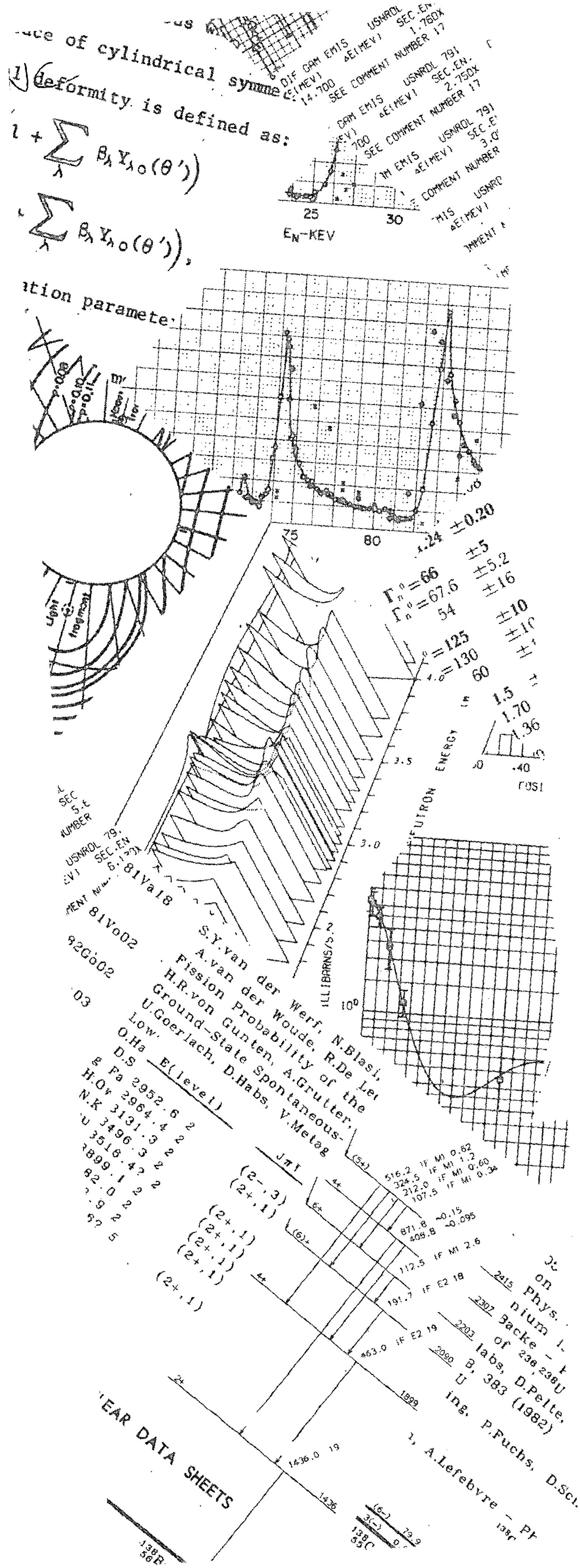

BNL-NCS-39266
DOE/NDC-43/U
NEANDC(US)-224/U
INDC(USA)-99L
INFORMAL REPORT
LIMITED DISTRIBUTION

REPORTS TO THE DOE NUCLEAR DATA COMMITTEE

Compiled by
NATIONAL NUCLEAR DATA CENTER
for the
U.S. Department of Energy
Nuclear Data Committee

May 1987

BROOKHAVEN NATIONAL LABORATORY
ASSOCIATED UNIVERSITIES, INC.
UPTON, LONG ISLAND, NEW YORK 11973

National
Nuclear
Data
Center

BNL-NCS-39266
DOE/NDC-43/U
NEANDC(US)-224/U
INDC(USA)-99/L
Informal Report
Limited Distribution

REPORTS TO

THE DOE NUCLEAR DATA COMMITTEE

MAY 1987

National
Nuclear
Data
Center

Compiled by the

NATIONAL NUCLEAR DATA CENTER
BROOKHAVEN NATIONAL LABORATORY
ASSOCIATED UNIVERSITIES, INC.

UNDER CONTRACT NO. DE-AC02-76CH00016 WITH THE
UNITED STATES DEPARTMENT OF ENERGY

Printed in the United States of America
Available from
National Technical Information Service
U.S. Department of Commerce
5285 Port Royal Road
Springfield, VA 22161

NTIS price codes:
Printed Copy: A09; Microfiche Copy: A01

PREFACE

The reports in this document were submitted to the Department of Energy, Nuclear Data Committee (DOE-NDC) in April, 1987. The reporting laboratories are those with a substantial program for the measurement of neutron and nuclear cross sections of relevance to the U.S. applied nuclear energy program.

The authors of the Status Report contributions are responsible for collecting and editing individual contributions from their laboratory and are not necessarily the sole authors of the contributions. The scientists responsible for the work described in each individual contribution are listed at the beginning of the contribution.

The material contained in these reports is to be regarded as comprised of informal statements of recent developments and preliminary data. Persons wishing to make use of these data should contact the individual experimenter for further details. The data which appear in this document should be quoted only by permission of the contributor and should be referenced as private communication, and not by this document number. Appropriate subjects are listed as follows:

1. Microscopic neutron cross sections relevant to the nuclear energy program, including shielding. Inverse reactions where pertinent are included.

2. Charged-particle cross sections, where they are relevant to (1.) above, and where relevant to developing and testing nuclear models.

3. Gamma ray production, radioactive decay, and theoretical developments in nuclear structure which are applicable to nuclear energy programs.

4. Proton and alpha-particle cross sections, at energies of up to 1 GeV, which are of interest to the space program.

These reports cannot be regarded as a complete summary of the nuclear research efforts in the U.S. A number of laboratories whose research is less programmatically oriented do not submit reports; neither do the submitted reports reflect all the work related to nuclear data in progress at the submitting laboratory.

This compilation has been produced almost completely from master copies prepared by the individual contributors listed in the Table of Contents, and reports are reproduced without change from these master copies.

The CINDA-type index which follows the Table of Contents was prepared by Norman E. Holden and Alyce Daly of the National Nuclear Data Center, Brookhaven National Laboratory, Upton, Long Island, New York.

TABLE OF CONTENTS

TABLE OF CONTENTS (cont.)

NEUTRON DATA REFERENCES

Element	Quantity	Energy (eV) Min	Max	Type	Documentation Ref	Page	Date	Lab	Comments
^{1}H	$\sigma_{el}(\theta)$	1.7+7		Expt	DOE-NDC-43	181	Apr87	TNL	Howell+ NDG. ANAL POWER.
^{1}H	σ_{pol}	1.7+7		Expt	DOE-NDC-43	181	Apr87	TNL	Howell+ NDG. ANAL POWER.
^{2}H	$\sigma_{el}(\theta)$	1.2+7		Expt	DOE-NDC-43	181	Apr87	TNL	Howell+ NDG. ANAL POWER.
^{2}H	σ_{pol}	1.2+7		Expt	DOE-NDC-43	181	Apr87	TNL	Howell+ NDG. ANAL POWER.
^{3}He	$\sigma_{n,p}$	5.0+5		Expt	DOE-NDC-43	134	Apr87	NBS	Behrens+ NDG. TBD.
^{6}Li	$\sigma_{el}(\theta)$	8.0+6	2.4+7	Expt	DOE-NDC-43	154	Apr87	OHO	Hansen+ NDG. ANG 15-150 DEGS.
^{6}Li	$\sigma_{el}(\theta)$	2.4+7		Exth	DOE-NDC-43	76	Apr87	OHO	Hansen+ NDG.
^{6}Li	$\sigma_{el}(\theta)$	1.7+7		Expt	DOE-NDC-43	176	Apr87	TNL	Walter+ NDG.
^{6}Li	σ_{pol}	1.7+7		Expt	DOE-NDC-43	176	Apr87	TNL	Walter+ NDG.
^{6}Li	$\sigma_{dif.inl}$	8.0+6	2.4+7	Expt	DOE-NDC-43	154	Apr87	OHO	Hansen+ NDG. ANG 15-150 DEGS.
^{6}Li	$\sigma_{dif.inl}$	2.4+7		Exth	DOE-NDC-43	76	Apr87	OHO	Hansen+ NDG.
^{6}Li	$\sigma_{n,p}$	1.2+8		Expt	DOE-NDC-43	154	Apr87	OHO	Pocanic+ NDG. 0-12.5 DEGS.
^{6}Li	$\sigma_{n,p}$	2.6+7		Expt	DOE-NDC-43	163	Apr87	OHO	Wang+ NDG. MEAS.SPECTRA.
^{6}Li	$\sigma_{n,d}$	2.6+7		Expt	DOE-NDC-43	163	Apr87	OHO	Wang+ NDG. MEAS.SPECTRA.
^{6}Li	$\sigma_{n,t}$	2.5-2		Eval	DOE-NDC-43	135	Apr87	NBS	Carlson+ NDG. ENDF/B-6 EVAL.
^{7}Li	$\sigma_{el}(\theta)$	8.0+6	2.4+7	Expt	DOE-NDC-43	154	Apr87	OHO	Hansen+ NDG. ANG 15-150 DEGS.
^{7}Li	$\sigma_{el}(\theta)$	2.4+7		Exth	DOE-NDC-43	76	Apr87	OHO	Hansen+ NDG.
^{7}Li	$\sigma_{dif.inl}$	8.0+6	2.4+7	Expt	DOE-NDC-43	154	Apr87	OHO	Hansen+ NDG. ANG 15-150 DEGS.
^{7}Li	$\sigma_{dif.inl}$	2.4+7		Exth	DOE-NDC-43	76	Apr87	OHO	Hansen+ NDG.
^{7}Li	$\sigma_{n,nt}$	NDG		Revw	DOE-NDC-43	10	Apr87	ANL	Smith. NDG. EVL TBD.
^{7}Be	$\sigma_{n,p}$	3.0-2	1.4+4	Expt	DOE-NDC-43	90	Apr87	LAS	Koehler+ σ (THERMAL) GIVEN.
^{7}Be	$\sigma_{n,p}$	1.0-2	1.0+6	Theo	DOE-NDC-43	101	Apr87	LAS	Hale+ GRPH. CALC AGREES EXPT.
^{9}Be	σ_{tot}	1.0+6	1.5+7	Expt	DOE-NDC-43	1	Apr87	ANL	Smith+ NDG.
^{9}Be	$\sigma_{el}(\theta)$	4.5+6	1.0+7	Expt	DOE-NDC-43	1	Apr87	ANL	Smith+ NDG.
^{9}Be	$\sigma_{el}(\theta)$	NDG		Expt	DOE-NDC-43	176	Apr87	TNL	Walter+ NDG. SEE NP/A 455,525.
^{9}Be	$\sigma_{dif.inl}$	4.5+6	1.0+7	Expt	DOE-NDC-43	1	Apr87	ANL	Smith+ NDG.
^{9}Be	$\sigma_{\alpha,emis}$	1.4+7		Expt	DOE-NDC-43	173	Apr87	AI	Kneff+ NDG.
^{10}B	$\sigma_{el}(\theta)$	3.0+6	1.2+7	Expt	DOE-NDC-43	155	Apr87	OHO	Sadowski+ NDG.
^{10}B	$\sigma_{el}(\theta)$	1.0+7	1.7+7	Expt	DOE-NDC-43	176	Apr87	TNL	Walter+ NDG.
^{10}B	σ_{pol}	1.0+7	1.7+7	Expt	DOE-NDC-43	176	Apr87	TNL	Walter+ NDG.
^{10}B	$\sigma_{dif.inl}$	3.0+6	1.2+7	Expt	DOE-NDC-43	155	Apr87	OHO	Sadowski+ NDG.
^{10}B	$\sigma_{n,n'\gamma}$	9.0+5	2.0+7	Expt	DOE-NDC-43	141	Apr87	ORL	Bywater+ NDG. SEE ORNL-TM-10191.
^{10}B	$\sigma_{n,p}$	2.5-2		Expt	DOE-NDC-43	88	Apr87	LAS	Reedy+ σ =6.4±0.5 MB.

NEUTRON DATA REFERENCES

Element	Quantity	Energy (eV) Min	Max	Type	Documentation Ref	Page	Date	Lab	Comments
^{10}B	$\sigma_{n,t}$	2.5-2		Expt	DOE-NDC-43	88	Apr87	LAS	Reedy+ σ = 0.89±0.09 B.
^{10}B	$\sigma_{n,\alpha}$	2.5-2		Eval	DOE-NDC-43	135	Apr87	NBS	Carlson+ NDG. ENDF/B-6 EVAL.
^{11}B	$\sigma_{el}(\theta)$	1.0+7	1.7+7	Expt	DOE-NDC-43	176	Apr87	TNL	Walter+ NDG.
^{11}B	σ_{pol}	1.0+7	1.7+7	Expt	DOE-NDC-43	176	Apr87	TNL	Walter+ NDG.
^{11}B	$\sigma_{n,\gamma}$	2.2+7		Expt	DOE-NDC-43	65	Apr87	KTY	Hanly+ NDG.
^{12}C	$\sigma_{el}(\theta)$	6.5+7		Expt	DOE-NDC-43	40	Apr87	DAV	Hjort+ NDG.
^{12}C	$\sigma_{el}(\theta)$	1.1+7	2.0+7	Eval	DOE-NDC-43	136	Apr87	NBS	Axton. FIT ENDF-5 σ, KERMA.
^{12}C	$\sigma_{el}(\theta)$	1.1+7	1.4+7	Expt	DOE-NDC-43	177	Apr87	TNL	Walter+ NDG.
^{12}C	$\sigma_{el}(\theta)$	1.6+7	1.7+7	Expt	DOE-NDC-43	177	Apr87	TNL	Walter+ NDG. JP/G TBP.
^{12}C	$\sigma_{el}(\theta)$	1.7+7		Expt	DOE-NDC-43	177	Apr87	TNL	Walter+ NDG.
^{12}C	σ_{pol}	1.6+7	1.7+7	Expt	DOE-NDC-43	177	Apr87	TNL	Walter+ NDG. JP/G TBP.
^{12}C	σ_{pol}	1.5+7	1.8+7	Expt	DOE-NDC-43	177	Apr87	TNL	Walter+ NDG.
^{12}C	σ_{pol}	1.6+7		Expt	DOE-NDC-43	181	Apr87	TNL	Howell+ NDG.
^{12}C	$\sigma_{dif.inl}$	1.1+7	2.0+7	Eval	DOE-NDC-43	136	Apr87	NBS	Axton. FIT ENDF-5 σ, KERMA.
^{12}C	$\sigma_{dif.inl}$	1.1+7	1.4+7	Expt	DOE-NDC-43	177	Apr87	TNL	Walter+ NDG.
^{12}C	$\sigma_{dif.inl}$	1.7+7		Expt	DOE-NDC-43	177	Apr87	TNL	Walter+ GRPH CFD MEAS.
^{12}C	$\sigma_{n,n'\gamma}$		2.0+8	Expt	DOE-NDC-43	96	Apr87	LAS	Nelson+ NDG. TBC.
^{12}C	$\sigma_{n,p}$	6.5+7		Expt	DOE-NDC-43	37	Apr87	DAV	Sorenson+ GRPH SPECTRA.
^{12}C	$\sigma_{n,d}$	1.1+7	2.0+7	Eval	DOE-NDC-43	136	Apr87	NBS	Axton. FIT ENDF-5 σ, KERMA.
^{12}C	$\sigma_{n,\alpha}$	1.1+7	2.0+7	Eval	DOE-NDC-43	136	Apr87	NBS	Axton. FIT ENDF-5 σ, KERMA.
^{12}C	$\sigma_{n,n\alpha}$	1.1+7	2.0+7	Eval	DOE-NDC-43	136	Apr87	NBS	Axton. FIT ENDF-V σ, KERMA.
^{12}C	$\sigma_{\alpha,emis}$	1.4+7		Expt	DOE-NDC-43	173	Apr87	AI	Kneff+ NDG.
^{13}C	$\sigma_{n,2n}$	NDG		Expt	DOE-NDC-43	156	Apr87	OHO	Resler+ NDG. SEQUENTIAL 2n DECAY.
^{13}C	$\sigma_{n,p}$	6.5+7		Expt	DOE-NDC-43	39	Apr87	DAV	Wang+ NDG.
^{14}N	$\sigma_{n,p}$	4.0-2	1.0+2	Expt	DOE-NDC-43	90	Apr87	LAS	Koehler+ NDG. TBC.
^{14}N	$\sigma_{\alpha,emis}$	1.4+7	1.5+7	Expt	DOE-NDC-43	173	Apr87	AI	Kneff+ NDG.
^{16}O	$\sigma_{el}(\theta)$	1.8+7	2.6+7	Expt	DOE-NDC-43	156	Apr87	OHO	Islam+ NDG.
^{16}O	$\sigma_{dif.inl}$	1.8+7	2.6+7	Expt	DOE-NDC-43	156	Apr87	OHO	Islam+ NDG.
^{16}O	$\sigma_{\alpha,emis}$	1.4+7	1.5+7	Expt	DOE-NDC-43	173	Apr87	AI	Kneff+ NDG.
^{19}F	$\sigma_{\alpha,emis}$	1.5+7		Expt	DOE-NDC-43	173	Apr87	AI	Kneff+ NDG.
Mg	$\sigma_{\alpha,emis}$	1.5+7		Expt	DOE-NDC-43	173	Apr87	AI	Kneff+ NDG.
^{27}Al	σ_{tot}	5.0+7	4.0+8	Theo	DOE-NDC-43	112	Apr87	LAS	Madland+ NDG. TBC.
^{27}Al	$\sigma_{el}(\theta)$	7.0+6		Expt	DOE-NDC-43	157	Apr87	OHO	Wang+ NDG.

NEUTRON DATA REFERENCES

Element	Quantity	Energy (eV) Min	Max	Type	Documentation Ref	Page	Date	Lab	Comments
^{27}Al	$\sigma_{el}(\theta)$	1.4+7	1.7+7	Expt	DOE-NDC-43	178	Apr87	TNL	Walter+ NDG. SEE PR/C 34,384.
^{27}Al	σ_{pol}	1.4+7	1.7+7	Expt	DOE-NDC-43	178	Apr87	TNL	Walter+ NDG. SEE PR/C 34,384.
^{27}Al	$\sigma_{dif.inl}$	7.0+6		Expt	DOE-NDC-43	157	Apr87	OHO	Wang+ NDG.
^{27}Al	$\sigma_{n,n'\gamma}$	9.5+6	1.9+7	Theo	DOE-NDC-43	83	Apr87	LRL	Blann+ NDG. CFD EXPT.
^{27}Al	$\sigma_{n,emis}$	7.0+6		Expt	DOE-NDC-43	157	Apr87	OHO	Wang+ NDG.
^{28}Si	$\sigma_{el}(\theta)$	2.0+7	2.6+7	Expt	DOE-NDC-43	158	Apr87	OHO	Alarcon+ NDG.
^{28}Si	σ_{pol}	8.0+6	1.7+7	Expt	DOE-NDC-43	178	Apr87	TNL	Walter+ NDG.
^{28}Si	σ_{pol}	1.9+7		Expt	DOE-NDC-43	181	Apr87	TNL	Howell+ NDG.
^{28}Si	$\sigma_{dif.inl}$	2.0+7	2.6+7	Expt	DOE-NDC-43	158	Apr87	OHO	Alarcon+ NDG.
S	$\sigma_{\alpha,emis}$	1.5+7		Expt	DOE-NDC-43	173	Apr87	AI	Kneff+ NDG.
^{32}S	$\sigma_{el}(\theta)$	2.0+7	2.6+7	Expt	DOE-NDC-43	158	Apr87	OHO	Alarcon+ NDG.
^{32}S	σ_{pol}	8.0+6	1.7+7	Expt	DOE-NDC-43	178	Apr87	TNL	Walter+ NDG.
^{32}S	$\sigma_{dif.inl}$	2.0+7	2.6+7	Expt	DOE-NDC-43	158	Apr87	OHO	Alarcon+ NDG.
^{33}S	σ_{tot}	1.0+4	2.0+6	Expt	DOE-NDC-43	142	Apr87	ORL	Coddens+ NDG.
^{34}S	$\sigma_{el}(\theta)$	2.0+7	2.6+7	Expt	DOE-NDC-43	158	Apr87	OHO	Alarcon+ NDG.
^{34}S	$\sigma_{dif.inl}$	2.0+7	2.6+7	Expt	DOE-NDC-43	158	Apr87	OHO	Alarcon+ NDG.
^{40}Ca	$\sigma_{el}(\theta)$	1.9+7	2.6+7	Expt	DOE-NDC-43	159	Apr87	OHO	Alarcon+ NDG
^{40}Ca	$\sigma_{el}(\theta)$	1.4+7	1.7+7	Expt	DOE-NDC-43	178	Apr87	TNL	Walter+ SEE PR/C 33, 1129.
^{40}Ca	σ_{pol}	1.1+7	1.7+7	Expt	DOE-NDC-43	178	Apr87	TNL	Walter+ SEE PR/C 33, 1129.
^{40}Ca	$\sigma_{dif.inl}$	2.2+7	2.6+7	Expt	DOE-NDC-43	159	Apr87	OHO	Alarcon+ NDG. CC ANALYSIS.
^{40}Ca	$\sigma_{dif.inl}$	1.4+7	1.7+7	Expt	DOE-NDC-43	178	Apr87	TNL	Walter+ PR/C 33, 1129.
^{48}Ca	σ_{tot}		1.0+7	Expt	DOE-NDC-43	141	Apr87	ORL	Carlton+ NDG.
^{48}Ca	$\sigma_{el}(\theta)$	NDG		Expt	DOE-NDC-43	61	Apr87	KTY	Hicks+ NDG.
^{48}Ca	$\sigma_{dif.inl}$	NDG		Expt	DOE-NDC-43	61	Apr87	KTY	Hicks+ NDG.
^{48}Ca	$\sigma_{n,\gamma}$		1.0+7	Expt	DOE-NDC-43	141	Apr87	ORL	Carlton+ NDG.
^{48}Ca	$\sigma_{n,n'\gamma}$	NDG		Expt	DOE-NDC-43	64	Apr87	KTY	Hicks+ NDG.TBC.
^{48}Ca	$<\Gamma>/D$		1.0+7	Expt	DOE-NDC-43	141	Apr87	ORL	Carlton+ $< 0.07*(10)^{-4}$.
^{51}V	Evaluation	NDG		Eval	DOE-NDC-43	10	Apr87	ANL	Smith+ NDG.
^{51}V	$\sigma_{el}(\theta)$	4.0+6	1.0+7	Expt	DOE-NDC-43	2	Apr87	ANL	Sugimoto+ NDG.
^{51}V	$\sigma_{dif.inl}$	4.0+6	1.0+7	Expt	DOE-NDC-43	2	Apr87	ANL	Sugimoto+ NDG.
^{54}Mn	$\sigma_{n,p}$	4.0-2	1.0+2	Expt	DOE-NDC-43	90	Apr87	LAS	Koehler+ NDG. TBC.
Fe	$\sigma_{el}(\theta)$	6.5+7		Expt	DOE-NDC-43	40	Apr87	DAV	Hjort+ NDG.
Fe	$\sigma_{el}(\theta)$	NDG		Eval	DOE-NDC-43	152	Apr87	ORL	Fu+ SEE ORNL-TM-9964.

NEUTRON DATA REFERENCES

Element	Quantity	Energy (eV) Min	Max	Type	Documentation Ref	Page	Date	Lab	Comments
Fe	$\sigma_{n,2n}$	NDG		Eval	DOE-NDC-43	152	Apr87	ORL	Fu+ SEE ORNL-TM-9964.
Fe	$\sigma_{n,emis}$	1.4+7	2.6+7	Theo	DOE-NDC-43	148	Apr87	ORL	Fu. NDG. CALC CFD EXPT.
Fe	$\sigma_{p,emis}$	NDG		Eval	DOE-NDC-43	152	Apr87	ORL	Fu+ SEE ORNL-TM-9964.
Fe	$\sigma_{\alpha,emis}$	NDG		Eval	DOE-NDC-43	152	Apr87	ORL	Fu+ SEE ORNL-TM-9964.
^{54}Fe	σ_{tot}	NDG		Expt	DOE-NDC-43	2	Apr87	ANL	Guenther+ ANE. TBP.
^{54}Fe	$\sigma_{el}(\theta)$	NDG		Expt	DOE-NDC-43	2	Apr87	ANL	Guenther+ ANE. TBP.
^{54}Fe	$\sigma_{el}(\theta)$	1.7+7		Expt	DOE-NDC-43	179	Apr87	TNL	Walter+ NDG.
^{54}Fe	σ_{pol}	1.7+7		Expt	DOE-NDC-43	179	Apr87	TNL	Walter+ NDG.
^{54}Fe	$\sigma_{dif.inl}$	1.1+7	2.6+7	Expt	DOE-NDC-43	159	Apr87	OHO	Mellema+ NDG
^{54}Fe	$\sigma_{dif.inl}$	1.7+7		Expt	DOE-NDC-43	179	Apr87	TNL	Walter+ NDG.
^{54}Fe	$\sigma_{n,n'\gamma}$	NDG		Expt	DOE-NDC-43	2	Apr87	ANL	Guenther+ ANE. TBP.
^{54}Fe	$\sigma_{n,p}$	2.6+7		Expt	DOE-NDC-43	163	Apr87	OHO	Wang+ NDG. MEAS.SPECTRA.
^{54}Fe	$\sigma_{n,d}$	2.6+7		Expt	DOE-NDC-43	163	Apr87	OHO	Wang+ NDG. MEAS.SPECTRA.
^{54}Fe	$\sigma_{\alpha,emis}$	1.0+7		Expt	DOE-NDC-43	173	Apr87	AI	Kneff+ NDG.
^{55}Fe	σ_{abs}	2.5-2		Expt	DOE-NDC-43	7	Apr87	ANL	Greenwood. σ < 50 BARNS.
^{55}Fe	$\sigma_{n,\alpha}$	2.5-2		Expt	DOE-NDC-43	7	Apr87	ANL	Greenwood. σ=13-40 MB.
^{56}Fe	σ_{tot}	5.0+7	4.0+8	Theo	DOE-NDC-43	112	Apr87	LAS	Madland+ GRPH CFD EXPT.
^{56}Fe	$\sigma_{dif.inl}$	1.1+7	2.6+7	Expt	DOE-NDC-43	159	Apr87	OHO	Mellema+ NDG
^{56}Fe	$\sigma_{n,2n}$	1.5+7		Expt	DOE-NDC-43	6	Apr87	ANL	Greenwood+ σ=454±35 MB.
^{56}Fe	$\sigma_{n,p}$	1.4+7		Expt	DOE-NDC-43	126	Apr87	MHG	Zasadny+ NDG.
^{56}Fe	$\sigma_{\alpha,emis}$	1.0+7		Expt	DOE-NDC-43	173	Apr87	AI	Kneff+ NDG.
^{57}Fe	$\sigma_{\alpha,emis}$	1.0+7		Expt	DOE-NDC-43	173	Apr87	AI	Kneff+ NDG.
^{58}Fe	$\sigma_{\alpha,emis}$	1.0+7		Expt	DOE-NDC-43	173	Apr87	AI	Kneff+ NDG.
^{59}Co	Evaluation	NDG		Eval	DOE-NDC-43	10	Apr87	ANL	Smith+ NDG.
^{59}Co	σ_{tot}	5.0+5	1.2+7	Expt	DOE-NDC-43	1	Apr87	ANL	Smith+ NDG.
^{59}Co	$\sigma_{el}(\theta)$	1.5+6	1.0+7	Expt	DOE-NDC-43	1	Apr87	ANL	Smith+ NDG.
^{59}Co	$\sigma_{dif.inl}$	1.5+6	1.0+7	Expt	DOE-NDC-43	1	Apr87	ANL	Smith+ NDG.
^{59}Co	$\sigma_{n,emis}$	5.0+6	1.0+7	Expt	DOE-NDC-43	4	Apr87	ANL	Guenther+ NDG. DOUBLE DIFF.
^{59}Co	$\sigma_{n,\alpha}$	5.0+6	1.0+7	Expt	DOE-NDC-43	5	Apr87	ANL	Meadows+ NDG.REL ^{238}U $\sigma_{(nf)}$.
Ni	$\sigma_{n,emis}$	5.0+6	1.0+7	Expt	DOE-NDC-43	4	Apr87	ANL	Guenther+ NDG. DOUBLE DIFF.
^{58}Ni	Evaluation	NDG		Eval	DOE-NDC-43	10	Apr87	ANL	Smith+ NDG.
^{58}Ni	σ_{tot}		1.2+7	Expt	DOE-NDC-43	2	Apr87	ANL	Smith+ NDG.
^{58}Ni	$\sigma_{el}(\theta)$	4.5+6	1.0+7	Expt	DOE-NDC-43	2	Apr87	ANL	Smith+ NDG.

NEUTRON DATA REFERENCES

Element	Quantity	Energy (eV) Min	Max	Type	Documentation Ref	Page	Date	Lab	Comments
^{58}Ni	$\sigma_{el}(\theta)$	1.7+7		Expt	DOE-NDC-43	179	Apr87	TNL	Walter+ NDG.
^{58}Ni	σ_{pol}	1.7+7		Expt	DOE-NDC-43	179	Apr87	TNL	Walter+ NDG.
^{58}Ni	$\sigma_{dif.inl}$	4.5+6	1.0+7	Expt	DOE-NDC-43	2	Apr87	ANL	Smith+ NDG.
^{58}Ni	$\sigma_{dif.inl}$	1.7+7		Expt	DOE-NDC-43	179	Apr87	TNL	Walter+ NDG.
^{58}Ni	$\sigma_{\alpha,emis}$	1.0+7		Expt	DOE-NDC-43	173	Apr87	AI	Kneff+ NDG.
^{60}Ni	$\sigma_{n,2n}$	1.5+7		Expt	DOE-NDC-43	6	Apr87	ANL	Greenwood+ $\sigma \approx 150$ MB.
^{60}Ni	$\sigma_{\alpha,emis}$	1.0+7		Expt	DOE-NDC-43	173	Apr87	AI	Kneff+ NDG.
^{61}Ni	$\sigma_{\alpha,emis}$	1.0+7		Expt	DOE-NDC-43	173	Apr87	AI	Kneff+ NDG.
^{62}Ni	$\sigma_{\alpha,emis}$	1.0+7		Expt	DOE-NDC-43	173	Apr87	AI	Kneff+ NDG.
^{64}Ni	$\sigma_{n,2n}$	1.5+7		Expt	DOE-NDC-43	6	Apr87	ANL	Greenwood+ σ=953±67 MB.
^{64}Ni	$\sigma_{\alpha,emis}$	1.0+7		Expt	DOE-NDC-43	173	Apr87	AI	Kneff+ NDG.
^{63}Cu	$\sigma_{n,p}$	1.5+7		Expt	DOE-NDC-43	6	Apr87	ANL	Greenwood+ σ=54±4 MB.
^{63}Cu	$\sigma_{\alpha,emis}$	9.0+6	1.1+7	Expt	DOE-NDC-43	160	Apr87	OHO	Ahmad+ NDG. σ, SPECTRA CFD CALC.
^{63}Cu	$\sigma_{d,emis}$	9.0+6	1.1+7	Expt	DOE-NDC-43	160	Apr87	OHO	Ahmad+ NDG. σ, SPECTRA CFD CALC.
^{63}Cu	$\sigma_{p,emis}$	9.0+6	1.1+7	Expt	DOE-NDC-43	160	Apr87	OHO	Ahmad+ NDG. σ, SPECTRA CFD CALC.
^{65}Cu	$\sigma_{n,2n}$	1.4+7		Expt	DOE-NDC-43	126	Apr87	MHG	Zasadny+ NDG.
^{65}Cu	$\sigma_{\alpha,emis}$	9.0+6	1.1+7	Expt	DOE-NDC-43	160	Apr87	OHO	Ahmad+ NDG. σ, SPECTRA CFD CALC.
^{65}Cu	$\sigma_{d,emis}$	9.0+6	1.1+7	Expt	DOE-NDC-43	160	Apr87	OHO	Ahmad+ NDG. σ, SPECTRA CFD CALC.
^{65}Cu	$\sigma_{p,emis}$	9.0+6	1.1+7	Expt	DOE-NDC-43	160	Apr87	OHO	Ahmad+ NDG. σ, SPECTRA CFD CALC.
^{64}Zn	$\sigma_{n,2n}$	1.5+7		Exth	DOE-NDC-43	106	Apr87	NMX	Rutherford+ GRPHS, EXPT CFD CALC.
^{64}Zn	$\sigma_{n,p}$	1.4+7		Expt	DOE-NDC-43	126	Apr87	MHG	Zasadny+ NDG.
^{64}Zn	$\sigma_{n,p}$	1.5+7		Exth	DOE-NDC-43	106	Apr87	NMX	Rutherford+ GRPHS, EXPT CFD CALC.
Ge	$\sigma_{\alpha,emis}$	1.5+7		Expt	DOE-NDC-43	173	Apr87	AI	Kneff+ NDG.
^{89}Y	$\sigma_{el}(\theta)$	8.0+6	1.7+7	Expt	DOE-NDC-43	180	Apr87	TNL	Walter+ NDG. PR/C TBP.
^{89}Y	σ_{pol}	8.0+6	1.7+7	Expt	DOE-NDC-43	180	Apr87	TNL	Walter+ NDG. PR/C TBP.
^{89}Y	$\sigma_{n,emis}$	5.0+6	1.0+7	Expt	DOE-NDC-43	4	Apr87	ANL	Guenther+ NDG. DOUBLE DIFF.
Zr	σ_{tot}	4.0+6	1.0+7	Expt	DOE-NDC-43	3	Apr87	ANL	Sugimoto+ NDG.
Zr	$\sigma_{el}(\theta)$	4.0+6	1.0+7	Expt	DOE-NDC-43	3	Apr87	ANL	Sugimoto+ NDG.
Zr	$\sigma_{dif.inl}$	4.0+6	1.0+7	Expt	DOE-NDC-43	3	Apr87	ANL	Sugimoto+ NDG.
^{93}Nb	$\sigma_{el}(\theta)$	7.0+6		Expt	DOE-NDC-43	157	Apr87	OHO	Wang+ NDG.
^{93}Nb	$\sigma_{el}(\theta)$	8.0+6	1.7+7	Expt	DOE-NDC-43	180	Apr87	TNL	Walter+ NDG. TBP.
^{93}Nb	σ_{pol}	8.0+6	1.7+7	Expt	DOE-NDC-43	180	Apr87	TNL	Walter+ NDG. TBP.
^{93}Nb	$\sigma_{dif.inl}$	7.0+6		Expt	DOE-NDC-43	157	Apr87	OHO	Wang+ NDG.

NEUTRON DATA REFERENCES

Element	Quantity	Energy (eV) Min	Max	Type	Documentation Ref	Page	Date	Lab	Comments
^{93}Nb	$\sigma_{dif.inl}$	FISS		Expt	DOE-NDC-43	43	Apr87	INL	Rogers+ NDG. ^{252}Cf, ^{235}U.
^{93}Nb	$\sigma_{n,n'\gamma}$	9.5+6	1.9+7	Theo	DOE-NDC-43	83	Apr87	LRL	Blann+ NDG. CFD EXPT.
^{93}Nb	$\sigma_{n,emis}$	7.0+6		Expt	DOE-NDC-43	157	Apr87	OHO	Wang+ NDG.
^{93}Nb	$\sigma_{n,emis}$	1.4+7	2.6+7	Theo	DOE-NDC-43	148	Apr87	ORL	Fu. NDG. CALC CFD EXPT.
^{93}Nb	$\sigma_{n,emis}$	5.0+6	1.0+7	Expt	DOE-NDC-43	4	Apr87	ANL	Guenther+ NDG. DOUBLE DIFF.
^{92}Mo	$\sigma_{n,np}$	1.5+7		Expt	DOE-NDC-43	6	Apr87	ANL	Greenwood+ $\sigma_{(nd+nnp)} \approx 300$ MB.
^{92}Mo	$\sigma_{n,d}$	1.5+7		Expt	DOE-NDC-43	6	Apr87	ANL	Greenwood+ $\sigma_{(nd+nnp)} \approx 300$ MB.
^{94}Mo	$\sigma_{n,p}$	1.5+7		Expt	DOE-NDC-43	6	Apr87	ANL	Greenwood+ $\sigma=53\pm5$ MB.
^{95}Mo	$\sigma_{n,\gamma}$	NDG		Expt	DOE-NDC-43	144	Apr87	ORL	Winters+ ASTRON.ASTROPHYS. TBP.
^{95}Mo	$\sigma_{n,np}$	1.5+7		Expt	DOE-NDC-43	6	Apr87	ANL	Greenwood+ $\sigma_{(nd+nnp)}=17\pm2$ MB.
^{95}Mo	$\sigma_{n,d}$	1.5+7		Expt	DOE-NDC-43	6	Apr87	ANL	Greenwood+ $\sigma_{(nd+nnp)}=17\pm2$ MB.
^{96}Mo	$\sigma_{n,\gamma}$	NDG		Expt	DOE-NDC-43	144	Apr87	ORL	Winters+ ASTRON.ASTROPHYS. TBP.
^{97}Mo	$\sigma_{n,\gamma}$	NDG		Expt	DOE-NDC-43	144	Apr87	ORL	Winters+ ASTRON.ASTROPHYS. TBP.
^{98}Mo	$\sigma_{n,\gamma}$	NDG		Expt	DOE-NDC-43	144	Apr87	ORL	Winters+ ASTRON.ASTROPHYS. TBP.
^{99}Tc	$\sigma_{n,\gamma}$	NDG		Expt	DOE-NDC-43	144	Apr87	ORL	Winters+ ASTRON.ASTROPHYS. TBP.
In	$\sigma_{el}(\theta)$	4.0+6	1.0+7	Expt	DOE-NDC-43	3	Apr87	ANL	Smith+ NDG.
^{116}Sn	$\sigma_{el}(\theta)$	8.0+6	1.4+7	Expt	DOE-NDC-43	181	Apr87	TNL	Walter+ NDG. TBP.
^{116}Sn	σ_{pol}	8.0+6	1.4+7	Expt	DOE-NDC-43	181	Apr87	TNL	Walter+ NDG. TBP.
^{116}Sn	$\sigma_{dif.inl}$	8.0+6	1.4+7	Expt	DOE-NDC-43	181	Apr87	TNL	Walter+ NDG. TBP.
^{118}Sn	$\sigma_{p,emis}$	6.5+7		Expt	DOE-NDC-43	39	Apr87	DAV	Romero+ NDG.
^{120}Sn	$\sigma_{el}(\theta)$	8.0+6	1.4+7	Expt	DOE-NDC-43	181	Apr87	TNL	Walter+ NDG. TBP.
^{120}Sn	σ_{pol}	8.0+6	1.4+7	Expt	DOE-NDC-43	181	Apr87	TNL	Walter+ NDG. TBP.
^{120}Sn	$\sigma_{dif.inl}$	8.0+6	1.4+7	Expt	DOE-NDC-43	181	Apr87	TNL	Walter+ NDG. TBP.
^{120}Sn	$\langle\Gamma\rangle/D$	NDG		Expt	DOE-NDC-43	60	Apr87	KTY	Harper+ S_0, S_1.
^{120}Sn	$\sigma_{p,emis}$	6.5+7		Expt	DOE-NDC-43	39	Apr87	DAV	Romero+ NDG.
Eu	$\sigma_{n,n'\gamma}$	4.0+2	3.0+6	Expt	DOE-NDC-43	92	Apr87	ORL	Wender+ NDG.
^{151}Eu	$\sigma_{n,\gamma}$	3.0+3	2.2+6	Expt	DOE-NDC-43	142	Apr87	ORL	Macklin+ SEE NSE 95,189.
^{153}Eu	$\sigma_{n,\gamma}$	3.0+3	2.2+6	Expt	DOE-NDC-43	142	Apr87	ORL	Macklin+ SEE NSE 95,189.
Gd	$\sigma_{n,n'\gamma}$	4.0+2	3.0+6	Expt	DOE-NDC-43	92	Apr87	ORL	Wender+ NDG.
^{152}Gd	Res.Params.		2.7+3	Expt	DOE-NDC-43	143	Apr87	ORL	Macklin. SEE NSE 95,189.
^{154}Gd	Res.Params.		2.8+3	Expt	DOE-NDC-43	143	Apr87	ORL	Macklin. SEE NSE 95,189.
^{165}Ho	$\sigma_{n,n'\gamma}$	4.0+2	3.0+6	Expt	DOE-NDC-43	92	Apr87	ORL	Wender+ NDG.
^{165}Ho	$\sigma_{n,emis}$	5.0+6	1.0+7	Expt	DOE-NDC-43	4	Apr87	ANL	Guenther+ NDG. DOUBLE DIFF.

Element	Quantity	Energy (eV) Min	Max	Type	Documentation Ref	Page	Date	Lab	Comments
^{181}Ta	$\sigma_{n,n'\gamma}$	1.4+7		Theo	DOE-NDC-43	83	Apr87	LRL	Blann+ NDG. CFD EXPT.
^{181}Ta	$\sigma_{\alpha,emis}$	1.5+7		Expt	DOE-NDC-43	173	Apr87	AI	Kneff+ NDG.
W	$\sigma_{\alpha,emis}$	1.5+7		Expt	DOE-NDC-43	173	Apr87	AI	Kneff+ NDG.
^{182}W	$\sigma_{\alpha,emis}$	1.5+7		Expt	DOE-NDC-43	173	Apr87	AI	Kneff+ NDG.
^{183}W	$\sigma_{\alpha,emis}$	1.5+7		Expt	DOE-NDC-43	173	Apr87	AI	Kneff+ NDG.
^{184}W	σ_{tot}	2.6+7		Theo	DOE-NDC-43	149	Apr87	ORL	Fu+ NDG. *TNG* CODE.
^{184}W	$\sigma_{el}(\theta)$	2.6+7		Theo	DOE-NDC-43	149	Apr87	ORL	Fu+ NDG. *TNG* CODE.
^{184}W	$\sigma_{dif.inl}$	2.6+7		Theo	DOE-NDC-43	149	Apr87	ORL	Fu+ NDG. *TNG* CODE.
^{184}W	$\sigma_{n,X}$	2.6+7		Theo	DOE-NDC-43	149	Apr87	ORL	Fu+ NDG. *TNG* CODE.
^{184}W	γ Spectra	5.0+5		Theo	DOE-NDC-43	85	Apr87	LRL	Gardner+ GRPH CFD EXPT.
^{184}W	$\sigma_{n,2n}$	2.6+7		Theo	DOE-NDC-43	149	Apr87	ORL	Fu+ NDG. *TNG* CODE.
^{184}W	$\sigma_{n,xn}$	2.6+7		Theo	DOE-NDC-43	149	Apr87	ORL	Fu+ NDG. *TNG* CODE.
^{184}W	$\sigma_{n,emis}$	2.6+7		Theo	DOE-NDC-43	149	Apr87	ORL	Fu+ NDG. *TNG* CODE.
^{184}W	$\sigma_{\alpha,emis}$	1.5+7		Expt	DOE-NDC-43	173	Apr87	AI	Kneff+ NDG.
^{186}W	$\sigma_{\alpha,emis}$	1.5+7		Expt	DOE-NDC-43	173	Apr87	AI	Kneff+ NDG.
Re	σ_{tot}	2.0+3	2.0+7	Theo	DOE-NDC-43	109	Apr87	LAS	Young. GRPH CFD EXPT.
Re	$\sigma_{n,\gamma}$	3.0+3	1.9+6	Expt	DOE-NDC-43	143	Apr87	ORL	Macklin. NSE TBP.
^{185}Re	$\sigma_{n,\gamma}$	1.0+3	2.0+7	Theo	DOE-NDC-43	109	Apr87	LAS	Young. GRPH CFD EXPT.
^{185}Re	$<\Gamma>/D$	NDG		Theo	DOE-NDC-43	109	Apr87	LAS	Young. TBL. CFD EXPT.
^{187}Re	$\sigma_{n,\gamma}$	1.0+3	2.0+7	Theo	DOE-NDC-43	109	Apr87	LAS	Young. GRPH CFD EXPT.
^{187}Re	$<\Gamma>/D$	NDG		Theo	DOE-NDC-43	109	Apr87	LAS	Young. TBL. CFD EXPT.
^{189}Os	$\sigma_{el}(\theta)$	6.3+4	9.7+4	Expt	DOE-NDC-43	67	Apr87	KTY	Hershberger+ NDG.ASTRO.ASTROPHYS.TBP
^{189}Os	$\sigma_{n,\gamma}$	2.0+2	5.0+5	Expt	DOE-NDC-43	143	Apr87	ORL	Winters+ ASTRON.ASTROPHYS. TBP.
^{189}Os	$\sigma_{n,\gamma}$	NDG		Expt	DOE-NDC-43	67	Apr87	KTY	Hershberger+ NDG.ASTRO.ASTROPHYS.TBP
^{189}Os	Res.Params.	NDG		Expt	DOE-NDC-43	143	Apr87	ORL	Winters+ ASTRON.ASTROPHYS. TBP.
^{189}Os	$<\Gamma>/D$	NDG		Expt	DOE-NDC-43	143	Apr87	ORL	Winters+ ASTRON.ASTROPHYS. TBP.
^{190}Os	$\sigma_{el}(\theta)$	NDG		Expt	DOE-NDC-43	58	Apr87	KTY	Hicks+ NDG.
^{192}Os	$\sigma_{el}(\theta)$	NDG		Expt	DOE-NDC-43	58	Apr87	KTY	Hicks+ NDG.
^{194}Pt	σ_{tot}	3.0+5	4.0+6	Expt	DOE-NDC-43	58	Apr87	KTY	Hicks+ NDG.
^{194}Pt	$\sigma_{el}(\theta)$	3.0+5	4.0+6	Expt	DOE-NDC-43	58	Apr87	KTY	Hicks+ NDG.
^{197}Au	$\sigma_{n,\gamma}$	2.5−2		Eval	DOE-NDC-43	135	Apr87	NBS	Carlson+ NDG. ENDF/B-6 EVAL.
^{197}Au	$\sigma_{n,n'\gamma}$	9.5+6	1.9+7	Theo	DOE-NDC-43	83	Apr87	LRL	Blann+ NDG. CFD EXPT.
Pb	$\sigma_{el}(\theta)$	6.5+7		Expt	DOE-NDC-43	40	Apr87	DAV	Hjort+ GRPH.

NEUTRON DATA REFERENCES

Element	Quantity	Energy (eV) Min	Max	Type	Documentation Ref	Page	Date	Lab	Comments
Pb	$\sigma_{dif.inl}$	6.5+7		Expt	DOE-NDC-43	40	Apr87	DAV	Hjort+ GRPH.
^{204}Pb	$\sigma_{el}(\theta)$	NDG		Expt	DOE-NDC-43	59	Apr87	KTY	Hanly+ NDG.
^{208}Pb	σ_{tot}	5.0+7	4.0+8	Theo	DOE-NDC-43	112	Apr87	LAS	Madland+ NDG. TBC.
^{208}Pb	σ_{tot}	5.0+4	1.0+6	Expt	DOE-NDC-43	150	Apr87	ORL	Horen+ SEE PR/C 34.
^{208}Pb	$\sigma_{el}(\theta)$	5.0+4	1.0+6	Expt	DOE-NDC-43	150	Apr87	ORL	Horen+ SEE PR/C 34.
^{208}Pb	$\sigma_{el}(\theta)$	6.0+6	8.0+6	Expt	DOE-NDC-43	181	Apr87	TNL	Howell+ NDG. ANAL POWER.
^{208}Pb	σ_{pol}	6.0+6	9.0+6	Expt	DOE-NDC-43	181	Apr87	TNL	Walter+ NDG. TBC.
^{208}Pb	σ_{pol}	6.0+6	8.0+6	Expt	DOE-NDC-43	181	Apr87	TNL	Howell+ NDG. ANAL POWER.
^{209}Bi	$\sigma_{el}(\theta)$	7.0+6		Expt	DOE-NDC-43	157	Apr87	OHO	Wang+ NDG.
^{209}Bi	$\sigma_{el}(\theta)$	4.5+6	1.0+7	Expt	DOE-NDC-43	3	Apr87	ANL	Smith+ NDG.
^{209}Bi	$\sigma_{dif.inl}$	7.0+6		Expt	DOE-NDC-43	157	Apr87	OHO	Wang+ NDG.
^{209}Bi	$\sigma_{n,emis}$	7.0+6		Expt	DOE-NDC-43	157	Apr87	OHO	Wang+ NDG.
^{209}Bi	$\sigma_{n,emis}$	1.4+7	2.6+7	Theo	DOE-NDC-43	148	Apr87	ORL	Fu. NDG. CALC CFD EXPT.
^{209}Bi	$\sigma_{n,emis}$	5.0+6	1.0+7	Expt	DOE-NDC-43	4	Apr87	ANL	Guenther+ NDG. DOUBLE DIFF.
^{230}Th	$\sigma_{n,f}$	1.5+7		Expt	DOE-NDC-43	5	Apr87	ANL	Meadows. REL ^{235}U $\sigma_{(n,f)}$.
^{230}Th	Fiss.Yield	FAST		Expt	DOE-NDC-43	145	Apr87	ORL	Dickens. NDG. SEE ORNL-6266.
^{232}Th	$\sigma_{el}(\theta)$	9.0+5	2.4+6	Expt	DOE-NDC-43	116	Apr87	LTI	Beghian+ GRPH. CFD CALC, ENDF.
^{232}Th	$\sigma_{dif.inl}$		3.0+6	Theo	DOE-NDC-43	102	Apr87	LAS	Arthur. GRPH CFD EXPT.
^{232}Th	$\sigma_{dif.inl}$	9.0+5	2.4+6	Expt	DOE-NDC-43	116	Apr87	LTI	Beghian+ GRPH. CFD CALC, ENDF.
^{232}Th	$\sigma_{dif.inl}$	2.0+6	3.0+6	Expt	DOE-NDC-43	118	Apr87	LTI	Beghian+ NDG. TBD.
^{232}Th	$\sigma_{dif.inl}$	NDG		Theo	DOE-NDC-43	119	Apr87	LTI	Sheldon. NDG.
^{232}Th	$\sigma_{n,f}$	1.5+7		Expt	DOE-NDC-43	5	Apr87	ANL	Meadows. REL ^{235}U $\sigma_{(n,f)}$.
^{232}Th	Fiss.Yield	FAST		Expt	DOE-NDC-43	145	Apr87	ORL	Dickens. NDG. SEE ORNL-6266.
^{232}Th	Photo-fissn	NDG		Expt	DOE-NDC-43	98	Apr87	LAS	Hollas+ GRAPH. γ-SPECTRA.
^{231}Pa	Fiss.Yield	FAST		Expt	DOE-NDC-43	145	Apr87	ORL	Dickens. NDG. SEE ORNL-6266.
^{233}U	$\sigma_{n,f}$	1.5+7		Expt	DOE-NDC-43	5	Apr87	ANL	Meadows. REL ^{235}U $\sigma_{(n,f)}$.
^{233}U	Fiss.Yield	FAST		Expt	DOE-NDC-43	145	Apr87	ORL	Dickens. NDG. SEE ORNL-6266.
^{234}U	$\sigma_{n,f}$	1.5+7		Expt	DOE-NDC-43	5	Apr87	ANL	Meadows. REL ^{235}U $\sigma_{(n,f)}$.
^{234}U	Fiss.Yield	FAST		Expt	DOE-NDC-43	145	Apr87	ORL	Dickens. NDG. SEE ORNL-6266.
^{235}U	σ_{tot}	2.5-2		Expt	DOE-NDC-43	147	Apr87	ORL	Spencer+ σ=690±5 B.
^{235}U	$\sigma_{el}(\theta)$	1.8+5	9.0+5	Expt	DOE-NDC-43	116	Apr87	LTI	Beghian+ NDG. TBP.
^{235}U	$\sigma_{dif.inl}$	1.8+5	9.0+5	Expt	DOE-NDC-43	116	Apr87	LTI	Beghian+ NDG. TBP.
^{235}U	$\sigma_{dif.inl}$	9.5+4		Expt	DOE-NDC-43	118	Apr87	LTI	Beghian+ NDG. TBD.

NEUTRON DATA REFERENCES

Element	Quantity	Energy (eV) Min	Max	Type	Documentation Ref	Page	Date	Lab	Comments
^{235}U	$\sigma_{n,f}$	1.0+6	4.0+8	Expt	DOE-NDC-43	96	Apr87	LAS	Lisowski+ NDG. TBC.
^{235}U	$\sigma_{n,f}$	2.5-2	1.0+3	Expt	DOE-NDC-43	130	Apr87	NBS	Schrack+ NDG. TBC.
^{235}U	$\sigma_{n,f}$	1.0+6	3.5+7	Expt	DOE-NDC-43	130	Apr87	NBS	Carlson+ NDG. TBC.
^{235}U	$\sigma_{n,f}$	2.5+6		Expt	DOE-NDC-43	132	Apr87	NBS	Duvall+ NDG.
^{235}U	$\sigma_{n,f}$	2.5-2		Eval	DOE-NDC-43	135	Apr87	NBS	Carlson+ NDG. ENDF/B-6 EVAL.
^{235}U	$\sigma_{n,f}$		1.0+5	Theo	DOE-NDC-43	83	Apr87	LRL	Gardner+ ISOMERIC STATE σ.
^{235}U	ν_d	FAST		Expt	DOE-NDC-43	97	Apr87	LAS	Atwater+ NDG. SPECTRAL MEAS.
^{235}U	ν_d	2.5-2		Expt	DOE-NDC-43	120	Apr87	LTI	Couchell+ GRPH. E_n-SPECTRA.
^{235}U	Spect.fiss n	5.5+5		Expt	DOE-NDC-43	8	Apr87	ANL	Sugimoto+REL ^{239}Pu.
^{235}U	Fiss.Prod γ	FAST		Expt	DOE-NDC-43	97	Apr87	LAS	Moss+ NDG. DELAY γ SPECTRAL MEAS.
^{235}U	Fiss.Yield	FAST		Expt	DOE-NDC-43	145	Apr87	ORL	Dickens. NDG. SEE ORNL-6266.
^{235}U	Fiss.Yield	2.5-2		Expt	DOE-NDC-43	166	Apr87	BNW	Ford+NDG. ^{138}Cs, ISOM.YLD.RATIO
^{235}U	Photo-fissn	NDG		Expt	DOE-NDC-43	98	Apr87	LAS	Hollas+ GRAPH. γ-SPECTRA.
^{236}U	$\sigma_{n,f}$	1.5+7		Expt	DOE-NDC-43	5	Apr87	ANL	Meadows. REL ^{235}U $\sigma_{(n,f)}$.
^{236}U	Fiss.Yield	FAST		Expt	DOE-NDC-43	145	Apr87	ORL	Dickens. NDG. SEE ORNL-6266.
^{238}U	$\sigma_{dif.inl}$	9.0+5	2.2+6	Expt	DOE-NDC-43	116	Apr87	LTI	Beghian+ NDG. SEE NSE 92,350.
^{238}U	$\sigma_{dif.inl}$	2.0+6	3.0+6	Expt	DOE-NDC-43	118	Apr87	LTI	Beghian+ NDG. TBD.
^{238}U	$\sigma_{dif.inl}$	NDG		Theo	DOE-NDC-43	119	Apr87	LTI	Sheldon. NDG.
^{238}U	$\sigma_{n,\gamma}$	2.3+4	9.6+5	Expt	DOE-NDC-43	128	Apr87	MHG	Quang+ TBC.
^{238}U	$\sigma_{n,\gamma}$	2.5-2		Eval	DOE-NDC-43	135	Apr87	NBS	Carlson+ NDG. ENDF/B-6 EVAL.
^{238}U	$\sigma_{n,\gamma}$	NDG		Theo	DOE-NDC-43	87	Apr87	LRL	Gardner+ NDG.
^{238}U	$\sigma_{n,\gamma}$	1.0+3	1.0+5	Expt	DOE-NDC-43	146	Apr87	ORL	Macklin+ TRANS.ANS. TBP.
^{238}U	$\sigma_{n,f}$	1.0+6	4.0+8	Expt	DOE-NDC-43	96	Apr87	LAS	Lisowski+ NDG. TBC.
^{238}U	$\sigma_{n,f}$	2.5-2		Eval	DOE-NDC-43	135	Apr87	NBS	Carlson+ NDG. ENDF/B-6 EVAL.
^{238}U	$\sigma_{n,f}$	5.0+6	1.0+7	Expt	DOE-NDC-43	5	Apr87	ANL	Meadows+ NDG.REL ^{59}Co $\sigma_{(n,\alpha)}$.
^{238}U	$\sigma_{n,f}$	1.5+7		Expt	DOE-NDC-43	5	Apr87	ANL	Meadows. REL ^{235}U $\sigma_{(n,f)}$.
^{238}U	ν_d	FAST		Expt	DOE-NDC-43	120	Apr87	LTI	Couchell+ NDG. SPECTRA.TBD.
^{238}U	Fiss.Yield	FAST		Expt	DOE-NDC-43	145	Apr87	ORL	Dickens. NDG. SEE ORNL-6266.
^{238}U	Photo-fissn	NDG		Expt	DOE-NDC-43	98	Apr87	LAS	Hollas+ GRAPH. γ-SPECTRA.
^{238}U	Photo-fissn	NDG		Theo	DOE-NDC-43	87	Apr87	LRL	Gardner+ NDG.
^{237}Np	$\sigma_{n,f}$	1.0+6	4.0+8	Expt	DOE-NDC-43	96	Apr87	LAS	Lisowski+ NDG. TBC.
^{237}Np	$\sigma_{n,f}$	1.5+7		Expt	DOE-NDC-43	5	Apr87	ANL	Meadows. REL ^{235}U $\sigma_{(n,f)}$.
^{237}Np	Photo-fissn	NDG		Theo	DOE-NDC-43	87	Apr87	LRL	Gardner+ NDG.

NEUTRON DATA REFERENCES

Element	Quantity	Energy (eV) Min	Max	Type	Documentation Ref	Page	Date	Lab	Comments
^{238}Pu	Fiss.Yield	FAST		Expt	DOE-NDC-43	145	Apr87	ORL	Dickens. NDG. SEE ORNL-6266.
^{239}Pu	σ_{tot}	2.5-2		Expt	DOE-NDC-43	147	Apr87	ORL	Spencer+ σ=1025±6 B.
^{239}Pu	$\sigma_{n,f}$	2.5-2		Eval	DOE-NDC-43	135	Apr87	NBS	Carlson+ NDG. ENDF/B-6 EVAL.
^{239}Pu	$\sigma_{n,f}$	1.5+7		Expt	DOE-NDC-43	5	Apr87	ANL	Meadows. REL ^{235}U $\sigma_{(n,f)}$.
^{239}Pu	ν_d	2.5-2		Expt	DOE-NDC-43	120	Apr87	LTI	Couchell+ GRPH. E_n-SPECTRA.
^{239}Pu	Spect.fiss n	5.5+5		Expt	DOE-NDC-43	8	Apr87	ANL	Sugimoto+REL ^{235}U.
^{239}Pu	Fiss.Yield	FAST		Expt	DOE-NDC-43	145	Apr87	ORL	Dickens. NDG. SEE ORNL-6266.
^{239}Pu	Res.Params.	NDG		Eval	DOE-NDC-43	144	Apr87	ORL	Derrien+ NDG. SEE ORNL-TM-10098.
^{239}Pu	Photo-fissn	NDG		Expt	DOE-NDC-43	98	Apr87	LAS	Hollas+ GRAPH. γ-SPECTRA.
^{240}Pu	σ_{tot}	2.5-2		Expt	DOE-NDC-43	147	Apr87	ORL	Spencer+ σ=284±2 B.
^{240}Pu	$\sigma_{dif.inl}$	NDG		Theo	DOE-NDC-43	119	Apr87	LTI	Sheldon. NDG.
^{240}Pu	Fiss.Yield	FAST		Expt	DOE-NDC-43	145	Apr87	ORL	Dickens. NDG. SEE ORNL-6266.
^{240}Pu	Res.Params.	1.1+0		Expt	DOE-NDC-43	147	Apr87	ORL	Spencer+ E_0, Γ_n, Γ_γ.
^{241}Pu	Fiss.Yield	FAST		Expt	DOE-NDC-43	145	Apr87	ORL	Dickens. NDG. SEE ORNL-6266.
^{241}Pu	Res.Params.	NDG		Eval	DOE-NDC-43	144	Apr87	ORL	Derrien+ NDG. NSE. TBP.
^{242}Pu	$\sigma_{dif.inl}$	NDG		Theo	DOE-NDC-43	119	Apr87	LTI	Sheldon. NDG.
^{242}Pu	$\sigma_{n,f}$	1.5+7		Expt	DOE-NDC-43	5	Apr87	ANL	Meadows. REL ^{235}U $\sigma_{(n,f)}$.
^{244}Pu	$\sigma_{dif.inl}$	NDG		Theo	DOE-NDC-43	119	Apr87	LTI	Sheldon. NDG.
^{244}Pu	Fiss.Yield	FAST		Expt	DOE-NDC-43	145	Apr87	ORL	Dickens. NDG. SEE ORNL-6266.
^{241}Am	Fiss.Yield	FAST		Expt	DOE-NDC-43	145	Apr87	ORL	Dickens. NDG. SEE ORNL-6266.
^{243}Am	Fiss.Yield	FAST		Expt	DOE-NDC-43	145	Apr87	ORL	Dickens. NDG. SEE ORNL-6266.
^{242}Cm	$\sigma_{n,f}$	1.0-1	1.0+5	Expt	DOE-NDC-43	169	Apr87	RPI	Alam+ GRPH.
^{242}Cm	$\sigma_{n,f}$	1.0-1	1.0+5	Expt	DOE-NDC-43	77	Apr87	RPI	Alam+ GRPH.
^{242}Cm	Res.Params.	1.4+1	6.0+1	Expt	DOE-NDC-43	169	Apr87	RPI	Alam+ TBL.
^{242}Cm	Res.Params.	1.4+1	6.0+1	Expt	DOE-NDC-43	77	Apr87	RPI	Alam+ TBL.
^{243}Cm	Fiss.Yield	FAST		Expt	DOE-NDC-43	146	Apr87	ORL	Dickens. NDG. NSE. TBP.
^{243}Cm	Fiss.Yield	FAST		Expt	DOE-NDC-43	145	Apr87	ORL	Dickens. NDG. SEE ORNL-6266.
^{243}Cm	Fiss.Yield	2.5-2		Expt	DOE-NDC-43	146	Apr87	ORL	Dickens. NDG. SEE PR/C 34,702.
^{244}Cm	Fiss.Yield	FAST		Expt	DOE-NDC-43	146	Apr87	ORL	Dickens. NDG. NSE. TBP.
^{244}Cm	Fiss.Yield	FAST		Expt	DOE-NDC-43	145	Apr87	ORL	Dickens. NDG. SEE ORNL-6266.
^{246}Cm	Fiss.Yield	FAST		Expt	DOE-NDC-43	146	Apr87	ORL	Dickens. NDG. NSE. TBP.
^{246}Cm	Fiss.Yield	FAST		Expt	DOE-NDC-43	145	Apr87	ORL	Dickens. NDG. SEE ORNL-6266.
^{248}Cm	Fiss.Yield	FAST		Expt	DOE-NDC-43	146	Apr87	ORL	Dickens. NDG. NSE. TBP.

NEUTRON DATA REFERENCES

Element	Quantity	Energy (eV) Min	Energy (eV) Max	Type	Documentation Ref	Page	Date	Lab	Comments
^{248}Cm	Fiss.Yield	FAST		Expt	DOE-NDC-43	145	Apr87	ORL	Dickens. NDG. SEE ORNL-6266.

ARGONNE NATIONAL LABORATORY

A. TOTAL AND SCATTERING CROSS-SECTION MEASUREMENTS

The fast-neutron total and scattering cross-section measurement program is directed toward achieving a fundamental understanding of physical processes, acquiring measured data and developing models useful for the provision of evaluations for applications, and determining basic nuclear properties which are essential for the analysis of directly-associated integral studies. Current emphasis is on the A = 50-60, 90 and 208 mass regions, and incident-neutron energies up to 10 MeV. The following titles refer to results of this program recently completed and/or nearing completion.

1. Neutron Total and Scattering Cross Sections of Beryllium
(A. Smith, P. Guenther and J. Whalen)

Neutron total cross sections have been measured from 1-15 MeV. Elastic- and inelastic-scattering cross sections have been measured from 4.5-10 MeV at incident-neutron energy intervals of approximately 0.5 MeV. The differential cross sections are determined at a minimum of 40 scattering angles distributed between 18-160 degrees. The inelastic excitation of the 2.43-MeV level is a prominent feature of the results. This beryllium study is a portion of a cooperative effort between ANL (measurements), LLNL (evaluation), Ohio University (analysis), and University of Illinois (integral test), which is a task force project established at the recent DOE fusion-data meeting.

2. Fast-Neutron Total and Scattering Cross Sections of Cobalt
(A. Smith, P. Guenther, J. Whalen and R. Lawson)

The work noted in the previous status report is now completed and a formal laboratory report is in press. The results are outlined in the following abstract submitted for the 1987 Spring APS Meeting:

"Energy-averaged total cross sections are measured from 0.5-12 MeV and elastic- and inelastic-scattering cross sections from 1.5-10 MeV, including the excitation of eleven levels in Co-59. The experimental results are interpreted in terms of spherical-optical-statistical and coupled-channels models. It is shown that the potential geometries are energy dependent, with a real-potential strength generally consistent with "global" representations and an imaginary strength that is relatively large and whose energy dependence is influenced by collective vibrational effects. The energy dependence of the real potential is almost completely due to the linking of real and imaginary potentials via the dispersion relation. Inelastically-scattered neutrons due to the excitation of the low-lying levels display angular distributions and cross-section magnitudes characteristic of collective vibrational reactions. Extrapolation of the potential to the bound-energy regime leads to binding energies of single-particle states in good agreement with experiment."

3. <u>Total, Scattering, and Gamma-Ray-Production Cross Sections for Few-MeV Neutrons on Fe-54</u>
(P. Guenther, D. Smith, A. Smith and J. Whalen)

This work, outlined in the previous report, has been formally completed and a manuscript accepted for publication in Annals of Nuclear Energy.

4. <u>Fast-Neutron Total and Scattering Cross Sections of Ni-58</u>
(A. Smith, P. Guenther, J. Whalen and R. Lawson)

The total cross section measurements have been completed to 12 MeV. Differential elastic- and inelastic-scattering results have been obtained at approximately 500-keV intervals from 4.5-10 MeV. At each incident energy the distributions contain 50-100 differential cross-section values. This information is combined with lower-energy results previously reported from this laboratory [1] to obtain a comprehensive data base extending from 1.4-10 MeV. These data are being interpreted using optical- and coupled-channels-models, with the objectives of obtaining physical understanding and a representation suitable for the evaluation cited elsewhere in this report. All of the data analysis will be completed in the near future.

1. C. Budtz-Jorgenson et al., Z. Phys. <u>A319</u>, 47 (1984).

5. <u>Neutron Total and Scattering Cross Sections of Yttrium</u>
(R. Lawson, P. Guenther, and A. Smith)

This work, cited in the prior report, has been published [1].

1. R. Lawson et al., Phys. Rev. <u>C34</u>, 1599 (1986).

6. <u>Elastic- and Inelastic-Scattering from Vanadium</u>
(M. Sugimoto*, A. Smith, P. Guenther and R. Lawson)

Measurements at 0.5-MeV intervals between 4-10 MeV are approaching completion. Combined with lower-energy data previously reported from this laboratory [1], these results provide a comprehensive data base from a few-hundred keV to 10 MeV. Optical-model and coupled-channels analyses are in progress, with the objectives of contributing to basic understanding and of providing of models essential to the associated on-going evaluation (see below).

---

* Visiting scientist from JAERI, Japan.

1. P. Guenther et al., Nucl. Sci. and Eng. 64, 733 (1977).

7. Fast-Neutron Scattering Cross Sections of Zirconium
(M. Sugimoto*, A. Smith, P. Guenther and R. Lawson)

An experimental study of the interaction of neutrons with energies up to 10 MeV with zirconium is nearing completion. The work includes neutron total and differential-scattering measurements, and it extends the investigation from the upper 4-MeV limit of that previously reported from this laboratory [1]. The measured results and associated interpretation are essential for the evaluation that is underway. That evaluation will contribute to the development of advanced fast-reactor systems (e.g., IFR).

---

* Visiting scientist from JAERI, Japan.

1. A. Smith and P. Guenther, ANL/NDM-69 (1982).

8. Neutron Elastic Scattering from Indium
(A. Smith, P. Guenther and R. Lawson)

Prior measurements in this group (to 4 MeV) [1] are being extended to 10 MeV in a search for the detailed behavior of the energy dependence of the optical potential well away from closed neutron or proton shells.

---

1. A. Smith et al., J. Phys. G11, 125 (1985).

9. Neutron Elastic Scattering From Bismuth
(A. Smith, P. Guenther, M. Sugimoto* and R. Lawson)

Detailed angular distributions resulting from the elastic scattering of fast neutrons from elemental bismuth have been measured at incident-energy intervals of appoximately 0.5 MeV from 4.5-10 MeV. Each angular distribution contains 40 to 100 differential values distributed in angle between approximately 15 and 160 degrees. These data were combined with lower-energy data previously reported from this laboratory [1,2], and with the lower-energy data of ref. 3, to obtain a detailed data base extending from a few-hundred keV to 10 MeV. This data base is being analyzed in terms of: i) a conventional optical-statistical model, and ii) a similar model extended to include the coupling between real and imaginary potentials prescribed by the dispersion relationship [4]. The preliminary results of this analysis indicate that: i) the real-potential radius slowly decreases with energy, ii) the imaginary diffuseness sharply increases with energy in a manner that extrapolates to a very small value at zero energy, iii) the imaginary-potential strength slowly increases with energy in an essentially linear manner, implying a small value at zero energy (i.e., a $J_W = (4\pi/A)\int W(r)\, r^2\, dr$ of approximately 30 MeV × fm³), and iv) the real strength (J_V) decreases with increasing energy in an approximately linear manner. Relatively small imaginary strengths have also been seen near N=50 [5,6], and they appear to be characteristic of nuclei near closed shells. Below approximately 2 MeV the volume integral of the real potential tends toward a constant (or perhaps even a slightly-decreasing value) as one approaches zero energy. This appears to be a manifestation of the Fermi surface anomoly suggested by theoretical considerations [7].

1. P. Guenther et al., Nucl. Sci. and Eng. 75, 69 (1980).
2. N. Olsson et al. Nucl. Phys. A385, 285 (1982).
3. E. Barnard et al., Nucl. Sci. and Eng. 41, 63 (1970).
4. G. Satchler, Direct Nuclear Reactions, Oxford, U.K.(1983).
5. A. Smith et al., Nucl. Phys. A455, 344 (1986).
6. R. Lawson et al., Phys. Rev. C34, 1599 (1986).
7. C. Mahaux and N. Ngo, Nucl. Phys. A378, 205 (1982).

10. Neutron Double-Differential Scattering
(P. Guenther and A. Smith)

The neutron double-differential scattering program continues with the objective of determining the energy dependence of level-density parameters. The incident energies extend from ≈ 5-10 MeV, in steps of ≈ 1 MeV. Particular attention is given to energies below the (n,2n) thresholds where interpretations are easier. All of the measurements are made relative to the well known Cf-252 prompt-fission-neutron spectrum, thus avoiding the complexities and uncertainties of independent detector calibrations. Measurements for niobium and yttrium are nearly complete, those for nickel and cobalt are well along, and measurements have been started in the heavy-mass region (e.g., bismuth and holmium). At present there is no clear experimental evidence for a significant precompound-emission component in either the energy spectra or angular distributions of emitted neutrons below 10 MeV. The compound-nucleus level-density parameters resulting from the measurements have an essentially linear energy dependence. More detailed analysis has been started using the code ALICE [1]. The results are being directly applied to the on-going evaluation activities cited below.

1. M. Blann, LLNL, private communication.

B. FISSION CROSS-SECTION MEASUREMENTS

1. Fission Cross Section Ratios at 14.7 MeV
(J. W. Meadows)

Measurements of the neutron-induced fission-cross-section ratios of nine isotopes relative to U-235 were completed at an average neutron energy of 14.74 MeV. Particular attention was paid to the determination of corrections and to sources of error. The error analysis was completed and the covariance matrix prepared. A report covering the experimental part of these measurements was prepared and an additional report covering the error analysis is in preparation. The experimental values for the nine ratios are: Th-230: 0.290 (± 1.9%); Th-232: 0.191 (± 1.9%); U-233: 1.132 (± 0.7%); U-234: 0.998 (± 1.0%); U-236: 0.791 (± 1.1%); U-238: 0.587 (± 1.1%); Np-237: 1.060 (± 1.4%); Pu-239: 1.152 (± 1.1)%; Pu-242: 0.967 (± 1.0%).

2. Integral Neutron-fission Cross-section-ratio Measurements in the Thick-target Be-9(d,n)B-10 Spectrum at 7-MeV Deuteron Energy
(J. W. Meadows, D. L. Smith and Y. Watanabe*)

Integral neutron-fission cross-section ratios have been measured to 1.4-2.5% accuracies for Th-232:U-235, Np-237:U-235, U-238:U-235, Np-237:U-238, Th-232:Np-237, U-236:U-235, Pu-239:U-235, U-233:U-235, U-234:U-235, U-234:U-238 and U-236:U-238 in the neutron spectrum produced by 7-MeV deuteron bombardment of a thick beryllium-metal target. These data will be used for two purposes: i) to test the ENDF/B-V evaluations in the few-MeV energy range, and ii) to test the contemporary representation of the beryllium neutron spectrum (which is based on direct time-of-flight measurements).

*Permanent address: Department of Nuclear Engineering, Kyushu University, Fukuoka, Japan.

C. ACTIVATION CROSS-SECTION MEASUREMENTS

1. The Co-59(n,α)Mn-56 Reaction
(J. W. Meadows and D. L. Smith)

The cross section for the Co-59(n,α)Mn-56 reaction was measured relative to the U-238 fission cross section from about 5 to 10 MeV neutron energy. Total errors, including the fission cross sections, were 5 to 6% except at the lowest energies where the counting statistics were less suitable. These data will be used in conjunction with prior experimental information and model calculations to produce a new evaluation for this reaction.

2. Neutron-activation Cross-section Measurements at 14.7 MeV
(J. W. Meadows, D. L. Smith, M. M. Bretscher and S. A. Cox)

Work on this project is now complete. Final cross-section values for 21 distinct reactions have been obtained. A complete covariance representation for the uncertainties in this data set has been developed. Comparisons were made, where relevant, to the results of a recent evaluation from this laboratory [1]. A paper on this work has been accepted for publication by the journal Annals of Nuclear Energy.

1. B. P. Evain, D. L. Smith and P. Lucchese, ANL/NDM-89 (1985).

3. Integral Activation-cross-section Measurements in the Thick-target Be-9(d,n)B-10 Spectrum at 7-MeV Deuteron Energy
(D. L. Smith, L. R. Greenwood and J. W. Meadows)

Data have been acquired and analysis is nearly complete for the following reactions: Fe-54(n,p)Mn-54, Fe-54(n,α)Cr-51, Fe(n,X)Mn-56, Ni-58(n,p)Co-58, Ni(n,X)Co-60, Aℓ-27(n,α)Na-24, Ti(n,X)Sc-46, Ti(n,X)Sc-47, Ti(n,X)Sc-48, Cu-65(n,p)Ni-65, Cu-63(n,α)Co-60, Cu-65(n,α)Co-62, Nb-93(n,2n)Nb-92m, Nb-93(n,α)Y-90m, Co-59(n,p)Fe-59, Co-59(n,2n)Co-58, Co-59(n,α)Mn-56, Zn-64(n,p)Cu-64, In-115(n,n')In-115m, In-115(n,p)Cd-115 and In-113(n,n')In-113m. These data will be used for two purposes: i) to test existing differential information (particularly ENDF/B-V evaluations) in the MeV-energy range, and ii) to test and possibly adjust the contemporary representation of the beryllium neutron spectrum (which is based on direct time-of-flight measurements).

4. Neutron Production of Long-Lived Isotopes near 14.8 MeV
(L. R. Greenwood and D. L. Bowers)

Recent research has focussed on the measurement of production rates for long-lived isotopes in fusion materials. Such data are needed for the determination of fusion-waste activities as well as for fusion-reactor dosimetry. Table I lists some of the reactions which we have measured. These measurements were performed by irradiating pure elements and separated isotopes at the Rotating Target Neutron Source II at Lawrence Livermore

National Laboratory (14.8 MeV). Chemical ion-exchange separations were performed to remove undesired activities, then the long-lived activities were measured using gamma spectroscopy, liquid scintillation counting, and accelerator mass spectrometry. These data can be directly applied in fusion-reactor design studies. As an example, using the STARFIRE design (22 MW-yr/m^2), our data for Mo would predict 75 μCi/g of 2.03(4)-yr Nb-94 and 12 mCi/g of 700-yr Nb-91, both of which are about 30% lower than previous estimates [1]. Other measurements in progress include reactions leading to 5730-yr C-14, 1.5(6)-yr Zr-93, 3.2(7)-yr Nb-92 and 3500-yr Mo-93.

Table I: Production of Long-Lived Isotopes near 14.8 MeV

Reaction	Half-life,y	Cross Section,mb
Fe-56(n,2n)Fe-55	2.7	454 ± 35
Ni-60(n,2n)Ni-59	7.5(4)	≈ 150
Ni-64(n,2n)Ni-63	100	953 ± 67
Cu-63(n,p)Ni-63	100	54 ± 4
Mo-94(n,p)Nb-94	2.0(4)	53 ± 5
Mo-95(n,x)Nb-94	2.0(4)	17 ± 2
Mo-92(n,x)Nb-91	700	≈ 300

1. L. R. Greenwood, D. G. Doran, and H. L. Heinisch, Phys. Rev. 34C, 1987 (in press).

5. Thermal-Neutron Helium Production from Fe-55
(L. R. Greenwood)

We have recently discovered that the isotope Fe-55 has a thermal-neutron helium-production cross section. Analyses of nine iron samples, irradiated to varying neutron fluences up to 2.0(23) n/cm-2 in the High Flux Isotopes Reactor at Oak Ridge National Laboratory, consistently show more helium than would be predicted from fast-neutron (n,α) reactions. Helium measurements were performed in collaboration with Dennis Kneff of Rockwell International (Canoga Park, CA), and neutron dosimetry was included with each sample to precisely determine the neutron fluence [1]. Anufriev reported a total absorption cross section for Fe-55 of less than 170 barns [2]. We are able to obtain excellent fits to our data if the Fe-55(n,α) thermal cross section is about 13-40 mb and the total absorption cross section is less than 50 barns. Additional helium and iron isotope mass spectrometry measurements now in progress should determine the thermal helium and total absorption cross sections more accurately. This reaction could be quite useful for fusion materials testing since it would allow us to obtain fusion-like helium production rates in iron or ferritic alloys irradiated in mixed-spectrum reactors. Helium measurements were also reported for Ni, Ti, Nb, Cr, and Cu in HFIR [1], and for 25 elements at 14.8

MeV [3]. The HFIR data for Ni, Fe, Cr, and Cu show good agreement with the Gas Production Files in ENDF/B-V, if we include thermal-neutron effects for Ni, Fe, and Cu. However, there are large discrepancies for Ti (230%) and Nb (30%). Further measurements are in progress.

---

1. D. W. Kneff, L. R. Greenwood, B. M. Oliver, and R. P. Skowronski, Helium Production in HFIR-Irradiated Pure Elements, Second Intl. Conf. on Fusion Reactor Materials, Chicago, April 13-17, 1986 (in press).
2. A. Anufriev, Fifth All-Union Conf. on Neutron Physics, Kiev, p. 161, Sept. 1980.
3. D. W. Kneff, B. M. Oliver, H. Farrar IV, and L. R. Greenwood, Nucl. Sci. Eng. 92, 491 (1986).

D. NEUTRON-SPECTRUM MEASUREMENTS

1. Ratio of the Prompt-Fission Neutron Spectrum of Pu-239 to that of U-235

(M. Sugimoto*, A. Smith and P. Guenther)

The prompt-fission neutron spectrum resulting from Pu-239 fission induced by ≈ 0.55-MeV incident neutrons was measured from 1-10 MeV relative to that of U-235 fission induced by the same incident-energy neutrons. Energy-dependent ratios of the two spectra were deduced from the measured values. The experimentally-derived ratio results were compared with those calculated from ENDF/B-V, revision-2, and the results of recent microscopic measurements. Using the ENDF/B-V U-235 Watt parameters to describe the U-235 spectrum, the experimental results imply a ratio of average fission-spectrum energy of Pu-239 to U-235 of 1.045 ± 0.003, compared to the value 1.046 calculated from ENDF/B-V, revision-2. The details of the work are available in a laboratory report [1].

---

* Visiting scientist from JAERI, Japan.

1. M. Sugimoto et al., ANL/NDM-96 (1986).

2. The Thick Target Neutron Emission Spectrum for Be-9(d,n)B-10 at 7-MeV Deuteron Energy

(D. L. Smith and J. W. Meadows)

The thick-target neutron spectrum from the beryllium (d,n) reaction promises to be a very useful high-intensity neutron source for integral measurements. However the shape of the spectrum is not known to the required accuracy. We have measured the spectrum at 7-MeV deuteron energy and zero-deg. emission angle, with emphasis on the lower-energy region. The source was contained in the recently-constructed shielded irradiation cavity

[1], and time-of-flight measurements were made over a 2.6-meter flight path using a U-235 fission detector. The resulting energy spectrum rises rapidly from about 0.2 MeV to about 0.8 MeV. At higher energies it is in fair agreement with the results of Crametz et al. [2].

---

1. D. L. Smith and J. W. Meadows, ANL/NDM-95, (1986).
2. A. Crametz, H. -H. Knitter and D. L. Smith, Nuclear Data for Science and Technology, edited by K. H. Bockhoff, D. Reidel Publishing Company, Dordrecht, Holland (1983), p. 902.

E. INTEGRAL DATA-TESTING MEASUREMENTS

1. Integral Testing for Beryllium and Niobium
(A. Smith and B. Micklich*)

Integral tests of evaluated data using time-of-flight measurement techniques to determine the neutron leakage spectra from solid spherical samples resulting from a burst of Be(d,n) (7-MeV deuterons) neutrons at their centers is continuing. Initial results have been obtained using a beryllium sphere several mean-free-paths thick. The results are compared with the results of Monte-Carlo calculations carried out by University of Illinois personnel on the MFE-LLNL Cray computer. There is qualitative agreement between observation and calculation, but there remain quantitative differences, some of which appear to be of an experimental origin. In particular, attention must be given to the details of the source spectrum and to instrumental perturbations. Both problems are being addressed, and the measurements are being repeated with improved accuracy. Concurrently, a niobium sphere of approximately 25-cm diameter is being prepared for similar studies, and the program plans extend to a number of other materials. The objective remains the integral testing of evaluated data files, particularly those resulting from this laboratory's microscopic measurement and evaluation program.

---

*University of Illinois, Urbana.

F. NUCLEAR-DATA EVALUATION ACTIVITIES

The program as a whole is a coordinated microscopic measurement and interpretation, evaluation, and integral-test effort. Evaluations currently in progress and nearing completion are cited below. All evaluations are submitted for consideration as a part of ENDF/B-VI.

1. <u>Vanadium</u>
(A. Smith, D. Smith, B. Micklich* and R. Howerton**)

The data base has been assembled, the necessary microscopic measurements and models are nearing completion, and parts of the evaluation are complete and documented (e.g., the total cross section). The major components yet to be completed are among the reaction cross sections.

---

* University of Illinois, Urbana.
**Lawrence Livermore National Laboratory.

2. <u>Cobalt</u>
(A. Smith, D. Smith, M. Sugimoto* and R. Howerton**)

The necessary microscopic measurements and models have been assembled and a comprehensive data base established. Portions of the evaluation are complete. We are particularly indebted to J. A. Harvey (ORNL) for undertaking and completing the total-cross-section measurements needed to fill a void in the required data base.

---

* Visiting scientist from JAERI, Japan.
**Lawrence Livermore National Laboratory.

3. <u>Nickel-58</u>
(A. Smith, D. Smith and R. Howerton*)

As cited above, microscopic measurements requisite to this evaluation are nearing completion and the data base is being established. This particular evaluation (unlike the preceding ones) will be limited to the unresolved resonance region and above.

---

*Lawrence Livermore National Laboratory.

4. <u>Compilation of Recent Data for the Li-7(n,n't)He-4 Reaction</u>
(D. L. Smith)

On the recommendation of a task force group convened at a recent fusion nuclear data meeting [1] all experimental data for the Li-7(n,n't)He-4 reaction which have become available since ~ 1981 have been compiled and carefully examined. A complete covariance matrix has been developed for each data set, based on the information available in the literature or through private communications. This compiled information has been transmitted to Los Alamos National Laboratory where it will be used in the conduct of a formal evaluation of this reaction for ENDF/B-VI.

---

1. Fifth coordination meeting of the Office of Basic Energy Sciences Program to Meet High Priority Nuclear Data Needs of the Office of Fusion Energy, held at Argonne National Laboratory, Argonne, Illinois, September 17-19, 1986.

5. Evaluated Data for the Development of Space-Power Sources
(A. Smith, D. Smith, J. Meadows and P. Guenther)

The suitability of available evaluated data for the development of high-temperature space-power sources was reviewed. Twenty-five materials were cited as being of interest by the system designers. Evaluated data for eleven of these were judged suitable for this particular use. Twelve of the files were judged to have shortcomings ranging from minor problems to serious concerns. Two files were judged to be so poor as to make quantitative prediction of system neutronic performance doubtful. Re-evaluation was very desirable in ten cases and desirable in four more. Basic measurement shortcomings were identified in fourteen cases, 70% of which were judged to be serious.

Predictably, those materials widely employed in conventional fast-reactor systems and/or extensively studied for standards or fundamental physics reasons are relatively well known. The problems are largely centered in the unusual materials that have received little attention for many years. An informal report of this survey is available.

G. NUCLEAR THEORY AND MODEL-CODE DEVELOPMENT

1. Spherical Optical-Model Fitting of Vibrational Nuclei
(R. Lawson, A. Smith and M. Sugimoto*)

It is common to use the spherical optical model to describe processes in nuclei that are obviously vibrational. The resulting effect on the conventional spherical parameters was examined using pseudo data. The results are summarized in the following abstract submitted for the winter APS meeting:

"We generated pseudo-data for neutron scattering from Ni-60 (assumed to be a vibrator), using the coupled-channels code ANLECIS. Zero, one and two phonon states were coupled with a $\beta = 0.25$. Shape-elastic and total cross sections, generated at various energies using conventional optical-model parameters, were then fitted using the spherical code ABAREX. Fits were obtained comparable to those for real nuclear data, and the fitted parameters varied smoothly with energy. The real potential was similar to that used in generating the pseudo-data. However, the imaginary potential resulting from the fitting was changed as follows: a) the radius was 6% smaller than that of the deformed well, and b) the volume integral decreased with increasing energy in contrast to the original deformed well where dJ_w/dE was greater than zero. Similar trends were in evidence in the analysis of the real Co-59 neutron-scattering data cited above."

---

* Visiting scientist from JAERI, Japan.

2. Neutron Scattering on Nuclei Near A=60 and A=90
(R. D. Lawson and A. B. Smith)

An invited paper with this title was presented at the first CRP Meeting on Methods for the Calculation of Fast Neutron Nuclear Data for Structural Materials. This meeting was held in Bologna, Italy, October 7-10, 1986, under the auspices of the IAEA. The paper deals with the optical-model parameters needed to fit neutron-scattering data in the energy region 4.5 to 10 MeV. The abstract of the paper reads as follows:

"Over a wide range of incident energies, the total cross section and angular distributions for elastic scattering of neutrons from nuclei in these mass regions are analyzed using the spherical-optical-statistical model. The effect of a real-surface-peaked potential, predicted by dispersion relations, is considered. It is found that when the data on a given nucleus between 4.5 and 10 MeV, are analyzed simultaneously one obtains a smooth energy variation of the optical-model parameters. Moreover, this parameterization may be used to predict, quite accurately, at least the total cross sections up to 20 MeV. The parameters characterizing the model are quite different in the two mass regions. However, a comparison of the optical model results for Y-89 and Nb-93 indicates that near A=90 the real-well parameters are nearly the same for the two nuclei, and that the volume integrals of the imaginary potentials are similar."

3. ABAREX
(R. D. Lawson)

Over the past two years many changes and additions have been made to the spherical-optical-statistical model code ABAREX. A new documentation of this program is now being made.

H. METHODS OF ANALYSIS IN NUCLEAR-DATA RESEARCH

1. Probability Theory in Nuclear-Data Research
(D. L. Smith)

An elementary guide to the basic concepts of probability, with emphasis on its role in nuclear-data research, has been written. Typing of the manuscript is nearly complete. This document will be issued as laboratory report (ANL/NDM-92) when the work is done. Meanwhile, work has commenced on a sequel volume dealing with more advanced properties of probability functions, and on errors. The material for this treatise has been compiled and organized, and writing is in progress.

2. Generation of Covariances for Experimental Data Sets
(D. L. Smith)

A careful examination has been made of methodology associated the generation of covariance information for an experimental data set, with particular emphasis on the type of data produced at this laboratory. It was concluded that determination of the magnitudes of various error sources which contribute to the total error is less problematic than estimation of the detailed (micro) correlations between specific error sources which are applicable to several elements of the set. However, it has also been determined that when the total error is comprised of a number of distinct components, the uncertainty concerning correlations between total errors (macro) can be substantially smaller than that involved in the estimation of individual micro correlations, primarily due to the effect of the law of large numbers from mathematical statistics. This effect has been investigated through simulation exercises as well as the examination of several real data sets from this laboratory. The results of this work were reported at a conference [1], and a paper has been submitted for journal publication.

---

1. D. L. Smith, J. W. Meadows and Y. Watanabe*, "Covariances for Measured Activation and Fission Ratios Data", IAEA Specialists' Meeting on Covariance Methods and Practices in the Field of Nuclear Data, Rome, Italy, 17-19 November 1986.

* Permanent address: Department of Nuclear Engineering, Kyushu University, Fukuoka, Japan.

3. Covariance Matrices for Collapsed Data Sets
(D. L. Smith)

A method has been developed for generating the covariance matrix of a set of experimental nuclear data which has been collapsed in size by the averaging of equivalent data points belonging to a larger parent set. The method resembles the NJOY procedures employed by Muir and McFarlane [1] for group-cross-section transformations, but there are significant differences because the mathematical problems themselves are quite different. Here it is assumed that the data values and covariance matrix for the parent set are provided. The collapsed set is obtained by a proper weighted-averaging procedure based on the method of least squares. It is then shown by means of the law of error propagation that the elements of the covariance matrix for the collapsed set are linear combinations of elements from the parent set covariance matrix. The coefficients appearing in these combinations are binary products of the same coefficients which appear as weighting factors in the data-collapsing procedure. A paper on this investigation has been submitted for journal publication.

---

1. D. W. Muir and R. E. McFarlane, LA-9303-M, Vol. IV, Los Alamos National Laboratory (1985).

1. BROOKHAVEN NATIONAL LABORATORY

The reactor-based neutron-nuclear physics research at BNL is composed of three categories: the study of nuclear structure with the (n,γ) reaction, the (n,γ) reaction mechanism and its application to pure and applied physics, and the spectroscopy of neutron-rich, fission product nuclides. These programs use the H-1 and H-2 beam ports of the HFBR. The tailored beam facility produces beams of thermal, 2- and 24-keV neutrons. A monochromator is used for resonance neutron studies. The TRISTAN on-line mass separator is used with a U-235 target to produce fission product nuclei. These facilities are operated in collaboration with a wide variety of collaborators from national laboratories and universities. In the following sections the complete program is outlined, and those sections of relevance to nuclear energy and other applications are described in detail.

A. NUCLEAR STRUCTURE WITH THE (n,γ) REACTION

The H-1 beam tube at the HFBR provides two beams used almost entirely for neutron capture γ-ray studies. These include the tailored beam facility, which provides beams of thermal, 2 and 24 keV neutrons, and the neutron monochromator, which provides thermal and energy-selected beams up to about 25 eV. These wide ranging beams provide a unique method of nuclear structure investigation due to the primarily nonselective character of the (n,γ) reaction. Indeed, in appropriate cases, all levels of a given spin-parity range in the final nucleus may be about equally populated without regard to the structure of the final state wave functions. This is primarily achieved with the use of the tailored beams, which provide resonance averaging of the primary transitions, and which are absolutely indispensable in the construction of level schemes. The primary transitions unambiguously disclose level positions, which can only be done indirectly from secondary transitions by the inferential application of the Ritz Combination Principle. The secondary transitions, however, are themselves of crucial importance for the information they provide on the electromagnetic matrix elements connecting low lying levels and, thereby, on the applicability of different nuclear models.

1. Background: The N_pN_n Scheme

Last year a proposal was made for a new parameterization of nuclear data. Called the N_pN_n scheme, it appears to be highly successful both in correlating the data within a given mass region and in relating different regions. Moreover, it has a simple microscopic basis. The idea has developed numerous offshoots and ramifications including such concepts as N_pN_n multiplets, radically simplified collective model calculations, a new approach to the study of evolving subshell structure, the relation of intruder states to deformation, and the prediction of properties of unknown nuclei far off stability.

The p-n interaction is the principal non-pairing residual interaction in nuclei that determines the evolution and development of collectivity. This has been known for decades and, indeed, is the basis behind the pioneering work of Talmi and of Federman and Pittel in explaining the origin of configuration mixing and nuclear deformation. Despite this well-recognized situation, there has been little systematic effort to exploit this idea to understand and interpret the evolution of nuclear structure as a function of A, N, and Z. The N_pN_n scheme, however, is explicitly based on the p-n interaction among valence nucleons. In it, nuclear observables are plotted, not against A, N, or Z, in terms of which they are complicated multi-dimensional functions, but rather against the product N_pN_n of the number of valence protons times the number of valence neutrons. This product approximates the total integrated proton-neutron interaction strength. It was shown that this scheme led to an enormous simplification of the systematics--each observable now follows a single smooth universal curve for a given region.

Moreover, in the N_pN_n scheme, different transitional regions, long thought to be highly diverse in character and systematics now appear nearly identical. They display nearly the same rate of evolution when measured in units of N_pN_n. This offers the hope, for the first time, of a truly unified understanding of the structure and evolution of heavy nuclei. In turn, of course, this greatly enhances the possibilities for predicting and studying the structure of unknown nuclei far off stability.

2. F-spin and N_pN_n Multiplets

Last year the concepts of F-spin and N_pN_n multiplets were described. Briefly, the former consists of a set of nuclei with the same total valence nucleon number (N_p+N_n), or F-spin (for the lowest levels, at least) but different values of N_p-N_n), that is, of the Z component, F_0, of F-spin. If the nuclear Hamiltonian is F-spin invariant and if F-spin is a good quantum value, then the energy levels of such a multiplet should be constant.

On the other hand, the N_pN_n scheme suggests that nuclei with the same value of the product N_pN_n should be similar. Empirically, the latter scheme works much better. The energy level structure of members of an F-spin multiplet are only constant to the extent that they have similar N_pN_n values.

This year, this relationship was further probed in collaboration with A. Jain of the University of Roorkee, India. A construction was developed, involving reflection about an isobaric mass line (A=164 for the rare earth nuclei) in which nuclei lying along a line perpendicular to this axis belong to an F-spin multiplet while pairs of nuclei systematically placed with respect to this axis have the same N_pN_n value. This combination allows one to select 9 pairs of rare earth nuclei as N_pN_n couplets in which their level schemes, even for such widely spaced pairs as ^{156}Dy and

^{172}W, are nearly identical. Secondly, it allows one to see easily the influence of N_pN_n along an F-spin multiplet and to predict exactly where the structure of the latter will begin to deteriorate.

3. Attempted Description of an Entire Shell with Constant IBA-2 Parameters

It was shown last year that the N_pN_n scheme allows the simplification of collective model calculations for extended sequences of nuclei. Since most observables are smooth functions of N_pN_n, an enormous reduction in the number of parameters can be achieved if they are written as functions of N_pN_n. This was illustrated with IBA-1 calculations for 100 nuclei in terms of only 6 constants. Moreover, since IBA-1 parameters can be written in terms of IBA-2 parameters, multiplied by functions of N_pN_n, it was thought that, perhaps, the required variations in IBA-1 parameters could be achieved by using constant IBA-2 parameters. Calculations in FY 1986 showed that this was not the case. Constant IBA-2 parameters could not reproduce a sufficient variation in collective properties in transition regions to match the data. However, an interesting result did emerge, namely that although the constant parameter IBA-2 calculations did not reproduce the data, they did display a nearly perfect N_pN_n dependence of most collective observables, with the exception of the 2^+_γ level whose systematics split into several branches according to the value of F_{max}.

4. The Extrapolation-interpolation Inversion in N_pN_n: Nuclei Far Off Stability

The N_pN_n scheme has numerous ramifications. One of particular importance relates to nuclei far off stability and therefore to the TRISTAN research program. The smoothness of the systematics for an observable in N_pN_n obviously aids in extrapolating to unknown nuclei. Secondly, the similarity of curves for different regions allows one region to serve as a paradigm for another, a procedure totally unusable in normal plots. Thirdly, and most importantly, the N_pN_n scheme frequently converts the process of extrapolation into one of interpolation with its attendent greater reliability. A nucleus far off stability but with a very unequal number of valence nucleons of each type will have a lower N_pN_n product than other nuclei, closer to stability (compare the unknown nucleus ^{148}Ba (Z=56, N=92), N_pN_n=60 with the known nucleus ^{154}Sm (Z=62, N=92), N_pN_n=120). During FY 1986 this idea was developed into detailed predictions for about 50 unknown neutron rich nuclei in the A=160-180 region. Many of these are of r-process interest as well and the testing and use of these predictions may help eliminate some of the uncertainties in the nuclear input parameters for r-process calculations.

5. <u>The P-Factor: A Universal Description of Collectivity in Heavy Nuclei</u>

Comparison of N_pN_n plots for different regions shows similar systematics but different displacements in the values of N_pN_n at which corresponding changes occur. The curves are congruent but not identical. This means that the absolute value of N_pN_n is of less significance than relative values. Unfortunately, it also implies that one cannot predict, a priori, the structure in a given region from the N_pN_n values alone. During FY 1987, work began on a related and much improved parameterization, in terms of the P-factor, defined as the normalized N_pN_n value, $P=N_pN_n/(N_p+N_n)$. P can be viewed as the <u>average number of interactions of each valence proton or neutron with those of the othertype</u>. It is also related to the relative strengths of the p-n and like-nucleon pairing interactions. It has been found that P-plots are significantly coalesced relative to N_pN_n plots and that deformation tends to set in universally when P reaches $P\approx 4$-5, independent of region. This provides a unified interpretation of all nuclear transition regions above A=80 as well as rules for the onset of deformation. Work on this is continuing and appears very promising.

6. <u>Nuclear Masses</u>

A study of nuclear masses in the N_pN_n and P-factor schemes has been initiated. Preliminary results suggest that when semi-empirical microscopic masses (i.e., empirical masses minus a spherical liquid drop component) are plotted against P, a remarkable linearization occurs for a given element or isotonic series. This seems to allow predictions of unknown masses to much greater reliability than heretofore possible. Work is continuing on this project.

7. <u>High Precision Spectroscopy in Well Deformed Nuclei: ^{162,164}Dy</u>

The combination of ARC studies at BNL with the high precision γ and β spectrometers at the ILL, Grenoble, provides data of unrivaled quality and extent, with the added bonus in many cases of a guarantee that all states within certain spin and excitation ranges will be populated. The best example to date of the application of these techniques was the case of ^{168}Er, which raised a host of new questions concerning the structure of deformed nuclei, as well as illuminating many aspects of the IBA. Two further studies of comparable scope have therefore been launched for ^{162,164}Dy. The ARC data is already published for both, while the ILL γ and β spectrometer measurements have been completed and the analysis of the former has been completed at BNL. The analysis of the conversion electron data is currently being finished at the ILL and in FY 1987 it should be possible to combine the two data sets to construct the final level schemes. These results should then allow many of the questions raised by the ^{168}Er study to be pursued, and provide further detailed tests of our understanding of the structure of well deformed nuclei.

8. The CQF for Odd Nuclei and Studies of Nuclei in the W-Os Region

The Consistent Q Formalism (CQF) has proved to be a particularly attractive starting point in the description of the collective structure of a broad range of even-even nuclei, with the framework of the Interacting Boson Model (IBM). The method is predicated on maintaining a consistent form for the IBM boson quadrupole operator in both the Hamiltonian and in the description of E2 transitions, and leads to a number of essentially parameter-free predictions for relative energies and B(E2) values across a wide region of nuclei. An equivalent approach for the boson-fermion Hamiltonian was achieved by recognizing that the pseudo-orbital angular momentum decomposition inherent in the various U(6/12) group chains allows the fermion generators to be split into components involving $(\ell,\ell')=(0,2)$ and (2,2), analogous to the s,d boson space. Thus the structure of the fermion quadrupole operator can be defined by the same parameter χ as used in the boson case, and then the wave functions and E2 operators are uniquely determined. It is then possible to predict the changes in relative energies, B(E2) values and single particle structure factors across the region from SU(3) (^{185}W) to O(6) (^{195}Pt) simply by varying χ between the values which generate these two symmetries.

Following the development of the CQF approach in the Interacting Boson-Fermion Model (IBFM) framework to describe the odd-N W-Pt region, an extensive set of (n,γ) studies has been undertaken on the odd-A, W, and Os nuclei. ARC measurements at neutron energies of 2 and 24 keV have been completed for all the nuclei. For ^{187}W, BILL and GAMS data from the ILL have also been obtained and an extensive level scheme has been constructed, which it should now be possible to interpret in some detail. A series of singles, coincidence, and angular correlation studies with Ge detectors have also been performed on ^{189}Os, using the neutron monochromator beam, and an the analysis of these data is now complete. Finally, new GAMS and BILL data on ^{191}Os are currently being obtained. The data, including existing single nucleon transfer results, for ^{189}Os has already been compared with the predictions of the CQF for odd nuclei. With the exception of the 216 keV level the agreement is rather good. This level was previously assigned $J^{\pi}=7/2^-$ and thought to be the 7/2, $7/2^-[503]$ bandhead. The new γ-γ angular correlation data shows that this J^{π} value is less than 0.19% probable. Since this level is not observed in ARC, it cannot be $1/2^-$ or $3/2^-$. The only remaining possibility, consistent with all the data, is $5/2^-$. This level cannot then be a single quasi-particle excitation but must correspond to coupling with some collective excitation of the core. This level then still presents an enigma for existing theoretical descriptions. The calculations will be extended to the other nuclei in this region when the experimental studies are completed. The results so far are the first test of the CQF for odd-mass nuclei and argue well for further tests of this scheme.

9. Tests of Extended Quartet-SUSY Schemes in ^{198}Au and ^{76}As

Recent theoretical work has postulated the existence of "supersymmetric quartets" of nuclei, consisting of an even-even, odd-neutron, odd-proton, and an odd-odd nucleus, in which all boson members are described by the same Hamiltonian. The crucial extension to earlier work centers on the odd-odd nucleus, since the claim is that, having fit the Hamiltonian to the appropriate even-even nucleus, the structure of the odd-odd nucleus can then be predicted without further parameterization. Two experimental investigations have been carried out to test these predictions. ARC data at 2 and 24 keV neutron energies have been taken and analyzed for ^{76}As and ^{198}Au. In addition, curved crystal spectrometer measurements have been completed for ^{76}As and are currently being analyzed. In the case of ^{198}Au the data are already sufficient to provide a sensitive test of the proposed quartet-SUSY scheme. The comparison with the predictions shows a 1-1 correspondence of low lying levels up to ≈600 keV but little if any detailed agreement in level patterns. It appears that the scheme, which combines a U(6/12) space for the neutron space, and U(6/4) for the protons, has approximately the correct single particle levels since the predicted density of states is reasonable. The omission of the $s_{1/2\pi}$ orbit seems not to be serious: large amplitudes for this single particle state probably occur above 600 keV. Of course, the O(6) core description is also appropriate. Therefore, one concludes that the disagreements are related to the specific core-particle interactions implied by the use of a Hamiltonian satisfying the SUSY. Although this particular extended SUSY description is inadequate the idea of quartet SUSY's may then still be useful in giving a starting point for numerical calculations.

10. ^{231}Th

A multi-laboratory study of ^{231}Th including (n,γ) data (ARC, GAMS, BILL) and (d,p) data has been completed and an extensive paper submitted. From these data, 70 excited levels in ^{231}Th were identified and, of these, 57 were placed in 18 rotational bands with assigned configurations. All expected Nilsson states below 750 keV have been identified; new configurations include $5/2^+[622]$, $7/2^+[624]$, $3/2^-[761]$, $1/2^-[770]$, $1/2^+[640]$, and $5/2^-[503]$. Several vibrational states have been identified; a special feature of these is the observation of greater fragmentation of single particle-0^+ mixed states than expected theoretically. Assuming degenerate parity doublets indicate the existence of stable octupole deformation, no evidence was found for a tendency toward this phenomenon in ^{231}Th. The neutron binding energy was determined to be 5118.13 ± 0.20 keV.

11. Collective M-1 Strength in ^{106}Pd

Over the past decade much attention has been focussed on searching for collective M-1 strength in nuclei. The giant M-1 resonance is known to be severely fragmented, or dissolved, into many fine structure states. This has made it difficult to ascertain the total strength. Resonance averaging allows the identification of M-1 strength in many nuclides in a rather unambiguous manner. Evidence for a collective giant resonance has been obtained for ^{106}Pd, where the large neutron binding energy of 9.6 MeV allows the examination of M-1 transitions over an energy range of almost 4 MeV. This collective strength amounts to about 150 units of μ^2-MeV, which is in good agreement with shell model calculations in this mass region.

12. Search for a Pygmy Resonance in ^{198}Au

Some years ago, Bartholomew proposed the existence of a doorway-state "pygmy resonance" located near 5 MeV. The resonance was ascribed to transitions across neighboring shells connecting components of the 2p-1h states of the doorways in neutron capture reactions. Evidence for the effects comes largely from (d,p) reactions and fast neutron capture, and the evidence has been ambiguous, at best. Efforts have been made to identify this "pygmy resonance" using resonance-averaging techniques. The ability of resonance averaging to isolate the E-1, M-1, and E-2 components give a new angle of attack on this problem. The $^{197}Au(n,\gamma)^{198}Au$ reaction has been studied at 2 and 24 keV neutron transmissions filters and analysis of the data are in progress.

13. Study of Photon Strength Functions and Brink's Hypothesis

A survey of electric dipole strength functions has been initiated with the aim of determining the validity of Brink's Hypothesis (also known as the Brink-Axel Hypothesis) in the low energy limit, $\omega \to 0$, where ω is the dipole oscillator frequency. The Brink Hypothesis is the assumption that the dipole oscillator is independent of nuclear structure and that a giant dipole resonance can be built on each excited state. This topic has received considerable attention in the high energy limit, where $\omega \geq \omega_R$, or the region at and above the giant dipole resonance. There has, however, been little work done with the low energy primary γ rays because of experimental limitations on the identification of soft E-1 γ rays. The use of the technique of resonance averaging has been extended to excitation energies of up to $\approx$3 MeV in the product nucleus, and this has allowed the study of photon strengths over a range of several MeV. Resonance averaging allows the separation of E-1, M-1, and E-2 strengths. The Lorentzian function describing the photoexcitation is known to fail as $\omega \to 0$, and alternate expressions have been developed. These alternate expressions are successful in predicting the total radiative widths of neutron resonances. This old problem, for whose solution Brink first proposed the concept of a giant resonance built on each excited state, may now be considered as solved.

14. Resonance Averaging in $^{173}Yb(n,\gamma)^{174}Yb$

Several years ago, highly correlated transitions were reported by groups at the Joint Institute for Nuclear Research (JINR), Dubna, for resonances of ^{173}Yb. It was suggested that resonance averaging at 2 and 24 keV be used to obtain averaged strengths for the transitions in question, so that their statistical behavior at higher neutron energies could be examined. These studies are currently under way. Preliminary data show some evidence for an enhanced strength for these transitions, and this enhancement could be interpreted in terms of a K-selection rule. This would indeed be surprising, since it has long been assumed that the K-quantum number is not valid at an excitation of 7-8 MeV. Additional data of high statistical quality are being collected so that a firm statement about these transition strengths can be made.

B. EXPERIMENTAL AND THEORETICAL STUDIES IN THE IBA

1. A New Analytic Expression for B(E2) Values in the IBA

In using g factors and B(E2) values to extract effective N_p and N_n values, it is necessary to have analytic formulas relating the empirical observables to N_p and N_n. For magnetic properties these expressions, containing matrix elements of the angular momentum operator, are essentially structure independent. For B(E2) values this is not the case and, heretofore, analytic expressions were available only in the three limiting symmetries of the IBA. This limitation effectively excludes nearly all deformed rare earth nuclei and, indeed, most others as well. We have developed a new approximate analytic expression, which describes B(E2) values for almost all deformed nuclei. It is accurate to about ±10% and is given by

$$B(E2{:}2^+_1 \to 0^+_1) = \frac{1}{2}\, e_B^2\, (1-0.1\chi)(N+1) \qquad \text{IBA-1}$$

$$= \frac{1}{2}\,(1-0.1\chi)\left(\frac{N+1}{N}\right)(e_\pi N_\pi + e_\nu N_\nu)^2 \qquad \text{IBA-2}$$

where e_B is an effective boson charge and where χ in the IBA-2 expression is given by $\chi = (\chi_n N_n + \chi_p N_p)/(N_p+N_n)$. This expression was used in the g factor study discussed later.

2. M1 Transitions in Collective Nuclei

In lowest order in the IBA, the collective M1 operator does not yield transitions since it is simply proportional to the total angular momentum. In IBA-2, however, this constraint is lifted, since the operator is specified in terms of the neutron and proton degrees of freedom separately. Transitions can then occur in cases where the wave functions of the states involved contain components which are not fully symmetric with respect to interchange of neutrons and protons. In general, the IBA-2 Hamiltonian gives rise to a set of low lying states which are n-p symmetric, and a set of higher lying states of mixed symmetry. The mixing between the two depends on the parameterization of the Hamiltonian, and can thus be tested via the M1 transition strengths among the lower lying states. For instance, a number of IBA-2 descriptions of deformed and

O(6)-like nuclei have recently been proposed which involve a substantially larger degree of mixing between symmetric and antisymmetric states than has hitherto been thought reasonable. However, an examination of the M1 properties shows that the predicted low lying B(M1) values are several orders of magnitude larger than the data. Also, a recent IBA-2 calculation for the transitional ^{148,150}Sm nuclei suggests that a particular high lying 2^+ state in each case is predominantly an antisymmetric mode. Again, it is possible to reject the hypothesis by demonstrating that the empirical B(M1) values to the first 2^+ state are too small. More generally, empirical B(M1) values for $\gamma \rightarrow \gamma$ transitions have been extracted for a large number of well deformed nuclei, by making use of a combination of existing data on mixing ratios, B(E2) values, bandmixing parameters, and conversion electron subshell ratios. The resulting systematics show a number of interesting features which should provide a key to determining the required form and extent of n-p symmetry mixing in the IBA-2 Hamiltonian. In particular, there are two ways in which intra-γ band M1 transitions can be produced. One involves using $\chi_\pi \neq \chi_\nu$ and the other large F-spin mixing. Calculations in both approaches show a definite preference for the former approach and set important constraints on the differences in χ_π and χ_ν in deformed nuclei.

3. The Pseudo-L Scheme and the Nilsson Model

One of the appealing features of the IBA is the close connection of its symmetries to geometrical models. These interrelationships have been extensively studied. The same is not true for the Bose-Fermi symmetries of the Interacting Boson-Fermion Approximation (IBFA). For example, in SU(3), it has been noted that rotational bands similar to the Nilsson scheme arise but little deep study of their structure and mixing has been carried out. In a project just completed, the pseudo-L structure of these symmetries has been exploited to address this issue. In describing the Fermion sector in a symmetry of the form $U^B(6) \times U^F(m)$ an essential step has been to cast the single particle angular momenta in terms of pseudo L and spin parts. Thus, the set of orbits j=1/2, 3/2 and 5/2 (e.g., $p_{1/2}$, $p_{3/2}$, $f_{5/2}$) can be described by coupling a pseudo spin s=1/2 to pseudo orbital states L=0 and 2. By decomposing the IBFA Hamiltonian corresponding to the SU(3) B-F symmetry into rotational and collective parts it was shown that the pseudo-L decomposition leads naturally to a pseudo Coriolis mixing between intrinsic states (as in the Nilsson model), but that, here, an attenuation or enhancement of the Coriolis coupling constant, relative to $h^2/2\ell$ naturally occurs, whereas it has always been an ad hoc insertion in the Nilsson description. Moreover, the intrinsic states here are not simply single particle excitations coupled to the ground state rotational band, as in the Nilsson scheme, but automatically include coupling to the full core spectrum. This means that a fragmentation of "Nilsson structure" (as observed empirically, for example in the near SU(3) W region) will be an automatic feature of this scheme.

4. Test of a Possible 0(6) Region near ^{124}Te

^{124}Te has been proposed as a possible 0(6) nucleus, but conflicting earlier (d,d') data appeared to disclose an extra state in conflict with the 0(6) description, thus prohibiting a definite conclusion. Therefore, ARC studies of ^{124}Te at 2 and 24 keV have been carried out and are being analyzed. The completeness guaranteed by the ARC technique will allow a definitive conclusion.

5. Further Evidence for the 0(6) Structure of ^{196}Pt

Recently, our earlier description of ^{196}Pt as an 0(6) nucleus was questioned and it was suggested that perhaps a U(5) description was equally good. At the same time, Talmi and co-workers pointed out that many features, typically associated with 0(6), actually pertain to its subgroup 0(5), which also occurs in the U(5) symmetry chain. They urged that experimental quantities which specifically distinguish 0(6) and U(5) be studied. We agreed completely with their arguments and analysis and, therefore, motivated by this, we reexamined the data for ^{196}Pt, looking specifically at properties of the high lying levels which are completely different in 0(6), where they comprise families with $\sigma<\sigma_{max}$ that mirror in their properties those of the ground state $\sigma=\sigma_{max}$ levels, and in U(5) where they are multi-phonon levels. It was shown that the U(5) limit cannot fit the energies of these levels, nor their (t,p) and (p,t) cross section, nor their E0 decay. The most important evidence, though, centered on the E2 branching ratios for their decay. The original data was rechecked to obtain a number of new limits. The full comparison of all the data revealed that the U(5) description is completely inadequate and that an 0(6) one provides an excellent description. This conclusion is also supported by absolute B(E2) values among low lying states which can also distinguish 0(6) and U(5) if measured to sufficient accuracy.

This study highlights once again the crucial value of data on high lying low spin states, and of complete spectroscopy as provided by nonselective reactions such as (n,γ). It is only by virtue of such data in ^{196}Pt that the important questions raised by Talmi and others could be addressed.

C. FERMION DYNAMICAL SYMMETRIES (FDS)

Recently, Ginocchio, Feng, Wu, and Guidry have proposed and developed a Fermionic model that aims at providing a microscopic understanding of the IBA and its U(6) symmetries. The model involves the truncation of the shell model to a space, consisting of pairs of fermions coupled to L=0 (S) and L=2 (D) and, therefore, can be mapped 1-1 onto the IBA basis. Yet the states and Hamiltonian are purely Fermionic. It has been shown that all three IBA symmetries, U(5), SU(3), and 0(6) emerge naturally in this scheme. However, in addition, the FDS model contains new symmetries. There are still important aspects of this model that need to be addressed, including its portrayal of the unique parity orbit primarily as a spectator "sink" for a certain number of valence nucleons, the nature of the implicit p-n interaction contained in the model, and the seriousness of the assumed degeneracy of different j orbits. Nevertheless, there have already been two interesting discoveries, relating to empirical data, that encourage interest and further work in this direction. These are described below.

1. Evidence for an SO(7) Fermion Dynamical (Pd-Ru Nuclei)

The FDS model contains an SO(7) dynamical symmetry that is not explicitly contained as a symmetry in the IBA (although its properties can be reproduced by numerical diagonalization in the IBA provided the IBA parameters are properly chosen and are mass dependent). It is a remarkable symmetry in that it does not correspond to a static structure but rather an evolving one that describes a transition region between the IBA symmetries U(5) and O(6).

Based on extensive (n,γ) and TRISTAN experiments in recent years on nuclei near A=100, it was possible, when the SO(7) limit was proposed, to recognize empirical evidence for it in the Pd and Ru nuclei with neutron numbers near 56-62. (Indeed, these nuclei had been previously treated, by us and others, as intermediate between O(6) and U(5) but with no clue that they corresponded to a simple analytic symmetry.) The particular feature automatically contained in SO(7) and reflected empirically, is a variation of properties (energy levels, B(E2) values, etc.) with mass (valence nucleon number). Normally, in a phenomenological model, such systematics must be introduced ad hoc via mass dependent parameter changes. Here it appears naturally and, in fact, is unavoidable. One assumption required to obtain a fit to the data in SO(7) is a particular and unexpected occupation of specific shell model orbits. A study of existing spectroscopic factor information, however, in fact reveals just the required assumptions (e.g., $g_{9/2\pi}$ orbit nearly filled near Z=44, with holes in the "lower lying" $p_{1/2}$, $p_{3/2}$, and $f_{5/2}$ orbits). Further study of this and other limits of the SO(7) model is urgently needed. The present results suggest that it may be a major new development in understanding the symmetry structure of nuclei. (Incidentally, it also includes high spin states and, therefore, has a natural link to this extremely active field of study as well.)

2. Explanation of the Particular Form of the O(6) Limit Observed Empirically

The O(6) eigenvalue expression of the IBA is: $E(\sigma,\tau,J)=A\sigma(\sigma+4) + B\tau(\tau+3) + CJ(J+1)$ where A, B, and C are completely free parameters. In both known O(6) regions, ^{196}Pt and the Xe and Ba isotopes, it is found that, of the infinite variety of relationships between A and B, their ratio A/B is always ≈1. This feature also emerges automatically in the CQF. It has long been a puzzling question as to why this particular paremeter relationship appears empirically. It turns out, however, that, now, the FDS model provides an explanation: the O(6) limit contained within it automatically predicts exactly this relationship between A and B. It arises directly from the relationship between the required magnitudes of the monopole pairing and quadrupole interactions between S and D Fermion pairs in the FDS model.

D. STUDIES OF NUCLEI FAR OFF STABILITY WITH THE TRISTAN FACILITY

The on-line isotope separator, TRISTAN, at the HFBR is a facility, unique in this country, for the study of neutron-rich nuclei far off stability, produced by thermal neutron induced fission of uranium. The reactor provides an intense external neutron beam, making excellent shielding possible. This combination of high beam intensity, long running time, low background, and the world's most powerful array of ion sources makes TRISTAN an unrivaled facility which can do experiments which are impossible elsewhere.

A high interest is associated with the study of nuclei far off stability for a number of reasons. The neutron-proton force is sensitive to the spatial overlaps of neutron and proton orbits, and, therefore, its effects vary with both neutron and proton number. By providing combinations of these not available elsewhere, neutron-rich nuclei provide the opportunity to study not just an extension of familiar phenomena but the possibility of observing entirely new effects. Particularly important areas of study center on the investigation of a wide variety of collective phenomena, of phase transitions, of deformation regions, of symmetries and, possibly, of supersymmetries. The latter two phenomena are especially relevant for odd nuclei where the predicted symmetries require specific combinations of single particle and core structure, some of which may not be available near stability. Besides the work on collective phenomena, TRISTAN provides access to nuclear regions that are expected to be magic in nature such as those near the doubly closed shell nuclei ^{132}Sn and ^{78}Ni. Nuclei far off stability also have a crucial importance in astrophysics since their lifetimes and β-decay energies affect the production of the heavier elements and can be used to distinguish different r-process models. Finally, the access to unstable nuclei with sufficiently large decay energies leads to the possibility of observing radioactivity in the form of β-delayed neutron emission and, in a few cases, of double delayed neutron radioactivity. Such studies are of both applied and structure importance, since they give information on the emission of decay heat from fission products and because they represent the inverse of neutron capture experiments on unstable targets, so that they can provide information on cross sections of neutron-rich nuclides, which is of particular interest for astrophysics and nuclear theory.

1. Nuclear Astrophysics: ^{80}Zn

During the past fiscal year, the first nuclear measurements at TRISTAN with astrophysical applications were completed. The half-life and Q_β value of ^{80}Zn were measured. ^{80}Zn is important due to its participation in the classical r-process. In the popular waiting point approximation model for this process, when neutron capture in stellar nucleosynthesis reaches a neutron closed shell (N=50 in this case), subsequent capture rates decrease enormously, and further production of heavy nuclei effectively ceases until significant quantities of the longer lived closed shell nuclei have decayed to a new element with higher neutron binding energy. These points are referred to as "waiting points" and their lifetimes critically restrict (see below) the time scale of r process nuclear synthesis and the stellar environments that are its site.

The waiting point approximation avoids the need for detailed nuclear information by making two simplifying assumptions: the time scale for neutron capture is assumed to be much shorter than that of beta decay, and an $(n,\gamma) \leftrightarrow (\gamma,n)$ equilibrium is envisioned. Then the abundance ratio of two adjacent isotopes depends, exponentially, in a nuclear Saha equation, on the ratio of the neutron binding energy, B_n, to the stellar temperature. Since B_n drops precipitously at neutron closed shells, points where the r-process path crosses N = 50, 82, and 126 specify the three most critical nuclides that determine the nucleosynthetic cycle time from Fe to the actinides. These nuclei are ^{80}Zn, ^{130}Cd, and ^{195}Tm. Thus, half-life measurements for these are critical for models of stellar nucleosynthesis, even including those that avoid the waiting point approximation. Until now, one has had to rely on theoretical estimates of these half-lives, but different calculations often differ by orders of magnitude: such differences lead in turn to marked differences in the stellar properties that must then be assumed to reproduce known elemental abundances.

Until now, it has not been thought possible to reach these nuclei, but recent developments in TRISTAN ion sources and experimental capabilities have now permitted the study of ^{80}Zn and the likelihood that ^{130}Cd will be attainable. In addition, the measurement of the neutron binding energy for even one of the waiting point nuclei can yield, from the Saha equation, the temperature regime in which stellar nucleosynthesis occurs and will also be valuable.

The half-life measured for ^{80}Zn was $T_{1/2}$=0.55 sec which is in agreement with the predictions of the microscopic model of Klapdor. Longer half-life predictions, as in the gross theory model of Takahashi, are excluded by our measurements. This shorter half-life implies a much shorter cycle time and removes a substantial constraint on the stellar neutron-exposure time required for r-process nucleosynthesis. This provides important information that constrains the stellar input parameters for r-process calculations.

Follow-up to this work lies in three areas. First, an attempt will be made to measure Q_β for ^{81}Zn and thereby extract a B_n value for the addition of a neutron to ^{80}Zn. This will make it possible to calculate directly, in the classical r-process approximation, the temperature regime for stellar nucleosynthesis. Secondly, ^{130}Cd will be studied in hopes of obtaining the same sort of data that was measured for ^{80}Zn. Thirdly, a general program will be developed to measure a more extensive set of $T_{1/2}$, and Q_β values and decay schemes of neutron-rich nuclei, especially for the crucial regions near A=80 and A=130 and for another important r-process abundance peak near A=160. The latter region has recently also become accessible at TRISTAN with improvements to the thermal ion source.

Indeed, it is worth emphasizing that plots of r-process abundances against A show five peaks, three major ones near A≈80, 130, and 195 and two smaller ones near A≈100 and 160. TRISTAN now provides access to four of these five critical regions.

The region of rare earth nuclides near A=160 has been studied in some preliminary experiments. Half-lives were measured for ^{156}Pm (28.2 ± 1.1 sec), ^{159}Sm (15 ± 2 sec), ^{160}Sm (8.7 ± 1.4 sec), and ^{161}Eu (27 ± 3 sec). The half-lives, and indeed any nuclear data, of these nuclei were previously unknown. Calculations by Klapdor et al predict 8.39, 10.1, 6.06, and 24.8 sec, respectively. These discrepancies hint at a systematic pattern and so a broader survey of half-lives measured since the work of Klapdor was made to test if a consistent pattern emerged. It is clear that many more empirical half-lives far off stability will be needed before firm conclusions can be drawn but, nevertheless, these appear to be repeated "jumps" in the relative experimental and theoretical half-life values. These "jumps" tend to occur at or near shell closures, suggesting that there may be some significant shell structure physics missing from the model. Further work on measurements and interpretation is in progress.

2. g-factor Measurements

One result of studies in the N_pN_n scheme is the recognition of the importance of subshell closures in affecting the active number of valence nuclei. It also appears that, in the middle of deformed regions, the number of valence nucleons effectively contributing to the collectivity may not be the same as inferred by simply counting from the nearest closed shells. Work in the past years on $g(2^+_1)$ factors has shown that such data can be used to extract effective N_p values. During the present period this work was extended, and combined with that from B(E2) values to provide both N_p and N_n effective values for the rare earth nuclei. The procedure is described as follows.

During FY 1986, experimental and theoretical work at TRISTAN has proven that magnetic moments of 2^+_1 states ($\mu(2^+_1)$) in even-even nuclei in the region around A=150 can be used to calculate the effective number of valence protons which take part in the collective nuclear motion. In particular, it was shown that this analysis provides direct evidence for the existence of the Z=64 closed subshell, and can be used to map its gradual dissipation as the number of neutrons increases beyond N=90. Specifically, it was found that for neutron numbers N<≈88 the numbers of valence protons, N_p, for nuclei like Sm and Nd were close to the values (2 and 4, respectively) that could be obtained if the effective proton shell were Z=50-64 while for N>≈92, the same nuclei are found to have N_p values close to 12 and 10, close to those for the Z=50-82 shell. This result gives strong support for recent theoretical work (see another paragraph) that describes the onset of deformation in this region as due to the role of the p-n interaction in eradicating the Z=64 shell gap and effectively increasing the number of valence nucleons.

Our purpose now is to extend the systematic investigation of magnetic moments in even-even nuclei to other regions, and to verify whether the simple linear relationship between the number of valence protons and neutrons and the magnetic moment as predicted by the IBA-2 model, which was found to hold very well in the A=150 region, is applicable to other nuclei as well. Preliminary work done in FY 1986 indicates that this is indeed the case. Of particular interest will be to compare the behavior of $\mu(2^+_1)$ of spherical and deformed nuclei and deduce the values of the g-factors of proton and neutron bosons in different nuclear regions. In addition, the TRISTAN isotope separator will be used to measure magnetic moments in the regions of A=100 and A=150, where existing experimental data is not sufficient to test all the predictions of the theoretical work.

Another line of research is the inclusion of B(E2) transition probabilities in our analysis of the systematics of even-even nuclei. The experimental technique for measuring the lifetimes necessary to deduce the B(E2) value is discussed in another paragraph. Our intention is first to check whether a simple analytical expression can be confidently used for this observable, in analogy to the one used for the magnetic moments, and to find the appropriate effective charges that should enter into this expression. Furthermore, we will use this relation in combination with the $\mu(2^+_1)$ data to extract the effective number of valence protons and neutrons in a wide variety of spherical, deformed and transitional nuclei. An important goal is to test whether a consistent analysis of B(E2) and $\mu(2^+_1)$ values is possible, and if it can provide valuable nuclear structure information regarding the existence of new subshell closures, the onset of deformation, the role of the proton-neutron interaction, and fundamental quantities in the IBA model such as boson g-factors and effective charges.

The g-factor of ^{142}Ba was measured. The result was compared to three models: the IBA-2 model, the hydrodynamic model calculations (Z/A), and Greiner's refinement to the hydrodynamical model that allows for differences in proton and neutron deformations. The simpler hydrodynamic model predicts g=Z/A for collective states. Greiner has shown, however, that the larger pairing force for protons implies a smaller deformation than for neutrons, which in turn implies that the neutron and proton degrees of freedom are no longer rotating in phase with each other. This results in a reduction in the absolute values of g below the Z/A estimate, but maintains the Z/A dependence of the hydrodynamic model since the model is still based on the idea of a collective flow involving all of the nucleons. In contrast, the IBA model considers only the valence nucleons, and predicts that the g factor will depend primarily on the ratio N_π/N_t, resulting in a more sharply changing value of $g(2^+_1)$ as A increases, for a particular Z. Indeed, when neutrons are filling past midshell, then valence number decreases with increasing A within an isotopic sequence and $g(2^+_1)$ is actually predicted to increase rather than decrease as in hydrodynamical model predictions. Such behavior has in fact been observed, for example, in the W isotopes. The accuracy of the g-factor previously obtained for ^{142}Ba was not sufficient to distinguish these models for which the IBA and Z/A predictions are nearly identical. For heavier Ba isotopes (measured a few years ago at TRISTAN), the data are in good agreement with the IBA and Greiner's corrections, but cannot completely exclude the Z/A calculations. An accurate $g(2^+_1)$ value for ^{140}Ba would be able to distinguish the three treatments. Similarly, a measurement on ^{148}Ba, or a more accurate determination of $g(2^+_1)$ for ^{142}Ba could distinguish between the IBA and Z/A predictions.

During this year, some of the above Ba measurements may be attempted, but emphasis will be placed on the A=100 region, specifically ^{98}Sr, where strong subshell effects (similar to those near Z=64) manifest themselves. In addition, newly available regions at TRISTAN, specifically the rare-earth nuclides, will be investigated.

3. Studies Near Closed Shells

a. The Structure of Odd-mass Sb Nuclei Near ^{132}Sn

An extensive series of experiments on the level structure of odd nuclei was mass Sb completed in FY 1986. The study resulted in the completed identification of the $\pi g_{7/2} \times 2^+$ multiplet in ^{127,129,131}Sb and has led to the identification of this multiplet in ^{123,125}Sb. In addition, several members of the $\pi d_{5/2} \times 2^+$ multiplet have also been identified. The structure of the levels arises predominantly from single particle states and states belonging to multiplets formed by the proton above the Z=50 shell interacting with an excited neutron core. These data provide a rather complete systematics of those states and thus offer an exciting region to test the shell model. Due to the proximity of the double closed shell at ^{132}Sn, the nuclear systems are very simple. Since there is only a single proton coupled to the neutron core, detailed calculations are possible. Shell model calculations have begun on these nuclei and will continue in the next year. Core polarization corrections will be investigated for nuclei in this region. Calculations for 1, 2, 3, and 4 quasi-particle nuclei have revealed some systematic problems in predicting the position of various states. Energies of well-predicted states will be used to further refine the calculations and explore the effective interactions for nucleons in these nuclei.

b. The Structure of Odd-mass Nuclei: ^{123}Ag, $^{123-129}$Cd

We have studied the decay of neutron-rich Ag and Cd nuclei in the ^{130}Cd region in order to measure $T_{1/2}$, Q_β and the decay patterns of nuclei in the close vicinity of the r-process path and the double shell closure at ^{132}Sn. The structure of odd mass In isotopes has attracted much attention due to the presence of the deformed shape isomer at low excitation energy in $^{107-121}$In. A good description of the lowest lying levels has been recently obtained by the Gent group. In these calculations single-hole and one-particle, two-hole proton configurations are considered, together with the collective excitations (quadrupole and octupole) of the underlying Sn core. The calculations reproduce both the vibrational muliplet and the rotational-like sequence of positive parity states at low excitation energies, which interact only weakly.

The study of heavier In isotopes A≥123 (from the decay of Cd) would extend the systematics of the intruder single particle hole excitations towards the closed shell at N=82, and particularly it would provide information on how the positive parity shell model intruder states will shift in excitation energy from their lowest energy at midshell towards the a shell closure at N=82.

Based on the γ multiscaling (GMS), singles and $\gamma\gamma$ coincidence results, decay schemes were constructed for the ^{123,125,127}In nuclei populated from the β-decay of Cd. Guided by very simple systematics of the low-lying levels E_x<1.7 MeV, characteristic of nuclei near Z=50 and on their decay properties, intruder levels have been tentatively identified in ^{123,125}In. This set of intruder levels (spins $1/2^+$, $3/2^+$, and $5/2^+$) has been tentatively identified in ^{123}In at excitation energies of 1926, 1616, and 1512 keV, respectively. These levels appear to shift towards higher excitation energy and are in a different sequence than was predicted by the Gent model. Conversion electron, angular correlation, and level half-life measurements are planned for this year to identify firmly those levels and to provide more specific spectroscopic data which would allow a detailed testing of the model.

c. Beta Decay of ^{126}Cd

The β decay rates in the vicinity of closed shell nuclei are generally enhanced as compared to other regions and thus provide a testing ground for theoretical models. The decay of the 0^+ level in ^{126}Cd to 2^+ and 2^- levels in the odd-odd nucleus of ^{126}In proceeds via fast β transitions with log ft≈4.0. Such log ft values are allowed G-T transitions and imply no parity change and the spin change of ±1.0. Our study of this decay via singles, GMS, γ-γ coincidences, and Q_β measurements confirmed the earlier results and failed to resole the discrepancy between the log ft values and the spin assignment. Further stucies of this decay and the decays of ^{128}Cd and ^{128}In are planned for this year.

d. Studies Near Z=28: ^{73,75}Ga

We have undertaken the study of odd-Ga isotopes populated from the decay of Zn nuclei in order to use the odd proton as a sensitive probe of the Z=28, N=50 core structure. The low shell and subshell degeneracies in this region lead to a complex interplay of shell structure and collective effects which manifest themselves by the presence of several transitional regions and which render a deep understanding elusive. A particular feature which is both perplexing and a likely clue to further insights is the fact that the N_pN_n systematics do not seem to apply to this region, in contrast to A>100 nuclei.

With $J^\pi=7/2^+$ for the ground state of ^{75}Zn and $Q_\beta \approx 6$ MeV one expects the complete set of low-lying levels to be populated directly or indirectly. Indeed, the lowest-lying levels in ^{75}Ga $E_x \leq 1.5$ MeV fully correspond to those found in the (^{3}He,d) work excluding perhaps a new $J^\pi=1/2^-$ level at 22.5 keV, which was not resolved in the particle transfer study. Based on our decay work and the results from the (^{3}He,d) reaction, a spin and parity was assigned to most of the low-lying levels. In addition, the data for the ^{73}Ga nucleus has been reevaluated to yield, along with ^{75}Ga, consistent systematics for Ga nuclei. The new data confirm the transitional character of heavy Ga nuclei, which is particularly manifested by a rapid lowering of a particular group of levels at N$\geq$40.

4. Octupole Versus Alpha Clustering Excitations in ^{146}Ba

Two models have been proposed to describe low lying negative parity excitations in even-even nuclei. The geometrical model uses octupole deformed shapes as the mechanism to generate these states, whereas the α clustering model assumes the coherent collective motion of a group of α particles outside the core. Exhaustive studies, both experimental and theoretical, in the actinide nuclei have yielded the conclusion that the models are virtually indistinguishable for these nuclei. However, it has been suggested that lighter nuclei, such as Ba, may represent a region in which the models will predict different structures that can be tested by experiment. We are carrying out a detailed spectroscopic study of ^{146}Ba in an attempt to distinguish these two interpretations. In particular, we are searching for the E2/E1 branching ratio $B(E2:3^-{}_1 \rightarrow 1^-{}_1)/B(E1:3^-{}_1 \rightarrow 2^+{}_1)$ as a key test of the models. However, the decay scheme of ^{146}Ba is only partially known and thus a more complete level scheme below 1.5 MeV must be obtained before any final conclusions can be reached.

5. A=100 Region: ^{96,98}Zr and Intruder State Systematics

The pioneering work of Federman and Pittel in the A=100 region suggested that the driving force for the onset of deformation was not simply the total number of valence nucleons, but the p-n interaction operating in certain crucial orbits. Since then, it has become more and more accepted that this is in fact an appropriate model for the development of collectivity and deformation in many regions. Thus, it is all the more crucial to fully understand the still poorly known A=100 region. A broad program of investigations of states at TRISTAN is therefore being carried out. The following paragraphs briefly discuss some of these projects.

A broad effort to investigate the levels of ^{96,98}Zr using a number of techniques has been started. In particular, advantage was taken of the ability of the TRISTAN mass separator to provide uncontaminated beams of mass 96 and 98, which allow an investigation of the Zr levels populated in the decay of the low spin isomers of $^{96,98}Y$. The $^{96,98}Zr$ nuclei are characterized by the closures of both neutron and proton subshells. In slightly heavier isotopes those subshell effects vanish. The object of the investigation was to provide information on the band built on the first excited 0^+_2 state (which is possibly a coexisting intruder band) and to understand further the mechanism underlying the A=100 spherical deformed transition region. Since the subshell closures reduce the size of the single particle space, this region is also amenable to microscopic calculations.

Angular correlation measurements were performed to supplement previous decay studies. The β^- feeding to the 0^+_2 level was more hindered ($\approx$1.5%) by comparison to the ground state feeding than previously estimated (25%). Furthermore, the small E2/M1 mixing ratio found for the $2^+_2 \rightarrow 2^+_1$ intraband transition relates to the question of a coexisting nature of the band. A third, 0^+_3 level has also been located from the angular correlation data.

Careful measurements of the β decay to these states has yielded log ft values for 0^- to 0^+ states in ^{96}Zr. Such transitions are of particular interest to the studies of the fundamental nature of the weak interaction (CP violations, meson exchange). For the nuclei near shell closures the $0^- \rightarrow 0^+$ β transitions are unhindered and in fact are enhanced as compared to the single-particle shell model estimates. For this class of β^- transitions, the initial and final state wave functions can be exactly determined, and thus provides a meaningful comparison of experiment and theory. Our results show a more enhanced transition rate to the 0^+ ground state relative to the first excited 0^+ states in ^{96}Zr than expected. The impact of those results onto the parameters deduced from previous theory-experiment comparisons is currently being assessed.

6. Exotic Neutron-rich Nuclei in the Rare Earth Region

Our recent measurement of the half-lives of these new isotopes indicats a systematic pattern of discrepancies with the most widely accepted predictions of the microscopic model of Klapdor *et al.* These discrepancies, which can be conveniently expressed as a ratio of experimental to calculated half-lives, R, change significantly in the vicinity of shell closures. In particular, approaching Z=28 R decreases almost monotonically to reach R$\approx$0.1 for Co nuclei and then jumps at Z=29 to R=2.5. Similar effects are observed in the rare earth region in the vicinity of Z=58 and 64, where the values of R change from 0.8 for Pr to 3.4 for Pm at Z$\approx$59 and then decrease monotonically to 0.9 for Tb and finally jump to R=3.9 for Dy nuclei at Z$\approx$65. These discrepancies, which significantly exceeds the uncertainties assigned to the model by its authors, have an impact on a wide range of problems (e.g., astrophysics, reactor environments) where those calculations are frequently the only source of vital input parameters.

We have deduced the decay schemes for $^{157}Sm \rightarrow {}^{157}Eu$ and $^{158}Sm \rightarrow {}^{158}Eu$ from the γ-γ coincidence and γ multispectra scaling measurements. This information will allow the measurement of Q_β values via β-γ coincidence techniques. The study of the β decay of ^{157}Sm revealed many previously unobserved levels in ^{157}Eu. Some of the levels populated by the β decay of ^{157}Sm are also populated in the ^{158}Gd (t,α) reaction; others are not. A combination of these two experiments will yield a more complete level scheme, which will be compared to IBFA model predictions. More detailed studies, including Q_β measurements are planned for the newly identified $^{159}Sm \rightarrow Eu$, $^{160}Sm \rightarrow Eu$, and $^{161}Eu \rightarrow Gd$ decays.

E. National Nuclear Data Center

1. Cross Section Evaluation Working Group (CSEWG) Activities

The annual CSEWG Meeting was held at BNL in May 1986. This meeting marked the 20th anniversary of the founding of CSEWG. In honor of the occasion, Associated Universities, Inc. hosted a banquet to which present and former members of CSEWG were invited. More than 70 persons attended the banquet including members of the original CSEWG committee. Henry Honeck, the evening's speaker and founding father of CSEWG, gave an amusing, enlightening and sometimes controversial review of the founding of CSEWG. Raphael LaBauve, retiring chairman of the Methods and Formats Committee, was honored for 20 years of continuous service. Former CSEWG Chairman, Sol Pearlstein, made the presentation.

The standards evaluations were completed in February 1987. Several iterations of the separate evaluations by Hale and Poenitz and the combination fit of Peelle were required to get a satisfactory final result. Recent evaluations of the 2200 m/sec cross sections by Axton were included. Results indicate not only an improved level of confidence in the standards but also improved evaluations for reactions closely related to the standards such as ^{235}U (n,γ) and ^{239}Pu (n,f).

New data needs in the areas of high energy charged particle data, data for space reactors, data for medical applications and data for exotic fusion were discussed at the meeting. A special session was organized by the Evaluations and Data Testing committees in which presentations on this topic were made. A Higher Energy Data subcommittee was formed within the Evaluation Committee to coordinate activity in the evaluation of both neutron and charged particle reaction data above the traditional CSEWG 20 MeV limit. The Charged Particle Subcommittee which was instrumental in developing the generalized incident particle approach used in the ENDF-6 format will continue to be active, concentrating its interest in data below 20 MeV.

Some progress has been made on ENDF/B-VI evaluations. New resonance region analyses for ^{239}Pu and Ni have been completed and one for ^{235}U has been started. New evaluations for B, ^{240}Pu, $^{151,153}Eu$, ^{165}Ho, ^{197}Au and ^{89}Y are complete or nearing completion.

While the ENDF-6 formats have been in principle frozen for the past year, there have in fact been some significant developments, particularly in the resonance region where more accurate R-matrix and R-function parameterizations are now proposed. An additional format has been added in file 6 to allow tabular representation of the secondary energy-angle spectra in the order E, μ, E′. Good progress has been made on the ENDF-6 format manual as a result of extensive cooperation between LANL and BNL. All sections not related to covariance formats should be completed by the 1987 CSEWG meeting.

2. Neutron Data Atlas

During the past year data reviews of $\sigma(E)$ were completed for all measured data from .01 eV to 200 MeV. We have also attempted to analyze activation measurements in order to include ground and metastable state production cross sections for the first time. As a useful byproduct of this review, we have been able to add to and correct the experimental neutron reaction data base (CSISRS).

Page layouts including overlay curves derived from ENDF/B-V, Mughabghab's resonance parameter evaluations or interactive curve fitting methods have been completed up to Z=90. A fall publication by Academic Press is envisioned.

3. Nuclear Data Sheets

The NNDC has been producing the Nuclear Data Sheets at the rate of about an issue a month. Of these, nine issues a year are devoted to the nuclear structure evaluation and the remaining three to the publication of Recent References.

The Center evaluated A=70, 73, 136, 138 and 140 and submitted them for publication; A=71, 138, 144, 147, 152 and 163 are being evaluated.

The U.S. is part of an international network of evaluators contributing recommended values of nuclear structure information to the Evaluated Nuclear Structure Data File (ENSDF). Publication of the Nuclear Data Sheets proceeds directly from this computerized file. In addition to the U.S., evaluations have been received or are anticipated from Germany, U.S.S.R., France, Japan, Belgium, Kuwait, Sweden, the People's Republic of China and

Canada. Italy and India have shown interest in joining the network and are expected to start evaluation in the near future.

A new concise format for the published A-chains in the Nuclear Data Sheets has been approved by the international network and adopted. This format reduces the size of the publication without omitting essential information and improves its readability.

4. On-line Data Services

During the past year, NNDC has improved on the on-line user access first provided last year. The data bases available are the neutron bibliography CINDA, the nuclear structure bibliography NSR, ENSDF; and nuclear structure, radioactivity, and ground and metastable state properties. Access is to the NNDC VAX 11/780 via telephone lines or PHYSNET (HEPNET).

5. Charged Particle Data

The NNDC chairs the Medium Energy Nuclear Data Working Group (MENDWG) which held its first meeting May 21-22, 1986. Seventeen organizations from the U.S., Canada, Federal Republic of Germany and the U.K. provided input to MENDWG. A partial list of data requirements were generated and some discrepancies between calculation and experiment were described. MENDWG recommendations are summarized in the report BNL-NCS-38404 (DOE/NDC-40) and circulated widely to encourage information exchange among the medium energy nuclear data community at large.

CROCKER NUCLEAR LABORATORY AND DEPARTMENT OF PHYSICS
UNIVERSITY OF CALIFORNIA, DAVIS

A. MEASUREMENTS

1. Results for the $^{12}C(n,p)^{12}B$ (g.s. + 1 MeV) Reaction at 65 MeV*.

(D.S. Sorenson, J.L. Romero, F.P. Brady, C.M. Castaneda, T.D. Ford, J.R. Drummond, and B.C. McEachern**, and N.S.P. King***)

We have measured (n,p) spectra using the zero degree dual target facility at CNL covering an angular range from 0 to 40 degrees. We have extracted cross sections for the g.s. + 1 MeV (which could not be resolved), the 4.4 MeV excited state(s) and the region between 6 and 10 MeV. Here we summarize our results for the g.s. + 1 MeV. Figure A-1 compares the present data with previous data also measured at CNL at 56 MeV[1] and 60 MeV[2]. When plotted as a function of the momentum transfer q, good agreement is observed between the 3 data sets. The curve is a DWBA microscopic calculation at

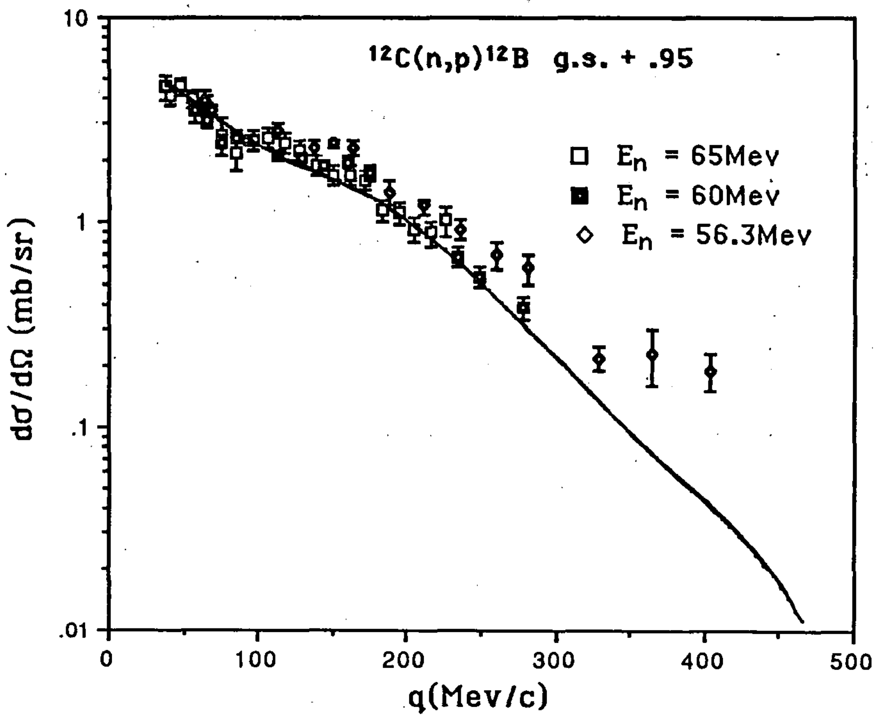

Figure A-1

* Supported by NSF grants PHY 81-21003 and 84-19380
** Associated Western Universities Graduate Fellow
*** Los Alamos National Laboratory
1 N.S.P. King, F.P. Brady et al., UCD-CNL 187, 80 (1976).
2 G.A. Needham, Ph.D. Thesis, UCD, 1980.

60 MeV using the code DW81[3]. The optical model potential of Comfort and Karp,[4] the transition densities of Cohen and Kurath,[5] and the M3Y N-N effective interaction[6] were used. Central, spin-orbit, and tensor components of the effective interaction are included normalized by 1.33. The calculations at 65 and 56 MeV are in good agreement with that at 60 MeV.

Figure A-2 compares the 65 MeV (n,p) data with available (p,n) at 62 MeV[7] and (p,p') at 65 MeV[8] (the latter multiplied by a isospin C-G factor of 2.0). Good agreement is found among the data sets. The two curves shown are DW81 calculations at 65 MeV for (n,p) of the g.s. + .95 MeV state, which agrees with corresponding calculations for (p,n) at 62 MeV and (p,p') at 65 MeV.

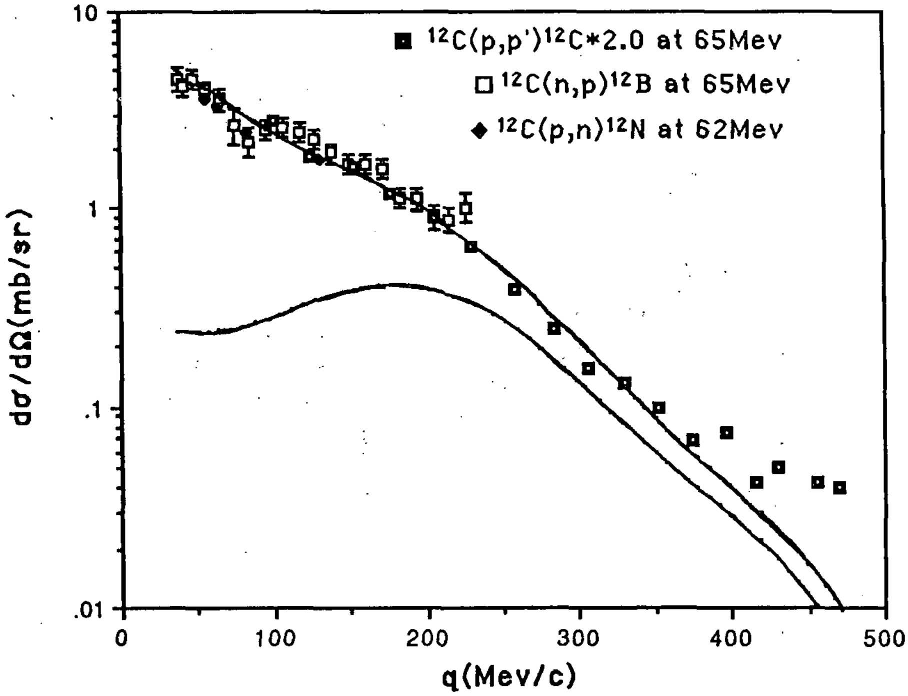

Figure A-2.

---

[3] R. Schaeffer and J. Raynal, Program DWBA70 (unpublished); extended version DW81 by J.R. Confort (unpublished).
[4] J.R. Comfort and B.C. Karp, Phys. Rev. C21:6 (1980).
[5] S. Cohen and D. Kurath, Nucl. Phys. 73:1 (1965).
[6] W.G. Love in "The (p,n) Reaction and the Nucleon-Nucleon Force", edited by C.D. Goodman, S.M. Austin, S.D. Bloom, J. Rapaport, and G.R. Satchler, Plenum Press, N.Y. (1980).
[7] C.A. Goulding et al., Nucl. Phys. A331:29-38 (1979).
[8] K. Hosono et al., Phys. Rev. Lett. 41:621 (1978).

2. <u>The C^{13}(n,p) Reaction at 65 MeV*.</u> (K. Wang,# D. Pocanic,# C.J. Martoff,# and S.S. Hanna#, F.P. Brady, J.L. Romero, C.M. Castaneda, J.R. Drummond, and B.C. McEachern**)

The $^{13}C(n,p)^{13}B$ reaction at 65 MeV was measured at the Crocker Nuclear Laboratory at U.C. Davis. A newly developed neutron facility[1] was used which can measure the 0° scattering and cover a large angle range from 0° to 60° in the laboratory system. The neutron production target is ^7Li, and the monoenergetic neutron beam is defined by a brass collimator. The primary proton beam current can be as high as 25 μA, and the 0° neutron yield is about 10^6 n/cm^2/sec. The cross sections for $^{13}C(n,p)^{13}B$ are normalized to n-p scattering. The $^{12}C(n,p)^{12}B$ reaction was also measured as a check of the whole system, since it is a well studied reaction. Angular distributions for $^{13}C(n,p)$ have been obtained for the transitions to the ground state and the three excited states of ^{13}B. A DWBA calculation was performed for comparison to the experimental results. The results are also compared with the reactions $^{13}C(\pi^-,\gamma)^{13}B$,[2] $^{13}C(\gamma,\pi^+)^{13}B$[3] and $^{13}C(p,n)^{13}N$.[4] The experimental value of log (ft) is 4.01, the strength for the GT transition from ^{13}B to ^{13}C is 0.386 and the 0° cross section for the (n,p) transition is 3.1 mb/sr in the center-of-mass system. Then the spin-isospin part of the effective N-N interaction is $V^c_{\sigma\tau}$ = 179 MeV - fm^3.

3. <u>The (n,px) Reaction on ^{118}Sn at 65 MeV*.</u> (J.L. Romero, E.J. Hjort, F.P. Brady, C.M. Castaneda, J.R. Drummond, B.C. McEachern, and D.S. Sorenson)

Zero degree scattering provides a tool to help separate excitation of the giant isovector monopole resonance (IVMR), expected to peak at forward angles.[5] The (n,p) reaction has the feature that only T_0+1 components of transitions are excited. Recent (π^-,π^0) data from LANL give evidence of the IVMR.[6] We have used our zero degree dual target facility at Crocker Nuclear Laboratory (which allows measurements from two targets simultaneously) to obtain energy spectra for the $^{120}Sn(n,px)$ reaction from 0 to 40 degrees. Using the same set-up we reported last year the excitation of the isovector monopole and quadrupole on $^{90}Zr(n,px)$.

---

* Work supported by NSF grant #84-19380
** Associated Western Universities Graduate Fellow
# Department of Physics, Stanford University, Stanford, CA 94305, supported by NSF Grant PHY83-1004-A1-3
† Supported by NSF grant 84-19380
1 F.P. Brady et al., in Neutron-Nucleus Collisions, ed. by J. Rapaport et al., No. 124, Proc. of AIP Conf. (Burr Oak State Park, Ohio, 1984), p. 382
2 C.J. Martoff et al., Phys. Rev. C27:1621 (1983).
3 K. Shoda et al., Phys. Rev. C27:443 (1983).
4 C.D. Boodman et al., Phys. Rev. Lett. 54:879 (1985).
5 N. Auerbach et al., Phys. Rev. C28:280 (1983).
6 J.D. Bowman et al., Phys. Rev. Lett. 50:1195 (183); A. Erell et al., Phys. Rev. Lett. 52:2134 (1984).

4. <u>(n,n) Elastic Cross Section and Continuum Measurements at 65 MeV</u>
(E.L. Hjort, F.P. Brady, J.L. Romero, C.M. Castaneda, J.R. Drummond, Zin Aung,#, B.C. McEachern,** and M.A. Hamilton***)

a. Elastic Measurements. The (n,n) elastic cross sections were measured for Pb, Fe, and C using a multiwire chamber system described earlier.[1] The original purpose of the experiment was to provide an absolute normalization for the inelastic scattering measurements made on Pb earlier in the year, and the experiment was extended to measure the elastic cross section of Fe also. In addition, data were also taken with CH2 and C targets to provide CH2-C spectra. Using the known n-p cross sections these data provide an absolute normalization for the cross section. The cross section obtained for Pb is shown in Fig. A-3, along with the optical model predictions of Schwandt[2] and Becchetti-Greenlees[3] for comparison.

b. Continuum Measurement. An experiment was also conducted to measure the (n,n') continuum and giant resonance excitations in Pb. An example of the final spectra is shown in Fig. A-4. It has been normalized to the elastic cross section for Pb presented above. Further analysis of the inelastic scattering spectra is on-going.

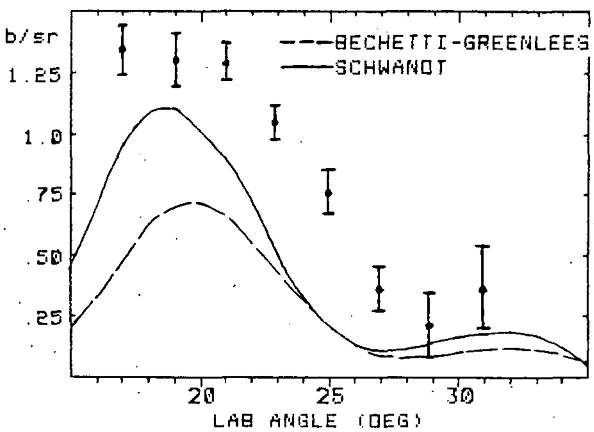

Figure A-3

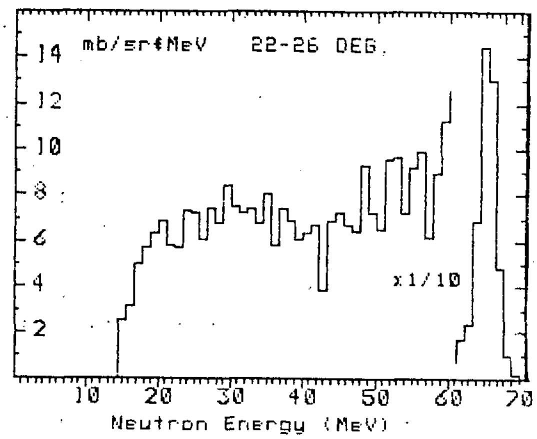

Figure A-4

---

* Supported by NSF Grant PHY84-19380
# University of Rangoon, Rangoon 11041, Burma
** Associated Western Universities Graduate Fellow
*** West Point Military Academy
[1] F.P. Brady et al., Nucl. Inst. and Meth. 228:89 (1984).
[2] P. Schwandt, private communication.
[3] F.D. Becchetti, Jr. and G.W. Greenless, Phys. Rev. 182:1190 (1969).

IDAHO NATIONAL ENGINEERING LABORATORY

A. EXPERIMENTAL STUDIES

1. International Program to Improve Decay Data for Transactinium Nuclides (R. G. Helmer, C. W. Reich)

To help meet an identified need for precise decay data for selected transactinium nuclides of importance to fission-reactor technology, in 1977 the International Atomic Energy Agency organized an international Coordinated Research Program to measure and evaluate such information. Five groups experienced in decay-data measurement were involved in the work of this Program. The categories of decay data considered by these participants included half-lives (both total and partial), γ-ray emission probabilities and α-particle emission probabilities. The goals of this Coordinated Research Program were: (1) to determine a list of data that needed improvement; (2) to make measurements of these data with the required precision; and (3) to evaluate the available data. The INEL participation in this effort involved the measurement of γ-ray emission probabilities, with the goal of obtaining uncertainties <1% for the prominent γ rays, for $^{238,239,240,241}Pu$, $^{232,233,235}U$, ^{233}Pa and ^{229}Th.

The work of this Coordinated Research Program is now completed, and the results have been summarized and published as a report in the IAEA Technical Reports Series.[1] A large quantity of precisely measured decay data has been produced by the participants in this Program. This information, together with the evaluations of these and other pertinent data, are believed to represent a major improvement in the status of our knowledge of the decay data of the transactinium nuclides.

2. Delayed-Neutron Spectral Measurements (R. C. Greenwood, A. J. Caffrey)

In a recent paper[2] we reported on measurements of the energy spectra of delayed neutrons for the isotope-separated fission-product precursors $^{93-97}Rb$ and $^{143-145}Cs$, over the region from $\sim$10 to $\sim$1300 keV. These data were obtained at the TRISTAN ISOL facility using gas-filled proton-recoil proportional counters. In that paper it was noted that, in the neutron-energy region above $\sim$800 keV, systematic deviations in intensities are apparent between the INEL data and other reported data sets. While the INEL proton-recoil data and the Rudstam ^3He ionization-chamber data[3]

---

1 "Decay Data of the Transactinium Nuclides", IAEA Technical Reports Series No. 261 (IAEA, Vienna, 1986).

2 R. C. Greenwood and A. J. Caffrey, Nucl. Sci. Eng. 91 (1985) 305.

3 G. Rudstam, Private Communication (1983), as reported in Ref. 2.

still appear to be reasonably consistent in that energy region, the normalized relative intensities in both of these data sets are significantly lower than those reported by Reeder[1] and Kratz[2], also measured with ^3He ionization chambers. It was further noted, however, that since finite-detector-size effects become significant above ~800 keV for the 2.6 Atm. CH_4 proton-recoil counter used to obtain the INEL data in this energy region, such discrepancies between the INEL data and ^3He data might be attributed to these effects.

Nevertheless, in an extension to our previously reported work[3], we thought it worthwhile to obtain additional delayed-neutron spectral information at these higher energies using higher pressure CH_4 gas-filled proportional counters together with a liquid scintillation counter, for comparison with the earlier ^3He data. To that end the following series of experiments was conducted: (1) measurements using a H_2 gas-filled proportional counter (2.6 Atm. pressure) with pulse-shape discrimination (between beta/gammas and neutrons) at a gain setting of 0.3 keV/channel; (2) measurements using a CH_4 gas-filled proportional counter (5.3 Atm. pressure) at a gain setting of 8 keV/channel; and (3) measurements using a 5.1-cm diameter x 1.27-cm thick BC-501 liquid scintillation detector with pulse-shape discrimination at a neutron gain setting of ~20 keV/channel.

Since, as noted above, it has been thought that finite-detector-size effects with the 2.6 Atm. CH_4 counter may have led to a distortion in the delayed-neutron spectral intensities reported above ~800 keV, it was thus of interest to compare the earlier intensity values with those obtained in the present work using the 5.3 Atm. CH_4 counter. This comparison, in the two highest energy groups (at 770.2 - 985.9 keV and 985.9 - 1262.0 keV) previously reported, shows that the intensity values obtained with the two separate detectors in these two energy regions are in rather good agreement, with no systematic deviations being apparent. Such agreement is somewhat surprising since the 2.6 Atm. CH_4 detector, as noted earlier, is operating in an energy region where it was thought that finite-size corrections could no longer be ignored.

In a somewhat complementary set of comparisons, the delayed-neutron intensity values for the precursors ^{95}Rb and ^{94}Rb measured using both the 5.3 Atm. CH_4 gas-filled proportional counter and the organic-liquid scintillation detector were compared for several energy groups over an energy region from ~1.4 MeV up to ~2.0 MeV. Bearing in mind that, for the 5.3 Atm. CH_4 counter, finite-detector-size effects are expected to become important above ~1250 keV, the degree of agreement between the neutron intensity values obtained with the two different detectors (with total

---

1 P. L. Reeder, Private Communication (1983) as reported in Ref. 3.

2 K.-L. Kratz, Private Communication (1983) as reported in Ref. 3.

3 R. C. Greenwood and A. J. Caffrey, Nucl. Sci. Eng. 91 (1985) 305.

discrepancies less than ±10%) is again somewhat surprising.

From these sets of comparisons we conclude that for these gas-filled proportional counters (with dimensions 2.54-cm diameter x 7.62-cm sensitive length) finite-detector-size corrections are still not too significant up to a neutron energy corresponding to a maximum proton range of ~15 mm. Also, our earlier assumption[1] that, in using the PSNS analysis code, differences between the response-corrected and uncorrected data represent the magnitude of the uncertainties resulting from finite detector size, seems at least reasonable, and probably conservative.

Improved delayed-neutron spectral-intensity distributions for $^{93-97}Rb$ and $^{143-145}Cs$ were then obtained by combining the present data with our earlier reported data[1] and are currently being prepared for publication. In regard to the comparison of the higher energy group intensities, the general conclusions cited in our earlier work remain unchanged, namely that, while the most recent INEL data and the Rudstam[2] data still appear to be reasonably consistent in this energy region, both of these data sets are significantly lower than those reported by Reeder[3] and Kratz[4].

3. <u>Niobium Irradiations in Standardized Neutron Fields</u> (J W Rogers, J. D. Baker, R. J. Gehrke)

Irradiations of niobium have been conducted in well characterized ^{252}Cf spontaneous fission neutron and ^{235}U fission neutron fields. The irradiated niobium material will be used to produce neutron fluence standards,and the activity produced by the $^{93}Nb(n,n')\,^{93m}Nb$ reactions will be used along with the neutron intensities to determine spectrum averaged neutron cross sections for this reaction.

High purity and well characterized niobium material has been obtained for these irradiations. The neutron field intensities of the ^{252}Cf and ^{235}U facilities have been measured by NBS using standardized fission chambers. Perturbations of the irradiations and measurements have been calculated to provide the necessary corrections. The ^{235}U facility at NBS and the ^{252}Cf facility at the University of Arkansas were used for the irradiations. The irradiated niobium material is being prepared for fluence standards at INEL. Since these irradiations could only produce low specific activity in the niobium material it will be necessary to produce sources with

1 R. C. Greenwood and A. J. Caffrey, Nucl. Sci. Eng. <u>91</u> (1985) 305.

2 G. Rudstam, Private Communication (1983) as reported in Ref. 1.

3 P. L. Reeder, Private Communication (1983) as reported in Ref. 1.

4 K.-L. Kratz, Private Communication (1983) as reported in Ref. 1.

large amounts (several mg) of niobium. To obtain the necessary accuracy in the activity, these sources nust be of uniform density and their attenuations accurately determined. Techniques to produce uniform sources have been developed and attenuation measuring techniques are being developed at INEL.

The results from these irradiations, measurements and calculations will produce accurately determined fission spectrum cross sections for these neutron fields, which will be used in data reduction and interpretation of neutron dosimetry with this reaction. Results will also be used to compare the measured reaction rates with calculated reaction rates as a test of the differential cross section data for these fission spectra. The results from these experiments will benefit nuclear technology by providing useful nuclear cross section data that will be applicable to light water reactors, breeder reactors, fusion reactors and any other fields which require fast neutron monitoring.

4. Intrinsic Reflection Asymmetry in Deformed Nuclei: the Odd-Mass Nuclide ^{225}Ra (C. W. Reich, R. G. Helmer, M. A. Lee, I. Ahmad* and G. A. Leander **)

Whether or not stable octupole-deformed equilibrium shapes occur as ground states of nuclei has been a topic of long-standing interest in nuclear physics. The light isotopes of radium have been almost everyone's leading candidate for the region of the Nuclide Chart where such states could occur, but only recently has substantial evidence emerged that effects related to octupole-deformed (or, more generally, intrinsic reflection-asymmetric) shapes do occur. Because of its location within this region, the nuclide ^{225}Ra has been the object of extensive study, using a wide variety of different experimental approaches, in the past few years. To provide additional information on the level structure of this important nuclide, we have carried out a detailed investigation of the level scheme of this nuclide, utilizing as a probe the α decay of ^{229}Th. This study has now been completed and the results submitted for publication.[1] It has provided a more complete, and somewhat different, picture of the low-energy level scheme of ^{225}Ra than was previously available. Careful analysis of the level structure of the $K\pi=\frac{1}{2}\pm$ "parity-doublet" bands has provided values for the decoupling parameters of the $\frac{1}{2}^+$ and $\frac{1}{2}^-$ bands of +1.89 and -2.56, respectively, considerably closer in absolute value than previously believed. We also propose a significantly different scheme of levels for the $K\pi=3/2+$ band at 149.87 keV, which implies a large amount of "staggering"

* Argonne National Laboratory

** Oak Ridge Associated Universities/UNISOR

1 R. G. Helmer, M. A. Lee, C. W. Reich and I. Ahmad, submitted for publication in Nuclear Physics A.

within this band. This study has also made possible an accurate determination of the "collective" E1 matrix element connecting the positive- and negative-parity members of the K=1/2 parity-doublet band. Utilizing the novel probe of the nuclear wave functions provided by these bands, we have also for the first time observed the effects of a $\Delta K = 1$ E1 matrix element in the reflection-asymmetric nuclei and deduced a value for it. These later results have been presented in a separate publication.[1]

5. Identification of New Neutron-Rich Rare-Earth Isotopes Produced in ^{252}Cf Fission (R. C. Greenwood, R. A. Anderl, J. D. Cole, H. Willmes*)

New neutron-rich isotopes of several rare-earth elements have been identified using the on-line mass separator system at the Idaho National Engineering Laboratory. In this system, spontaneous fission of ^{252}Cf is used as the source of fission products, with transport to the mass separator being achieved using a He gas-jet arrangement. The observed decay rates of K x rays in the mass-separated fractions, together with the associated γ-decay spectra provided direct isotopic identifications. New isotopes observed to date using the INEL ISOL system include ^{153}Pr, ^{155,156}Nd, ^{157,158}Pm and ^{162}Eu, with improved half-life values also being obtained for the recently reported isotopes, ^{153,154}Nd, ^{156}Pm, ^{159}Sm and ^{160}Sm.

Half-lives, together with the beta-decay energies and the distribution of Gamow-Teller strength, in neutron-rich nuclides such as those reported here are of importance in astrophysical calculations involving the rapid neutron-capture process (r-process). In calculations involving the r-process, because of lack of experimental data, it has been necessary to utilize predicted values of the half-lives of the relevant nuclides. Thus, as new data become available, it is desirable to check the validity of these predictions. At the present time, there exist two sets of half-life predictions, an earlier set by Takahashi *et al.*[2] based on the gross theory of beta decay and a recent set by Klapdor *et al.*[3] based on a microscopic model employing a description of the distribution of beta strength.

The new neutron-rich isotopes identified in this work extend the region of experimentally measured half-lives by roughly one unit of Z (along lines of constant A) and, therefore, present an opportunity to further expand

---

* University of Idaho

1 C. W. Reich, I. Ahmad and G. A. Leander, Physics Letters 169B (1986) 148.

2 K. Takahashi *et al.*, At. Data Nucl. Data Tables 12 (1973) 101.

3 H. V. Klapdor *et al.*, At. Data Nucl. Data Tables 31 (1984) 81.

TABLE A-1. Half-life values measured for the new neutron-rich rare-earth isotopes and their comparison with the results of two theoretical predictions.

Isotope	Experimental Half-Life: Present Work (sec)	Experimental Half-Life: Previous Work (sec)	Theoretical Half-life: Takahashi *et al.*[1] (sec)	Theoretical Half-life: Klapdor *et al.*[2] (sec)
^{153}Pr	4.3 ±0.2		14	2.81
^{153}Nd	28.9 ±0.4	32 ±4 (Ref. 3)	58	
^{154}Nd	25.9 ±0.2	26 ±2 (Ref. 4)	77	
^{155}Nd	8.9 ±0.2		18	15.3
^{156}Nd	5.47±0.11		24	8.36
^{156}Pm	26.70±0.10	28.2±1.1 (Ref.5)	25	8.39
^{157}Pm	10.90±0.20		22	4.68
^{158}Pm	4.5 ±0.5		10	2.31
^{159}Sm	11.37±0.15	15 ±2 (Ref.5)	31	10.1
^{160}Sm	9.6 ±0.3	8.7±1.4 (Ref.5)	67	6.06
^{162}Eu	10.6 ±1.0		18	9.35

1 K. Takahashi *et al.*, At. Data Nucl. Data Tables 12 (1973) 101.

2 H. V. Klapdor *et al.*, At. Data Nucl. Data Tables 31 (1984) 81.

3 J. A. Pinston *et al.*, Atomic Masses and Fundamental Constants 6, edited by J. A. Nolan, Jr., and W. Benenson (Plenum, New York, 1980) p. 493.

4 T. Karlewski *et al.*, Z. Phys. A 322 (1985) 177.

5 H. Mach *et al.*, Phys. Rev. Lett. 56 (1986) 1547.

the range over which experiment and model predictions can be compared. The adopted half-life values for the new isotopes and those other isotopes measured in this work are given in Table A-1. These values generally represent an average of the individual values measured for the K x-rays and the prominent γ rays which could be associated with each isotope. Shown in Table A-1, for comparison, are the theoretical predictions of Takahashi _et al._[1] and Klapdor _et al._[2] Further discussion of the comparison between the observed and the predicted half-lives is the subject of a paper presently in preparation.

6. _Ion-Source Development at the INEL ^{252}Cf ISOL Facility_ (R. A. Anderl, J. D. Cole, R. C. Greenwood)

The ISOL (Isotope Separation On Line) system at the INEL utilizes the He-gas-jet technique to transport fission products from ^{252}Cf spontaneous-fission sources (using up to $\sim$1 mg electrodeposits of ^{252}Cf) to the ion source of an electromagnetic mass separator. To ensure versatile and reliable operation of this ISOL system, the following ion-source design requirements were deemed to be most important: (1) high-pressure operation (several tens of Pascals of internal pressure); (2) long operating lifetime (no filament, insulator or other component failure for at least 100 hours); and (3) efficient and stable production of nongaseous fission-product elements.

The initial ion source design that evolved over the course of testing various ion-source configurations relative to the above requirements has focussed on the development of a gas jet-coupled, hollow-cathode ion source in which the cathode is heated by electron bombardment from an external filament. This design utilizes a cylindrical anode and a cylindrical cathode in a coaxial arrangement with insulators placed in the cooler portions of the source assembly. The arrangement for electron-bombardment heating of the cathode, namely the heat shielding and filament support structure is similar to that developed by Johnson _et al._[3] for a high-temperature ion source. These construction features were found to give a rugged ion-source assembly well suited to long lifetime operation at moderately high temperatures. The latest version of this ion source has a tungsten anode (6.4 mm ID x 0.5 mm W) and a tungsten cathode (9.5 mm ID x 1.0 mm W) with a 0.6 mm diameter outlet hole. Each tungsten cylinder is screwed into a tantalum base.

The performance of the high-temperature (surface ionization) mode of

---

1 K. Takahashi _et al._, At. Data Nucl. Data Tables _12_ (1973) 101.

2 H. V. Klapdor _et al._, At. Data Nucl. Data Tables _31_ (1984) 81.

3 P. G. Johnson, A. Bolson and C. M. Henderson, Nucl. Instrum. and Methods _106_ (1973) 83.

operation of this ion source has most recently been tested in the mass range 153 to 162. Estimates of the total separation efficiencies for selected rare-earth elements were obtained by analysis of some of the data acquired in conjunction with these studies. This determination was contingent on measuring gamma data for radionuclides for which absolute decay information is available. In the present series of experiments this was the case for ^{154}Pm and ^{158}Sm. Total separation efficiencies, defined as the ratio of radionuclide activity collected at the focal plane of the mass separator to radionuclide activity generated by the ^{252}Cf source, were estimated to be $\sim$1% for both ^{154}Pm and ^{158}Sm. Analysis of early data for Cs isotopes in which the ion source was operated at a lower temperature yielded estimates of the total separation efficiencies for ^{140}Cs, ^{141}Cs and ^{142}Cs of 1% to 2%.

Arc-discharge performance of the ion source was assessed by means of measured Kr and Xe ionization efficiencies. These efficiencies were determined by injecting stable Kr and Xe gas into the ion source through controlled leaks and then measuring the appropriate beam currents at the focal plane of the mass separator. Maximum Kr and Xe ionization efficiencies of only a few percent were achieved with the ion source operating in a closed configuration, that is, uncoupled from the gas-transport arrangement. In the coupled configuration, the Kr and Xe ionization efficiencies were typically reduced to a few tenths of a percent. Post-test inspection of the various anode components typically showed significant erosion along the outer surface of the anode cylinder with less erosion of the end facing the cathode outlet. This indicated that the most intense discharge was occurring radially between the cathode and anode. The implication of these observations is that the cylindrically concentric, anode-cathode configuration is not suitable for efficient ionization and extraction of trace atoms.

7. <u>The Muon-Catalyzed Fusion Alpha Sticking Probability and the Infuence of ^{5}He(3/2+) Nuclear Resonance.</u> (A. J. Caffrey, C. De W. Van Siclen)

Muon-catalyzed fusion research has undergone a vigorous rebirth in recent years. In particular, the prediction[1] and experimental confirmation[2, 3] of a resonant mesomolecular formation process in deuterium-tritium mixtures have renewed interest in this field, including possible energy production. Our laboratory is engaged in muon-catalysis

---

1 S. S. Gershtein and L. I. Ponamarev, Phys. Lett. <u>72B</u> (1977) 80.

2 V. M. Bystritskii, <u>et al</u>., Sov. Phys. JETP <u>53</u> (1981) 887.

3 S. E. Jones, <u>et al</u>., Phys. Rev. Lett. <u>51</u> (1983) 1757.

experiments at LAMPF[1], in collaboration with groups from Brigham Young University and Los Alamos National Laboratory. In this brief note, we will outline the muon catalysis cycle in d-t mixtures, and discuss the possible influence of the $^5He(3/2^+)$ nuclear resonance.

As shown in Fig. A-1, the catalysis cycle begins with the stopping of a free negative muon in the d-t mixture. Next, either a d-mu or t-mu atom is formed. If the muon binds to a deuteron, it usually transfers to a triton, since, due to reduced-mass effects, the binding energy of a t-mu atom is 50 electron volts greater than that of a d-mu atom. The t-mu is a small, neutral body, on an atomic scale, and it easily penetrates the electron cloud of the D_2 and DT molecules in the gas mixture. If the energy of the t-mu atom meets the resonance condition, the formation rate of the dt-mu molecule is greatly enhanced over the non-resonant (Auger) process. Fusion follows molecular formation in about a picosecond. The muon is usually free to catalyze further cycles.

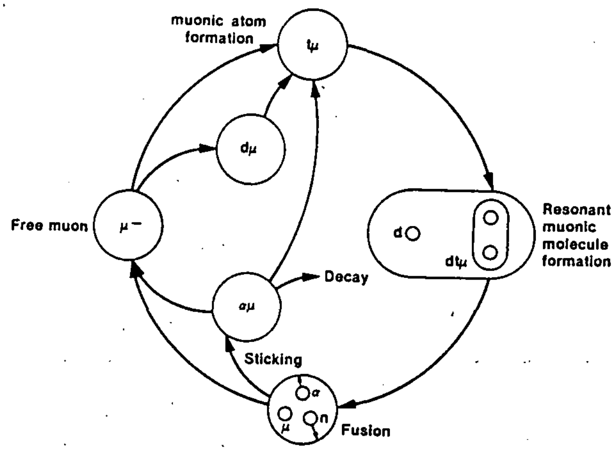

Figure A-1
Muon Catalysis Cycle

Two loss mechanisms dominate the cycle. The muon can beta-decay at any point in the cycle. However, under favorable conditions, the cycling rate is high enough to permit perhaps 1000 cycles during the two microsecond muon lifetime. Also, the muon can stick to the outgoing alpha particle. This loss mechanism is more serious, limiting the possible number of cycles to about 200; in other words, the alpha sticking probability is about 0.5%.

At present, the alpha sticking probability following muon-catalyzed d-t fusion is the outstanding theroretical and experimental problem in this field. Our present knowledge of the alpha sticking probability is summarized in Table A-2.

1 A. J. Caffrey, et al., Proceedings of the International Symposium on Muon-Catalyzed Fusion, Tokyo, Japan, 1-3 September, 1986, to be published.

Table A-2. Alpha Sticking Probability

Probability(%)	Method	Authors	Year
0.86	Theory	Aristov *et al.*[1]	1981
0.91	Theory	Bracci and Fiorentini[2]	1982
0.89	Theory	Ceperley and Alder[3]	1985
(0.35±0.05)	Experiment	Jones *et al.*[4]	1986
0.58	Theory	Bogdanova *et al.*[5]	1986
(0.40±0.05)	Experiment	Breunlich *et al.*[6]	1987

Experiments at LAMPF[4] and SIN[6] both report sticking probabilities 0.4% or less, while theoretical work generally predicts sticking should 0.6% or greater. The uncertainties of the experimental measurements are probably 0.1% or better. In an effort to resolve this

1 Aristov *et al.*, Yad. Fiz. 33 (1981) 1066. [Sov. J. Nucl. Phys. 33 (1981) 564.]

2 L. Bracci and G. Fiorentini, Phys. Rep. 86 (1982) 169.

3 D. Ceperley and B. J. Alder, Phys. Rev. A 31 (1985) 1999.

4 S. E. Jones, *et al.*, Phys. Rev. Lett. 56 (1986) 588.

5 L. N. Bogdanova *et al.*, Preprint JINR E4-85-425, 1985, Dubna; Proceedings of the International Symposium on Muon-Catalyzed Fusion, Tokyo, Japan, 1-3 September, 1986, to be published.

6 W. H. Breunlich, *et al.*, Phys. Rev. Lett. 58 (1987) 329.

discrepancy, J. Rafelski and colleagues[1] have calculated that the $^5He(3/2+)$ nuclear resonance may have a strong effect on the sticking coefficient, perhaps reducing it as much as an order of magnitude. The theoretical debate centers on the effect of the nuclear fusion reaction on the muonic wave function, or in simple terms, how well does the "sudden approximation" describe the muon-alpha system after fusion?[2]

Recently, Takahashi[3] demonstrated the sensitivity of the alpha sticking probability to the energy and width of the $^5He(3/2+)$ nuclear resonance. In 1983 the resonance energy and width were re-measured by Haesner and colleagues[4] in a time-of-flight experiment over a 180 meter flight path. Their results differ from the most recent evaluation[5], likely due to the impressive energy resolution ($\Delta E/E = 1.3 \times 10^{-3}$ at 40 MeV) in their measurement. We would like to learn if the measurements of Haesner _et al_. are considered definitive at this time, and if improved values of the resonance energy and width will become available.

B. NUCLEAR DATA EVALUATION

1. Mass-Chain Evaluation for the Nuclear Data Sheets (M. A. Lee, R. G. Helmer, C. W. Reich)

As part of our involvement in the work of the International Nuclear Structure and Decay Data Evaluation Network, which carries out the evaluation of basic nuclear-physics data for publication in the Nuclear Data Sheets, we have the evaluation responsibility for the ten mass chains in the region $153 \leq A \leq 162$. The plan for the evaluation of these mass chains has been to undertake those most out of date first.

---

1 J. Rafelski, B. Mueller, and M. Danos, Proceedings of the International Symposium on Muon-Catalyzed Fusion, Tokyo, Japan, 1-3 September, 1986, to be published.

2 L. N. Bogdanova _et al_., Preprint JINR E4-85-425, 1985, Dubna; Proceedings of the International Symposium on Muon-Catalyzed Fusion, Tokyo, Japan, 1-3 September, 1986, to be published.

3 H. Takahashi, J. Phys. G: Nucl. Phys. 12 (1986) L271.

4 B. Haesner, _et al_., Phys. Rev. C 28 (1983) 995.

5 F. Ajzenberg-Selove, Nucl. Phys. A413 (1984) 9.

The status of the evaluation work for our region of responsibility can be summarized as follows:

A Chain	Status (according to currency)
158	evaluation underway; last published 1980.
157	evaluation underway; last published 1983 (literature cutoff date: 12/80).
154	submitted for publication (1986).
159	submitted for publication (1986).
155	to appear in NDS (early 1987).
156	NDS 49 (1986) 383.
160	NDS 46 (1985) 187.
162	NDS 44 (1985) 659.
161	NDS 43 (1984) 1.
153	NDS 37 (1982) 487.

As is evident from this listing, with the completion of the A=157 and 158 evaluations, our mass chains will satisfy one of the desired objectives of the international evaluation network, namely currency < 5 years.

The mass-chain evaluation effort at INEL is beginning to be affected favorably by our increasing use of IBM-AT PC's to construct and edit the various individual data sets. This year, the ability to use lower-case characters, which has not been possible in the past, has been developed. In addition, an effort to convert a number of the major processing codes used in the mass-chain evaluation from main-frame-type (e.g.,CYBER) computer systems for use on PC's was initiated. The Belgian group of mass-chain evaluators has taken the lead in doing this. We have implemented three of these programs during the past year. However, in order to avoid problems arising from the potential proliferation of various versions of these codes (based on variants in the underlying processing codes employed by different groups), we have suggested that some standardization and coordination be set up for these conversions. This suggestion has been accepted, and our code-conversion effort will be coordinated with that of other evaluation groups.

2. <u>IAEA Coordinated Research Program on Decay Data for Ge Detector Efficiency Calibration</u> (R. G. Helmer)

An advisory group meeting was convened May 30-31, 1985 in Grenoble by the International Atomic Energy Agency (IAEA) to discuss the status of the quality of the decay data for the nuclides commonly used for the efficiency calibration of Ge detectors for gamma- and X-ray spectrometry. The participants in the meeting were from nine laboratories in seven countries, including R. G. Helmer from the INEL.

The goal of this group will be to get subsequent evaluators to use the values it recommends and, thereby, generate one internationally adopted set of values. To achieve this goal will require some promotion after the technical work is done. In order to reach this goal it was agreed that even in cases where the decay data are sufficiently accurate for efficiency calibration, this group should generate an evaluated value on which it agrees. The quantities to be evaluated are the nuclide half-life and the emission probabilities of the gamma and X rays that are used for Ge detector efficiency calibrations. It is also the purpose of the group to identify cases for which new measurements are needed, that is, where the data are poor or discrepant. The Advisory Group recommended the formation of a Coordinated Research Program (CRP) to address these issues. This CRP has now been formed.

The group agreed on the preliminary list of 32 nuclides given in Table B-1. A preliminary evaluation of the data for these nuclides has been carried out. At INEL we have evaluated the gamma-ray emission probabilities for ^{152}Eu and ^{155}Eu. We have also supplied a list of the X- and gamma-ray energies for all 32 nuclides.

TABLE B-1. Nuclides to be Considered in IAEA Review of Decay Data

^{22}Na	^{75}Se	^{137}Cs
^{24}Na	^{85}Sr	^{139}Ce
^{46}Sc	^{88}Y	^{152}Eu
^{51}Cr	^{93m}Nb	^{154}Eu
^{54}Mn	^{94}Nb	^{155}Eu
^{55}Fe	^{95}Nb	^{198}Au
^{56}Co	^{109}Cd	^{203}Hg
^{57}Co	^{111}In	^{228}Th(with daughters)
^{58}Co	^{125}I	
^{60}Co	^{133}Ba	^{241}Am
^{65}Zn	^{134}Cs	^{243}Am

3. <u>Participation in One of the Working Groups of the ICRM (R. G. Helmer)</u>

R. G. Helmer of INEL has been named Coordinator of the Gamma- and Beta-Ray Spectrometry Working Group of the International Committee for Radionuclide Metrology (ICRM). During the year he has been in contact with members of this Working Group (which represents metrology groups in 23 countries) to determine a new program for the Group. In response to inquiries concerning technical interest and leadership availability, three actions have developed. These are: the measurement of the emission probabilities of the gamma rays from ^{75}Se decay, to be led by R. Jedlovszky of the National Office of Measures in Hungary; a study of detection limits, to be led by J. E. Cline of Science Applications International, U.S.A., and one on peak-area fluctuations, to be led by F. E. Schima of the National Bureau of Standards, U.S.A.

DECAY STUDIES OF FISSION PRODUCTS WITH TRISTAN AT THE HFBR AT BNL

The TRISTAN on-line mass separator facility at the High Flux Beam Reactor at Brookhaven National Laboratory is used to study the decays of mass-separated neutron-rich nuclides produced in thermal neutron fission of ^{235}U. A number of different elements can be ionized and separated using a variety of ion sources. Measurements made at TRISTAN are discussed below. Members of the Ames Laboratory group (John C. Hill, F. K. Wohn, and J. A. Winger) have collaborated with other users from BNL (R. F. Casten, R. L. Gill, and H. Mach), R. Moreh, A. Wolf and Z. Berant (Nuclear Research Centre, Beer Sheva, Israel) and R. F. Petry (U. of Oklahoma). Experiments involved decay scheme studies via γ-ray spectroscopy, $\gamma\gamma$ angular correlations, $\beta\gamma$ coincidences and perturbed angular correlations.

1. Decay of ^{80}Zn to Levels in Odd-Odd ^{80}Ga (Winger *et al.*, Gill *et al.*)

The decay of ^{80}Zn to levels in ^{80}Ga was studied at TRISTAN. Based on γ singles and coincidence measurements, 26 γ rays were placed in a level scheme for ^{80}Ga with 13 excited states up to 2655 keV. The emission of a γ ray following delayed neutron emission of ^{80}Ga was observed. Five levels in ^{80}Ga were observed to be fed by allowed β transitions. They were postulated to be proton-particle neutron-hole states. The measured properties reported for ^{80}Zn and ^{80}Ga are also of astrophysical interest for modeling the r process of nucleosynthesis. This work has been published[1] in a brief form in a recent letter and the more complete results have been submitted to Phys. Rev. C.

2. Decay of ^{82}Ga by Beta and Delayed-Neutron Decay (Winger *et al.*)

The decay of ^{82}Ga to levels in the N=50 isotone ^{82}Ge was studied by γ singles, $\gamma\gamma$ coincidence, and angular correlations. The structure of ^{82}Ge is of interest since it can be pictured as 4 protons outside of a doubly-magic ^{78}Ni core. The half-life was measured to be 0.62 ± 0.02 s. ^{82}Ga decays to 7 excited states in ^{82}Ge ranging up to 3257 keV by the emission of 11 γ rays. Delayed-neutron decay from ^{82}Ga results in the emission of 6 γ rays which depopulate excited states in ^{81}Ge up to 1723 keV. The structure of ^{82}Ge is being modeled using a large-space shell-model calculation.

---

[1] Gill, Casten, Warner, Piotrowski, Mach, Hill, Wohn, Winger, and Moreh, Phys. Rev. Lett. 56, 1874 (1986).

3. Decay of ^{83}Ge to Levels in the N=50 Isotone ^{83}As (Winger *et al.*)

The decay of ^{83}Ge to levels in the N=50 isotone ^{83}As was investigated by γ singles, multispectral scaling, and $\gamma\gamma$ coincidence techniques. The structure of ^{83}As is of interest since it can be pictured as 5 protons outside of a doubly-magic ^{78}Ni core. We have measured the half-life to be 1.85±0.07 s. A total of 50 γ rays have been assigned to ^{83}Ge decay. The level scheme for ^{83}As includes 27 excited states from 306 to 4841 keV. Calculations on the structure of ^{83}As are being carried out in collaboration with B. H. Wildenthal. Preliminary results imply that the region around ^{78}Ni is doubly magic in character.

4. Decay of ^{100}Sr and a Pairing-Free $K^{\pi}=1^{+}$ Rotational Band in Odd-Odd ^{100}Y (Wohn *et al.*)

The decay of ^{100}Sr (193 ms) to the low-spin ^{100}Y isomer (735 ms) was studied from mass-separated activity produced in thermal neutron fission of ^{235}U. γ singles and $\gamma\gamma$ coincidence measurements resulted in the placement of 67 γ transitions in a decay scheme with 26 levels below 2 MeV. Multipolarities of low-energy transitions were determined from internal conversion electron measurements. An absolute γ intensity determination for the A=100 decay chain beginning with ^{100}Sr allowed log*ft* determinations to be made. The 1^{+} levels in ^{100}Y at 10.7 and 974.6 keV each receive ~ 40% of the β feeding from ^{100}Sr. A $K^{\pi}=1^{+}$ rotational band, with 1^{+}, 2^{+}, and 3^{+} levels at 10.70, 76.15, and 172.03 keV, can be characterized as a nearly pairing-free band. Other levels in ^{100}Y are discussed in terms of two-quasiparticle Nilsson orbitals.

5. Decay of ^{101}Sr and Rotational Structure of ^{101}Y (Wohn *et al.*)

The level structure of ^{101}Y has been studied through the decay of ^{100}Sr ($T_{1/2}$=121±6 ms). 90 γ rays have been placed in a level scheme with 32 levels. Five rotational bands are identified which include all but 3 levels below 1.2 MeV. The 5 lowest bands, which are associated with the Nilsson orbitals (and bandhead energies in keV) 5/2[422] (0), 3/2[301] (510), 5/2[303] (666), 3/2[431] (996), and 1/2[431] (1217), are similar in many respects to those observed for ^{99}Y. As is the case for ^{99}Y, the rotational characteristics of ^{101}Y indicate an axially symmetric deformation in the range of 0.3 to 0.4 However, unlike ^{99}Y, where simple particle-rotor calculations were quite successful in producing a self-consistent picture of the nuclear structure, several ambiguities remain after similar calculations for ^{101}Y.

6. Identification and Decay of ^{102}Sr (Hill *et al.*)

A study of the decay of ^{102}Sr to levels in ^{102}Y was reported earlier. This material has now been published in Phys. Rev. C.[2]

7. Decay of ^{102}Y to the Even-Even Nucleus ^{102}Zr (Hill *et al.*)

Past studies[3] of the decay of ^{102}Y to levels in ^{102}Zr indicate that ^{102}Zr is quite deformed. In these studies at the JOSEF separator population was probably mostly from the decay of a high-spin isomer of ^{102}Y. At TRISTAN we have carried out similar studies but in this case population of the low-spin isomer of ^{102}Y is enhanced due to feeding from even-even ^{102}Sr. Analysis of γ singles and coincidence data is in progress.

8. g-Factor of the 359-keV Level in ^{142}Ba (Wolf *et al.*, Winger)

The g-factor of the 2^+, 359-keV level in ^{142}Ba has been measured using the time-differential perturbed angular correlation method. A preliminary value of 0.41±0.06 is an improvement over a previously reported value.[4] This value compares quite well with the value of $g(2_1^+)=0.40$ predicted by the IBA-2 model. Continued analysis of the data is presently in progress.

9. Decay of ^{148}Cs to Levels in ^{148}Ba (Hill *et al.*)

The decay of ^{148}Cs to levels in the even-even nucleus ^{148}Ba was studied by γ singles and $\gamma\gamma$ coincidence measurements. The ^{148}Cs half-life was determined to be 171 ms. A total of 9 γ rays were placed in a level scheme with 5 excited states up to 1049 keV. Values of $E(2_1^+)$, $E(4_1^+/2_1^+)$, and $E(2_2^+)$ are in excellent agreement with interpolative predictions from systematics of the valence-nucleon product. These results have been published[5] in a recent issue of Phys. Rev. C.

---

[2]Hill, Winger, Wohn, Petry, Goulden, Gill, Piotrowski, and Mach, Phys. Rev. C 33, 1727 (1986).

[3]Shizuma, Hill, Lawin, Shaanan, Selic, and Sistemich, Phys. Rev. C 27, 2869 (1983).

[4]Gill, Warner, Wolf, and Winger, Phys. Rev. C 34, 1983 (1986).

[5]Hill, Wohn, Leininger, Winger, Nieland, Gill, Piotrowski, Petry, and Goulden, Phys. Rev. C 34, 2312 (1986).

10. Search for New Isotopes in the Mass 149-152 Region (Mach *et al.*, Winger)

The decay of several new isotopes in the mass 149-152 region have been investigated using γ singles, multispectral scaling, xγ and $\gamma\gamma$ coincidences. The previously known mass 149 nuclei ^{149}Ba and ^{149}La have been observed with half-lives of 0.4 and 1.2 s respectively. Three γ-ray transitions were found in the decay of ^{149}Ba, and 8 were found for ^{149}La. Three new isotopes have been identified: ^{150}Ba ($T_{1/2}$=0.3 s), ^{150}La ($T_{1/2}$=0.7 s) and ^{151}Pr ($T_{1/2}$=14 s). Analysis of the data is still in progress.

DIRECT MASS MEASUREMENTS OF LIGHT NUCLEI WITH TOFI AT LAMPF AT LANL

The TOFI (time-of-flight isochronous) spectrometer located on-line to the main beam line of the LAMPF accelerator at Los Alamos National Laboratory is used to determine the atomic masses of neutron-rich light nuclei produced in heavy-target fragmentation reactions. F. K. Wohn of the Ames Laboratory collaborates with Los Alamos scientists D. J. Vieira, J. M. Wouters, and G. W. Butler in the TOFI project. Other collaborators are H. Wollnik (Justus-Liebig Univ., Giessen, Germany), K. Vaziri (Utah State Univ.) and R. H. Kraus, Jr. and D. S. Brenner (Clark Univ.). The first completed study is reported below. Future studies will extend mass measurements up to Z $\simeq$ 40.

1. Direct Mass Measurements of Neutron-Rich Light Nuclei Near N=20 (Vieira *et al.*, Wollnik, Vaziri, Kraus, Wohn, Wapstra)

This study was published in a recent letter[6]. It reports on the simultaneous direct mass measurements of 21 neutron-rich nuclei ranging from ^{19}C to ^{37}P. The masses of ^{19}C, $^{27-28}$Ne, $^{32-34}$Al, ^{36}Si, and ^{37}P were determined for the first time. The most notable feature in the data is the smoothly decreasing trend in the two-neutron separation energies with increasing neutron number for $^{30-32}$Mg and $^{32-34}$Al, which is consistent with the smooth trend for $^{33-36}$Si but contrasts sharply with the behavior for $^{31-33}$Na. These trends indicate that, just below N=20, Mg, Al and Si nuclei can be well described within the sd shell. Only the Na nuclei give clear indications of a broken sd shell and consequent deformation for N near 20.

[6] Vieira, Wouters, Vaziri, Kraus, Wollnik, Butler, Wohn, and Wapstra, Phys. Rev. Lett. 57, 3253 (1986).

UNIVERSITY OF KENTUCKY

That part of the research program at the University of Kentucky carried out in the local Van de Graaff laboratory continues to be centered on four main areas of work; neutron scattering studies, nuclear structure studies using the (n,n'γ) reaction, nucleon and alpha particle studies, and experiments to answer questions of astrophysical interests. The facility for doing capture experiments became operational in the past year and two experiments are in progress. A fifth area of study, the study of an anomaly in the imaginary part of the optical potential, was reactivated this past year. Detailed descriptions of recent progress in each of these five areas is given below. Research in intermediate energy and radioactive decay carried out in laboratories at other sites is not appropriate for inclusion in this report and has been omitted.

A. NEUTRON SCATTERING

1. Collective Excitations in Neutron Scattering

Several neutron scattering studies for well deformed target nuclei were completed in the late 70's and early 80's. These showed that quadrupole rotational excitations were coupled into the scattering with the same basic strength in neutron scattering as in proton scattering or in Coulomb excitation. Valence proton and neutron motions in these nuclei seem to be tightly coupled, so that the same surface excitations are excited with any hadronic probe. There were hints in some of those studies, though, that γ-band excitations were not so well described in the scattering analyses. But the major emphasis had been on the ground band excitations, so the effects of other excitations had not been very carefully examined.

a. Os-Pt Scattering Studies at Low Energies (S.E. Hicks, M.T. McEllistrem)

An extensive program of experiments and analyses was begun some time ago in this laboratory to study the shape-transitional osmium and platinum nuclei through neutron scattering. These nuclei were selected for study because they are in a nuclear region where γ-band excitations are very strong and also quite variable from one nuclide to another. Since earlier work had taught us that accurate knowledge of total cross sections was indispensable for a confident interpretation of the role of structure effects in scattering, these were measured for neutron energies (E_n) from 300 keV to 4 MeV, as well as differential scattering cross sections at several neutron energies. An 8-MeV scattering experiment was performed in France, and the others were done in our laboratory. Data taking and interpretations are complete for ^{194}Pt, so that results of that study can help guide future efforts in other nuclei.

A large surprise from the ^{194}Pt study was that quadrupole coupling amplitudes in the quasi-ground band are 15% stronger for neutrons than the amplitudes of

Coulomb excitation. There are several recent Coulomb excitation and electromagnetic decay studies, and they result in amplitudes substantially weaker than previously thought. The neutron scattering data is so extensive that the coupling is quite well defined for this probe. The difference is quite striking, and clear, for the coupling in the two classes of experiments.

Since ^{194}Pt is generally regarded as a strongly collective nucleus, although not clearly deformed, equality of coupling strengths for hadron scattering might have been expected. Instead we find differences at least as large as those reported for semi-magic nuclei, well away from strong collective excitations. Even though different probes have excitation strengths which scale differently, both proton and neutron scattering are shown to be best characterized with ^{194}Pt regarded as a nucleus very soft to changes in shape upon excitation. All hadron scattering experiments are best described with γ-soft models. This character of ^{194}Pt is much better manifested in scattering studies than in bound state decay studies; this is a very strong conclusion.

Preliminary analyses of neutron scatttering by ^{190,192}Os show γ-band excitations very different from those of ^{194}Pt. These nuclei do show clear prolate deformation, and hence direct coupling strengths may behave quite differently than was found in the Pt study. Scattering is also being studied for ^{196}Pt, which is structurally quite similar to ^{194}Pt, except that it does seem to have a well defined oblate shape at low excitation energies. It will be very interesting to see whether nuclei that are more clearly deformed will have excitation strengths more nearly equal for all hadronic probes.
Another surprising finding of the ^{194}Pt study was that the scattering potential strength saturates below 5 MeV neutron energy, in a manner similar to that observed for scattering from ^{208}Pb. This non-linear energy dependence of scattering potential has been attributed to effective mass anomalies near the Fermi surface. We also found that the scattering geometry is energy dependent, again in a manner similar to that attributed earlier to effective mass anomalies. In Pt nuclei, even at low energies, we are well above the Fermi energy. This surprising potential behavior presents a question clearly important to pursue in other nuclei in this mass region. One paper dealing with this Pt study has been published.[1]

b. Pb Isotope Scattering Study (J.M. Hanly, G.R. Shen, M.T. McEllistrem)

Several years ago data taken here with incident neutron energies between 7 and 9 MeV showed that strong, well grouped collective excitations existed in ^{208}Pb up to about 5.5 MeV excitation energy. These included known odd-parity excitations and some which are probably even parity, though not yet completely identified. Data taken here also for ^{206}Pb showed

---

[1] Mirzaa, Delaroche, Weil, Hanly, McEllistrem and Yates, Phys. Rev. C32, 1488 (1985).

most of the same collective excitations, except that some of the higher energy ones seemed to be diffusing into nearby levels, so that isolated collective groups were not so visible. Data are now being taken for ^{204}Pb, far enough from doubly magic ^{208}Pb that collective excitations might be quite indistinct.

2. Neutron Scattering from Spherical Nuclei

a. The Five Even-A Sn Isotopes (R. Harper, Z. Zhou, J.L. Weil)

An extensive study of neutron scattering in the spherical, even-A Sn isotopes has been concluded, to test whether nuclear dynamics of the target structures must be explicitly included when determining scattering potentials, even when target excitations are weakly coupled, as in the Sn isotopes. A part of the test was to determine whether including the target excitations would be important to seeing properly the systematic behavior of scattering potentials at low neutron energies.

Previous work[1,2] in this laboratory at low energies (E_n < 5 MeV) and with strongly collective nuclei demonstrated clearly that target dynamics have very strong effects on scattering potentials; spherical or single channel scattering models are useless in describing scattering for such nuclei. Other work carried out near 7 MeV and above show that at those energies elastic scattering is insensitive to the nature of collective excitations, even in strongly collective nuclei. The question of the role of dynamics for weakly coupled excitations in spherical nuclei is really a low energy question.

A second aspect of our study of scattering in the Sn nuclei was that those nuclei provide an excellent testing ground, at low energies, for modified forms of statistical models for distribution of absorbed flux into the various open scattering channels. At quite low energies, 1.63 MeV, only a few strongly coupled channels are present, while at E_n = 4 MeV many strongly and weakly excited levels are open. The two situations provide excellent opportunities for testing appropriate modifications which accommodate level width fluctuations and channel-channel correlations, both modifications needed to the original form of the statistical model of Wolfenstein, Hauser, and Feshbach (WHF) formulated in 1952. Neutron scattering from spherical nuclei provides a sensitive test of the new forms of the statistical model.

The analytical approximations to fluctuation and correlation corrections of Herman, Hofmann, and Weidenmuller (HHW)[3] were used to treat compound elastic and inelastic scattering at neutron energies of 1.63 and 4.0 MeV. At 1.63 MeV

---

[2] Coope, Tripathi, Schell, Weil, and McEllistrem, Phys. Rev. C16, 2223 (1977).

[3] Tepel, Hofmann and Herman, Proc. Int. Conf. Nucl. Cross Sect. for Technology, NBS Spec. Pub. 594, 762 (1980).

only two scattering channels are open, providing a good test of the model in this limited situation, where it should work with least difficulty. The results are that the modifications of the statistical model are clearly shown to be necessary; no realistic changes in the scattering potentials can mask the need for the corrections. When corrections are applied via the HHW approximation, the resulting fits are excellent.

Further tests done at E_n = 4.0 MeV, where many weakly excited, and a few strongly excited channels are open, provide exactly the same results. The HHW form of the model provides excellent fits to the measured cross sections. We feel that this is the first definitive test of these correction models for scattering, in that the scattering potential has been carefully developed to fit low energy scattering properties, total cross sections over a wide energy range, and differential scattering cross sections at several energies. The potential is unusually well determined.

The results of tests of including target excitations for the Sn nuclei are that a consistent fit to all of the measurements could not be obtained unless the quadrupole collectivity, not only of the first 2^+ level, but also of the two phonon triplet were both included. Without such dynamics coupled into the analyses, one could write interpretations which would work for a single incident energy, but the different incident energy scattering experiments could not have a consistent interpretation.

Another long standing problem was resolved through the careful measurements of total cross sections and two phonon coupled channels modelling of differential scattering cross sections. The s-wave strength function for ^{120}Sn had been carefully determined to be $S_o = 0.13 \times 10^{-4}$, while the p-wave value is about 2×10^{-4}. It had been commonly understood that such sharply different absorption properties in s-wave and p-wave scattering, differing by more than a factor of ten, could not be accommodated within a single model which also fit all of the other scattering data. However the results of the present coupled channels model shows that all of the scattering properties are well represented, within their experimental uncertainties. Even in weakly collective nuclei like the Sn isotopes, that collectivity must be incorporated into the interpretation to 2nd order, if the data are to be properly described. The analyses of this Sn study are essentially complete. After a few tests for consistency are completed, the work will be published. Two papers on portions of the project have already been published.[4]

b. Ca Isotopes Scattering Study (S.F. Hicks, M.T. McEllistrem)

Preliminary data have been taken for scattering from a separated isotope sample enriched in ^{48}Ca. The nucleus ^{49}Ca has a low neutron separation energy and, in consequence, clean, well separated resonances in low energy neutron scattering. Some of the broad resonances are either known to

---

[4] Harper, Godfrey and Weil, Phys. Rev. C26, 1432 (1982). Harper, Weil, and Brandenberger, Phys. Rev. C30, 1454 (1984).

arise, or suspected of arising, from coupling of collective bound states of ^{48}Ca into the continuum. These coupled excitations are true intermediate resonances, based on collective excitations rather than the expected particle-hole configurations. The coupling to these excitations, and the degree to which that coupling spreads the collective excitations into the scattering continuum, provides insights into reaction mechanisms which are very important not only for neutron scattering but also for other projectiles.

B. NUCLEAR STRUCTURE STUDIES

1. Studies of Dynamical Symmetries

a. O(6) Symmetry (R. Gatenby, E.W. Kleppinger, S.W. Yates)

The O(6) symmetry of the Interacting Boson Approximation (IBA) was first found to be exhibited by the nucleus ^{196}Pt, and many nuclei in this mass region have been subsequently described in terms of small, systematic departures from this limit. Partly within the spirit of examining the applicability of the IBA, we have studied the structures of Pt nuclei with A = 194, 196, and 198. The lighter two were adequately characterized as noted above, but ^{198}Pt seemed not to fit any of the collective models employed to represent nuclei in this mass region. Studies of the Os isotopes with A = 190 and 192 have also been completed, and examined in the light of IBA predictions. Recently, Fewell has suggested that the U(5) description is more appropriate than O(6) for ^{196}Pt. In view of the large mass of data which seem to argue for the O(6) interpretation, it is difficult to support Fewell's contentions. But it is clear that parts of the ^{196}Pt spectrum which have yet to be studied, at higher excitation energies, will need examination.

It is appropriate to mention here that, in a desire to examine the O(6) region of Pt nuclei in a comprehensive manner, we have pursued measurements at other laboratories which extend our knowledge of ^{198}Pt and ^{200}Pt. In recent measurements at the JYFL-Jyvaskyla, Finland, we have performed a preliminary $(p,p'\gamma)$ study of ^{198}Pt. The ultimate aim is to measure the lifetime of the anomalously low-lying first excited 0^+ state. In the nucleus ^{200}Pt we have put together an extensive picture of the low-lying collective states with results from the (t,pe^-) and $(t,p\gamma\gamma)$ reactions performed at LANL with the LLNL Spectroscopy Group. The latter study marks the first observation of γ decay in this nucleus.

Recently Casten and von Brentano have recognized that another extensive O(6) region exists in the Xe-Ba nuclei. To examine this region in greater detail we have initiated a study of ^{134}Ba, the lightest isotope for which sufficiently large scattering samples can be obtained. There is an amazing similarity between this nucleus and ^{196}Pt, and all of the properties of ^{134}Ba which we have measured to date support the contention that this is indeed also a good O(6) nucleus.

2. Nuclei Near Closed Shells and Subshells

a. Nuclei near ^{208}Pb (R. Gatenby, E.W. Kleppinger and S.W. Yates)

Our previous studies of nuclei in the Pt region have led us quite naturally to explore the nuclei closer to the ^{208}Pb double shell closure. We have in progress detailed studies of the heaviest stable mercury nuclei, ^{202}Hg and ^{204}Hg. Since only very small (<1.5 g) scattering samples of these isotopes are available, these studies severely test our techniques. While data analyses are still in progress, and additional measurements will be necessary and are planned, we are pleased that we have been able to uncover a great deal of new information about these nuclei, especially ^{204}Hg. It is our feeling that this nucleus, with two neutron holes and two proton holes, should provide an excellent test of shell model calculations in this region.

b. Nuclei near ^{146}Gd (S.W. Yates)

Extensive work by Kleinheinz and coworkers has shown that ^{146}Gd exhibits many of the properties of a doubly magic nucleus, and thus that a proton shell closure exists at $Z = 64$. We have recently enjoyed very successful collaborations with Peter Kleinheinz and his group at the Kernforschungsanlage-Julich, and the nuclear spectroscopy group at LLNL, in studying the important ^{146}Gd nucleus with a variety of techniques.[5] We were able to identify many proton particle-hole excitations from the $(\alpha,2n)$ spectroscopic measurements and neutron excitations from the (p,t) reaction data.

c. A Double Subshell Closure at ^{96}Zr (G. Molnar, R. Gatenby, E.W. Kleppinger and S.W. Yates)

Following the arrival of Dr. Gabor Molnar from the Institute of Isotopes in Budapest, we commenced an extensive series of $(n,n'\gamma)$ measurements on the doubly closed subshell nucleus ^{96}Zr. This nucleus is one of the few which exhibits this unique property of double subshell closure and is at the same time most amenable for study. Our measurements have been supplemented by β-decay measurements which included γ-γ angular correlations at the TRISTAN facility at Brookhaven National Laboratory and an attempt to measure Doppler-shifted lifetimes following the $(^{18}O,^{16}O)$ reaction at the Notre Dame heavy-ion tandem. Some of these results for ^{96}Zr have already been published and other reports are planned or recently written.[6] Here some highlights are mentioned.

Our initial discovery was that a band of states could be associated with the 0_2^+ excitation in ^{96}Zr. This band could be understood as a four particle,

---

[5] Yates, Julin, Kleinheinz, Rubio, Mann, Henry, Stoeffl, Decman and Blomqvist, Z. Phys. A234, 417 (1986). Yates, *et al.* Phys. Rev. C, submitted.

[6] Molnar, Yates and Meyer, Phys. Rev. C33, 1843 (1986).

four hole state having quadrupole deformation. The coexisting, normal shell model excitations were also identified. The extent of mixing between spherical and deformed configurations was determined to be small by assessment of interband decay rates. These results, together with the clear signatures of subshell closure from neighboring nuclei, permitted us to understand better the influence of the double subshell closure on the delayed onset of deformation in the mass 100 region.

d. A Study of Doubly Magic ^{48}Ca (S.F. Hicks, G. Molnar, and S.W. Yates)

As noted in the neutron scattering section, ^{48}Ca has been the subject of study to explore the spreading of collective excitations coupled into the continuum. The availability of this sample--despite complications introduced by its small size, complex composition, and awkward geometry--has dictated that we examine it with (n,n'γ) spectroscopic techniques. Accurate knowledge of the excited levels and excitation strengths of closely spaced levels above 4 MeV excitation is quite important to proper interpretation of the neutron scattering study. Preliminary studies demonstrate that we will be able to characterize many of the states up to 6 MeV excitation energy in this important nucleus.

e. Level Structure of Even-A Sn Isotopes (Z. Gácsi and J.L. Weil)

Decay schemes for $^{116,120,124}Sn$ up to excitations of 3.5-4.0 MeV have been constructed from the results of (n,n'γ) and (n,γ) measurements made in recent years. A level scheme for ^{124}Sn calculated by Bonsignori and Allart using the two-broken-pair model has been received. A preliminary comparison to the experimental results shows fairly good agreement for about 25 levels up to 3.1 MeV excitation. The worst disagreement is in the energies of the 3^- and 5_2^+ levels. All but two experimentally observed levels up to 3.1 MeV excitation can be accounted for by the model, although some of the experimental spin-parity assignments are not unique above 2.7 MeV. Generally speaking, the calculated positive parity levels tend to have higher energies than their experimental counterparts, the lowest 1^+ and 6^+ states being the only exceptions. The reverse is true for many of the negative parity levels.

f. ^{204}Pb Levels at Low Excitation (J.M. Hanly and M.T. McEllistrem)

An important complementary study for our exploration of the shape-transitional nuclei in neutron scattering in the Os-Pt region is the study of scattering from a Pb nucleus viewed as likely to provide a normal statistical spectrum of excitations, without strongly coupled resonances in the scattering or strongly coupled collective excitations. Scattering from both ^{208}Pb and ^{206}Pb have been shown to excite resonances which are believed to come from coupling of scattering from excited levels into the scattering from the ground states. One expects that with four valence holes, ^{204}Pb will not show strong excitations of this isolated character; its scattering will be describable with statistical models at low energies.

Study of the low-lying level scheme is important so we can properly characterize its excitations, if we are to test the sensitivity of scattering to those excitations. Furthermore, with four valence particles it is a good testing ground for shell model calculations, and several attempts to describe its level scheme have already been made. But the knowledge of spins and even of the level scheme is not adequate for comparison with model calculations.

Our measurements completed to date show that up to 1.6 MeV the previously known level scheme was complete, except that a level thought to be the first excited 0^+ level, at 1583 keV, is actually $J^\pi = 2^+$. The group at Jyvaskyla, Finland, having now observed the ground state conversion electron decay of a level at 1583 keV, agree that there must be a 2^+ level at this energy, but argue that there must also be a 0^+ level within about 1 keV of the 2^+ level. We see no evidence of such a level. The clear existence of the 2^+ level will seriously alter perceptions about the degree of configuration mixing present at low excitations in this nucleus. Additional work is in progress to characterize all of the low energy excitations, for comparison with the rather extensive shell model calculations made by the ORNL theory group and other investigators.

3. Lifetimes from DSAM Measurements (R.D. Mullins and J.L. Weil)

The use of observed γ-ray energies at different scattering angles to obtain lifetimes from $(n,n'\gamma)$ experiments has been inhibited by the lack of stopping power information for the very slow moving heavy recoil ions from nucleon scattering with $v/c < 0.01$. Recent compilations of stopping powers for such slow heavy ions have been made by Ziegler, who has needed them for ion implantation work and other surface studies with ions from accelerators. We have taken advantage of the availability of these new compilations, and incorporated them into the computer program used in analyzing the Doppler shift measurements. We measured lifetimes for 14 levels of ^{56}Fe, six of which are new measurements. Comparisons with previous work for other levels show good agreement, with uncertainties ranging from 20% to 50% for lifetimes from 15 to 500 fs.

The good agreement now achieved encourages us to deploy this method for transitions in the heavier Zr and Sn isotopes. Four lifetimes have been determined, with data for several other levels to be analyzed.

C. CHARGED PARTICLE AND FAST NEUTRON CAPTURE

1. ^{11}B (n,γ) and Giant Resonances Built on Excited Nuclear Configurations (S.L. Hanly, B. Pugh, M. Wang and M.A. Kovash)

Since the discovery in 1979 that radiative capture reactions in light nuclei at energies greater than about 20 MeV preferentially populate high-lying final states of a simple particle-hole nature, considerable experimental and theoretical efforts have been made to understand this mode of nuclear excitation. In the $^{11}B(p,\gamma)^{12}C$ reaction, an excitation function for γ-ray transitions to final states near 19 MeV excitation shows a resonance-like structure near 42 MeV excitation in ^{12}C. This feature is nearly 20 MeV wide. The unresolved final states near 19 MeV in ^{12}C, which include the 'stretched configuration' 4^- states, are predominantly of the simple $d_{5/2}$-$p_{3/2}^{-1}$ particle-hole configuration, and lie near the centroid of the $1\hbar\omega$ excitation in this nucleus. The strong dipole transitions to these final states are identified as arising from electromagnetic transitions of the type $2\hbar\omega \to 1\hbar\omega$. Because of the analogy with the strong giant dipole resonance transitions of the form $1\hbar\omega \to 0\hbar\omega$, we had named this excitation a Second Harmonic Giant Resonance.

In the late Spring of 1986 the construction of a new capture experimental apparatus was completed. This included the beam line, the γ-ray spectrometer, goniometer, and a new data acquisition system (hardware and software). For the initial experiment, we chose to study the $^{11}B(n,\gamma)^{12}B$ reaction. The $T(d,n)^4He$ reaction is used at E_d = 5.5 MeV to produce an intense high energy neutron beam of 22 MeV. A boron target has been developed containing about 70 g of enriched ^{11}B. Gamma rays are detected in our segmented NaI(Tℓ) spectrometer which consists of an eight inch diameter central element, ten inches long. The central element is surrounded by six annular segments of NaI of 1.75 inch thickness, and a front plate of NaI two inches thick. From each detection element both time and energy signals are derived and recorded in the new CAMAC acquisition system. The CAMAC acquisition and replay system has been used to determine the response function for the spectrometer by reconstructing the energy distribution of each event. Cosmic rays are distinguished and rejected, while the escape-shower energy detected by the annular elements is digitally resummed into the primary core energy. This technique increases the efficiency of the core detector by more than 200% while maintaining the energy resolution of a detector operated strictly in the annulus-veto mode.

Neutron backgrounds are made with cross sections of mbarns up to barns, while capture yields correspond to total cross sections of about a microbarn in this reaction. The energy spectrum from the spectrometer is time-gated by a window on the γ peak of the TOF spectrum, as well as gated by several other background rejection conditions. In a three hour test run with 1 μA of 5.5 MeV deuterons incident on a 2.5 cm long gas cell containing tritium at 1 atm pressure, γ-ray peaks are observed in the time-gated energy spectrum which are in very good correlation with the excitation energies of final states in ^{12}B. This preliminary result encourages us to continue in these studies with plans for measurements of full angular distributions and limited excitation functions. The direct capture code HIKARI has been obtained and calculations will soon be done to compare with these new data.

2. Remeasurement of the Reactions $^{12}C(\alpha,\gamma_0)^{16}O$ and $^{12}C(\alpha,\gamma_3)^{16}O$
(J. Trice, B. Pugh, J.L. Weil, M.T. McEllistrem, M.Z. Wang, T.R. Donoghue†, and M.A. Kovash)

These capture reaction studies are quite important for confirming or modifying the C burning rates as they sensitively determine the production of heavy elements and the explosive evolution of many stars. Background and target tests have commenced at the end of September, 1986. For these first studies we are using natural carbon foils and detecting only the γ-ray singles yield to the ground state. In an energy spectrum from the NaI detector taken with only 10 minutes of beam, the ground state transition at the position of the 2^+ resonance is clear, and little background remains. We have taken preliminary angular distributions with this target at this energy and at the position of the 1^- resonance near 9.6 MeV. We find very encouraging results even with this crude initial setup, and believe we will have much better sensitivity than in previous studies of this process, of which there have been many. The enhanced sensitivity results from the carefully developed and large efficiency, background-rejecting spectrometer. Not only does the segmented NaI spectrometer offer high efficiency and moderate resolution (2%), it also rejects cosmic ray backgrounds with very high efficiency. Just as importantly, we are using TOF techniques with pulsed beams, at pulse widths of only 2.7 ns, to reject time delayed backgrounds produced by charged particles and neutrons. With a demonstrated time resolution of 0.8 ns, fast neutron backgrounds from contaminant reactions are rejected with an efficiency which is presently limited only by the duration of the beam pulse.

D. NUCLEAR ASTROPHYSICS PROJECTS

1. Re/Os Cosmochronology and Neutron Capture in Os Isotopes (R.L. Hershberger, M.T. McEllistrem, R.L. Winters[††] and R.L. Macklin[*])

A very careful and sensitive neutron scattering experiment had been completed on ^{187}Os and ^{188}Os to fix the neutron scattering properties upon which determination of a scattering potential depended. Both model independent phase shift fits to the scattering data and potential modelling of the scattering led to the same conclusions. The neutron scattering and absorption cross sections were well characterized. With that neutron analysis, an excellent fit was obtained to the ^{187}Os(n,γ) and ^{188}Os(n,γ) cross sections measured in two other laboratories. These determinations led to a new Re/Os age for the galaxy of 16 Gyr, which was satisfying to some groups of astrophysicists and a source of skepticism for others. These results were published[7] at the end of 1983, and part of the measurements were indirectly confirmed in another scattering experiment at ORNL.

Doubts persist about the correct description of capture in Os, because some mechanisms of capture cross sections in these heavy nuclei would rely on γ-ray average widths which are not dependent on the distribution of angular momenta of capture states in the compound system. This would be the case for models

---

† Dept. of Physics, Ohio State University

†† Dept. of Physics, Denison University, Granville, OH

* Oak Ridge National Laboratory

7 Hershberger, Macklin, Balakrishnan, Hill, and McEllistrem, Phys. Rev. C28, 2249 (1983).

which do not see capture proceeding through a compound nucleus. Hence a proposal to redo the entire neutron scattering and capture problem in the nucleus ^{189}Os was made, where the angular momentum dependence will be different than in ^{187}Os.

An 8 g sample of highly isotopically enriched ^{189}Os was used as a scattering sample, and differential scattering cross sections were measured for incident neutron energies of 63, 73, and 97 keV. These data are yet to be fully corrected and interpreted, but all data taking has been completed for this project, and all yields extracted from the data.

Based on the ^{187}Os potential determined earlier, a new analysis has been made for the ^{189}Os neutron capture, under the assumption that the neutron scattering potential for ^{189}Os would be very similar to that determined for ^{187}Os. This reanalysis and its consequences for the Re/Os chronology will be published this year in Astronomy and Astrophysics.

2. ^{81}Br - ^{81}Kr Mass Difference and Neutrino Detection (Y. Wang, G.R. Shen, S.F. Hicks and M.T. McEllistrem)

The proposal to use bromine cleaning solution as a relatively inexpensive, large volume solar neutrino detector requires accurate knowledge of the detection efficiency of the $^{81}Br + \nu \rightarrow {}^{81}Kr + e$ reactions. Direct measurements should provide a capture rate for one transition, but those to excited levels will have to be calculated. Neutrino capture rates often vary with mass difference at the level of several percent per keV. Hence measurement of the mass difference with an uncertainty under 1 keV becomes very important. Preliminary data have been taken on the $^{81}Br(p,n)^{81}Kr$ reaction to assess the accuracy achievable with such a measurement. For this purpose reasonably stable KBr targets have been developed. Our tests indicate that the deterioration rate of these targets is low enough that good data on the $^{41}K(p,n)^{41}Sc$ and $^{81}Br(p,n)^{81}Kr$ reactions can be simultaneously obtained. Thus the desired Q-values for the reaction can be obtained through comparison with the accurately known $^{41}K(p,n)$ reaction, $Q = -1.210 \pm 0.5$ keV. There is, however, only one accurate determination of this Q-value, so it will also have to be remeasured.

E. THE IMAGINARY PART OF THE OPTICAL POTENTIAL

1. $^{103}Rh(p,n)$ and $^{103}Rh(p,p)$ Measurements (C.E. Laird† and F. Gabbard)

The study of proton reactions and scattering on the mass range $90 \leqslant A \leqslant 130$ has continued with measurements on ^{103}Rh. The "anomaly" in the imaginary potential observed when data is analyzed using a spherical optical model (SOM) has a maximum in the W vs. A plot near A = 103. Cross sections of the $^{103}Rh(p,n)$ reaction and of $^{103}Rh(p,p_o)$ were measured in the energy range E_p = 1.7-6.5 MeV. This data is being analyzed to obtain a more precise value of W near the peak of the anomaly.

---

† Department of Physics, Eastern Kentucky University, Richmond, Ky.

LAWRENCE BERKELEY LABORATORY

A. NUCLEAR DATA EVALUATION

1. Isotopes Project (E. Browne, R.B. Firestone, and V.S. Shirley)

The Isotopes Project compiles and evaluates nuclear structure and decay data. The group coordinates its efforts with those of the U.S. Nuclear Data Network and the International Nuclear Data Committee of the IAEA. The Isotopes Project has authored seven editions of the Table of Isotopes and recently completed the Table of Radioactive Isotopes. The group evaluates the mass chains $167 \leq A \leq 194$ and develops evaluation methodology. The Isotopes Project maintains the LBL/ENSDF database, provides remote access to nuclear data, and offers an extensive reference library.

2. Table of Radioactive Isotopes (E. Browne, R.B. Firestone, and V.S. Shirley)

The Table of Radioactive Isotopes was published by John Wiley & Sons, New York, in July, 1986. It is a comprehensive and critical evaluation of the nuclear and atomic properties of radioactive isotopes. The book is especially tailored to the needs of applied users in nuclear energy, industry, biology, medicine, and other fields, but serves also as an indispensable reference for nuclear physicists and chemists. Detailed radiation data for about 2000 of the 2755 known nuclides are presented in this up-to-date and concise single-volume book.

3. Table of Isotopes, 7th Edition (C.M. Lederer and V.S. Shirley, editors, E.Browne, J.M. Dairiki, and R.E. Doebler principal authors)

The Seventh Edition of the Table of Isotopes was reprinted by John Wiley & Sons, New York in 1986. The first printing in 1978 sold over 9000 volumes and the book continues to sell about 500 volumes per year. The Table of Isotopes is an indispensable reference book for nuclear physicists, chemists and applied users of radioactivity. It is the only comprehensive, single-volume source of nuclear structure data available. No future editions of the Table of Isotopes are envisioned due to the scope of such a project. Considerable interest has been expressed for such a book, and the Isotopes Project is investigating the possibility of producing a less ambitious book on nuclear structure.

4. Mass Chain Evaluation (E. Browne, R.B. Firestone, V.S. Shirley)

The Isotopes Project has recently submitted evaluations for A = 168, 180, and 183. Because radioactivity data for $A \leq 44$ had been evaluated for the Table of Radioactive Isotopes, the group additionally provided decay data for $33 \leq A \leq 44$ for ENSDF. The Isotopes Project is currently evaluating A = 173, 178, and 182.

5. Evaluation Methodology (E. Browne and R.B. Firestone)

The Isotopes Project has been developing methodology for nuclear data evaluation. Topics of particular interest include the normalization of radiation intensity data for decay schemes, and the adoption of transition energies and branching ratios. Computer codes have been developed to implement the new methodology, and are being distributed to other evaluation centers.

6. LBL/ENSDF Database (E. Browne and R.B. Firestone)

The LBL/ENSDF database contains nearly all of the numerical data from the ENSDF file, adopted decay data from the Table of Radioactive Isotopes, and Wapstra's 1983 Atomic Mass Table. The LBL version of ENSDF contains cross-referencing linkage between levels and transitions measured in different experiments. The database has been organized using DATATRIEVE, a DEC database management system. DATATRIEVE provides simple, English commands for retrieving, sorting and printing the desired data. DATATRIEVE also has a straightforward native programming language for performing more complex retrievals. The database is maintained on a dedicated 456 megabyte disk of the LBL VAX-9600 computer cluster which is accessible by telephone and via PHYSnet, MILNET, and TYMNET. Interested users should contact the Isotopes Project for further information.

The Isotopes Project received about 12 major requests in 1986 for data from the LBL/ENSDF database. These included data requests for books, nuclear physics research, and nuclear applications. The Isotopes Project is investigating the possibility of providing decay data to Idaho Nuclear Engineering Laboratory for producing ENDF/B.

7. Remote Access (E. Browne and R.B. Firestone)

The Isotopes Project has established a guest account for users of the LBL/ENSDF database. This account provides access to the LBL/ENSDF file, the databases maintained by the NNDC at BNL, and to the LBL Physics Program Library (PPL). Data retrieval procedures are available for the LBL/ENSDF database as well as direct access through DATATRIEVE at command level. The PPL library contains interactive computer codes for calculating internal conversion coefficients, logft values, E0 atomic subshell and pair production ratios, multipole mixing ratios, and simple or weighted averaging. Access to the guest account can be obtained by contacting the Isotopes Project.

8. Calculated Uncertainties of Absolute γ-ray Intensities and Decay Branching Ratios and Decay Branching Ratios Derived from Decay Schemes* (E.Browne)

Accurate values for absolute radiation intensities, i.e, the

* Condensed from E. Browne, Nuclear Instruments and Methods in Physics Research A249, 461 (1986), North-Holland, Amsterdam.

percentages of various types of radiations emitted in a nuclear transformation, are frequently required. For example, they are the basic quantities from which transition probabilities may be derived for testing nuclear models; and these intensities, together with their corresponding energies, are often used in applications of radioactivity to other fields for calculating average radiation energies emitted per disintegration. Hence it is important to report absolute radiation intensities and their uncertainties accurately. The concurrent determination of decay branching ratios is of course mandatory.

It generally requires elaborate calibrated detector systems and delicate measuring techniques to determine absolute radiation intensities. For short-lived isotopes and for isotopes which decay through more than one mode, e.g. ß- and electron capture, the experimental difficulties may be even greater. Chemical and isotopic purities of the source are also important, especially for a beta emitter, for which it is difficult to remove contributions from possible impurities from the continuous-energy beta spectrum. Consequently, most of the known absolute radiation intensities have been derived from it relative intensities (i.e., intensities measured relative to that for a nominal transition for each radiation type) and from the knowledge of the isotope's decay scheme (which often includes assumptions based on nuclear-structure theory). A set of radiations, usually gamma rays which represent the full disintegration intensity of the isotope, provides the it normalizing factor between the relative and absolute scales. It is important to choose this set carefully, because the accuracy of the resulting absolute radiation intensities is of course affected by the relative intensities and assumptions for the set. This paper presents analytical methods for calculating uncertainties of absolute γ-ray intensities and decay branching ratios derived from decay schemes. The equations have been derived with standard mathematical error-propagating techniques, using first-order approximations in Taylor series expansions of absolute γ-ray intensities.

B. EXPERIMENTS WITH OASIS

1. ß-Delayed Proton Emission in the Lanthanide Region (P.A. Wilmarth, J.M. Nitschke, R.B. Firestone, and J.Gilat)

Table I summarizes the decay properties of very neutron-deficient ß-delayed proton emitters produced in 1986 at the SuperHILAC's on-line isotope separator OASIS. Unambiguous Z-identifications were obtained in all cases by observing characteristic x-rays coincident with the protons.

Table I. E_{lab} = bombarding energy; $T_{½}$ = weighted half-life from all available OASIS data; $\bar{E}_p$(range) = average energy and energy range of the observed protons.

Isotope	Reaction	E_{lab} (MeV)	$T_{½}$ (s)	$\bar{E}_p$(range) (MeV)
^{124}Pr	$^{92}Mo(^{36}Ar,p3n)$	174	1.2 ± 0.2	3.7(2.1 - 5.9)
^{125}Ce	$^{92}Mo(^{36}Ar,2pn)$	153	9.2 ± 1.0	3.3(1.7 - 5.1)
^{127}Nd	$^{92}Mo(^{40}Ca,2p3n)$	208	1.8 ± 0.4	3.7(2.2 - 6.0)
^{131}Nd	$^{94}Mo(^{40}Ca,2pn)$	168	25 ± 4	3.1(1.7 - 6.4)
^{131}Sm	$^{96}Ru(^{40}Ca,2p3n)$	208	1.2 ± 0.2	3.7(1.8 - 6.6)
^{140}Tb	$^{92}Mo(^{54}Fe,3p3n)$	298	2.4 ± 0.4	4.2(2.2 - 6.6)
^{141}Gd	$^{92}Mo(^{54}Fe,4pn)$	276	20 ± 4	3.6(2.2 - 4.9)
^{141}Dy	$^{92}Mo(^{54}Fe,2p3n)$	276	0.9 ± 0.2	4.1(2.1 - 7.2)
^{142}Dy	$^{92}Mo(^{54}Fe,2p2n)$	247	2.3 ± 0.8	3.9(2.5 - 5.2)
^{144}Dy	$^{92}Mo(^{56}Fe,2p2n)$	245	9.1 ± 0.5	3.2(2.6 - 4.5)
^{144}Ho	$^{92}Mo(^{58}Ni,3p2n)$	325	0.7 ± 0.1	4.2(2.2 - 7.0)
^{146}Ho	$^{92}Mo(^{58}Ni,2p2n)$	261	3.1 ± 0.5	4.1(2.4 - 6.3)

2. <u>Decay Studies of Neutron-Deficient Rare Earth Isotopes: A=140,141,142</u> (R.B. Firestone, J. Gilat, P.A. Wilmarth, and J.M. Nitschke)

The decay of the very neutron-deficient nuclides in the A=140,141, and 142 isobaric chains were investigated at the SuperHILAC with the OASIS on-line mass separator facility. Preliminary decay schemes have been constructed. These results are summarized in the following table.

Table I. Decay Summary of A = 140,141,142 Isotopes Produced with OASIS

Isotope Z,A	Half-life This work	Half-life Literature	Radiations
^{140}Tb	2.4 ± 0.4 s	-	βp, γ-ray 329
^{140}Gd	16 ± 1 s	-	γ-rays 175,192,379,722,750 (10 more)
^{140g}Eu	1.5 ± 0.1 s	1.3 s	γ-rays 460,531,1068 (10 more)
^{140m}Eu	~ 0.1 s	20 s	γ-rays 175,185
^{141}Dy	0.9 ± 0.2 s	-	βp, γ-rays 53,140,190
^{141}Tb	3.5 ± 0.3 s	-	γ-rays 113,136,198,258,293 (25 more)
^{141g}Gd	20 ± 2 s	22 s	βp?, γ-rays 120,216,336
^{141m}Gd	25 ± 4 s	-	βp?, γ-rays 60,113,119,145,198,224,258,351,361,521, (20 more)
^{141g}Eu	40 ± 5 s	40 s	γ-rays 369,383,385,394,396 (20 more)
^{141m}Eu	3.5 ± 0.3 s	3.3 s	γ-rays 96,519,804,1595
^{142}Dy	2.3 ± 0.8 s	-	βp, γ-rays 182,212 (20 more)
^{142g}Tb	0.8 ± 0.4 s	-	βp?, γ-rays 389,465,515,853
^{142m}Tb	0.3 ± 0.1 s	-	γ-rays 182,212,465,515
^{142}Gd	71 ± 1 s	90 s	γ-rays 179,280,284,526,620 (30 more)
^{142g}Eu	2.4 ± 0.2 s	2.4 s	γ-rays 768,890,1288,1405,1658,2056
^{142m}Eu	~ 70 s	73 s	γ-rays 556,768,1024

3. <u>Radioactive Decay of ^{144}Dy</u> (R.B. Firestone, W.-Y. Chen, P.A. Wilmarth, and J.M. Nitschke)

The decay of ^{144}Dy was investigated at the SuperHILAC with the OASIS on-line mass separator facility. A preliminary decay scheme was constructed on the basis of γ-ray singles, coincidence, and half-life measurements. ß-delayed protons were assigned to ^{144}Dy decay on the basis of x-ray coincidences. These results are summarized in Table I. The half-life of ^{144}Dy was measured as 9.1±-0.5 s. Levels at 0(1^+)-, 196.5(1^+)-, 298.7(2^-)-, 532.2-, 615.9-, 620.0-, 774.4-, 793.3- and 1237.2-keV in ^{144}Tb are postulated. The J^{π} value for the 196.5-keV level is based on strong ß-decay feeding from the 0^+ parent and, for the 298.7-keV level, from no feeding by the 5^- isomer at 396.7-keV and no direct ß-decay feeding. Weak evidence exists for a level at 469.5 keV which deexcites through the 283.7-keV level that is strongly populated by IT decay.

γ rays from ^{144}Dy Decay

E_{γ}	I_{γ}	Placement
185.8	3	469.5 - 283.7 ?
196.5	100	196.5 - 0.0
260.9	9	793.3 - 532.2
298.7	85	298.7 - 0.0
305.1	2	774.4 - 469.5 ?
317.3	17	615.9 - 298.7
321.3	10	620.0 - 298.7
335.4	8	532.2 - 196.5
419.4	9	615.9 - 298.7
423.5	6	620.0 - 196.5
462.5		1237.2 - 774.4 ?
469.6	7	469.5 - 0.0 ?
475.7	44	774.4 - 298.7
494.6	5	793.3 - 298.7
532.2	12	532.2 - 0.0
596.0	13	793.3 - 196.5
615.9	5	615.9 - 0.0
620.0	7	620.0 - 0.0
793.3	20	793.3 - 0.0
1040.7	17	1237.2 - 0.0
1237.4	21	1237.2 0 0.0

4. <u>Radioactive Decay of $^{144m+g}$Tb</u> (R.B. Firestone, W.-Y. Chen, P.A. Wilmarth, and J.M. Nitschke)

The decay of $^{144m+g}$Tb was investigated at the SuperHILAC with the OASIS on-line mass separator facility. Preliminary decay schemes have been constructed on the basis of γ-ray singles, coincidence, and half-life measurements. The results are summarized in Table I. ^{144m}Tb was reported by Nolte et al[1] and Sousa et al[2] Our half-life of 4.1+-0.1 s consistent with Nolte (4.5+-0.5s) and Sousa (5+-1s). We propose $J^{\pi}=5^-$ for the isomer on the basis of an E3 transition to the 283.7-keV (2^+) level, an (M4) transition to the 1 ± ground state, and strong β-decay feeding to the $J^\pi = 5^-$ level at 2302.7 keV. Nolte et al [1] previously reported ^{144g}Tb decay with a half-life of 1.5±-1.0 s decaying to the levels at 0.0(0^+)- and 743.0(2^+)-keV in ^{144}Gd. We propose two additional levels at 1877.2(2^+)- and 1886.8(0^+)-keV. A half-life as long as 4s could not be eliminated in these experiments because ^{144g}Tb was produced in equilibrium with the isomer and ^{144}Dy.

Table I. γ rays from $^{144m+g}Tb$ Decay

	E_γ	I_γ	Placement
^{144m}Tb	113.0(IT)	3.7	396.7 - 283.7
	139.7(ϵ+β+)	1.5	2442.5 - 2302.7
	169.1(ϵ+β+)	3.6	2471.8 - 2302.7
	283.7(IT)	100	283.7 - 0.0
	315.1(ϵ+β+)	3.1	2786.9 - 2471.8
	396.7(IT)	1.2	396.7 - 0.0
	544.5(ϵ+β+)	0.8	3016.2 - 2471.8
	558.1(ϵ+β+)	8.4	2302.7 - 1744.6
	600.4(ϵ+β+)	5.9	2302.7 - 1702.3
	628.5(ϵ+β+)	1.5	2330.8 - 1702.3
	697.9(ϵ+β+)	2.5	2442.5 - 1744.6
	713.5(ϵ+β+)	2.0	3016.2 - 2302.7
	743.0(ϵ+β+)	~53	743.0 - 0.0
	959.3(ϵ+β+)	11	1702.3 - 743.0
	1001.6(ϵ+β+)	19	1744.6 - 743.0
^{144g}Tb	743.0	~10	743.0 - 0.0
	1134.1	1.5	1877.2 - 743.0
	1143.8	7.7	1886.8 - 743.0
	1877.3	2.2	1877.2 - 0.0

a E. Nolte, S.Z. Gui, G. Columbo, G. Korschinek, Z. Phys. A306, 223 (1982).

b D.C. Sousa, K.S. Toth, C.R. Bingham, A.C. Kahler, and D.R. Zolnowski, Phys. Rev. C25, 1012 (1982).

A. NUCLEAR DATA APPLICATIONS - MEASUREMENTS

1. Discovery of Two New Lr Isotopes
(Lougheed, Moody, Wild, Dougan and Hulet)

We bombarded a target of ^{254}Es with 126-MeV ^{22}Ne ions from the 88-in cyclotron at LBL. We periodically collected recoiling reaction products on Mo foils after several hours of bombardment and chemically separated the Lr fractions using cation-exchange chromatography. These fractions were counted with surface-barrier detectors using a multichannel analyzer for alpha-energy analysis and detection of SF events. In an analysis of more than 200 events, we have observed two SF components with half-lives of 39 and 216 min and cross sections of 240 and 37 nb, respectively. Because of our chemical separation procedure, we know that the activity is from Lr; the magnitudes of these cross sections are consistent with the 39-min activity being ^{261}Lr and the 216-min activity being ^{262}Lr. The longest-lived previously known isotope of Lr is the alpha-emitter 3-min ^{260}Lr. A preliminary examination of the alpha spectra from this experiment indicates that these SF activities are not due to contamination from Es, Fm, or Md isotopes and, thus, are likely to arise from either the decay of the Lr isotopes themselves or electron-capture decay to No daughters followed by SF decay. We searched for this latter mode of decay but observed no SF activity in separated No chemical fractions, indicating that either electron capture is not a significant mode of decay for these Lr isotopes, or that the half-lives of the daughter No isotopes are too short ($\leq$ 5 min) to be observed by this method. We have not yet calculated upper limits for alpha-decay branches.

2. Energy-level Structure of ^{93}Mo
(Bauer, Becker, Cizewski*, Sale and Warburton**)

The energy-level structure of ^{93}Mo was studied by in-beam γ-ray measurements using the ^{89}Y(^{7}Li,3nγ)^{93}Mo fusion evaporation reaction at bombarding energies up to 24 MeV. The emphasis of our experiments was to investigate transitions involving levels at excitation energies ranging from 1 to 3 MeV located in the vicinity of isomers. A large number of states were observed, with angular momenta extending to $21/2^{+}$ and possibly above. Partial decay schemes were constructed on the basis of γ-ray excitation functions, angular distribution and linear polarization measurements, γ-ray coincidences, and level lifetimes determined from Doppler shift attenuation measurements.

*Rutgers University, Piscataway, NJ
**Brookhaven National Laboratory, Upton, NY

3. Probe of the Shell Crossing at $A = 40$ Via Beta Decay: Experiment and Theory
(Warburton, Alburger, Becker, Brown and Raman)

The β^- decays of ^{35}P, ^{37}S, ^{38}Cl were studied both experimentally and via shell-model calculations. The four decaying nuclei were formed by bombardment of 81% enriched ^{36}S by triton and deuteron beams. γ-ray spectroscopy was carried out with Ge detectors, either bare or surrounded by a Compton suppression NaI(Tl) shield. One new Gamow-Teller decay was observed in ^{35}P decay, and one new first-forbidden decay was observed in ^{38}S decay. Otherwise γ-ray measurements of E_γ and I_γ (and limits on I_γ for unobserved transitions) were improved significantly over previous results. Shell-model studies were undertaken in order to bring these beta decay results to bear on an understanding 1f the shell structure in the (sd) to (fp) transition region at $A = 40$. An interaction wws constructed in the $1d_{5/2}$, $1d_{3/2}$, $2s_{1/2}$, $1f_{7/2}$, $1f_{5/2}$, $1p_{3/2}$, $1p_{1/2}$ model space. This interaction started from the Wildenthal "USD" (sd) interaction and the van Hees-Glaudemans (fp) interaction, which were connected by the cross-shell Millener-Kurath interaction. Certain important two-body matrix element and single-particle energies were adjusted to fit experimental binding energies in $A = 40, 41, 42$. This interaction was then used to calculate level spectra for the daughter nuclei ^{35}S, ^{37}Cl, ^{38}Cl and ^{38}Ar as well as Gamow-Teller and unique first-forbidden beta decays leading to these nuclei.

4. Proton and Neutron Transition Densities in $^{6,7}Li$ from a Comparative Study of Proton and Neutron Scattering at 24 Mev
(Hansen, Rapaport and Petrovich)

Elastic and inelastic neutron scattering for ^{6}Li [GS (0^+), 2.184 MeV (3^+) levels] and ^{7}Li [GS ($3/2^-$), 0.478 ($1/2^-$), 4.63 MeV ($7/2^-$) levels] were measured[1] at 24.0 MeV at the Ohio University Tandem Van de Graaff accelerator. These data have been analyzed in conjunction with the existing proton scattering data[2] for these levels at 24.4 MeV. The measurements have been compared with DWBA calculations done with the code DWBA79. (For details on these calculations see Ref. 2). These comparisons have allowed us to infer that $\rho_n = \rho_p$ in ^{6}Li and ^{7}Li, in contrast with the result $\rho_n \simeq (N/Z)\rho_p$ deduced from the earlier proton work[2].

---

[1]Hansen, Rapaport, Wang and Barrios, APS Bull.31, 1237 (1986).

[2]Petrovich, Howell, Poppe, Austin and Crawley, Nucl. Phys. A383,, 355 (1982).

5. Measurement of the Neutron Induced-Fission Cross Section of ^{242}Cm (Alam, Block, Sovacek and Hoff)

The measurement of the neutron-induced ^{242}Cm fission cross section is extremely difficult because the nucleus has a very high alpha decay rate and an intense spontaneous fission background. For the present measurement, we used the large neutron flux from the Rensselaer Intense Neutron Spectrometer (RINS) to obtain an adequate neutron-induced fission signal above the spontaneous fission background. The RINS system, a lead slowing-down-time spectrometer coupled to the RPI Linac, produces a very intense neutron flux of broad resolution in the 0.1 to 100,000 eV energy range. In this experiment, the fission chamber, which contained five pairs of hemispherical electrodes, was coupled to nano-second rise-time electronics to suppress the α-decay pile-up effects. The samples inside the ionization chamber were 1.15 μg of ^{242}Cm, 12.5 μg of 99.995 % ^{238}Pu, a mixture of 6.4 μg of highly enriched ^{235}U and 2.86 pg of ^{252}Cf, and 960 pg of ^{252}Cf. The flux normalization factor was determined from the present experimentally measured ^{235}U fission data and the resolution-broadened ^{235}U ENDF/B-V data. These data were further corrected for 2.7% ^{238}Pu buildup using the simultaneously measured ^{238}Pu data and the final results are shown in Fig. 1. The data show several low-energy resonances; the parameters of which have been determined and these are shown in Table 1 on the next page.

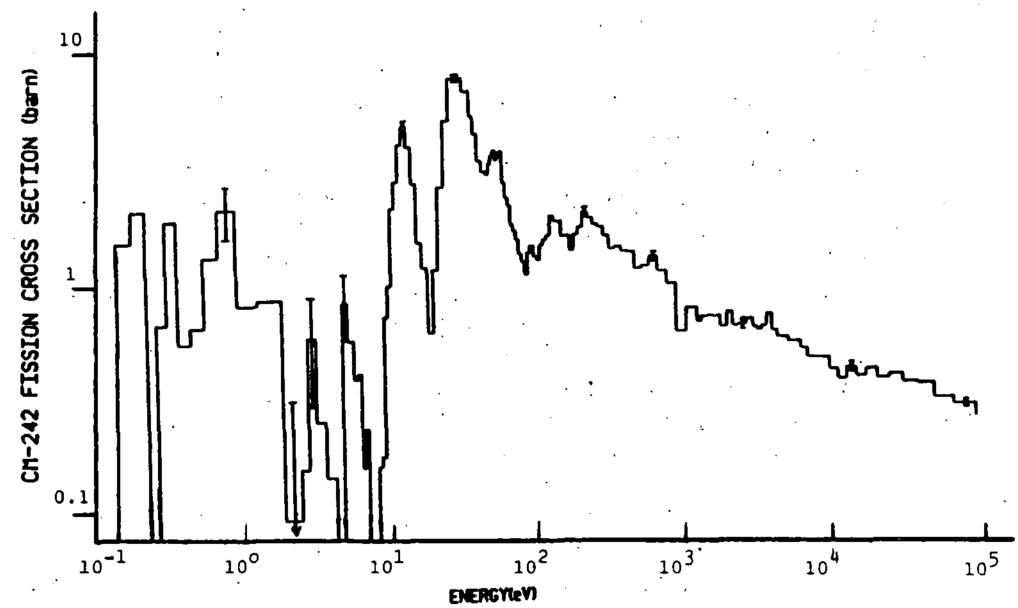

Fig. 1 Fission cross section vs neutron energy for the ^{242}Cm isotope.

Table 1: ^{242}Cm resonance parameters.

E_0 (eV) From Ref.(1)	Measured A_f (b-eV)	g	Γ_n (meV) From Ref.(1)	Γ_γ (meV)	Γ_f (meV)
13.62	20.8 ± 1.9	1	1.82 ± 0.05	34 ± 6 From Ref.(5)	1.42 ± 0.27
30.33 37.49	130 ± 8 (Area under ~31 eV peak)	1	3.1 ± 0.3 4.4 ± 0.3	34 34 (Assumed)	6.41 ± 1.53
60.1	52.8 ± 5.5	1	23.6 ± 4.0	34 (Assumed)	1.96 ± 0.46

6. Gamma Ray Emission from Oxygen Pulsed with 14 MeV Neutrons
(Goldberg, Hansen, Howerton, Komoto and Pohl)

The integral measurements of the gamma emission spectra in the energy interval 1-8 MeV from materials pulsed with 14 MeV neutrons were reported earlier[1]. The calculational analysis has been carried out with the neutron-photon Monte Carlo (MC) Transport code TART using the ENDL library. Direct comparisons of these calculations with the measured electron recoil spectra (ERS) have been done using the three-dimensional, photon-electron cascade MC code SANDYL. We have found good agreement between the calculations and the measurements for C, Al, Cu, Au, ^{232}Th, and ^{238}U. For oxygen (a water target) and Fe, the calculations over-estimate (20-30%) the measured gamma spectra, while for Ta and W the latter are higher than the calculated values. In Fig. 1 (see next page) we show a comparison of the measurements and calculations for the ERS from water (13.4 cm thick). The dashed-dotted curve was obtained with the gamma production cross sections for the interactions of 14 MeV neutrons with ^{16}O as existed in the ENDL library. A revision of these cross sections together with the recent measurements[2] of helium production have resulted in the calculation given by the solid line. The measured ERS have also been compared with the TART calculations using the ENDF/B-V library (dashed line). The latter underpredict the gamma production from oxygen over the whole energy range of the measurements.

Presently we are looking into sources of the discrepancies obtained in the comparisons done for Fe, Ta, and W with the ENDL library. Calculations with the ENDF/B-V are in progress for all the other materials.

[1]Mathews and Lanier, Lawrence Livermore National Laboratory, UCID-18987-86, 6 (1986).

[2]Kneff, Oliver, Farrar IV and Greenwood, Nucl. Sci. & Eng. 92, 491 (1986).

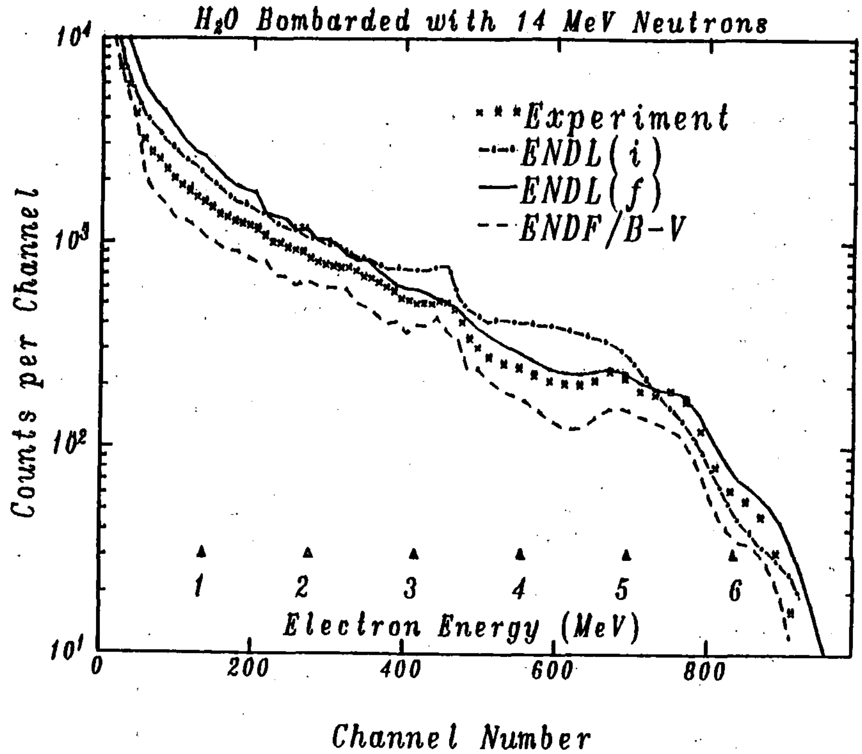

Fig. 1 Comparison of measurements and calculations for the electron recoil spectra from water (13.4 cm thick).

7. Quadrupole Moments and Spectroscopy of ^{210}Po with the ^{209}Bi(t,2nγ) Reaction
(Maier, Aprahamian, Becker, Decman, Estep, Henry, Lanier, Mann, Meyer, Struble, Berger and Stoeffel).

Nuclear quadrupole moments have been measured for the 8^+, 11^-, 13^-, 16^+ isomers of ^{210}Po by perturbed angular distribution in a Bi single crystal as $Q(8^+) = -57.9$ fm^2 (used for normalization, $Q(11^-) = -105(15)$ (from ^{209}Bi + ^{15}N), $Q(13^-) = 94(9)$ and $Q(16^+) = 136(8)$. The results give the quadrupole moment of the $i_{13/2}$ proton and agree well with our understanding of electromagnetic moments close to ^{208}Pb and of the proposed structure of ^{210}Po, as described by two protons coupled to ^{208}Pb.

8. Excitation Functions for ^{89}Y + p over the Range 5 to 40 MeV
(O'Brien, West, Lanier and Mustafa)

We studied the excitation functions[1] of the radioactive nuclides produced by the proton bombardment (from 5 to 40 MeV) of ^{89}Y. Results were obtained for ^{89}Y(p,n)^{89}Zr, ^{89}Y(p,2n)^{88}Zr, ^{89}Y(p,pn)^{88}Y, and ^{89}Y(p,αn)^{85m,g}Sr, and we have made progress in studying several other nuclides produced from the same bombardments. We used the STAPRE and ALICE statistical-model codes to calculate the excitation functions, and we found reasonable agreement between calculation and experiment for the energy range over the peak of the excitation function where compound statistical effects are dominant. However, significant disagreement is found at the higher energies, where preequilibrium effects are dominant.

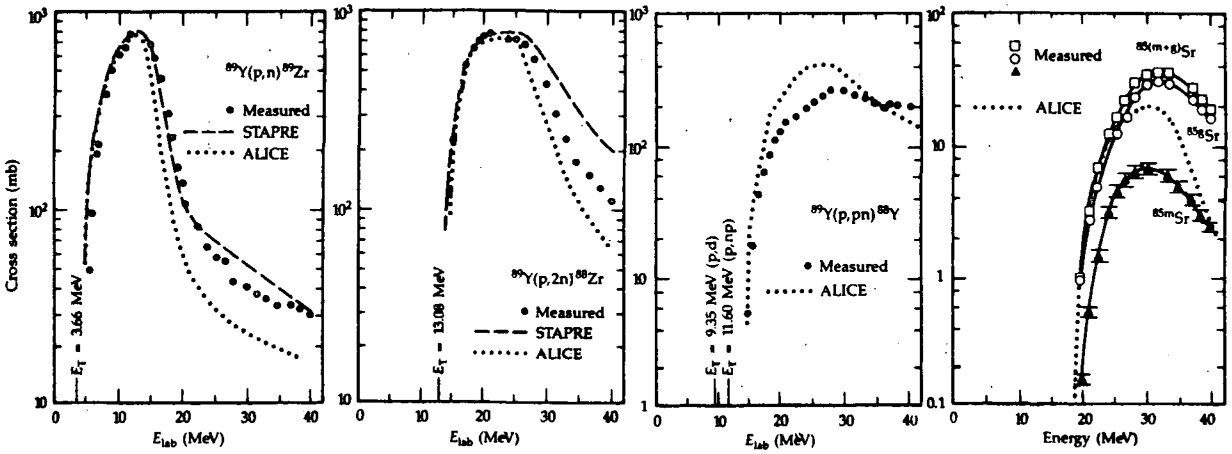

Fig. 1. Excitation functions for (a) ^{89}Y(p,n)^{89}Zr, (b) ^{89}Y(p,2n)^{88}Zr, (c) ^{89}Y(p,pn)^{88}Y, (d) ^{85m}Sr, ^{85g}Sr, and ^{85m}+ ^{g}Sr from the ^{89}Y(p,αn)reaction.

[1] O'Brien, West, Jr., Lanier, and Mustafa, Lawrence Livermore National Laboratory, UCAR-10062/86, (1986).

9. ^{36}S(t,pγ)^{38}S reaction
(Olness, Warburton, Becker, Decman, Henry, Mann and Ussery)

The ^{36}S(t,p$_\gamma$)^{38}S reaction was used to populate levels in ^{38}S up to 3-MeV excitation. A definite 2^+ assignment to the 1292-keV first-excited state was obtained from a (t,p$_\gamma$) angular correlation. Doppler shift information provided lower limits of 0.45 and 0.2 ps for the mean lifetimes of the 1291 → 0 and 2825 → 1291 transitions. Evidence for a possible new level at 2805 keV was obtained from p-γ coincidence data. The known level spectrum of ^{38}S has been compared to predictions of a shell-model interaction utilizing the full sdpf model space. This calculation has also predicted the E2 and M1 transition rates.

10. <u>Excitation Functions for $^{89}Y + d$ Over the Range 3 to 40 MeV.</u>
(West, Lanier, O'Brien and Mustafa)

We studied the excitation functions[1] of the radioactive nuclides produced by the deuteron bombardment (from 3 to 40 MeV) of ^{89}Y. Results were obtained for $^{89}Y(d,2n)^{89}Zr$, $^{89}Y(d,3n)^{88}Zr$, $^{89}Y(d,2np + nd)^{88}Y$, and $^{89}Y(d,p)^{90m}Y$, and we have made progress in studying several other nuclides produced in the same bombardments. In agreement with our earlier work on the excitation functions of titanium and chromium [2], we find deviations between the STAPRE and ALICE models and experimental results that support the concept of the occasional breakup of the loosely bound deuteron in the entrance channel.

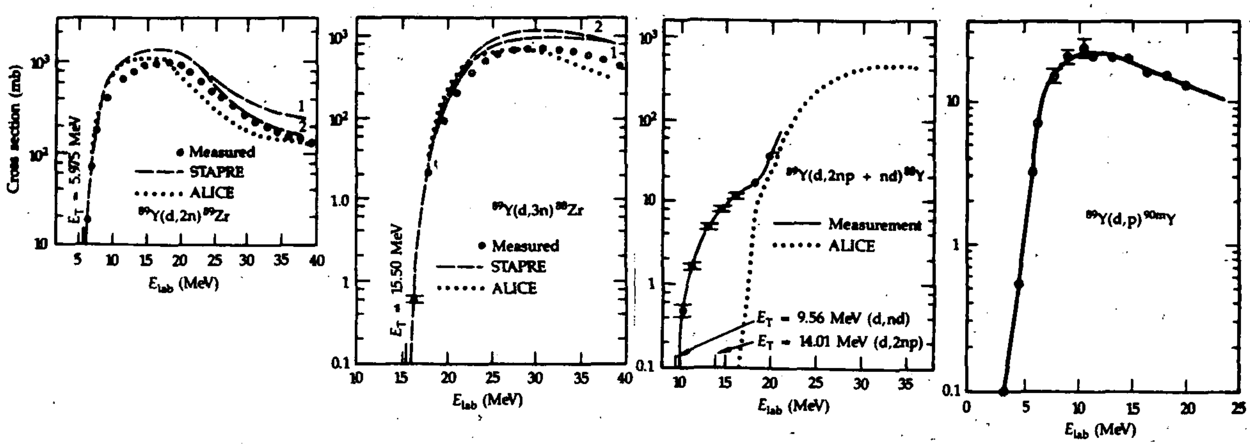

Fig. 1 (a) The $^{89}Y(d,2n)^{89}Zr$ excitation function. Curve (1) allows for a greater contribution from preequilibrium effects than does (2). The difference between calculations and experiment near the peak in distribution is attributed to deuteron breakup in the entrance channel. (b) The $^{89}Y(d,3n)^{88}Zr$ excitation function. Curves (1) and (2) are for different assumptions in the STAPRE code (see (a)). (c)The $^{89}Y(d,2np + nd)^{88}Y$ excitation function. (d) The $^{89}Y(d,p)^{90m}Y$ excitation function. We have not measured the excitation function of ^{90g}Y, which decays approximately 100% by β^- emission with a 64.1-h half-life.

---

[1] West, Lanier, O'Brien and Mustafa, Lawrence Livermore National Laboratory, UCAR-10062/86 (1986).

[2] West, Lanier and Mustafa, Lawrence Livermore National Laboratory, UCAR-10062/85-1 (1985).

11. <u>Nuclear Structure of ^{231}Th</u>
(White, Borner, Hoff et al)

The nuclide ^{231}Th was investigated with the reactions ^{230}Th(n,γ)^{231}Th, ^{230}Th(n,γe)^{231}Th and ^{230}Th(d,p)^{231}Th. Gamma rays from average resonance capture were measured, in addition to the usual thermal neutron capture spectroscopy. From these data, 70 excited levels in ^{231}Th were identified and, of these, 57 were placed in 18 rotational bands with assigned configurations. Candidates have been proposed for all expected Nilsson states below 750 keV, albeit with varying degrees of confidence, including the $5/2^{+}$[622], $7/2^{+}$[624], $3/2^{-}$[761], $1/2^{-}$[770], $1/2^{+}$[640], and $5/2^{-}$[503] configurations. Several vibrational states have been identified; a special feature of these is the observation of greater fragmentation of single particle-0^{+} mixed states than expected theoretically. The existence of nearly degenerate parity doublets indicates that the nucleus may possess a stable octupole deformation; no evidence was found for such states in ^{231}Th. The neutron binding energy was determined to be 5118.13 $\pm$ 0.20 keV.

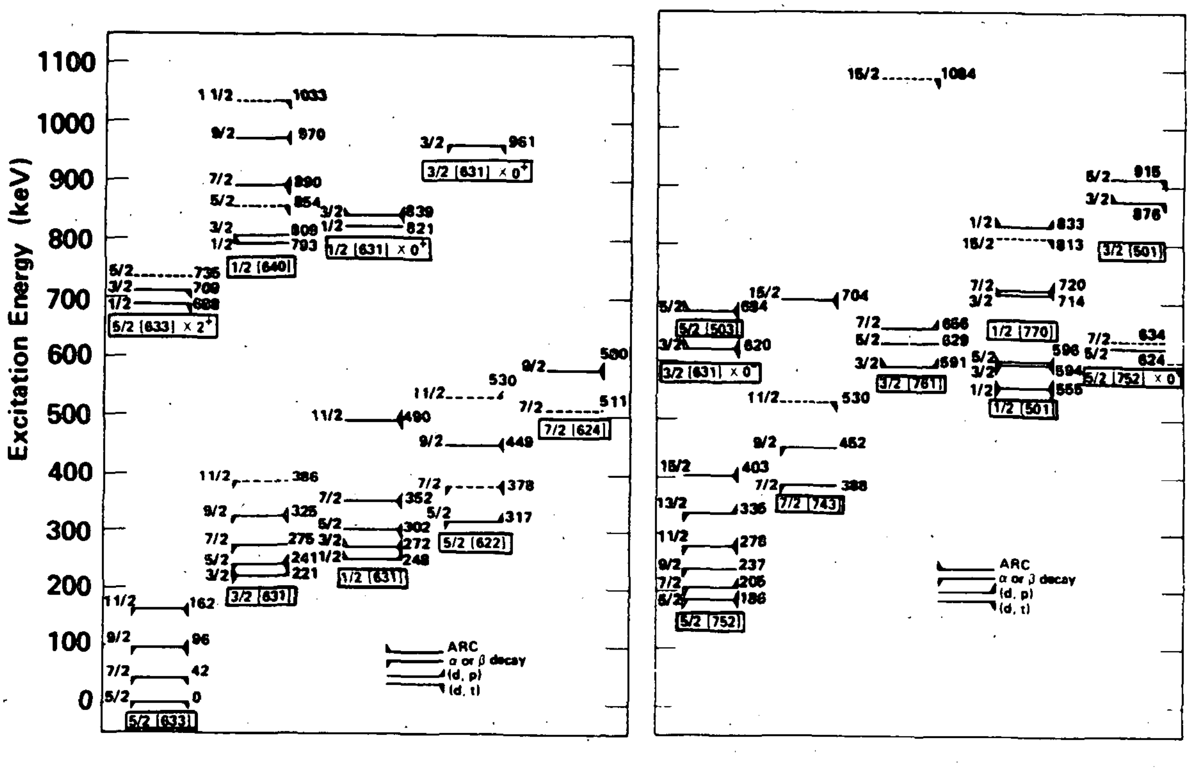

Fig. 1 (a) Positive-parity and (b) negative-parity levels in ^{231}Th assigned to rotational bands with Nilsson configuration assignments.

B. NUCLEAR DATA APPLICATIONS - CALCULATIONS

1. Calculation of γ-ray Cascades in Code ALICE
(Blann, Reffo and Fabbri)

We have modified the nuclear modeling code ALICE to include compound and precompound γ-rays. No additional input is required for the new capability. Spectra calculated with this modified code have been compared with experimental spectra for ^{93}Nb (n,x$_\gamma$), ^{27}Al (n,x$_\gamma$) and ^{197}Au (n,x$_\gamma$) at ε_n = 9.5, 14.3 and 18.5 MeV (average bin energies), and for ^{181}Ta (n,x$_\gamma$) at 14 MeV. The ^{93}Nb and ^{181}Ta γ-ray spectra are also compared with results of the ENEA code PENELOPE. The results of the simpler ALICE calculation compare very favorably with results of the more sophisticated codes, and require less than 1% of the CPU time to perform.

2. Low Energy Neutron Capture of Neutron Rich Target Nuclides
(Reffo, Blann, Komoto and Howerton)

Nuclear modeling codes have been used in conjunction with a careful analysis of nuclear systematics to calculate (n,γ) cross sections for 76 neutron rich nuclides at incident neutron energies between 1 and 500 keV. The physics of the modeling used and the systematics involved in parameter selection have been summarized in report UCRL-95370. A discussion is given of the likely uncertainties of these capture cross sections of very unstable target nuclides which are in a region of interest to astrophysics.

3. Exploratory (n,f) Cross-Section Calculations for the ^{235}U 1/2$^+$ Isomer
(Gardner and Gardner)

We have made some exploratory cross-section calculations for the ^{235}U 1/2$^+$, 0.073-keV isomeric state to determine whether it might fission better than the ground state with incident low-energy neutrons. This was thought possible because the lowest fission barrier in ^{236}U is 0$^+$. Therefore, any low-lying 0$^+$ and 1$^+$ states readily made by low-energy neutrons on the 1/2$^+$ isomer might prefer to fission rather than emit neutrons or dipole photons. Unfortunately, there appear to be no low-lying 1$^+$ discrete fission channels, and presently we find that the isomer undergoes less neutron fission than the ground state for neutron energies below 100 keV. We intend to carry out further calculations with updated discrete-level information and improved fission modeling.

4 <u>Calculated Photon-Induced Isomer Production in ^{176}Lu and Its Impact on the Use of ^{176}Lu as a Stellar Chronometer and/or Thermometer</u>
(Gardner, Gardner and Hoff)

The isotope, ^{176}Lu, is astrophysically important because it is made only by the s-process. Moreover, with a ground state half-life of 3.6×10^{10}y, it would function as an excellent galactic s-process chronometer were it not for the 3.7-h isomeric state at 123 keV. We have calculated the production and destruction of the isomer by photons and neutrons, using absolute photon strength functions and well-tested, modeled, discrete nuclear level sets for $^{175-177}$Lu. We find that our calculations predict photo-production cross sections for ^{176m}Lu that are much larger than previously thought, and that the threshold for such production is lower than had been assumed. These two facts combine to exert an enormous effect, a decrease of a factor of 10^7, on the half-life for photoexcitation of the ^{176m}Lu as a function of temperature (Fig. 1).

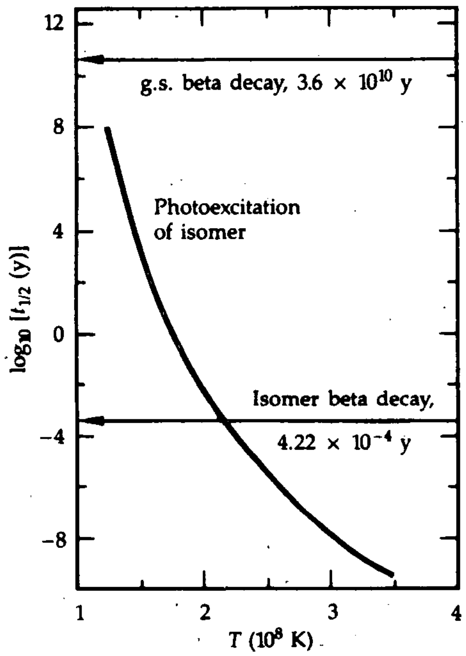

Fig. 1 The half-life for photoproduction of the ^{176}Lu isomer from the ground state as a function of the temperature of the Planck photon-density energy distribution.

We conclude: (1) that the ground state and isomer will be in equilibrium near 2×10^8 K(kT = 15-20 keV), a much lower temperature than previous literature estimates of kt = 30 keV; and (2) that the average temperature during the s-process could not exceed about 1.2×10^8 K(kT = 10 keV) if ^{176}Lu were to function as a chronometer. With our complete set of calculated cross sections, the possible usefulness of ^{176}Lu as a stellar thermometer can be extended to even lower temperature ranges where the ground state and isomer are not in thermal equilibrium. This work should be useful in delimiting the parameters in various current models of the s-process in nucleosynthesis.

5. Disagreement Between Measured Capture γ-Ray Spectra and Our Calculations
(Gardner and Gardner)

We found disagreement when we compared our calculated capture γ-ray spectra for incident 0.5 MeV neutrons on various target nuclei with those measured and recently published by Voignier, Joly and Grenier (NSE 93 (1986) 43). For example, a comparison (see Fig. 1) of our calculated spectrum for ^{184}W with that published showed the measured spectrum to be lower by about a factor of four or more over most of the energy range. Further, this experimental spectrum, together with the capture cross section measured at 0.5 MeV by the same workers, would only account for about 25% of the energy emitted as γ-rays. Our calculated spectrum and capture cross section (the computed cross section being in agreement with the measured one) reproduced the total energy to within a percent. We observed the same sort of discrepancies for the targets ^{89}Y, ^{159}Tb, ^{181}Ta and ^{209}Bi when we compared the data of Voignier, et al, either with our

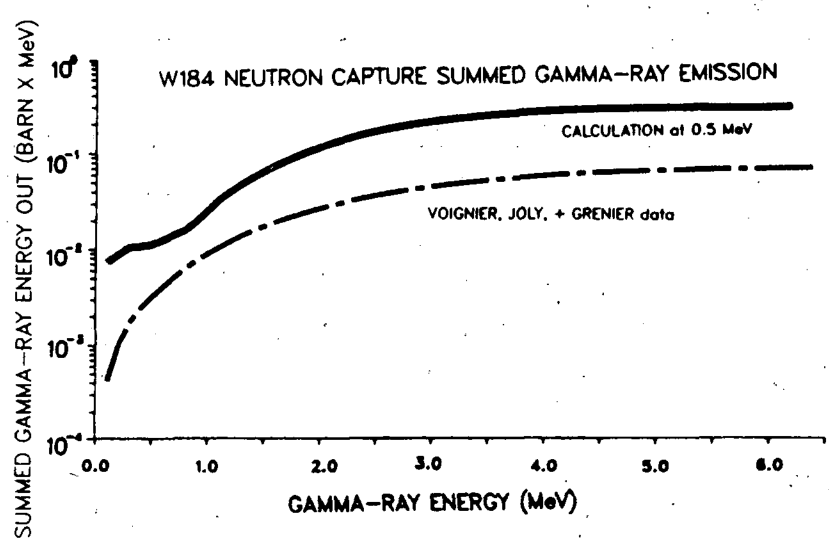

Fig. 1. A Comparison of the summed γ-ray energy out for ^{184}W obtained from the Voignier, et al, data and from our calculation.

calculations or with other measured spectra. We wrote to the experimenters about these discrepancies and understand that indeed each of the spectra published does not include its own unique average γ-ray multiplicity determined from the experiment.

6. <u>Electromagnetic Moments for $^{88,86}Sr$</u>
(Becker and Warburton)

The quantities $B(E2;\, J_i \rightarrow J_i-2)$, $g(J_i)$ and $Q(J_i)$ have been calculated for $J_i = 2^+, 4^+, 6^+$ and 8^+ in order to compare to recent experimental results. Calculations were done using the shell model code OXBASH and the (realistic) PMM two-body interaction. The model space for both $^{88,86}Sr$ assumed an inert ^{56}Ni core. The minimum-maximum valence particles allowed for the orbitals ($f_{5/2}$, $p_{3/2}$, $p_{1/2}$, $g_{9/2}$) are:

^{88}Sr(10-12, 6-8, 2-4, 8-10);
^{86}Sr(12-12. 4-8, 0-4. 8-12).

A comparison of these results with experiments is presented in Table 1.

Table 1.

Moments ^{88}Sr ^{86}Sr

		Calculation				Experiment	
		2_1^+	4_1^+	6_1^+	8_1^+	2_1^+	8_1^+
^{88}Sr	$Q(efm^2)$	23.4	36.0	-9.8	-48.9		
^{88}Sr	g	1.23	1.16	1.36	1.36	0.96(17)[a]	
^{88}Sr	$B(E2)_{WU}$	5.8	1.2	2.0	2.8	7.04(41)[a]	<0.86[a]
^{86}Sr	$Q(efm^2)$	+7.8	-4.4	+7.0	+22.3		
^{86}Sr	g	+0.36	-0.17	-0.18	-0.18	0.265(50)[a]	-0.243(3)[b]
^{86}Sr	$B(E2)_{WU}$	5.03	1.51	1.83	0.98		

a) A. Kucharska, Ph.D. Thesis, Oxford University Nuclear Physics Laboratory (1986).

b) Nucl. Phys. <u>A237</u>, 182 (1975).

7. Shell-Model Calculations of First-Forbidden Beta Decay in the Mass 40 Region.
(Warburton, Millener, Brown and Becker)

First-forbidden beta decay with selection rules $\Delta J = 0, 1, 2,$; $\Delta\pi = -$ is a good test of nuclear structure near the interface between major shells such as ^{16}O and ^{40}Ca. Recently, we have developed a cross-shell interaction for use in the model space 1d5/2, 2s1/2, 1d3/2, 1f7/2, 2p3/2, 1f5/2, 2p3/2 (the SDPF interaction) and used it to calculate unique first-forbidden rates in the decay of ^{35}P, ^{37}S, ^{38}S, and ^{38}Cl. These calculations have now been extended to include non-unique rates including an interesting $0^{+} \rightarrow 0^{-}$ ^{38}S decay.

8. Dipole Strength Function Studies in the Actinide Mass Region
(Gardner, Gardner and Hoff)

We have calculated photon- and neutron-induced reaction cross sections for the ground and isomeric states of a number of actinide isotopes, using large sets of modeled discrete levels in each nucleus together with absolute E1 and M1 (and occasionally E2) γ-ray strength functions. We studied the reactions $^{238}U(n,\gamma)^{239}U$, $^{238}U(\gamma,f)$, $^{237}Np(\gamma,f)$, and $^{237}Np(\gamma,\gamma')^{237m}Np$. We obtain good agreement between our calculations and measurements reported in the literature if we increase our absolute E1, M1 and E2 strength functions, previously reported to be valid for elements from Sr to Bi[1] by about 27%. In our study of the photon production and destruction of the 68ns $5/2^{-}$ isomer of ^{237}Np at 0.06 MeV, a possible candidate for a γ-ray laser, we found that the modeling of the M1 dipole strength function determines whether we obtain an average m/g ratio value that is greater than one for photons in a continuous energy range of about 0.4 to 1.15 MeV. An experimental measurement of the population of this isomer, using photons in the energy range of 0.4 to 4.0 MeV, would be valuable in shedding light on the magnitude and energy dependence of the M1 strength function at these low energies.

---

[1] M. Gardner, Proc. Int. Conf. on Nuclear Data for Basic and Applied Science, Santa Fe, NM, 2, 1481 (1985).

LOS ALAMOS NATIONAL LABORATORY

A. NUCLEAR DATA MEASUREMENTS

1. <u>Low Energy Fusion Cross Sections:</u> Charged Particle Reactions (N. Jarmie and R. E. Brown)

The goal of this project is to determine cross sections for interactions among the hydrogen isotopes in the bombarding-energy range 10-120 keV. Such cross sections are fundamental to the operation of future controlled-fusion reactors. Experimental work with the facility constructed for this purpose [LEFCS: Low-energy Fusion Cross Sections] is complete. Analysis and publication are continuing.

Work on the completion of the D(t,α)n reaction is continuing from last year because of an interesting development in the R-Matrix analysis of the data (with G. Hale). Bound states and resonances of a compound system are often represented as S-Matrix poles in the complex-energy plane. What is interesting is that the analysis appears to require a pole on a continued complex sheet ("second Riemann sheet")--a so-called "shadow" pole. This result is unusual and is being explored.

G. Hale of Los Alamos is also extending R-Matrix phenomenology to be able to handle 3-body breakup. This development is of great interest to us to help analyze the three-body breakup alpha spectra of the T(t,α)nn reaction; and, in particular, to be able to estimate the shape of the neutron spectra, which we have found impossible to measure.

A review paper was prepared and given for the IAEA Advisory Group Meeting on Nuclear Data for Fusion Reactor Technology, Dec. 1-5, 1986 in Gaussig/Dresden, GDR entitled *Requirements for Charged-Particle Reaction Cross Sections in the D-T, D-D, T-T, and D-^{3}He Fuel Cycles* [Los Alamos preprint LA-UR-86-3705] which covers the status of data and evaluation of the low energy reactions: ^{2}H(t,α)n, ^{2}H(d,p)^{3}H, ^{2}H(d,^{3}He)n, ^{3}H(t,α)nn, ^{3}He(d,p)^{4}He, ^{3}He(^{3}He,α)pp, and the associated elastic scattering and capture reactions. This paper emphasizes the need for a standard "handbook" of the best evaluated fuel-cycle cross sections and reactivities. Some fusion-reactor designers are still using old and sometimes grossly inaccurate data and there exists no world standard collection of charged-particle data such as exists for neutron data.

2. <u>The (n,p) and (n,t) Cross Sections for Thermal Neutrons Reacting with Boron-10</u> (R. C. Reedy; D. Lal, K. Nishiizumi, and W. Rison (Univ. Calif., San Diego); Y. D. Dande (BARC, Trombay, India); and M. Suter and W. Woelfli (ETH, Zurich, Switzerland))

The cross sections for the $^{10}B(n,p)^{10}Be$ and $^{10}B(n,X)^3H$ reactions using thermal neutrons were measured, the former for the first time and the latter giving a much high value than the previously reported value.[1] Samples of dilute orthoboric acid (about 1 ml) were sealed in quartz ampoules and irradiated with neutrons in the thermal column of the Omega West Reactor (OWR) at Los Alamos. Iron wires were used to monitor the neutron fluences, which were about 10^{17} neutrons/cm^2. Two ampoules were analyzed for their ^{10}Be activities. After a known amount of ^9Be was added to the solution and the beryllium separated and purified, the $^{10}Be/^9Be$ ratio was determined by accelerator mass spectrometry at the ETH in Zurich. The cross sections measured for the production of ^{10}Be in the two vials were 6.2 and 6.6 mb. Including an uncertainty in the neutron fluence, the measured cross section for the $^{10}B(n,p)^{10}Be$ reaction with thermal neutrons was 6.4 ± 0.5 mb.

The other quartz vials were sealed within 15 days in 1720 glass to minimize the diffusion of ^3H and its decay product ^3He from the vials. After several months, helium was extracted from the vials and analyzed. The results showed large variability, which we ascribe to the fact that OWR used tank helium to push the samples into and out of the thermal column. To set a lower limit to the $^{10}B(n,t)$ cross section, the ^3H in two vials was converted to HTO and all the helium was removed. These samples gave a lower limit the the $^{10}B(n,t)$ cross section of 0.3 barns. To measure this cross section, we irradiated 1720 glass that contained 1.516% boron and a quartz vial like that used at OWR in the Apsara Swimming Pool Reactor of the Bhabha Atomic Research Centre in Trombay, India, to a fluence of about 10^{17} neutrons/cm^2. As before, the helium in the samples was measured. For the glass, a correction for the production of ^3H and helium from lithium had to be made. The measured cross section for the $^{10}B(n,t)$ reaction with thermal neutrons was 0.89 ± 0.09 barns. This value is much higher than the 50 mb cross section reported previously for this reaction.[1] As pointed out by G. M. Hale (priv. comm.), this substantially higher thermal $^{10}B(n,t)$ cross section could have implications for the discrepancy in the helium production measurements for boron in several critical assemblies relative to calculations using ENDF/B-V cross sections.

The much higher cross section for the (n,t) channel (0.89 b) than for the (n,p) channel (6.4 mb) in the reaction of thermal neutrons with ^{10}B is not predicted on the basis of normal theoretical considerations of the Coulomb barrier, and new models to explain the results are being considered. These cross sections will be very useful in interpreting ^{10}Be and ^3He measurements in geophysical samples that had been deeply buried and in which it had previously been assumed that the

---

[1] F. Cserpak, T. Biro, and J. Csikai, "Measurement of Cross Sections for (n,t) Reactions on Light Nuclei," Neutron Physics and Nuclear Data for Reactor and Other Purposes, Proc. Int. Conf., Harwell, Sept., 1978, OECD Nucl. Energy Agency, Paris (1978), 761.

production of these nuclides was negligible, such as ^{10}Be in material near subduction zones or ^{3}He in diamonds. Papers on these measurements have been submitted to Nuclear Physics.

3. Low-Energy (n,charged particle) Cross Sections on Unstable Nuclei: The $^{7}Be(n,p)^{7}Li$ Cross Section from 0.03 eV to 13.5 keV (P. E. Koehler, C. D. Bowman, F. J. Steinkruger, D. C. Moody, J. W. Starner, S. A. Wender, R. C. Haight, P. W. Lisowski and W. L. Talbert)

Our initial measurements at WNR of the $^{7}Be(n,p)^{7}Li$ cross section from 0.03 eV to 200 eV reported here last year have been extended to 13.5 keV. We have also measured the absolute thermal cross sections for the ground state (38400 ± 800 b) and first excited state (420 ± 120 b) groups at the Omega West Reactor. These results are considerably different than the previously accepted value of 48000 ± 9000 b for the total ^{7}Be + n thermal cross section.[1] Our new results are compared to the old thermal value[1], previous $^{7}Li(p,n)^{7}Be$ measurements[1,2] (converted to $^{7}Be(n,p)^{7}Li$ using reciprocity), and an R-matrix calculation[3] in Fig. A-1. Our data agree well with the R-matrix calculation and the $^{7}Li(p,n)^{7}Be$ data of ref. 1, while the $^{7}Li(p,n)^{7}Be$ data of ref. 2 and the previous thermal value[1] are about 15% and 20% higher than our data respectively. In addition, we see no indication of the narrow resonance recently reported at approximately 170 eV.[4] We expect to publish these results soon, exploring their implications on the big bang nucleosynthesis of ^{7}Li and the structure of ^{8}Be.

---

[1] R. C. Hanna, "The Disintegration of ^{7}Be by Slow Neutrons", Phil. Mag. 46 (1955) 381.

[2] R. L. Macklin and J. H. Gibbons, "Study of the $T(p,n)He^{3}$ and $Li^{7}(p,n)Be^{7}$ Reactions", Phys. Rev. 109 (1958) 105.

[3] G. Hale *et al.*, This report Section B-2.

[4] Y. M. Glendenov *et al.*, "On the Study of the $^{7}Be(n,p)^{7}Li$ Reaction in the Neutron Energy Range from 0.025 to 500 eV", JINR Rapid Communications, N17-86, Dubna, 1986, p 36.

4. Low-Energy (n,charged particle) Cross Sections on Unstable Nuclei: The $^{54}Mn(n,p)^{54}Cr$ and $^{14}N(n,p)^{14}C$ Cross Sections from 0.04 eV to approximately 100 eV. (P. E. Koehler, H. A. Obrien, and C. D. Bowman)

In our continuing effort to measure (n,charged particle) cross sections of importance to a better understanding of nucleosynthesis and basic nuclear physics, we have completed preliminary measurements on ^{54}Mn and ^{14}N. The data are currently being analyzed and the initial results are very encouraging. The measurements were made with the Proton Storage Ring (PSR) operating at only 10% of its design intensity. Our results show that when the PSR reaches its design intensity we should be able to extend these measurements to neutron energies of a few keV. The measurements will also be extended to include other targets such as ^{22}Na, ^{26}Al, ^{36}Cl, and ^{55}Fe. The results should be very important to the study of stellar nucleosynthesis.

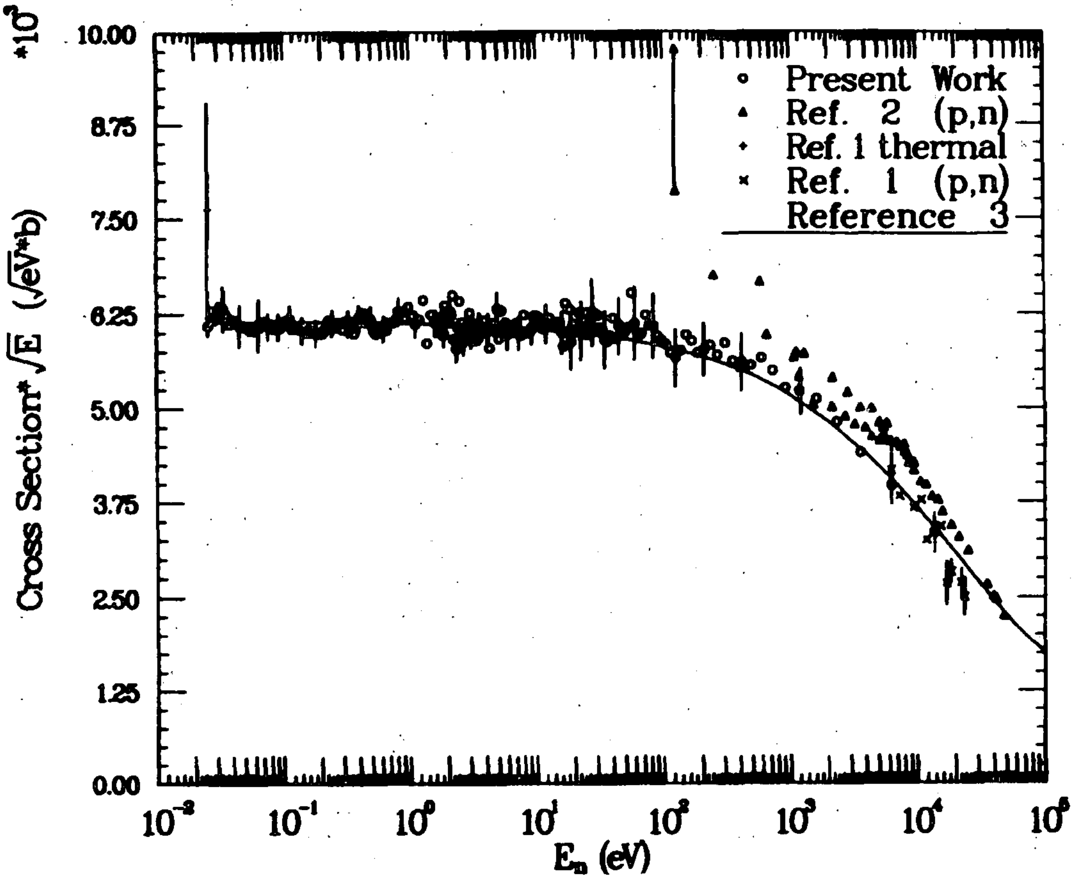

Fig. A-1 The ^{7}Be(n,p)^{7}Li cross section from 0.025 eV to approximately 100 keV. Our new data (circles) are compared to previous ^{7}Li(p,n)^{7}Be data of refs. 1 and 2 (triangles and crosses), the thermal cross section of ref. 1 (plus) and the R-matrix calculation of ref. 3 (solid line).

5. Parity Violation in Neutron Resonances (C. D. Bowman, J. D. Bowman, V. W. Yuan)

The first measurements in the U.S. on parity violation in neutron resonances were conducted on the 0.734-eV resonance in ^{139}La. Ordinarily these measurements are conducted by passing a polarized beam through the sample with the beam polarization parallel and antiparallel to the neutron velocity. A difference in the transmission signals parity violation in the resonance.

Because we did not have beam polarization equipment operational, we devised a different experiment. The unpolarized beam from the PSR was first transmitted through a thick La sample. The difference in cross section for the two equally abundant polarization components in the beam results in a weakly polarized beam at the resonance. This beam was then passed through a spin flipper and through a second sample of the same material. The difference in transmission for the flipped and unflipped beam can then be converted to a matrix element for parity violation. From a preliminary analysis of the data, we believe that our uncertainty will be small compared to the difference between two other measurements at KEK and at Dubna.

6. First Results from LANSCE Benchmark Program (C. D. Bowman)

A program of benchmark measurements for testing neutron transport codes in the 10-eV to 100-keV range has begun at Los Alamos. The measurements are being conducted at a 50-meter flight path associated with the Los Alamos Neutron Scattering Facility (LANSCE). Two simple assemblies have been studied. The first consisted of a 0.8 gm/cm^2 plate of ^{235}U placed against a cylindrical 11.4 cm diam., 5.1-cm thick NE-213 liquid scintillator with low energy neutron isolation from the scintillator provided by a 0.08-cm thick layer of Cd. The second assembly was the same but with a 0.48-cm thick layer of polyethylene and a 6 gm/cm^2 layer of ^{235}U added. A 10.2-cm diameter neutron beam directed along the P. M. tube axis struck the assembly, encountering the ^{235}U sample first in each geometry. Pulse shape discrimination was used to eliminate gamma-ray background from the fission neutrons which we wished to detect. Measurements were made from 4 to 300 eV.

A sample of the results from 78-102 eV are shown in Fig. A-2. The upper panel shows the thicker assembly; the lower panel looks very much like the ^{235}U fission cross section. The data are not normalized. The dramatic difference between these two assemblies should provide a stringent test of the performance of neutron transport codes and of the accuracy of ^{235}U data. The difference between these two data sets is believed to arise primarily from variations in the capture-to-fission ratio. This kind of experiment might be useful in improving the parameterization of the data in the unresolved resonance region.

The upper data were taken in one hour using an energy independent beam filter which reduced the intensity by a factor of 100. With the PSR running at full power and without this attenuator, this data in principle could have been measured in about three seconds.

7. Gamma-Ray Production in Ho, Eu, and Gd (S. A. Wender, S. Hansen, J. Aubrey, and D. Larson (Oak Ridge National Laboratory)

We are continuing our measurements of continuum gamma-ray production in rare earth elements. Data similar to that already taken on Ho has been taken on natural Eu and Gd samples. The data, which were taken at ORELA, consist of gamma-ray pulse-height spectra for gamma energies from 0.5 to 12 MeV. Twenty pulse-height spectra were obtained for neutron energy bins from 400 eV to 3 MeV. The detector was a 7.6 x 7.6-cm BGO detector located at 125° with respect to the incident neutron beam. The results of the measurements are presently being analyzed.

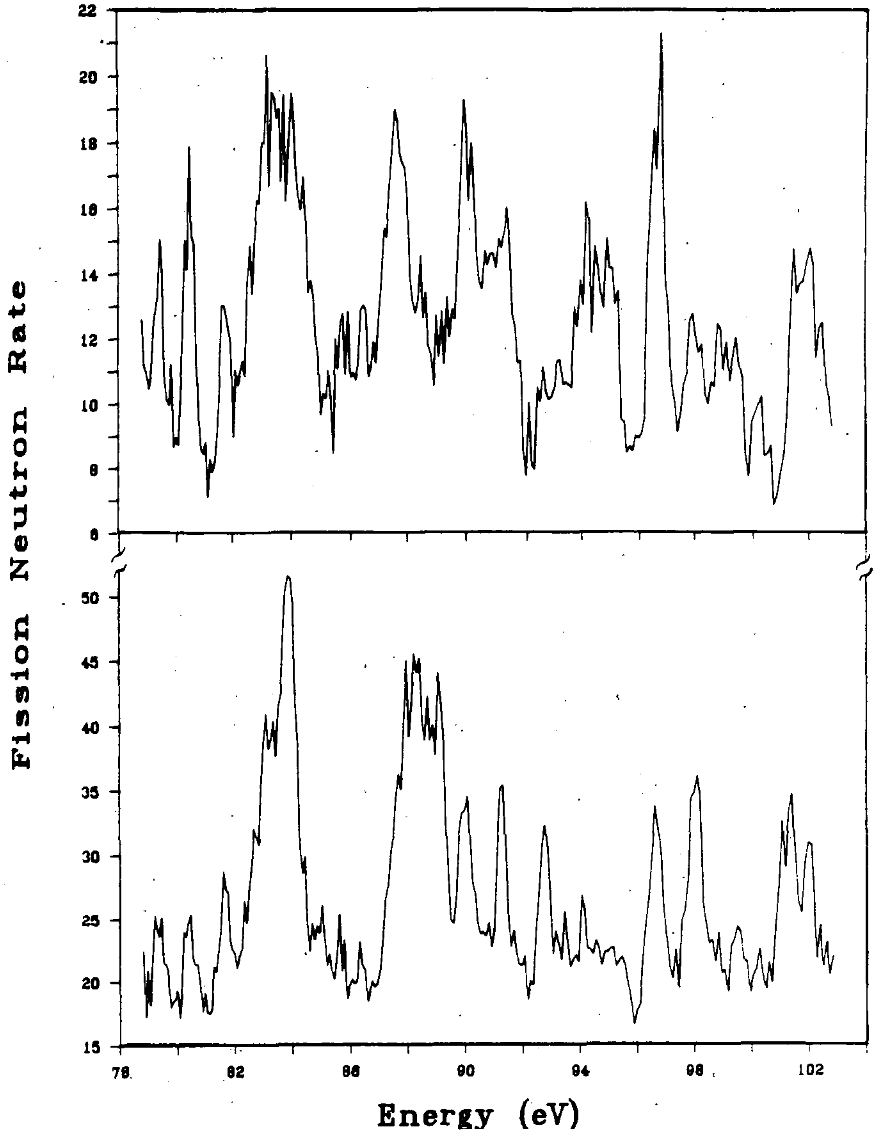

Fig. A-2 The upper panel shows the data from the complex ^{235}U assembly. The lower panel shows data from the simple assembly for which the structure approximates that of the ^{235}U fission cross section. The correlation in the structure of the data is not nearly so strong as one might expect. The fluctuation amplitude is at least as great in the upper panel as the lower panel.

8. <u>Status of the WNR Facility</u> (P. W. Lisowski and S. A. Wender)

The capability of the Weapons Neutron Research (WNR) facility has been significantly enhanced for fast-neutron time-of-flight experiments with the completion of the first phase of construction of a new white-neutron spallation source. The facility was commissioned in December, 1986, and at present, has shielding for up to 200 nA of 800 MeV beam from the Los Alamos Meson Physics Facility (LAMPF). Because this area is multiplexed with the PSR/LANSCE complex, experiments receive approximately a factor of five more operating time each LAMPF cycle. Improvements to the chopping and bunching system have resulted in an increase of a factor of four in the number of protons/pulse. Although the facility received beam for only one week during December, six experiments were performed; 1) neutron-induced fission cross section ratios for $^{235,238}U$ and ^{237}Np from 1 to 400 MeV; 2) studies of neutron-induced gamma ray production from ^{11}B, ^{12}C and ^{181}Ta; 3) (n,p) reaction studies; 4) ^{235}U fission cross section measurements between 50 and 200 MeV; 5) SDI detector calibrations; and 6) high resolution 800 MeV (p,n) angular distributions. A plan view of the WNR facility and time-of-flight yard as it is presently configured is shown in Figure A-3. Plans are now underway for the second phase of construction which will increase the shielding to be adequate for 20 micro-amperes of proton beam.

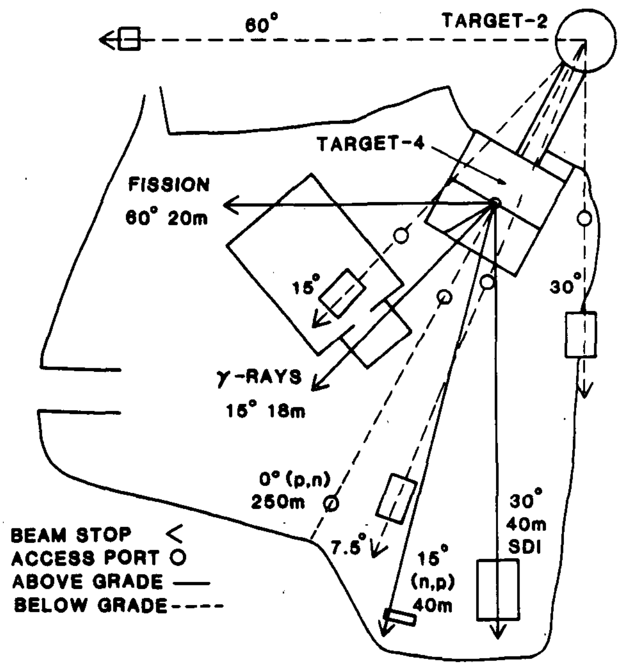

<u>Fig. A-3</u> Plan view of the Los Alamos WNR facility. The proton beam enters through target-2 and can be used in either the target-2 or target-4 complex.

9. Cross Sections and Yields for (p,xn) Reactions at Medium Energies (M. M. Meier, C. A. Goulding, G. L. Morgan, H. Robinson, G. J. Russell, J. L. Ullmann)

The goal of this project is to provide microscopic production cross sections and yield data for reactions initiated by medium energy protons. These data are used to refine nuclear models (e.g. HETC) and provide benchmarks for codes that are used to estimate the primary and secondary production processes as well as transport through extended media. Such codes are useful in accelerator breeding, hadron calorimetry and shielding design.

The 800 MeV (p,xn) data at 7.5 and 15 degrees have been reported at the April 1986 APS meeting and submitted for publication (Phys. Rev. C). This year we extensively modified the WNR Target 2 facility to include beamlines at 7.5, 15, 30, 60, 120 and 150 degrees and made measurements on stopping length and thin targets at 256 MeV bombarding energy.

The lengths of the flight paths are between 30 and 70 meters and neutron backgrounds were typically less than 3%. The neutron collimation can be varied on all flight paths to produce either 25 cm dia. beams at the detector stations for thin targets or to view 35 cm extended targets at the target location. The 256 MeV neutron yield measurements were made with stopping length and 200 MeV thick targets of elemental C, Al, Fe and depleted U. As reported in contribution A-10 to this report, gamma-ray data were also obtained at 30 and 120 degrees for these targets. In addition, cross-section data were obtained for thin targets of C, Fe and depleted U. In addition to the yield and cross-section measurements, several auxiliary measurements were performed. Transmissions for the U filters (used to increase the neutron/gamma detection ratio in the neutron measurements) were measured over the energy range of interest. The total cross section for C was measured in the flux from a stopping length U target. This provided a length calibration for the flight paths using resonance energy standards above 500 keV as well as a check on the relative charge normalization, background estimation and deadtime correction. Neutron detector efficiency was determined using monoenergetic neutron source reactions between 1 and 35 MeV using the Los Alamos Ion Beam Facility and from 150 MeV to 800 MeV using the 800 MeV Pb(p,xn) cross section. The secondary emission monitor for charge normalization of runs was absolutely calibrated against activation foils several times during the course of the yield measurements. The calibration constants obtained agreed to ± 1%, the accuracy of the foil counting measurement. A new data acquisition system with 1 μsec storage time enabled us to acquire data at rates that are roughly twenty times higher than in the past.

10. Proton Induced Gamma-Ray Production (R. O. Nelson, S. J. Seestrom-Morris, C. E. Moss, S. A. Wender, N. W. Hill (Oak Ridge National Laboratory)

We measured the gamma-ray yield following bombardment of targets of natural carbon, aluminum, iron and uranium by 256 MeV protons. Target thicknesses were stopping length and stopping length less 50 MeV. These measurements were made at two angles using four detectors. The 120° measurements were made with a flight path of 65 m using a Ge(Li) detector and a 7.6 x 7.6-cm BGO detector. At 30°, the flight path was 30 m and a 7.6 x 7.6- NaI detector and a 7.6 x 7.6-cm BGO detector was used. The results of these measurements are being analyzed and yields/incident proton will be obtained.

11. Neutron Induced Gamma-Ray Production (R. O. Nelson, S. J. Seestrom-Morris, S. A. Wender, C. R. Gould, and G. E. Mitchell (North Carolina State University/TUNL), N. W. Hill (Oak Ridge National Laboratory)

We measured the cross section and angular distribution of the 4.44 and 15.1 MeV gamma-rays in ^{12}C induced by neutrons from the recently completed Phase-I white neutron source at the WNR facility. The experimental apparatus consists of five 7.6 x 7.6-cm BGO detectors spanning an angular range from 40° to 140° in the reaction plane. The results of the measurements are being analyzed now and we expect to obtain the cross sections and angular distributions of these gamma-rays from threshold up to approximately 200 MeV.

12. Neutron Induced Fission Cross Section Ratios for $^{235,238}U$ and ^{237}Np from 1 to 400 MeV (P. W. Lisowski, J. L. Ullmann, S. B. Balestrini; A. D. Carlson, and O. A. Wasson, National Bureau of Standards); N. W. Hill, (Oak Ridge National Laboratory))

Time-of-flight measurements of neutron induced fission cross section ratios for $^{235,238}U$ and ^{237}Np were performed using the newly commissioned spallation neutron source located at the Los Alamos WNR facility. A multiple-plate gas ionization chamber was used at a 20-m flight path to simultaneously measure the fission rate for all samples over the energy range from 1 to 400 MeV. At energies below 30 MeV, cross sections are being obtained relative to hydrogen using a proton-recoil spectrometer. From 30 to 200 MeV, cross sections for ^{238}U and ^{237}Np are being determined relative to ^{235}U by comparison with data obtained in a separate experiment. During the next LAMPF operating cycle, experiments will be performed to improve the ^{235}U fission cross section standard.

13. Delayed Neutron Spectral Measurements (H. F. Atwater, C. A. Goulding, C. E. Moss, and A. A. Robba)

We have initiated a program of delayed neutron spectral measurements for neutron energies above 1 MeV. This program consists of two parts: 1) measurement of integrated precursor spectra and 2) measurement of spectra from separated individual precursors.

The integrated spectral measurements were performed by using the Godiva burst reactor to irradiate ^{235}U samples. The samples were moved to a counting location by a pneumatic sample transport system. The neutron spectra were measured by a liquid scintillator spectrometer system. Preliminary neutron spectral data has been taken between 1 and 30 sec. after the fission burst. These data have been sorted into three time bins and extend to 4 MeV neutron energy. These data have been compared to the model predictions of England and Mann and, in general, confirm the validity of those predictions. In the future, we hope to take data at 0.5 sec. after fission where the high energy neutron emitting precursors are accentuated.

The separated precursor measurements were performed at the Tristan separated isotope facility of the Brookhaven High Flux Beam Reactor. Measurements were performed on three isotopes, $^{96,97,98}Rb$. The neutron spectra were measured to 4 MeV. The analysis of these data is now in progress. The ^{96}Rb data will serve as a benchmark because the neutron spectrum below 2 MeV is well known. Also, the neutron emission probability has been measured by many groups and, therefore, the absolute normalization of the neutron spectrum is known. In the future we hope to measure the spectra of some of the bromine isotopes with particularly large energy windows.

14. Delayed Gamma-Ray Spectral Measurements (C. E. Moss, R. A. Pederson, T. F. Wimett (Los Alamos); P. Reeder and R. Warner (Battelle Pacific Northwest Lab))

Delayed gamma-ray spectra were measured in conjunction with the delayed neutron spectral measurements (reported separately). The emphasis was on detecting high energy gamma rays and on identifying gamma rays from very neutron-rich isotopes which emit high energy delayed neutrons.

Integrated spectral measurements were performed on a ^{235}U sample irradiated by the Godiva burst reactor. Two pneumatic transport systems were used. A 10-m system transferred the sample in less than one second to a shielded area where two pulse-height distributions were acquired. The first was between 1 and 61 seconds after the burst and the second was between 300 and 1200 seconds. Alternatively, a 240-m system transferred the sample to a counting laboratory in less than 15 seconds where pulse-height distributions were acquired. The detectors were a bismuth germanate (BGO) detector, which has good efficiency at high energy, and a germanium detector. Analysis is in progress. In future measurements we hope to use electronics more suitable for extremely high counting rates (10^6 Hz) and to acquire the spectra into sixteen time bins.

Spectral measurements on individual mass numbers were performed at the TRISTAN isotope separator of the Brookhaven National Laboratory. The mass numbers surveyed were A = 79 through 101 and A = 127 through 146. The detectors were BGO and germanium; there was no time binning. Preliminary analysis indicated some 6-MeV gamma rays from neutron unbound states but no gamma-ray energies greater than 10 MeV. In future measurements we hope to refine our setup and use a different ion source to produce different isotopes.

15. <u>Gamma Rays From Fission Products Produced By Photofission</u>
(C. L. Hollas, D. A. Close, and C. E. Moss)

Spectra of gamma rays from fission products produced by photo-fission of ^{232}Th, ^{235}U, and ^{239}Pu have been measured. The target samples were irradiated with bremsstrahlung gamma rays produced by 10-MeV electrons from a small linear accelerator. The electron beam had a macro-structure of 4-μsec duration pulses at a 10-Hz repetition rate. The peak current in each pulse was 80 mA. The gamma-ray spectrometer was an 11% efficient coaxial, high-purity germanium detector equipped with a standard resistive feedback preamplifier. The germanium detector was paralyzed from the beginning of the beam pulse for 13 msec. The multichannel analyzer was gated off for 13.6 msec by a gate pulse derived from the electron beam burst and remained on for 86.4 msec until the next burst. Each target was irradiated approximately 2 hours. The portion of the gamma-ray spectra from 1000 to 1500 keV, shown in Fig. A-4, reveals a distinctive intensity distribution for the four isotopes studied. The source of the differences for these distributions is presently under investigation.

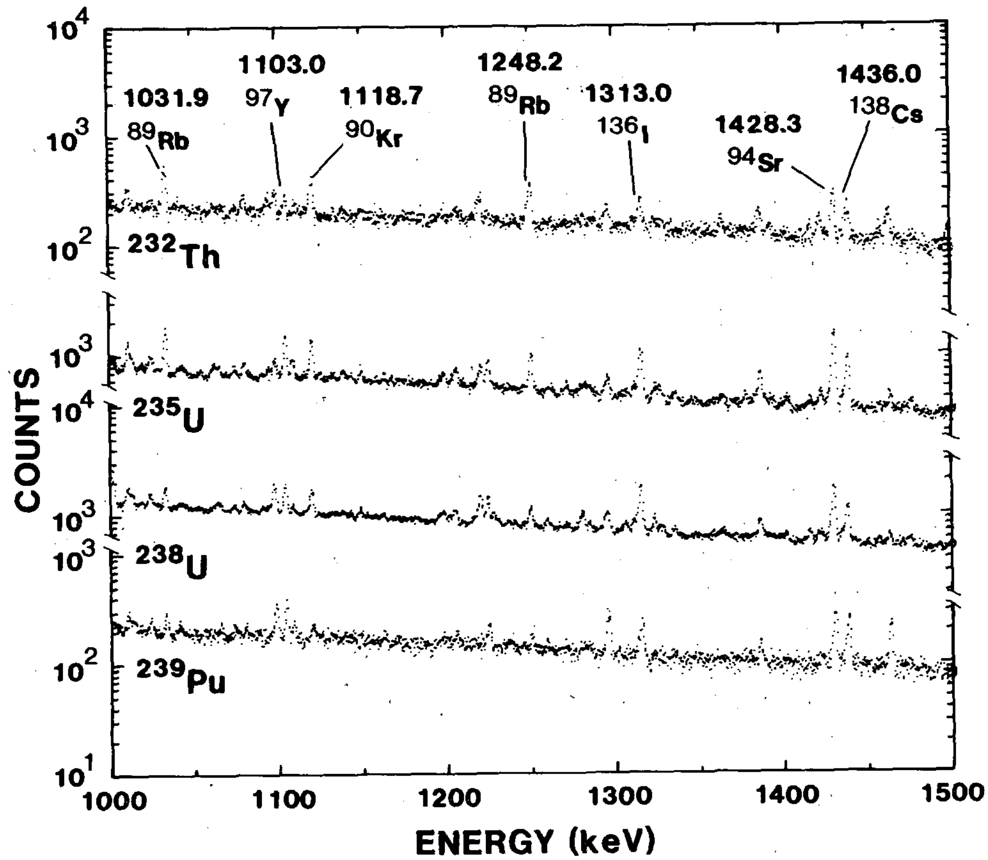

Fig. A-4 Gamma rays between 1000 and 1500 keV from fission products resulting from photofission of ^{232}Th, ^{235}U, ^{238}U and ^{239}Pu. Selected peaks are labeled with the energy and associated fission product

B. NUCLEAR DATA EVALUATION

1. Pole Structure of the $J^{\pi} = 3/2^{+}$ Resonance in ^{5}He (G. Hale, R. Brown, N. Jarmie)

The parameters from our R-matrix fit of reactions in the ^{5}He system, which includes the latest measurements of the T(d,n)[1] and n-α total[2] cross sections over the $J^{\pi} = 3/2^{+}$ resonance at $E_x = 16.76$ MeV, have been used to explore the S-matrix pole structure of the compound system. The correct procedure for finding poles and residues of the S matrix from R-matrix parameters involves calculating Coulomb functions in the complex energy plane, which has been done using the elegant numerical routine of Thompson and Barnett.[3]

For $J^{\pi} = 3/2^{+}$, the R-matrix level corresponding to the resonance just above the d-t threshold gives two poles on different unphysical sheets of the many-channel Riemann energy surface. Resonance parameters for the poles are given in the table below.

TABLE B-1. Resonance parameters for the $J^{\pi} = 3/2^{+}$ state in ^{5}He. Energies and widths are given in keV in the center-of-mass sytem relative to the d-t threshold.

Pole	Resonant Energy	Γ_d	Γ_n	Γ
M	46.97	27.69	46.51	74.20
S	81.57	7.11	0.17	7.28

The pole designated "M" is clearly the main pole associated with the structure observed in the low-energy T(d,n) reaction cross section and in the n-α total cross section at neutron energies near 22.13 MeV. The total width of 74.2 keV is in good agreement with the value 76 ± 12 keV found by Haesner et al.[2] from a single-level Breit-Wigner fit to their n-α total cross section measurements over the resonance, although our partial neutron width disagrees with their value of 37 ± 5 keV.

The other pole, designated "S" for "shadow" pole in the terminology introduced by Eden and Taylor,[4] lies much closer to the real energy axis at a center-of-mass energy of about 82 keV; it is responsible for the approach of the reaction S-matrix element to its unitary limit at a deuteron energy of about 137 keV, giving nearly the maximum possible single-transition cross section at that energy.

Similar results have been obtained from a two-level fit[5] to low-energy data for the T(d,n) reaction cross section alone.

---

[1] N. Jarmie, R. E. Brown, and R. A. Hardekopf, Phys. Rev. C 29, 2031 (1984), and the data contained in Ref. 5.

2 B. Haesner, W. Heeringa, H. O. Klages, H. Dobiasch, G. Schmalz, P. Schwarz, J.. Wilczynski, and B. Zeitnitz, Phys. Rev. C 28, 995 (1983).

3 I. J. Thompson and A. R. Barnett, Comp. Phys. Comm. 36, 363 (1985).

4 R. J. Eden and J. R. Taylor, Phys. Rev. 133, B1575 (1964).

5 R. E. Brown, N. Jarmie, and G. Hale, "Fusion Energy Reaction $^3H(d,\alpha)n$ at Low Energies," submitted to Phys. Rev. C (1987).

2. R-Matrix Analysis of Reactions in the ^{8}Be System [G. M. Hale, R. E. Seamon, and D. C. Dodder (X-Division Consultant)]

In order to obtain better ^{8}Be level parameters for our calculations of ^{6}Li(t,n) spectra[1], and also to provide a theoretical description of the ^{7}Be(n,p)^{7}Li reaction in support of ongoing Los Alamos measurements of the cross section at low energies,[2,3] we have begun an R-matrix analysis of reactions in the ^{8}Be system.

The first stage of the analysis considered α-α scattering at energies E_α below 34 MeV (E_x < 17.1 MeV). Despite the simple channel structure of this problem, discrepancies among the cross-section measurements hindered a definitive determination of the level structure in this energy range. We obtained a reasonable fit to most of the data by using the five known levels of ^{8}Be that occur below E_x = 17 MeV.

In view of the relatively small overlap between α-α and p-^{7}Li or n-^{7}Be states, the next stage was a separate analysis of the two-channel system p-^{7}Li, n-^{7}Be at energies $0 \leqq E_p \leqq 3$ MeV ($17.25 \leqq E_x \leqq 19.88$ MeV). This analysis uses, for the first time to our knowledge, a charge-symmetric R-matrix framework in which the reduced widths for the charge-conjugate p-^{7}Li and n-^{7}Be channels are constrained to have the same magnitudes, and equal or opposite signs depending on whether the isospin of the level is T = 1 or T = 0. Thus, there are effectively free parameters for only one channel (we take it to be p-^{7}Li) in our simultaneous fit to ^{7}Li(p,p)^{7}Li and ^{7}Li(p,n)^{7}Be cross-section and polarization data, along with a newly measured thermal value[2] for the ^{7}Be(n,p) cross section.

The level structure emerging from our fit appears to agree fairly well with previously determined P-wave resonances. The S-wave structure is somewhat different, however, with 2^- levels located both below and above the n+^{7}Be threshold in order to account for the significant threshold effects in p+^{7}Li elastic scattering and large ^{7}Be(n,p) thermal cross section with a charge-symmetric description.

Our present prediction for the ^{7}Be(n,p) cross section at energies up to E_n = 1 MeV is shown in Fig. B-1. The calculated value of the thermal cross section is 38,701 b, within ~ 1% of the measurement. One sees strong deviations from 1/v behavior at energies above 100 eV, caused by broad

S-wave and P-wave resonances, and narrower structure at about 400 keV, which is also due to a P-wave resonance. The deviations from 1/v at energies below 50 keV have been substantiated by further recent measurements of Koehler et al.[3]

---

[1] G. Hale, D. George, and P. Lisowski, "Neutron Spectra for the t + ^{6}Li Reaction," in Los Alamos National Laboratory report LA-10513-PR, Applied Nuclear Science and Development Progress Report June 1, 1985-November 30, 1985 (April 1986), p. 1.

[2] P. Koehler et al., Bull. Am. Phys. Soc. 31, 854 (1986).

[3] P. Koehler et al., contribution to this report (1987).

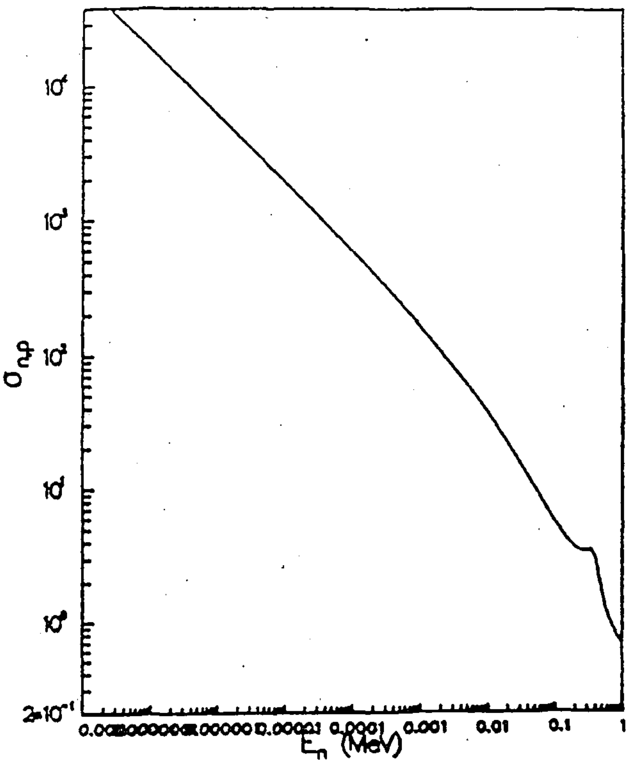

Fig. B-1 R-matrix prediction for the ^{7}Be(n,p)^{7}Li cross section in barns for neutron energies between thermal and 1 MeV.

3. <u>Calculation of (n,n') Reactions from Vibrational Levels in ^{232}Th (E. D. Arthur)</u>

Calculations were made of neutron inelastic scattering from levels in ^{232}Th occupying higher-lying vibrational bands. A primary motivation behind this effort was determination of direct-reaction contributions to scattering from such levels, as well as to compare results with newly reported $^{232}Th(n,n')$ data.[2] The techniques were identical to those we reported in Ref. 3 for $^{238}U(n,n')$ reactions. In particular, coupled-channel optical model transmission coefficients were utilized in Hauser-Feshbach calculations of compound nucleus contributions to elastic and inelastic scattering, as well as for determination of competing capture and fission reaction cross sections. Such coupled-channel calculations also produced direct-reaction components for scattering involving levels of the ground-state rotational band. For the higher-lying levels of primary interest here, we used distorted wave Born approximation (DWBA) calculations to provide the required direct-reaction components. In a fashion identical to that described in Ref. 3, we normalized such DWBA cross sections using $B(E\ell)$ data determined from (p,p'), (d,d') or Coulomb excitation measurements. Use of such techniques produced direct-reaction contributions of 10-15 mb in contrast to significantly larger contributions (50-100 mb) determined in other theoretical analyses.[4,5]

Figure B-2 compares our calculated results with cross sections measured for scattering from the 0.774 MeV 2^+, 0.7741 MeV 3^-, and 0.785 MeV 2^+ levels. Our results agree well with the new direct measurements of (n,n') cross sections available from the Univ. of Lowell[2] but disagree with data inferred from $(n,n'\gamma)$ measurements.[6] Figure B-3 compares our calculations with scattering data available for the 1.054-MeV 2^- state. In this instance, no direct-reaction calculations were attempted so that the curve represents compound nucleus contributions only. Again, there is good agreement with the new (n,n') data. Thus, from the analysis of scattering from these and other ^{232}Th states, we find that direct-reaction contributions to scattering involving higher-lying band members appear to be small. This conclusion is in contrast to that from other theoretical calculations[4,5] but is supported by similar data for $^{238}U(n,n')$.[3]

---

1 E. D. Arthur, Bull. of Am. Phys. Soc. 31, 1238 (1986).

2 C. Giarcia, G. Couchell, J. Egan, G. Kegel, S. Li, A. Mittler, D. Pullen, W. Schier, and J. Shao, Nucl. Sci. Eng. 91, 428 (1985).

3 J. Shao, G. Couchell, J. Egan, G. Kegel, S. Li, A. Mittler, D. Pullen, W. Schier, and E. Arthur, Nucl. Sci. Eng. 92, 350 (1980).

4 A. M. Street and P. E. Hodgson, Nucl. Sci. Eng. 92, 459 (1986).

5 D. W. S. Chan and E. Sheldon, Phys. Rev. C 26, 861 (1982).

6 J. Egan, J. Menachery, G. Kegel, D. Pullen, Nucl. Cross Sections for Technology, NBS Special Pub. 594, p. 685, Eds. Fowler, Johnson, Bowman (1980).

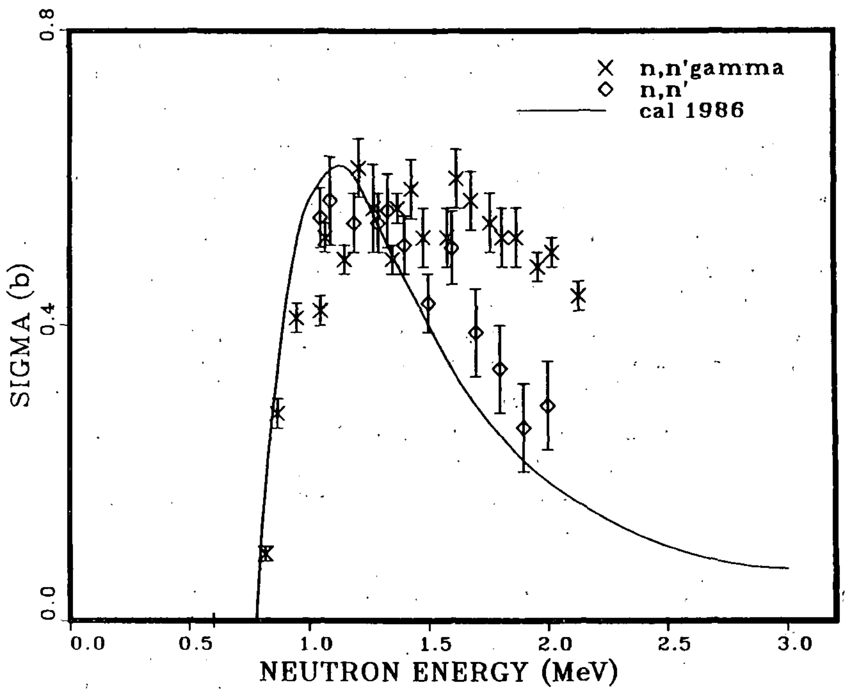

Fig. B-2 Comparison of the present theoretical calculations with (n,n')[2] and (n,n'γ)[6] data available for neutron scattering from the sum of states at 0.774, 0.7741, and 0.785 MeV. Direct reaction contributions were included using the techniques described in the text.

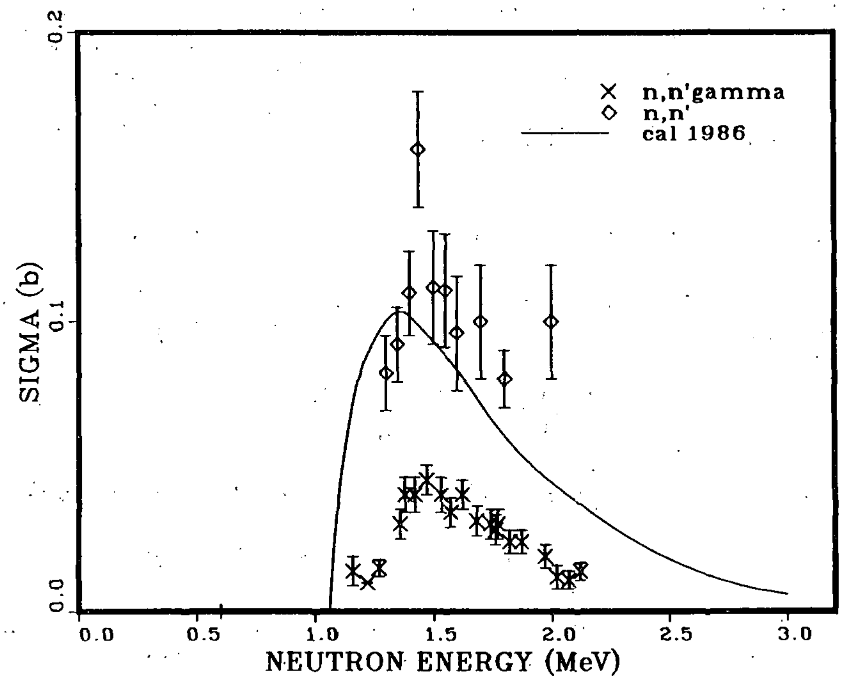

Fig. B-3 A comparison of our calculations with data available for scattering from the 1.054-MeV 2^- state in ^{232}Th. Here only compound nucleus contributions were included in the calculation.

4. Calculation of Deuteron-Induced Reaction Data Using an Improved Version of the GNASH Nuclear Model Code (E. D. Arthur)

The ability to account for components of particle emission spectra resulting from projectile stripping reactions has been added to the GNASH nuclear model code system. Basically, the formalism follows that originally developed by Serber,[1] which has been recently confirmed via sophisticated DWBA calculations of projectile fragmentation to unbound states.[2,3] The Serber model was implemented in full detail including entrance and exit-channel Coulomb deflection effects important for determination of (d,xp) emission spectra. To date, benchmark calculations have been made for deuteron reactions on aluminum, copper, gold, and bismuth for both thin and stopping-length targets. Figure B-4 compares (d,xp) spectra calculated for 80 MeV d + ^{27}Al reactions at angles of 20, 40, and 60° with the data of Ref. 4. At 20° the strong stripping component is evident, while by 40° it has almost disappeared. Figure B-5 compares calculated 0° neutron spectra obtained for 55-MeV deuterons stopping in an aluminum target with the data of Schweimer.[5] Both these examples indicate that the GNASH calculations reproduce well emission spectra components arising from projectile fragmentation.

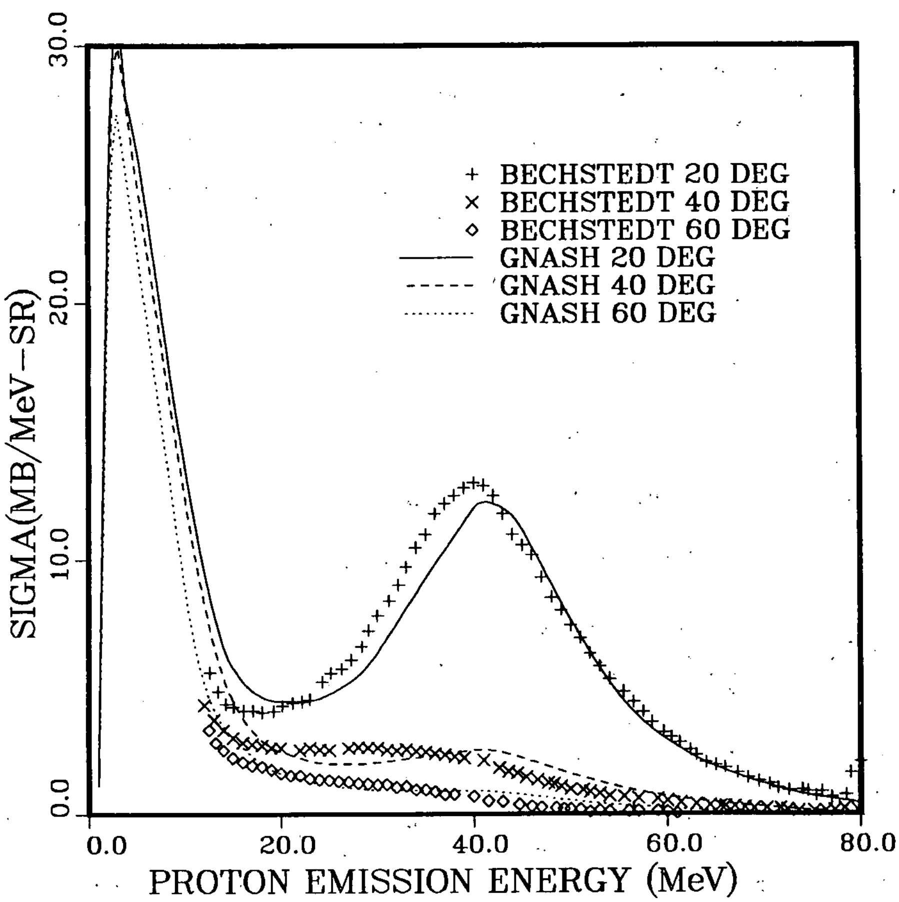

Fig. B-4 The present calculated proton spectra at 20, 40, and 60° produced from 80-MeV d+^{27}Al reactions are compared with the data of Ref. 4.

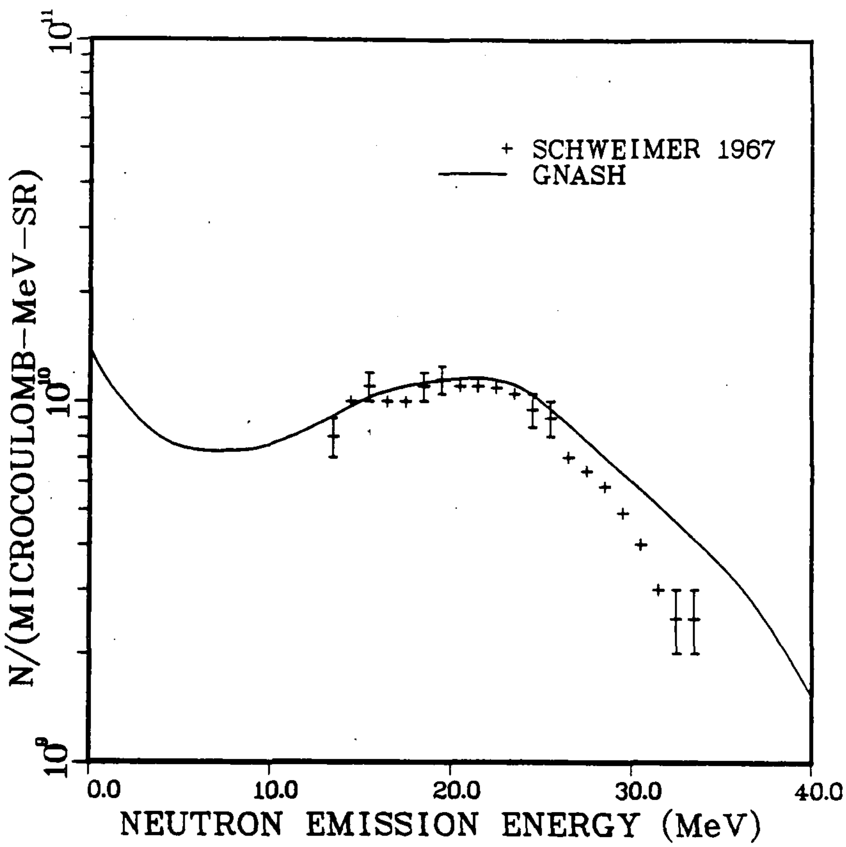

Fig. B-5 A comparison of calculated 0° neutron spectra produced by 55-MeV deuterons stopping in a thick aluminum target with the data of Schweimer.[5]

---

[1] R. Serber, Phys. Rev. 72, 1008 (1947).

[2] G. Baar et al., Helv. Physica Acta 53, 506 (1980).

[3] A. Sitenko et al., Sov. J. Nucl. Phys. 43, 50 (1980).

[4] U. Bechstedt et al., Nucl. Phys. A 343, 221 (1980).

[5] G. Schweimer, Nucl. Phys. A 100, 537 (1967).

6. Experimental and Theoretical Neutron Cross Sections for the $^{64}Zn(n,2n)^{63}Zn$, $^{64}Zn(n,p)^{64}Cu$ Reactions (D. A. Rutherford* and P. G. Young)

Accurate measurements of the $^{64}Zn(n,p)^{64}Cu$ and $^{64}Zn(n,2n)^{63}Zn$ cross sections at 14.8 MeV have been made using the neutron generator at the University of New Mexico and the activation technique. A NaI spectrometer[1] (using two 6" x 6" NaI detectors/crystals), was used to measure the gamma radiation emitted in coincidence from the positron-emitting decay products. The measurements were made relative to $^{65}Cu(n,2n)^{64}Cu$ and

---

* University of New Mexico

$^{63}Cu(n,2n)^{63}Cu$ cross sections, which have similar half-lives, radiation emission, and were previously measured to high accuracy (2%).[1]

In concert, a theoretical analysis of neutron-induced reactions on ^{64}Zn was performed using the GNASH code.[2] Starting from parameters obtained earlier for ^{58}Ni,[3] a neutron optical potential was obtained by fitting neutron elastic angular distributions, total cross sections, and low-energy average resonance parameters. Using proton and alpha optical potentials from earlier work,[4] Hauser-Feshbach statistical theory calculations[2] were carried out from 10 keV to 20 MeV. The calculations include width fluctuation corrections, direct reaction contributions, and preequilibrium corrections above 6 MeV.

The neutron optical model potential is given in Table B-2. Calculated cross sections for the $^{64}Zn(n,p)^{64}Cu$ and $^{64}Zn(n,2n)^{63}Zn$ reactions are compared with the new measurements in Figs. B-6 and B-7, along with a selection of older data. The theoretical values agree with the new 14.8-MeV (n,2n) measurement to within experimental error (~ 3%) but fall 10% below the (n,p) measurement. Results from the analysis will be made available in ENDF/B format for fusion applications.[5]

---

[1] F. Ghanbari and J. C. Robertson, "The $^{63}Cu(n,2n)^{62}Cu$ and $^{65}Cu(n,2n)^{64}Cu$ Cross Sections at 14.8 MeV," Proc. Int. Conf. Nucl. Data for Basic and Applied Sci., Santa Fe., N.M., 13-17 May 1985 [Gordon and Breach Science Pub., New York (1986)], p. 179.

[2] P. G. Young and E. D. Arthur, "GNASH: A Preequilibrium Statistical Nuclear Model Code for Calculation of Cross Sections and Emission Spectra," Los Alamos National Laboratory report LA-6947 (1977).

[3] R. C. Harper and W. L. Alford, J. Phys. G: Nucl. Phys. 8, 153 (1982).

[4] E. D. Arthur and P. G. Young, "Evaluated Neutron Cross Sections for $^{54,56}Fe$ to 40 MeV," Los Alamos National Laboratory report LA-8626-MS (1980).

[5] E. T. Cheng, "Nuclear Data Needs for Fusion Energy Development," GA Technologies report GA-A17881 (1985).

TABLE B-2 Neutron Optical Parameters for ^{64}Zn

	r_0	a
$V_R = 49.11 - 16\eta - 0.376E$	1.295	0.58
$W_D = 8.545 - 8\eta$	1.295	0.48
$W_v = - 0.094 + 0.197E$	1.295	0.58
$V_{so} = 6.2$	1.12	0.48

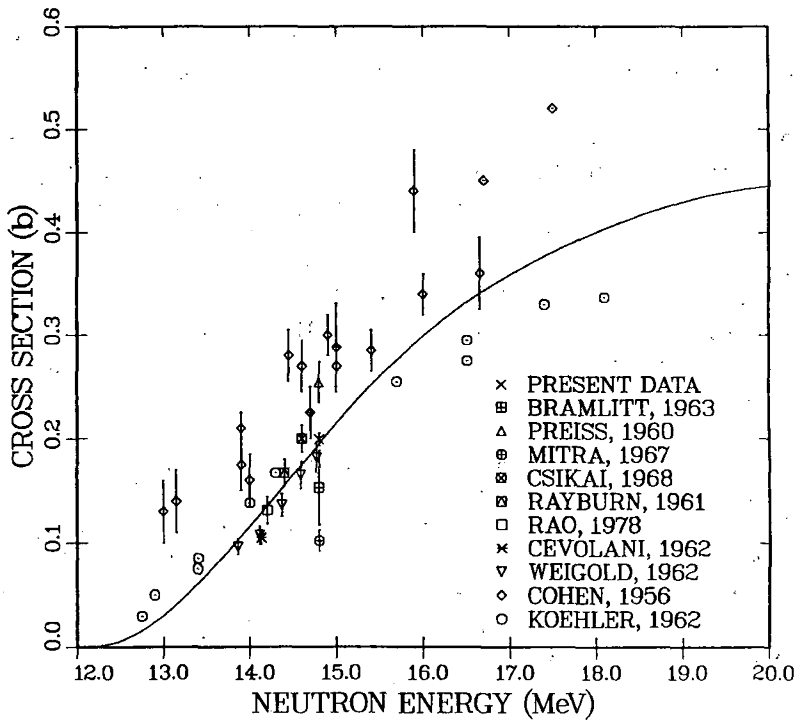

Fig. B-6 Calculated and measured values of the $^{64}Zn(n,2n)^{63}Zn$ cross section from threshold to 20 MeV.

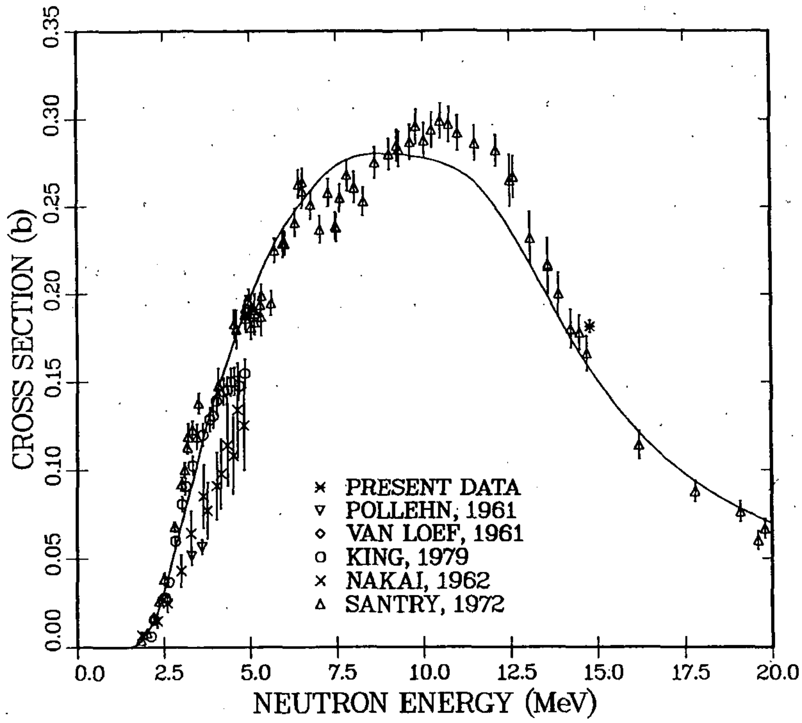

Fig. B-7 Comparison of calculated and measured values of the $^{64}Zn(n,p)^{64}Cu$ cross section up to 20 MeV.

7. Theoretical Analysis of ^{185}Re and ^{187}Re Neutron Cross Sections (P. G. Young)

A deformed optical model analysis of n + Re reactions was performed with the ECIS coupled-channel computer program.[1] The lowest three members of the ground state rotational bands of ^{185}Re and ^{187}Re(J^{π} = $5/2^{+}$, $7/2^{+}$, and $9/2^{+}$) were coupled in the calculations. The optical model parameters were obtained by matching the calculations with published s- and p-wave neutron strengths (S_0,S_1) and potential scattering radii (R'), as well as measured neutron total cross sections for natural rhenium between 10 keV and 15 MeV.[3] Values of the deformation parameters β_2 and β_4 from several previous studies were tried in the analysis; best results were obtained with parameters interpolated from the calculations of Goetz et al.[4] The deformed optical model parameters that result from this analysis are given in Table B-3. Values of the s- and p-wave neutron strength functions and potential scattering radii calculated at E_n = 10 keV are compared with experimentally inferred values[2] in Table B-4. The neutron total cross section for natural rhenium from the optical model analysis is compared with experimental data[3] between 2 keV and 20 MeV in Fig. B-8.

Hauser-Feshbach statistical theory calculations with width-fluctuation corrections were carried out with the GNASH computer code.[5] Neutron transmission coefficients were obtained from the deformed optical model parameters, and a giant dipole resonance model was used to calculate gamma-ray strength functions. Experimental spins and parities were used directly in the calculations up to excitation energies of ~ 800 keV for ^{185,187}Re and to ~ 300 keV for ^{186,188}Re. Phenomenological level densities from Gilbert and Cameron[6], smoothly matched to the experimental levels and parameterized to agree with observed $\langle D_0 \rangle$ values at the neutron binding energy, were used in the calculations at higher energies.

Calculated radiative capture cross sections for ^{185}Re and ^{187}Re are compared with the available measurements in Fig. B-9. The shapes of the cross sections for the two isotopes are quite similar and the absolute magnitudes differ by less than 20% between 1 and 200 keV. Larger differences occur at higher energies where inelastic scattering competition becomes important, with differences of a factor of two occurring near 1 MeV. The slight evidence of broad structure or shoulders in the calculated cross sections above 100 keV results from inelastic competition to discrete states (or groups of states) in ^{185}Re and ^{187}Re.

---

1 J. Raynal, "Optical Model and Coupled-Channel Calculations in Nuclear Physics," IAEA-SMR-9/8, International Atomic Energy (1972).

2 S. F. Mughabghab, M. Divadeenam, and N. E. Holden, Neutron Cross Sections, Vol. 1B, Academic Press, New York (1984).

3 Obtained from the National Nuclear Data Center, Brookhaven National Laboratory, Upton, N. Y.

[4] U. Goetz, H. C. Pauli, and K. Alder, Nucl. Phys. A192, 1 (1972).

[5] P. G. Young and E. D. Arthur, "GNASH: A Preequilibrium-Statistical Nuclear Model Code for Calculations of Cross Sections and Emission Spectra," Los Alamos Scientific Laboratory report LA-6947 (1977).

[6] A. Gilbert and A. G. W. Cameron, Can. J. Phys. 43, 1446 (1965).

TABLE B-3 Deformed Optical Model Parameters for n + ^{185}Re and n + ^{187}Re Interactions.

Potential[+] (MeV)		r_i, a_i (fm)
$V_R = 49.8 - 16\eta - 0.30E$		1.26, 0.61
$W_D = 4.02 - 8\eta + 0.75E$	$E < 9$	1.26, 0.47
$= 10.77 - 8\eta - 0.05(E - 9)$	$E \geq 9$	
$W_V = -1.8 + 0.2E$		1.26, 0.61
$V_{SO} = 7.5$		1.26, 0.61

$\beta_2(^{185}\mathrm{Re}) = 0.22$ $\beta_2(^{187}\mathrm{Re}) = 0.21$

$\beta_4(^{185}\mathrm{Re}) = -0.085$ $\beta_4(^{187}\mathrm{Re}) = -0.085$

[+] $\eta = (N - Z) / A$

TABLE B-4 S- and P-Wave Neutron Strength Functions (S_0,S_1) and Potential Scattering Radii (R') for ^{185}Re and ^{187}Re.

	^{185}Re			^{187}Re		
	S_0 (10^{-4})	S_1 (10^{-4})	R' (fm)	S_0 (10^{-4})	S_1 (10^{-4})	R' (fm)
Experiment[+]	2.1 ±0.2	1.7 ±0.7	8.7 ±0.3	2.5 ±0.3	1.0 ±0.7	8.7 ±0.3
Calculation	2.3	0.8	7.7	2.3	0.7	7.7

[+] Reference 2

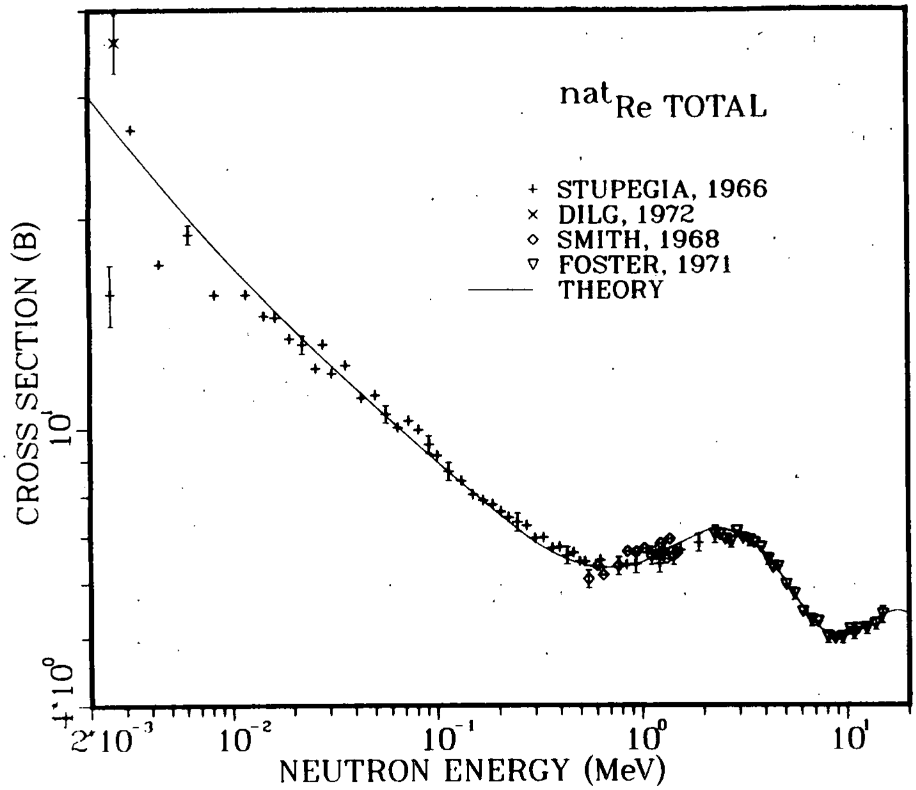

Fig. B-8 Comparison of the calculated neutron total cross section of elemental rhenium with the available experimental data.[3]

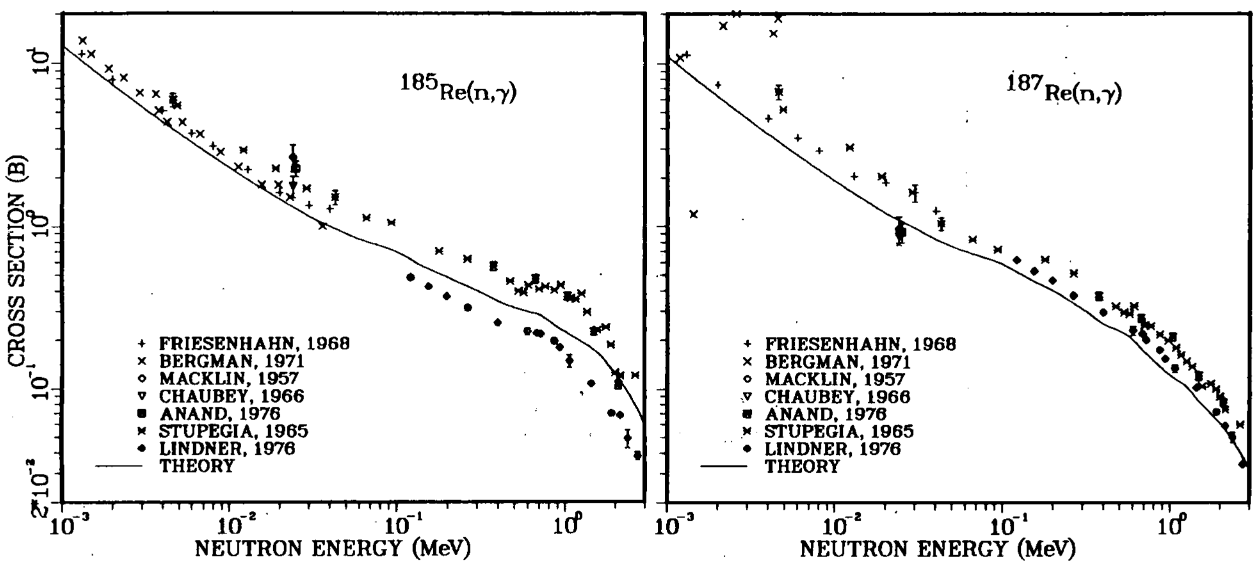

Fig. B-9 Calculated and measured[3] radiative capture cross sections of ^{185}Re and ^{187}Re.

8. Medium Energy Nucleon-Nucleus Reaction and Total Cross Sections from Phenomenological Optical-Model Calculations (D. G. Madland)

Preliminary results have been obtained for calculations of the proton reaction cross section and the neutron total cross section for ^{27}Al, ^{56}Fe, and ^{208}Pb over an incident energy range of 50 to 400 MeV. Using a relativistic Schrödinger-type wave equation generated by appropriate reduction of the Dirac equation, the starting point for these calculations is the phenomenological optical-model potential determined by Schwandt et al.,[1] which is based on measured elastic scattering cross sections and analyzing powers for polarized protons ranging from 80 to 180 MeV. This potential was modified to optimally reproduce experimental proton reaction cross sections as a function of energy, while allowing minimal deterioration in the fits to the elastic cross sections and analyzing powers. Further modifications, especially in the absorptive part, were found necessary to extrapolate the modified potential to higher energies. The final potential was then converted to a neutron-nucleus potential by use of standard Lane model assumptions and by subtraction of a simple form of the Coulomb correction. Comparisons of calculated and measured reaction and total cross sections for ^{56}Fe are shown in Figs. B-10 and B-11, respectively.

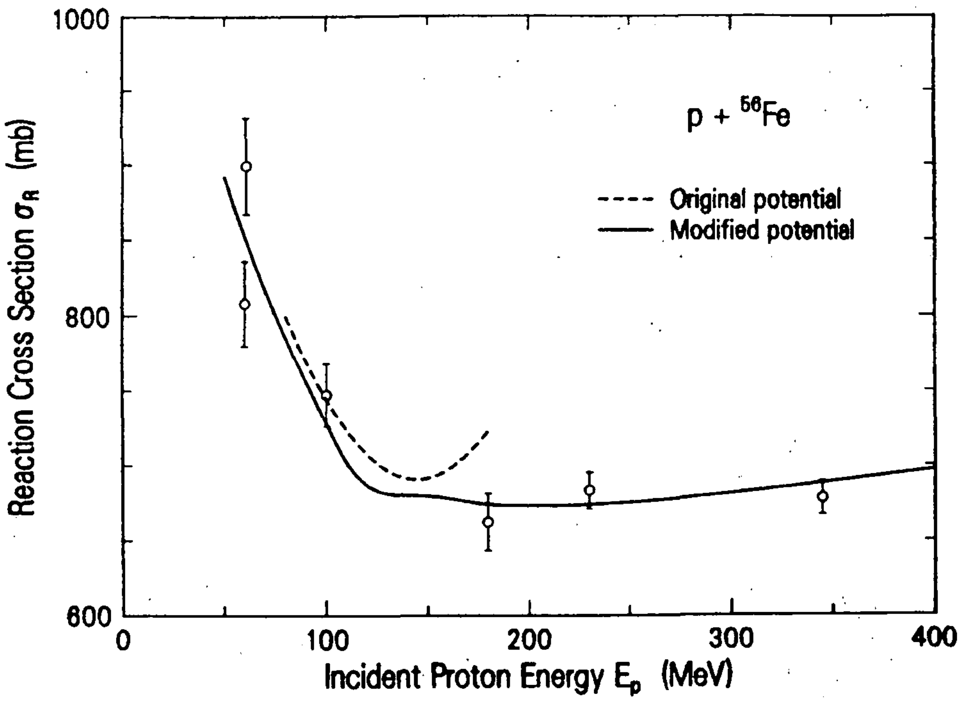

Fig. B-10 Comparisons of calculated and experimental proton total reaction cross sections for ^{56}Fe. Calculations using the original potential of Schwandt et al.[1] are shown with the dashed curve while those using the modified potential are shown with the solid curve.

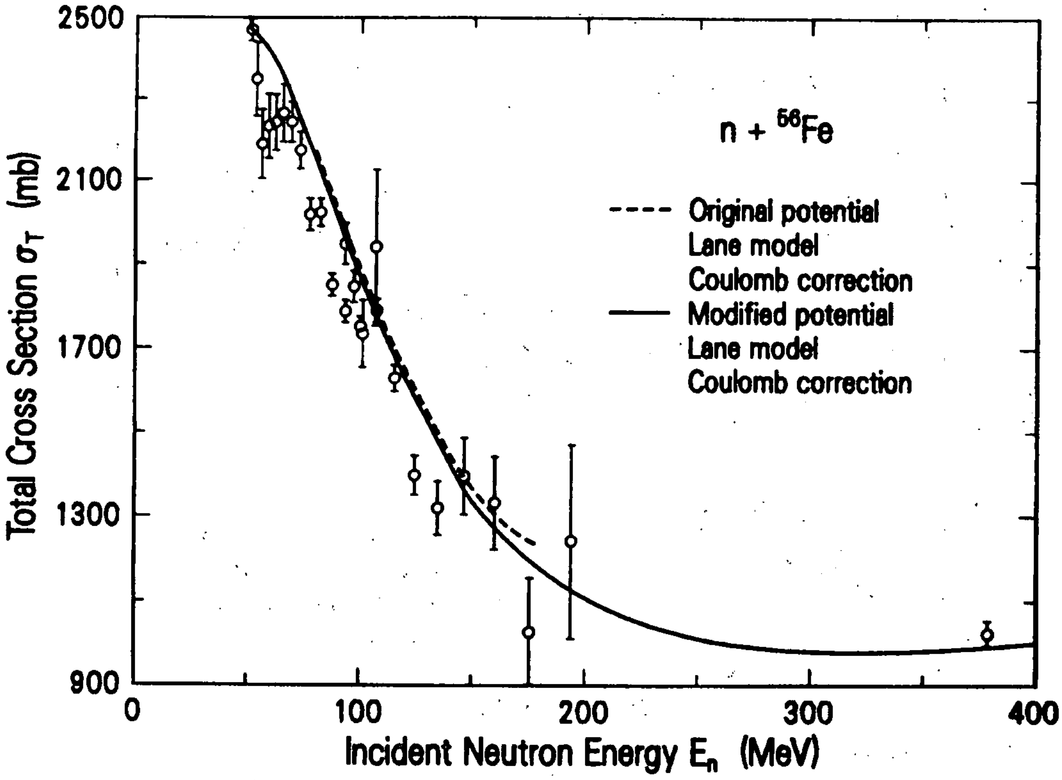

Fig. B-11 Identical to Fig. B-10 except for neutron total cross sections.

[1] P. Schwandt et al., Phys. Rev. C 26, 55 (1982).

9. New Model of the Average Pairing Gap and Average Residual n-p Interaction Energy (D. G. Madland and J. R. Nix)

Work has been completed on a new model of the average neutron pairing gap $\bar{\Delta}_n$, the average proton pairing gap $\bar{\Delta}_p$, and the average residual n-p interaction energy $\bar{\delta}$. The new model is based upon the isospin dependencies of the pairing strengths, G_n and G_p, and is derived by use of the BCS approximation applied to equispaced levels. The model explains not only the dependencies of $\bar{\Delta}_n$ and $\bar{\Delta}_p$ upon isospin, but also the experimental result that $\bar{\Delta}_n$ is generally smaller than $\bar{\Delta}_p$. In addition, we take into account the shape dependencies of $\bar{\Delta}_n$, $\bar{\Delta}_p$, and $\bar{\delta}$ and introduce a new expression for $\bar{\delta}$. Contour plots of the average neutron and proton pairing gaps calculated are shown in Figs. B-12 and B-13, respectively. Our model should permit extrapolation of these quantities to nuclei farther removed from the valley of β stability than do previous parameterizations. We expect tests and applications of the new model to occur in nuclear structure calculations, atomic mass formulas, and microscopic level-density calculations.

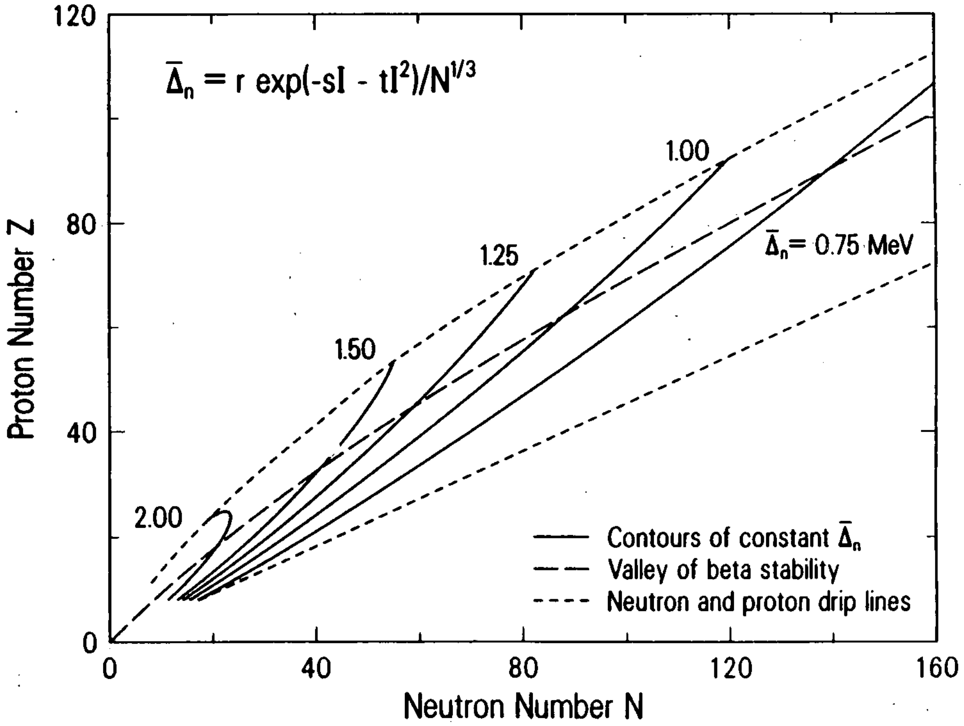

Fig. B-12 Contours of constant $\bar{\Delta}_n$ calculated using the new model. Also shown are the valley of β stability and the neutron and proton drip lines.

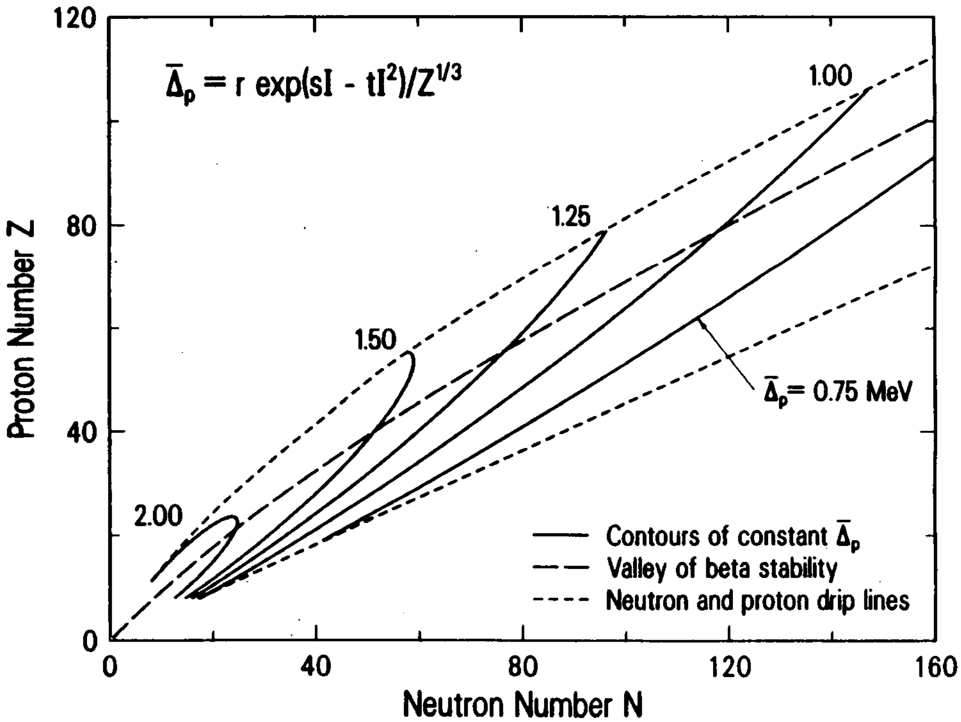

Fig. B-13 Identical to Fig. B-12 except for contours of constant $\bar{\Delta}_p$.

10. Delayed Neutron Precursor Evaluation (T. R. England, M. C. Brady, R. J. LaBauve, E. D. Arthur, and C. Goulding)

Almost a third of the fission products are delayed neutron precursors. Using measurements, systematics, and nuclear models, we have created a preliminary file for 272 nuclides consisting of emission probabilities (Pn's) and spectra;[1] parameters for six-groups, dervived from aggregate calculations, are in progress. For reactors, the limited precursor measurements (34 spectra and 85 Pn values) are nearly adequate in that they account for > 80% of the delayed neutrons. For other purposes, such as fission yield evaluations, complete data are needed.

Measured spectra $\gtrsim$ 3 MeV did not exist until recently. All measurements were therefore extended using nuclear models to include the full energy range. The extension for ^{96}Rb and a subsequent preliminary measurement are shown in Fig. B-14; the measurement, discussed in another contribution (see C. Goulding, et al.) may require some additional change in normalization.

[1] T. R. England, M. C. Brady, E. D. Arthur, R. J. LaBauve, and F. Mann, "Status of Evaluated Precursor and Aggregate Spectra," to be published in Proc. of Specialists' Meeting on Delayed Neutrons at the University of Birmingham, Birmingham, England, September 15-19, 1986 (LA-UR-86-2983).

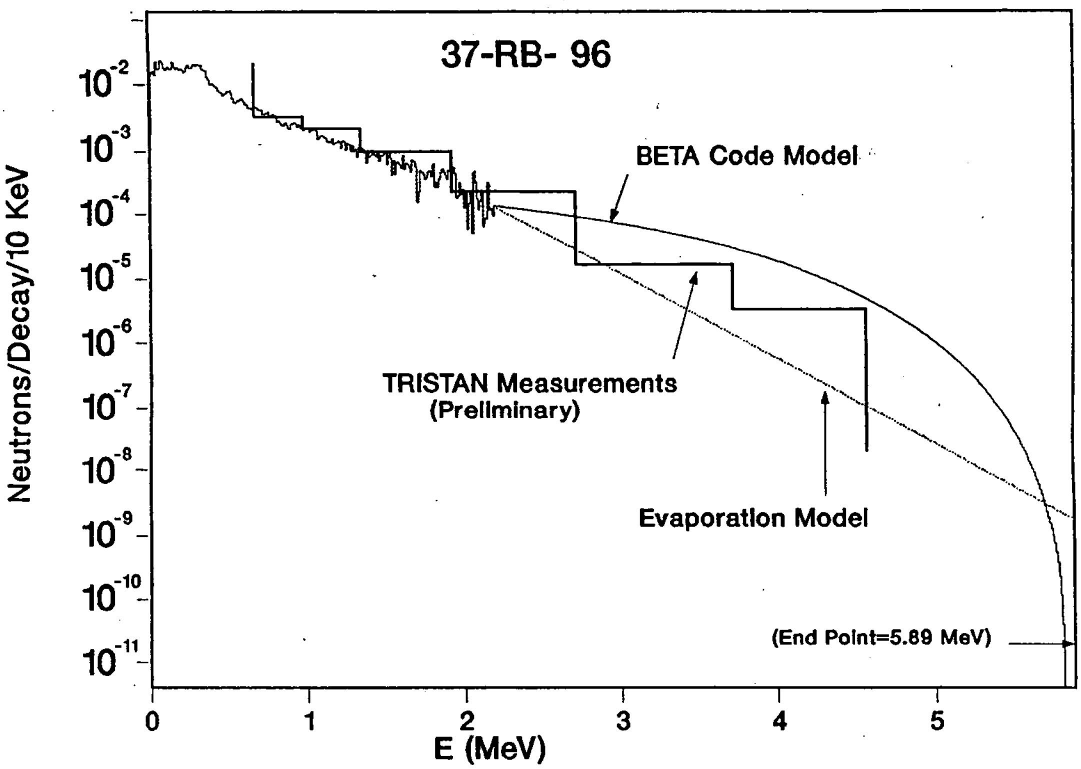

Fig. B-14 Comparison of delayed neutron spectra for ^{96}Rb.

UNIVERSITY OF LOWELL

A. NEUTRON SCATTERING CROSS SECTIONS IN THE ACTINIDES

(L.E. Beghian, G.H.R. Kegel, J.J. Egan, A. Mittler, G.C. Goswami, E. Sheldon, A. Aliyar and C.A. Horton)

1. Completed Work

During the past year we have published the results of our (n,n') cross section measurements on ^{238}U states from 680 to 1530 keV in the incident energy range 0.9 to 2.2 MeV. The theoretical analysis in this work was carried out by E.D. Arthur of Los Alamos National Laboratory who is a co-author on the paper.[1] We have prepared a manuscript for publication[2] of our work on the first three members of the ground state rotational band of ^{232}Th. In this paper we report measurements of: (1) excitation functions in the incident energy range 185 - 2400 keV for the 0^+ (ground) and 2^+ (49 keV) states, and in the 480 - 2400-keV range for the 4^+ (162 keV) state; (2) angular distributions of the 0^+ and 2^+ states at 185 keV and for the 0^+, 2^+ and 4^+ states at 550 keV. The excitation functions were measured at 125° and level cross sections were obtained using our measured angular distributions and those published previously by Haouat et al[3]. Figure A-1 shows these level cross sections compared to ENDF/B-V[4] (solid line) and, in the case of the inelastic cross sections, with several theoretical calculations. The dashed curves were obtained using an incoherent sum of the results from the compound nucleus (CN) code "CINDY"[5] and direct interaction results from the

---

[1] J.Q. Shao, G.P. Couchell, J.J. Egan, G.H.R. Kegel, S.Q. Li, A. Mittler, D.J. Pullen, W.A. Schier and E.D. Arthur, Nucl. Sci. Eng. <u>92,</u> 350 (1986).

[2] G.C. Goswami, J.J. Egan, G.H.R. Kegel, A. Mittler and E. Sheldon, "Neutron Scattering Cross Sections Up to 2.4 MeV for the Ground and First Two Excited States of ^{232}Th," (manuscript, 1987).

[3] G. Haouat, J. Lachkar, Ch. Lagrange, J. Jary, J. Sigaud and Y. Patin, Nuclear Sci. Eng. <u>81,</u> 491 (1982).

[4] J.W. Meadows, W.P. Poenitz, A.B. Smith, D.L. Smith, J.F. Whalen, R.J. Howerton, B.R. Leonard, G. de Saussure, R.L. Macklin, G. Gwin, and M.R. Bhat, "Evaluated Nuclear Data File, Version - V for ^{232}Th, MAT 1390," National Nuclear Data Center, Brookhaven National Laboratory, Upton, New York, (1979).

[5] E. Sheldon and V.C. Rogers, Comput. Phys. Commun. <u>6,</u> 99 (1973).

coupled-channel code "KARJUP"[6], a variant of Tamura's code "JUPITOR"[7]. The dotted curves were obtained in a similar fashion except the "CINDY" calculations were replaced by CN computations using "JACQUI", a variant of Jary's code "NRLY"[8]. The dot-dashed curves were computed by the program "NANCY"[9] based on the statistical S-matrix formalism of Hofmann, Richert, Tepel and Weidenmüller[10] in which "fluctuation" and "nonfluctuation" amplitudes are combined coherently.

We are currently preparing a paper on the angular distributions for two composite levels in ^{235}U consisting of ground + 77-eV + 13-keV and the 46 + 52-keV states. These measurements were made at 185 and 550 keV.

A summary of this work on ^{232}Th, ^{235}U, and on ^{238}U ground state rotational band states at incident energies from 185 to 900 keV is being prepared for presentation at the Crystal City meeting of the American Physical Society in April 1987.

Several other papers of a primarily theoretical nature have been published in the past year and still others are about to appear in print. These are referred to in Section B of this report.

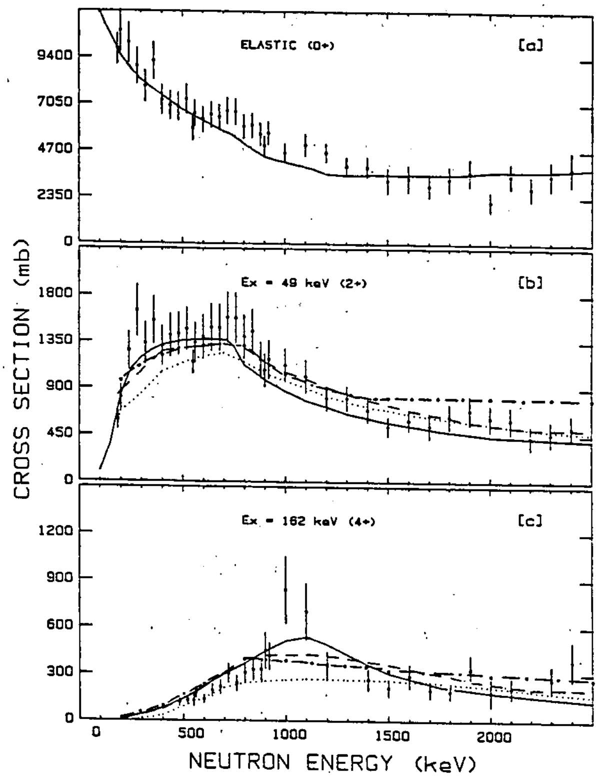

Fig. A-1 Angle integrated cross sections for the ground state and first two excited levels of ^{232}Th compared with ENDF/B-V (——), CINDY/KARJUP (----), JACQUI/KARJUP (••••), and NANCY (-•-•-).

---

[6]H. Rebel and G.W. Schweimer, "Improved Version of Tamura's Code for Coupled Channel Calculations," Kernforschungszentrum Karlsruhe Report KFK-1333.

[7]T. Tamura, Rev. Mod. Phys., 37, 679 (1965).

[8]J. Jary, "NRLY," Report PNN-771/81, Bruyeres-le-Chatel (1981).

[9]D.W.S. Chan and E. Sheldon, Phys. Rev. C, 26, 861 (1982).

[10]H.M. Hofmann, R. Richert, J.W. Tepel, and H.A. Weidenmüller, Ann. Phys. 90, 403 (1975).

2. Work In Progress

a. Cross Section Measurements Using 82-keV Iron-Filtered Neutrons

The neutron detector in an iron-filtered neutron experiment (82-keV window) must combine good time resolution (FWHM $\sim$1ns) and excellent signal to background ratio. We have determined through preliminary measurements that the signal amplitudes obtained from a BC418 scintillator and a Phillips XP-2020 photomultiplier tube for 82-keV neutrons is in the same amplitude range as the 1 to 3 photoelectron "dark current". The count rate for this noise is 100 to 300 counts per second. To reduce this background we tried chilling the PM tube but have finally decided to use coincidence techniques to reject the noise.

Hill et al.[11] at Oak Ridge have described a system using three low noise photomultiplers in majority logic offering outstanding signal to noise ratio. We have developed a similar device using a matched pair of XP-2020 photomultipliers viewing the same BC418 scintillator. Our system employs special wide band (2 GHz) strip-line integrated amplifiers to obtain good time resolution.

Our cross section measurements will initially focus on the 13-keV excited state of ^{235}U for incident neutrons of 95 keV. The iron filter will be placed in the scattered neutron path[12] so only 82-keV neutrons reach the detector.

b. ^{232}Th and ^{238}U Cross Sections for $E_n > 2.0$ MeV

The inelastic scattering cross sections for levels in ^{232}Th and ^{238}U in the 600-to 1000-keV excitation energy range for incident energies above 2.0 MeV are of interest because of their importance in establishing and testing theoretical reaction models for scattering from these rotational and vibrational states. As recently as the Fall Meeting of the Nuclear Physics Division of the Americal Physical Society in Vancouver, B.C., E.D. Arthur emphasized the need for such measurements.[13] In preliminary work these have proven to be difficult measurements requiring extremely stable accelerator operation and premium time resolution over periods of 12 hours or so. We have modified our time-resolution monitoring program[14] and now

---

[11] N.W. Hill, J.A. Harvey, D.J. Horen, G. L. Morgan and R.R.Winters, I.E.E.E. Trans. Nuc. Sci. 32, 367 (1985).

[12] R.L. Macklin, R.R. Winters, N.W. Hill and J.A. Harvey Astro. J. 274, 408 (1983).

[13] E.D. Arthur, Bull. Am. Phys. Soc. 31, 1238 (1986).

[14] G.H.R. Kegel, Nucl. Instrum. & Meth. 135, 53 (1976).

consistently achieve proton beam pulse durations of less than 350 ps for extended periods of time. We are using pulse-shape discrimination which has significantly reduced gamma-ray background. We have also made several modifications to our time-of-flight spectrometer during exploratory measurements which have yielded somewhat better results for ^{232}Th than for ^{238}U. In the coming months we will carry out the cross section measurements from 2 MeV up to as high an energy as feasible, probably somewhere near 3 MeV.

B. LEVEL CROSS-SECTION CALCULATIONS FOR NEUTRON INELASTIC SCATTERING ON ACTINIDES (E. Sheldon)

The latest computations of angle-integrated and differential cross sections for (n,n') scattering to rotational and vibrational levels of ^{232}Th, ^{238}U and $^{240, 242,244}$Pu, as detailed in previous (1983-86) Reports to the DOE Nuclear Data Committee, for analysis of level excitation functions and angular distributions on the basis of standard (CN+DI) and statistical S-matrix (HRTW) formalisms have now been published[1-5] or

---

[1]E. Sheldon, in HEAVY IONS IN NUCLEAR PHYSICS, Proceedings of the 16th Polish Summer School of Nuclear Physics, Mikolajki, Masuria, August 27 - September 7, 1984, edited by Z. Wilhelmi and M. Kicinska-Habior (Harwood Academic Publishers, Chur, London, Paris, New York, 1986), p. 377.

[2]E. Sheldon, L.E. Beghian, C.A. Ciarcia, G.P. Couchell, J.H. Dave, J.J. Egan, G. Goswami, G.H.R. Kegel, S.Q. Li, A. Mittler, D.J. Pullen, W.A. Schier, J.Q. Shao, J. Phys. G. - Nucl. Phys. 12, 237 (1986).

[3]E. Sheldon, L.E. Beghian, J.J. Egan, D.W.S. Chan, G.P. Couchell, G.Goswami, G.H.R. Kegel, S.Q. Li, A. Mittler, D.J. Pullen, W.A. Schier, J.Q. Shao and A. Wang, J. Phys. G. - Nucl. Phys. 12, 443 (1986).

[4]E. Sheldon, L.E. Beghian, G.C. Goswami, G.H.R. Kegel and A. Mittler, in Proceedings of the International Conference on Fast Neutron Physics, Dubrovnik, Yugoslavia, May 26 - 31, 1986, edited by D. Miljanic, B. Antolkovic and G. Paic (Rudjer Boskovic Nuclear Institute, Zagreb, 1986), p. 279.

[5]E. Sheldon, in HARROGATE 86, Proceedings of the International Nuclear Physics Conference, Harrogate, U.K., August 25 - 30, 1986 (Institute of Physics, London, 1986), Vol. I, Contributed Paper C74, p. 261.

are in imminent publication,[6] together with results[7] for ^{235}U rotational states. Fission corrections have now been incorporated, with the aid of the program "JACQUI" derived from the Bruyeres code "NRLY" compiled by Jacqueline Jary for total (angle-integrated) cross sections.

With the impending replacement of our CDC Cyber 170-825 computer facility by a DEC VAX system, current computational activity has been halted as transfer of the existing programs, and their recompilation into a VAX-compatible form, is pursued.

C. DELAYED-NEUTRON MEASUREMENTS

(G.P. Couchell, D.J. Pullen, W.A. Schier, L. Fisteag, M.H. Haghighi, E.J. Saunders and Q. Sharfuddin)

The study of composite delayed neutron (DN) spectra as a function of time following fission of U-235 and Pu-239 addresses the specific need for such measurements cited at the NEANDC Specialists meeting at BNL in 1983. U-235 is important in providing benchmark data for DN spectra as well as for its probable use as a major fuel component in compact, enriched fast reactors, e.g. space reactors. Our next major thrust is the investigation of DN spectra from the fast fission of U-238. The study of these spectra was recommended at the 1986 Specialists Meeting on Delayed Neutrons (Birmingham, England) due to their important contribution to the kinetic behavior of large fast reactor systems.

1. Thermal Neutron Fission of Pu-239

We are continuing our study of composite (aggregate) DN energy spectra following thermal neutron induced fission of Pu-239. For these studies BC501 liquid scintillators, incorporating a pulse-shape discrimination (PSD) system for neutron-gamma discrimination, have been used for measuring each neutron energy spectrum from 0.13-4.00 MeV. The spectrum in the 0.01-0.30 MeV region was determined in separate measurements using NE912 Li-6 loaded glass scintillators with PSD. A helium jet system transported fission products to a low-background counting area. Neutron energies were measured by the time-of-flight technique using beta-neutron correlations. Measurements of Pu-239 DN spectra have been completed for seven nearly contiguous delay time intervals ranging from 0.17 s to 29.0 s after fission. Results for two delay time intervals are shown in Fig. C-1, where the Pu-239 spectra are compared

---

[6] E. Sheldon and D.W.S. Chan, J. Phys. G. - Nucl. Phys. (1987 - in publication).

[7] E. Sheldon, J.J. Egan, G.C. Goswami, G.H.R. Kegel and A. Mittler, in HIGHLY EXCITED NUCLEI, Processings of the 18th Polish Summer School of Nuclear Physics, Mikolajki, Masuria, September 1 - 13, 1986, edited by Z. Wilhelmi and G. Szeflinska (Harwood Academic Publishers, New York, 1987 - in publication).

with the corresponding ones from U-235 fission.[1] Although each Pu-239 spectrum was measured over the energy range 0-4 MeV, only the region 0-2 MeV is depicted in Fig. C-1 since this was the full range of the U-235 DN measurements. The Pu-239 DN yield in the 2-4 MeV energy range was generally quite small, about 1% for delay times less than 2 s and rapidly decreasing for times greater than 2 s. Comparison of the Pu-239 DN spectra with the corresponding ones from U-235 fission reveals a great similarity in shape for delay times less than 2 s and in the 12.5-29.0 s range. However, there is a relative softening of the Pu-239 spectra in the 2-10 s range, where average energies are about 50 keV less than those of U-235.

The Pu-239 measurements will be analyzed using a constrained least-squares fitting method, similar to that dscribed below for U-235, to obtain 6-group DN spectra useful for reactor kinetics calculations. The 6-group spectra can also be used to determine the Pu-239 equilibrium DN spectrum, either directly by summing the 6-group spectra weighted by their fractional yield, or by using them to supplement measurements for those delay time intervals where data is lacking. Results of these analyses will be published shortly.

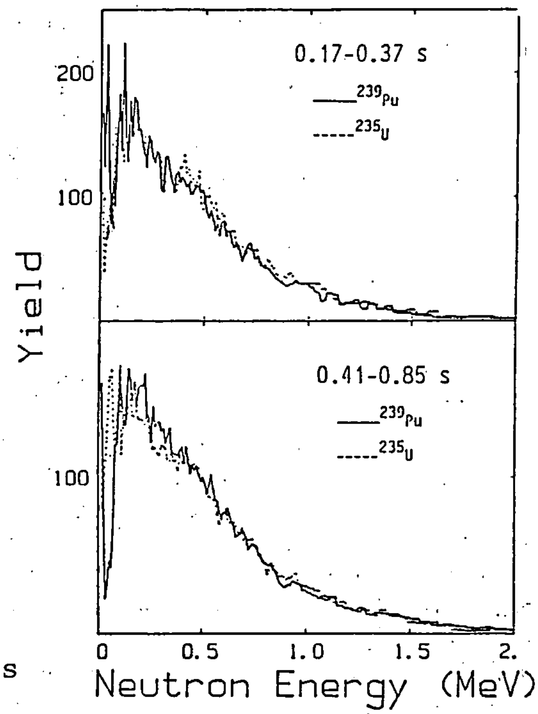

Fig. C1 A Comparison of composite DN energy spectra from thermal neutron induced fission of ^{239}Pu (solid curve)and ^{235}U (dotted curve).

2. <u>Search for Dependence of Composite DN Spectra on Incident Neutron Energy</u>

In seeking differences in spectral structure due to the energy of neutrons inducing fission, it is clearly desirable to perform the thermal and fast measurements successively for each delay time interval and under as nearly identical experimental conditions as possible. For our studies this required that both sets of measurements be made using the accelerator and Li-7(p,n) reaction as a neutron source, whereas our earliest thermal measurements were performed with the fission chamber in the thermal column of our reactor.

---

[1]R.S. Tanczyn, Q. Sharfuddin, W.A. Schier, D.J. Pullen, M.H. Haghighi, L. Fisteag and G. P Couchell, Nucl. Sci. Eng. <u>94</u>, 353 (1986).

To make thermal neutrons the dominant mode for inducing fission using the accelerator, the fission chamber and thick lithium target assembly were encased in a paraffin block (0.3 m^3). For the fast neutron measurements a nearly bare geometry was used, with the fission chamber wrapped in cadmium to shield against any residual thermal neutrons. The primary neutrons typically spanned an energy range 0.3-3.2 MeV in an approximately rectangular distribution with a mean energy similar to that of a prompt fission spectrum.

In studying the energy dependence in a fast-induced/thermal-induced pair of TOF spectra, the spectra were first normalized and then subtracted from one another. Since the gamma peak and random background largely cancelled, only differences in the neutron spectra remained. The resulting 'difference' TOF spectrum was then converted to a 'difference' energy spectrum in the usual manner using our code DENTS.[2]

U-235 'fast-induced minus thermal-induced' DN difference spectra for four of the eight successive delay time intervals are presented in Fig.C-2. The vertical and horizontal scales are consistent with 10^4 counts in each DN spectrum. The low-energy portions of the two shortest time intervals are missing because background conditions became unfavorably large in the NE 912 measurement, particularly for U-235 fission induced by fast neutrons. Representative error bars are superimposed on the difference spectra.

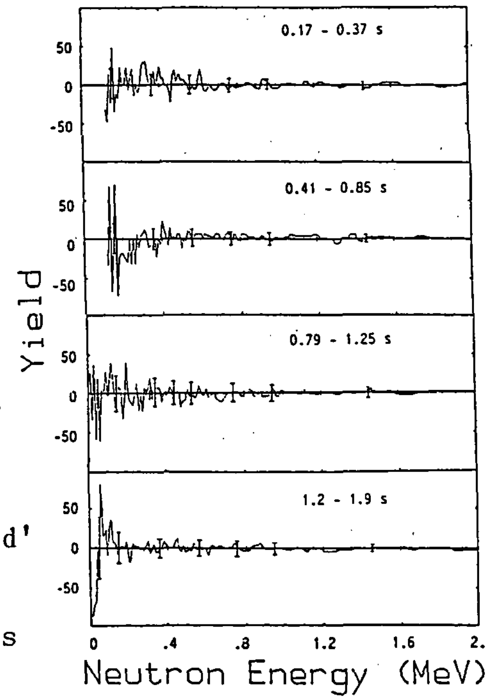

Fig.C-2 U-235 fast-minus thermal-induced fission DN difference spectra for four delay time intervals. Representative uncertainties are indicated.

It is evident that the difference spectra shown display structures that can be attributed mainly to statistical uncertainties. Thus no significant variation between thermal and fast fission was observed in U-235 DN spectra. The completed energy dependent study will soon be submitted to Nucl. Sci. Eng.

---

[2] C. A. Ciarcia, W.A. Schier, G.P. Couchell, D.J. Pullen, R.S. Tanczyn M.H. Haghighi and Q. Sharfuddin, Comp. Phys. Comm. 39, 233 (1986).

3. Six-Group Decomposition of Composite DN Measurements

For convenience of reactor kinetics calculations, it is desirable to parameterize the composite DN spectra by a six-group approach as suggested by Keepin. However, decomposition of composite DN spectra into group spectra often lead to oscillatory, physically unacceptable solutions[3-5] due to such effects as statistical uncertainties, energy shifts in data sets, poor sensitivity of the data to certain groups, and inadequacy of the six-group approach. By adding a constraint in the first iteration of a least squares decomposition approach, we have been able to obtain physically acceptable, nearly unique solutions.

The procedure is demonstrated here using our eight DN spectra measured after the thermal neutron fission of U-235, which spanned delay times from 0.17 s to 85.5 s.[1] This time range provided good sensitivity to DN groups 2-6, but not to group 1 ($T_{1/2}$ = 55.5 s). The group 1 spectrum was thus taken to be that reported by Rudstam,[6] and the eight measured spectra $S_{\nu i}$ (ν=1,...,8) were used to determine solutions for groups 2-6 from the equations

$$S'_{\nu i} = S_{\nu i} - a_{\nu 1}\chi_{1i} = \sum_{\mu=2}^{6} a_{\nu\mu}\chi_{\mu i} \;, \quad (\nu = 1,\ldots,8)$$

where $S'_{\nu i}$ are the spectra which result when the group-1 contribution is removed from each of the measured spectra. The equations are not redundant due to the statistical uncertainties in the measured spectra and due to the fact that the 6-group parameterization is an approximation.

In the conventional weighted least-squares method one minimizes the quantity

$$\Phi_i^2 = \sum_{\nu=1}^{8} (S'_{\nu i} - F_{\nu i})^2 \frac{1}{\sigma_{\nu i}^2}$$

---

[3]K.L. Kratz and H. Gabelmann, Proc. Int. Conf. on Nucl. Data for Basic and Applied Science, Sante Fe, May 1985, vol. 1, p. 661, Gordon and Breach Sci. Publ. (1986).

[4]S.J. Chilton, D.R. Weaver, J. Walker and J.G. Owen, Proc. Spec. Meeting on Delayed Neutrons at Birmingham, England (1986) (to be published).

[5]G.P. Couchell, W.A. Schier, D.J. Pullen, L. Fisteag, M.H. Haghighi, Q. Sharfuddin and R.S. Tanczyn, Ibid.

[6]G. Rudstam, Nucl. Sci. Eng. 80, 238 (1982).

where

$$F_{\nu i} = \sum_{\mu=2}^{6} a_{\nu\mu}\chi_{\mu i}$$

are the fits and $\sigma_{\nu i}$ is the uncertainty in $S'_{\nu i}$. In order to exclude a large class of mathematically good solutions that were not physically acceptable, it proved beneficial to introduce a constraint condition by minimizing the modified quantity

$$\phi^2_{Mi} = \sum_{\nu=1}^{8} (S'_{\nu i} - F_{\nu i})^2 \frac{1}{\sigma^2_{\nu i}} + \alpha \sum_{\mu=2}^{6} (C_{\mu i} - \chi_{\mu i})^2 \frac{1}{w^2_{\mu i}} \quad i = 1,\ldots,200$$

where $\alpha > 0$ is an adjustable parameter, $\{C_{\mu i}\}$ is a suitable set of positive spectra and $w_{\mu i}$ is a measure of their uncertainty. To start one might choose $C_{\mu i} = \bar{S}_i$, the average of the eight measured DN spectra, and solve for $\chi_{\mu i}^{(1)}$. If the parameter α is chosen large enough, the solution $\chi_{\mu i}^{(1)}$ will be positive nearly everywhere. Let $\chi_{\mu i}^{(1)}(POS)$ be these spectra with any negative counts set equal to zero and then renormalized, e.g.

$$\sum_{i=1}^{200} \chi_{\mu i}^{(1)}(POS) = 1$$

These are the first-order solutions for the six-group energy spectra. For further iteration one can set $C_{\mu i} = \chi_{\mu i}^{(1)}(POS)$ and obtain a second set of solutios $\chi_{\mu i}^{(2)}$ and corresponding positive energy spectra $\chi_{\mu i}^{(2)}(POS)$.

We have found with our computer program that for all values of $\alpha \geq 0.3$, the group spectra obtained were nearly identical. Group 2-6 DN energy spectra obtained with $\alpha = 0.3$ are shown in Fig.C-3. Each of the five spectra has the general shape expected for a DN spectrum, and shows little or no evidence of the oscillatory structure observed in the $\alpha = 0$ 'best-fit' solutions. Moreover, the fit to the eight measured DN spectra is excellent, as evidenced by a normalized 'chi-square' value of 3.5 that is only about 50% higher than that of the $\alpha = 0$ 'best-fit'. The "uniqueness" of the solutions will be investigated in a paper soon to be submitted to Nucl. Sci. Eng.

4. Fast Fission of U-238

Most large, fast reactor prototypes are of heterogeneous design with typical fuel cores comprising 20-25% PuO_2 and 78-80% UO_2. The percentage contributions of each fuel isotope to the fission rate and delayed-neutron yield within the core region of a 1000 MWe reactor of this

Table C-1. Isotope Contribution to Fission and DN Production in the Core of 1000-MWe Heterogeneous Fast Reactor at the End of its Equilibrium Cycle.

Isotope	% of Core Fissions	ν_d (DN/Fission) (Ref. 34)	% of DN
U-235	0.6	0.0167	0.86
U-238	10.6	0.0439	40.0
Pu-239	70.2	0.0063	38.0
Pu-240	5.4	0.0095	4.4
Pu-241	12.1	0.0152	15.8
Pu-242	0.5	0.0221	0.95

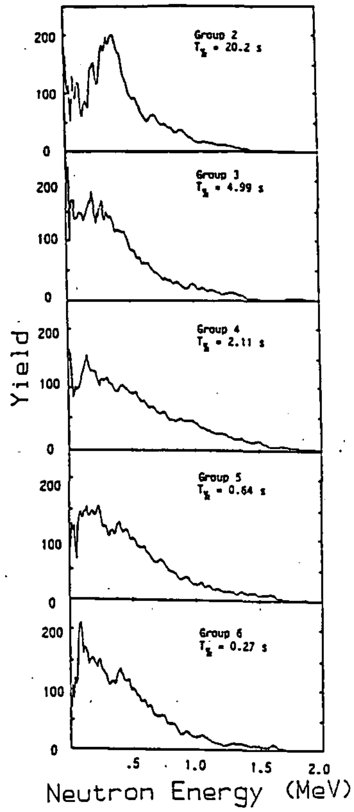

Fig. C3 Normalized 6-group spectra obtained from measured U-235 DN spectra.

type and near the end of its fuel cycle are given in Table C-1. The values are from Waltar and Reynolds.[7]

Whereas the fission rate is dominated by the plutonium isotopes, it is seen that U-238 is in fact the highest contributor to the DN yield. This results from the very high ν_d for U-238 relative to the other core constituents. At earlier times in the fuel cycle the DN fractional contribution from U-238 is even higher. It is evident, therefore, that for such reactors measurements of time-dependent DN spectra for U-238 are equally as important as those for Pu-239. Although there have been a few near-equilibrium composite DN studies for U-238,(8,9) there exists little direct information on their time dependence. We are now beginning a comprehensive study of DN spectra following fast fission of U-238.

---

[7]A.E. Waltar and A.B. Reynolds, Fast Breeder Reactors, publ. Pergamon Press, New York, 1981.

[8]G.W. Eccleston and G.L. Woodruff, Nucl. Sci. Eng. 62, 636 (1977).

[9]A.E. Evans and M.S. Krick, Nucl. Sci. Eng. 62, 652 (1977).

THE UNIVERSITY OF MICHIGAN
DEPARTMENT OF NUCLEAR ENGINEERING

A. INTRODUCTION

Over the past year, the cross section project at the University of Michigan has continued activities in two major areas. In the Neutron Experimental Bay, we have been employing a 150 kV Cockcroft-Walton accelerator as a 14 MeV neutron generator in the measurement of a number of activation cross sections. These have included the completion of a measurement of the $Cr(n,X)^{52}V$ cross section, and the near-completion of measurements of the $^{65}Cu(n,2n)^{64}Cu$, $^{64}Zn(n,p)^{64}Cu$, and $^{56}Fe(n,p)^{56}Mn$ cross sections. Over the past year, we have also taken steps to place these measurements on a more nearly absolute basis through the use of a proton recoil fast neutron monitor on loan from the National Bureau of Standards. In the Photoneutron Laboratory, we have continued work on the measurement of the U-238 capture cross section at neutron energies between 23 and 964 keV.

We have also begun work on planning for a major redirection of our 14 MeV program. We have made plans for the conversion of our present steady state neutron generator into a facility capable of generating 14 MeV neutron pulses of 1 - 2 nanosecond duration. Ion beam optics codes have been adapted to predict the performance of various components that are needed to carry out this conversion. Construction of first components is now underway.

B. ABSOLUTE MEASUREMENT OF THE $^{65}Cu(n,2n)^{64}Cu$, $^{64}Zn(n,p)^{64}Cu$ AND $^{56}Fe(n,p)^{56}Mn$ CROSS SECTIONS AT 14 MeV

(K. Zasadny, G. Knoll)

The $^{65}Cu(n,2n)^{64}Cu$ and $^{64}Zn(n,p)^{64}Cu$ reaction cross sections are being measured using the $^{56}Fe(n,p)^{56}Mn$ cross section as a neutron flux standard. The $^{56}Fe(n,p)^{56}Mn$ cross section is then measured using the "dual-thin scintillator" (DTS) detector developed at the National Bureau of Standards (NSF) as a neutron flux monitor.[1] The absolute efficiency of the DTS detector has previously been measured at NBS using the time-correlated associated particle technique.

---

[1] M. Dias, R. Johnson, O. Wasson, Nucl. Inst. and Meth., 224 p. 532 (1984).

1. Measurement of the $^{65}Cu(n,2n)^{64}Cu$ and $^{64}Zn(n,p)^{64}Cu$ Reactions at 14 MeV

A copper or zinc foil, sandwiched between two iron foils, is irradiated at a relatively high neutron flux (about 5-8 cm from the neutron source). The iron foils act as a flux monitor and the resulting ^{56}Mn activities are counted in a 4π-proportional counter. The absolute efficiency of the proportional counter is determined by a separate $4\pi\beta$-γ coincidence counting measurement. The time-varying behavior of the 14 MeV neutron emission is measured by a BF_3 long counter in multiscaling mode.

The induced ^{64}Cu activities are measured using opposing 3" x 3" NaI(Tl) detectors, each located approximately 10 cm from the ^{64}Cu source. The two detectors are operated in coincidence mode to detect the angularly correlated photon emission from the annihilation of the ^{64}Cu decay positrons. The branching parameters in the ^{64}Cu decay are taken from the measurements of Christmas, et al.[2] The copper or zinc foil is sandwiched between copper absorbers with a thickness chosen to stop the most energetic positron. The efficiency of the counting system for annihilation photons is determined using a standard ^{22}Na source of similar geometry to the copper or zinc foil-absorber package. This efficiency requires a small correction for 511 keV photon counting losses due to summing of the annihilation photons and 1274 keV ^{22}Na gamma rays. Summing losses are kept to less than 2% through choice of the source-detector geometry.

The absolute decay of the ^{22}Na source is measured by positron-gamma coincidence counting techniques. The positron is detected by counting annihilation photons, the gamma ray in coincidence is the 1274 keV gamma ray emission of ^{22}Na.

2. Measurement of the $^{56}Fe(n,p)^{56}Mn$ Cross Section

The $^{56}Fe(n,p)^{56}Mn$ cross section measurement is performed by irradiating an iron foil in a well-determined geometry with the NBS DTS detector system, on loan to The University of Michigan from the neutron measurements group at the National Bureau of Standards. The resulting activity of ^{56}Mn is counted, as before, by $4\pi\beta$ counting. The neutron flux at the iron foil is then determined by solid-angle calculation from the measured flux at the DTS detector. Neutron source-to-iron foil separations are kept large (20-30 cm) compared to iron foil-to-DTS detector spacing (about 5 cm) to minimize sensitivity to the solid angle and flux determination. Details

---

[2] P. Christmas, S. Judge, et al., Nucl. Inst. and Meth. 215 p. 397 (1983).

on the DTS detector system can be found in reference (1).The efficiency of the DTS detector system was previously measured at NBS at 14.041 MeV neutron energy by the time-correlated associated-particle method. A Monte Carlo computer program also simulates the resulting pulse height spectrum and efficiency determination to less than 2% uncertainty. This program is used to extend the measured efficiency at d-d and d-t neutron energies to the neutron energy of our cross section measurements (about 14.6 MeV). Small corrections must be assessed for the contributions of neutron scattering, since our measurements are not made in the time-correlated sense.

C. PLANNING FOR PULSED BEAM FACILITY
(J. Yang, V. Rotberg, G. Knoll)

During the past year, we have begun work on a study of the feasibility of converting our present 14 MeV facility to a nanosecond pulsed source. In conjunction with Dr. Alan Smith of Argonne National Laboratory, we have carried out a preliminary design for a beam sweeper, bending magnet, focussing quadrupoles, and klystron buncher to be used with our current neutron generator to produce short-duration pulses suitable for fast neutron time-of-flight spectroscopy. As part of this process, we have adapted and augmented several ion optics codes to permit a detailed description of beam focussing and time behavior of the pulser components. Based on these studies, the design and fabrication of several components of the system is now underway.

D. MEASUREMENT OF THE U-238 CAPTURE CROSS SECTION
(E. Quang, S. Melton, G. Knoll)

We are proceeding with steps described in the progress report of a year ago for the measurement of the capture cross section of U-238 at energies between 23 and 964 keV. As part of the procedure, we must carry out a chemical separation of the induced Np-239 activity from the much larger natural activity of the uranium target sample. A considerable experimental effort has gone into investigating a number of alternative chemical separation steps that will achieve the following objectives: clean separation of the Np-239 from the uranium, concentration of this activity into a small volume for convenient counting purposes, and high yield of the activity throughout the separation process.

The procedures now adopted involve a sequence of four different chemical separation techniques. Both solvent extraction and precipitation techniques are involved. The final activity is concentrated into a liquid sample of no more than 2 to 3 cm^3 final volume. Because of the clean separations achieved, we rely on close geometry sodium iodide scintillation counting of the induced neptunium activity. At the same time, the effectiveness of the separation is monitored using gamma counting with a high resolution germanium detector. Detector efficiencies are determined using a source of Am-243 in which an equivalent Np-239 activity exists in equilibrium. The absolute Am-243 activity is now being determined through absolute alpha counting using a newly constructed alpha counting facility. In the apparatus, a silicon surface barrier detector is used to measure the alpha activity transmitted through sharp edge apertures under low solid angles conditions. The aperture is remotely variable to allow cross checks on the consistency of the activity measurement.

As part of the experiment, the chemical separation yield must also be determined. We have worked out procedures for the use of Np-238 as a tracer that can be used to quantify the separation yield. We are currently investigating several techniques to reduce the interference that can occur between the Np-238 and Np-239 activities.

A. NUCLEAR DATA MEASUREMENTS

1. $^{235}U(n,f)$ Fission Cross Section Measurements from Thermal to 1 keV (R. A. Schrack, A. D. Carlson, and R. G. Johnson)

The dual ionization chamber containing both B-10 and U-235 foils has been rebuilt and the data taking system revised. Preliminary tests of the new system have been made.

The lessons learned from the experimental tests made in the previous year have been incorporated in the new system and have successfully accomplished the desired goals. The resolution of the chamber has reduced to the point where geometry no longer plays a role and interaction between the two detector systems has been eliminated. The chamber is now operated with a constraint flow of P-10 gas (95% argon, 5% CO_2) at about 0.5 cu ft/hour at a nominal measure of 1 atm to eliminate degradation of the pulse height distribution due to gas poisoning.

Background measurements have been made using filters having resonances in the energy range from 1.26 to 2850 eV. The measured backgrounds are on the order of 1% of the foreground rates and are a function of the background yield rate. Preliminary results show good agreement with other recent experiments from thermal to about 50 eV. Current work is directed toward enhancing the stability of the system to get more consistent results at higher energies.

2. Measurements of the $^{235}U(n,f)$ Cross Section in the MeV Energy Region (A. D. Carlson, O. A. Wasson, P. W. Lisowski,* J. L. Ullman,* and N. W. Hill**)

The $^{235}U(n,f)$ cross section is often considered the most favorable of the neutron cross section standards. Above a few MeV, however, the uncertainties are still unacceptably large. There is a need for improved measurements of this cross section especially in the upper MeV energy region where very little data exist. In an effort to improve the accuracy and range of this standard, measurements have been initiated at the new LANL WNR Target 4 facility which provides a very intense source of high energy neutrons. These measurements are being made at the 20 m flight path end station. The fission detector is a LANL fission chamber with new fission deposits recently made at ORNL. The neutron flux detector is an annular proton telescope which was used in earlier cross section measurements at NBS.[1]

* Los Alamos National Laboratory, Los Alamos, NM
** Oak Ridge National Laboratory, Oak Ridge, TN.
[1] A. D. Carlson and B. H. Patrick, Neutron Physics and Nuclear Data, pp. 880-886 (1978).

The first phase of the experiment involved tests of the detector systems and measurements of fission cross section ratios at the LANL Van de Graaff facility. From this work timing determinations for the telescope obtained with a simple α-particle system were verified.

The initial work on the WNR facility allowed experimental tests, diagnostic studies and some preliminary results to be obtained in the 1-35 MeV energy range.

3. International ^{235}U Fission Foil Mass Intercomparison
(I. Schröder, D. M. Gilliam, A. D. Carlson, S. W. Bright, and J. M. R. Hutchinson)

In the measurement of neutron fission cross sections, one of the larger uncertainties is associated with the mass determination of the fissionable deposit. Inconsistencies in determinations of the fission cross sections may be a result of systematic errors associated with the measurement of the deposit mass.

As part of a study to check the consistency of mass scales at a number of laboratories throughout the world, two ^{235}U deposits from the Khlopin Radium Institute (KRI) in Leningrad, U.S.S.R. were made available through the assistance of the IAEA for measurements at NBS and ANL. These deposits are directly traceable to foils used in very precise measurements of the $^{235}U(n,f)$ cross section made in a collaborative effort by KRI and the Technical University of Dresden (TUD), GDR.

The study undertaken at the NBS consisted of two parts.[2] One consisted in the measurement of the alpha-decay rates of the two ^{235}U samples (KRI-VI and KRI-XV) with a low geometry counting spectrometry facility. The other consisted of the measurement of the total alpha disintegration rate of the samples employing a 2π alpha-counter.

The ^{235}U mass determinations obtained at KRI, ANL, and NBS are summarized in Table 1. The results shown as ANL-LG are low geometry alpha counting measurements of Poenitz and Meadows. As can be seen from this table, all measurements agree within their stated uncertainties. In addition, Poenitz and Meadows have determined values for the KRI samples based on an intercomparison of measurements of foils from a number of contributing laboratories. The values they obtained in this evaluation are 760.2 ± 1.4 for KRI-VI and 893.0 ± 1.8 for KRI-XV. The outcome of the KRI mass scale determination will have a direct effect on the KRI-TUD fission cross section measurements and their uncertainties. This effort should contribute to the long-sought objective of 1% accuracies for this cross section.

---

[2] Trans. Am. Nucl. Soc. 53, 473 (1986).

TABLE A-1. Mass determination of KRI-VI and KRI-XV Foils (μg)

	KRI	NBS-LG	NBS-2π	ANL-LG
KRI-VI	757.9 ± 7.6	763.9 ± 2.9	755.4 ± 6.0	762.7 ± 3.3
KRI-XV	901.0 ± 9.0	898.9 ± 3.4	894.0 ± 7.0	896.2 ± 3.9

4. Use of the Dual Thin Scintillator as a Neutron Fluence Monitor for 14 MeV Activation Cross Section Measurements (K. Zasadny, G. Knoll, R. G. Johnson, and O. A. Wasson)

The dual-thin scintillator (DTS) neutron fluence monitor which was developed at NBS[3] is being used at the 14 MeV neutron generator facility at the University of Michigan as a neutron fluence monitor for 14 MeV neutron activation cross section measurements. The detector has been used in its various modes of operation and its performance compared to the calculated response. The results of the measurements are given in the contribution from the University of Michigan.

5. Measurement of the ^{235}U(n,f) Cross Section Standard at 2.5 MeV Neutron Energy (K. C. Duvall, H. Ma,* and O. A. Wasson)

In order to apply the time-correlated associated-particle technique using the D(d,n)^{3}He reaction to a measurement of the ^{235}U(n,f) cross section standard at 2.5 MeV neutron energy, it is necessary to use larger diameter ^{235}U deposits than were used in the measurement at 14 MeV.[4] This is because the neutron beam is much wider. A total of six ^{235}U-Tetra fluoride deposits with a diameter of 50 mm and a thickness of 250 μg/cm^{2} have been obtained from the Central Bureau of Nuclear Measurements in Belgium for use in this measurement. Preliminary measurements are in progress at the 100 kV ion generator.

6. Intercomparisons for Development of a 15 MeV Neutron Dosimetry Standard (L. J. Goodman, H. Ma,* and D. M. Gilliam)

An intercomparison was completed between instruments of the Bureau International des Poids et Mesures (BIPM) and instruments of the National Bureau of Standards (NBS). The intercomparison was made for a 15-MeV neutron radiation field produced by the T(d,n)^{4}He reaction with a 500 keV deuteron beam produced by the NBS 3 MV Positive Ion Accelerator. The instruments used consisted of tissue-equivalent ionization chambers and photon-energy-compensated Geiger-Müller dosimeters. The neutron tissue

---

* Guest Scientist from the Institute of Atomic Energy, Beijing, PRC.

[3] Dias, Johnson, and Wasson, Nucl. Instr. and Meth. 224, 532 (1984).

[4] Wasson, Carlson, Duvall, Nucl. Sci. and Eng. 80, 282 (1982).

kermas determined by the two sets of instruments were in excellent agreement (0.1 percent difference) and the radiation field was found to have a gamma-ray kerma of about three percent of the total kerma.

A second intercomparison was made in the NBS 15 MeV neutron field to compare the neutron tissue kerma determined with tissue-equivalent ionization chambers and a Geiger-Müller dosimeter to that calculated by applying an appropriate kerma factor to the neutron fluence measured with a double-foil ^{235}U fission chamber. The agreement between the two methods was poor (15 percent difference). These measurements will be repeated with an unused TiT target.

B. DETECTORS AND FACILITIES FOR NUCLEAR DATA MEASUREMENTS

1. Data Acquisition System Development (R. G. Johnson)

The data acquisition systems for the Linac Dedicated Pulsed Neutron Facility and the 3 MV Positive Ion Accelerator are being upgraded. Orders have been placed for two computer systems to replace the last of our Harris/5 computers. The new computers are based on the Motorola 68020 microprocessor and the VME bus. PC AT clones will be used as intelligent front ends in the data acquisition system. Our intention is to take advantage of the extensive hardware and software developments made at CERN to reduce the necessary development time and work in replacing data acquisition systems.

2. Design of an Induction Linac for Neutron Research (R. G. Johnson)

The conceptual design of a linear induction accelerator for neutron and high-LET radiation research has been improved by incorporating the latest technological developments. The basic parameters of the design remain unchanged, i.e., a final energy of 100 MeV, beam currents of 250 A of electrons or 2.5 A of protons, and a pulse structure with pulse width of up to 100 ns and repetition rates to 1000 Hz. The changes are primarily connected with the development of magnetic switching techniques at Lawrence Livermore National Laboratory. This development has eliminated much of the uncertainty in the design of pulse forming networks and also simplifies the design of the induction modules. A report on the improved conceptual design of the induction linac was presented at the IAEA Advisory Group Meeting on Neutron Source properties (June 9-13, 1986, Leningrad, U.S.S.R.).

3. Continued Development of a Standard 2.5 MeV Neutron Source (K. C. Duvall)

A recently purchased 100-kV ion generator is being fitted with aft-acceleration focusing and steering components to provide up to 200 microamps of deuteron beam current within a 2-mm beam spot. The beam is expected to produce the needed neutron intensity to carry-out a $^{235}U(n,f)$ cross section measurement at 2.5 MeV using the $D(d,n)^3He$ reaction and the time-correlated associated-particle method. The fixed setup will be dedicated solely to the production of a reference 2.5 MeV neutron source with stable field characteristics. The facility is further described in a recent publication that will appear in the April issue of Nuclear Instruments and Methods. The facility should provide a means of establishing the 2.5 MeV spot energy as an intermediate energy normalization point.

4. Progress in the Development of a ^3He Gas Scintillation Counter. (J. W. Behrens, H. Ma, O. A. Wasson, and C. R. Westerfeldt*)

We report the progress made during the past year to implement a detector to measure the $^3He(n,p)T$ reaction from thermal to several MeV neutron energy. In order to improve on the prototype detector reported last year, we constructed a $^3He/Xe$ gas scintillation counter consisting of a cubic gas cell with 150 mm sides.[5] Four faces of the cube contained pyrex windows with photomultiplier tube modules while the remaining two faces were for the neutron beam. Using research purity Xe gas with diphenylstilbene (dps) wavelength shifter coated on the glass, the resolution was 10% (FWHM) for a ^{238}Pu alpha-particle source. Variations in the dps thickness and light collection geometry have produced improvements in detector resolution. It is planned to first use this system to measure the $^3He(n,p)T$ cross section at 0.5 MeV.

5. Absolute Thermal Neutron Counter Development (D. M. Gilliam and G. P. Lamaze)

A gamma-alpha coincidence method is being employed to make an accurate calibration of a totally absorbing ^{10}B capture-gamma neutron beam monitor; and subsequently, the "black" ^{10}B detector will be used to calibrate a thin ^{10}B transmission monitor. These neutron counters have potential applications, such as improvement of thermal neutron cross section standards and improved calibration of the NBS manganese bath, with possible implications for ^{252}Cf nubar data.

The immediate stimulus for these neutron counter developments is the need for a high-accuracy thermal neutron beam monitor for a DOE sponsored

---

* Duke University

5 Behrens, Hongchang Ma, and Wasson, Trans. Am. Nucl. Soc., Vol. 53, p. 163 (1986).

measurement of the free neutron lifetime. The overall uncertainty of the neutron lifetime measurement is intended to be well under 0.5% (one sigma), so that the accuracy demands for the neutron beam monitor are even more stringent (0.1% to 0.3%). The gamma-alpha technique being developed at NBS will be intercompared with a cryogenic calorimetric ^{6}Li monitor, which is under development at LANL.

C. NUCLEAR DATA EVALUATIONS AND COMPUTATIONS

1. The Neutron Cross Section Standards Evaluations for ENDF/B-VI (A. D. Carlson, W. P. Poenitz,* G. M. Hale**, and R. W. Peelle†)

The evaluation process for the ENDF/B-VI standards is more thorough and logically consistent than that used in earlier versions. The primary effort is focused on a simultaneous evaluation using generalized least squares, R-matrix evaluations and a procedure for combining the results of these evaluations. The simultaneous evaluation is important to this process since ratio measurements in addition to shape and absolute determinations are treated properly. Correlations within and among experimental data sets are also taken into account. Also the output results from the thermal constants evaluation by Axton, including the associated variance-covariance matrix, has been used as input for this evaluation. The R-matrix evaluations provide a method which allows charged-particle measurements involving the same compound nuclei (^{7}Li and ^{11}B) to be included in the evaluation process. These evaluations also provide a smooth meaningful expression for the energy dependence of the cross sections. Independent data bases are used in the simultaneous and R-matrix evaluations. The combining procedure is used to combine the information obtained from these analyses in a proper way to form the final evaluation and its variance-covariance matrix. The standards being evaluated are ^{6}Li(n,t), ^{10}B(n,α_1), ^{10}B(n,α), ^{197}Au(n,γ), and ^{235}U(n,f). Evaluations for the important reactions ^{238}U(n,γ), ^{238}U(n,f), and ^{239}Pu(n,f) are also being performed. The new R-matrix evaluation of the hydrogen scattering cross section by Dodder and Hale has already been accepted as the hydrogen standard for ENDF/B-VI.

A large number of complete cycles of the evaluation procedure have been performed in order to implement various improvements, changes, and checks into the process. The work has gone relatively smoothly except for some problems concerning the ^{10}B cross sections. For this case, the adequacy of the linear approximation being used in the combining process was questioned. The ^{10}B results were verified by performing a second iteration cycle in which second derivative terms were included. The basic problem with the ^{10}B data is the relatively poor data base available for use in the evaluation effort.

---

* Argonne National Laboratory, Argonne-West, Idaho Falls, ID.
** Los Alamos National Laboratory, Los Alamos, NM.
† Oak Ridge National Laboratory, Oak Ridge, TN.

At the present time a final cycle of the process is underway to include additional data and improvements. Smoothing of the capture and fission data and data testing will then be performed. It is anticipated that this work will be completed by about May 1987.

2. Calculation of Carbon Cross Sections at ENDF/B Energy Values (R. A. Schrack)

The evaluation of the neutron total cross section for carbon requires the data from the experimental determinations be recalculated to supply cross section values and associated errors at a common set of energy values. The energy grid used for the ENDF/B neutron total cross section for carbon was chosen so that linear interpolation between any two given data points would not introduce an error greater than 1%. This property of the energy set justifies the condensation of other energy sets to ENDF/B set. For example, about 1700 values of the cross section are supplied for the energy region between 10 and 20 MeV in an experimental data set supplied by Karlsruhe. This set can be condensed to 163 values of the ENDF/B set covering the same energy range. Data obtained by experiments at NBS, Los Alamos, and Karlsruhe have been recalculated for inclusion in the evaluation procedure.

3. A Simultaneous Evaluation of Kerma in Carbon and the Carbon Cross Sections (E. J. Axton)

Recent measurements of kerma in carbon indicate that values of this quantity calculated on the basis of cross sections taken from the ENDF/B-V file are probably too high, particularly in the energy range from 15 to 20 MeV. Measurements of the inelastic scattering cross section to the first excited state, and of the n-n'3α cross section in this energy range which have appeared since the establishment of ENDF/B-V suggest that the former should be higher, and the latter lower. The purpose of this exercise is to perform a least squares fit to the available data for kerma and the cross sections in order to find best values for these parameters.

A preliminary calculation has already been carried out with a very simple model in order to get some feeling for the problem. In this simple model the cross sections are taken from ENDF/B-V and multiplied by various factors which are initially unity, but which are allowed to float in the least squares fit within the constraints of their uncertainties. Thus, the absolute values of the cross sections can change, but not their shapes as a function of energy, which is another way of saying that there is 100% correlation between cross sections at different energies.

The data set is by no means complete, but it probably gives a reasonable initial estimate of the eventual outcome. The calculation covers the energy range from 11 to 20 MeV. The total kerma at 14.1 MeV is reduced by 16% from the initial value. The n-n'3α cross section is reduced by 20%.

This is achieved by reducing the total, elastic, n-α, and n-d cross section by 6, 5.2, 12, and 2.6%, respectively, and increasing the inelastic by 6.4%. This latter increase is supported by inelastic angular distribution measurements which appeared after ENDF/B-V.

Probably the main defect in the simple model described above is the rather improbable shape of the n-n'3α cross section. It has become obvious that a complete reevaluation of the carbon cross sections is necessary, and this is in progress. If time permits, the energy range will be extended to 5-35 MeV.

4. Bibliography of Photon Cross Section Measurements 10 eV to 13.5 GeV (J. H. Hubbell, E. B. Saloman)

A bibliography of measured absolute cross section data for photons (XUV, x ray, gamma ray, bremsstrahlung) has been completed and is available as an NBS internal report[6] from the NBS Photon and Charged Particle Data Center. This bibliography lists 512 independent literature sources, each annotated as to substances (elements and compounds) covered. These sources, spanning the time period 1907 to 1986, cover 82 elements ranging from Z = 1 to 92, and our over-all energy range from 10 eV to above 10 GeV. This bibliography represents about 20,000 data points, available in machine-readable form. This bibliography has been prepared as part of a critical evaluation of photon attenuation coefficients, and additions to this data base are solicited from researchers in this subject area.

5. X-Ray Attenuation Data 0.1 to 1000 keV (E. B. Saloman, J. H. Hubbell, M. J. Berger)

The NBS Photon and Charged Particle Data Center has carried out a comparison in both graphical and tabular form, of measured x-ray attenuation coefficients with state-of-the-art theoretical values and with a widely-used semi-empirical data set. The measured coefficients in this comparison are from the Data Center computerized file. The theoretical data set is based on the 1 to 1500 keV relativistic Hartree-Slater atomic photoeffect calculation by J. H. Scofield (Lawrence Livermore National Laboratory) extended at NBS request down to 0.1 keV, plus theoretical scattering data developed by NBS in collaboration with other laboratories. For atomic numbers Z = 2 to 54 the tabular comparisons include an alternative of Scofield photoeffect values, renormalized to the Hartree-Fock atomic model. This comparison suggests that the Scofield values without renormalization are more realistic. The semi-empirical set

[6] J. H. Hubbell, H. M. Gerstenberg, and E. B. Saloman, "Bibliography of Photon Total Cross Section (Attenuation Coefficient) Measurements 10 eV to 13.5 GeV," NBSIR 86-3461 (1986).

is that of B. L. Henke et al. (Lawrence Berkeley Laboratory) covering the energy range 0.03 to 10 keV. The present comparison, available as an NBS internal report,[7] extends from 0.1 to 100 keV and includes all elements Z = 1 to 92.

6. Evaluation of the Thermal Constants of ^{233}U, ^{235}U, ^{239}Pu, and ^{241}Pu and the Fission Neutron Yield of ^{252}Cf. (E. J. Axton)

This work was performed at the Central Bureau for Nuclear Measurements in Geel, Belgium. In 1982 a simultaneous evaluation of the thermal neutron constants of ^{233}U, ^{235}U, ^{239}Pu, and ^{241}Pu, together with the fission neutron yield from the spontaneous fission of ^{252}Cf, was performed with, for the first time, a full covariance matrix to describe the correlations in the uncertainties of the input data. The input data set was limited in that measurements in Maxwellian reactor spectra were excluded.[8] In 1984 the Maxwellian data were added, and all measurements were renormalized to the latest values of reference data such as half-lives and cross sections, and some of the earlier measurements were re-interpreted.[9] In this third paper on the subject the input data are again renormalized to the latest reference data, new measurements added, and some older measurements reinterpreted, in order to provide an up-to-date set of values for possible inclusion in the evaluated nuclear data files of ENDFB. This paper should be regarded as a supplement to the earlier two in this series. It will be published as a European Research Report, but meanwhile it is available an an internal CBNM Report GE/PH/01/86.

7. Photonuclear Data Abstract Sheets (H. M. Gerstenberg)

The complete set of Photonuclear Data-Abstract Sheets[10] has been published as a fifteen volume work and distributed to forty-five research and educational institutions throughout the world. These abstract sheets cover most classes of experimental nuclear data leading to information of the electromagnetic matrix elements between the ground and excited states of a given nucleus. The set, containing nearly 7200 abstract sheets and covering 89 chemical elements from hydrogen through americium, represents a twenty-seven year history of the study of electromagnetic interactions.

---

[7] C. B. Saloman and J. H. Hubbell, "X-Ray Attenuation Coefficients (Total Cross Sections): Comparisons of the Experimental Data Base with the Recommended Values of Henke and the Theoretical Values of Scofield for Energies Between 0.1 - 100 keV," NBSIR 86-3431 (1986).

[8] E. J. Axton, (1984), European Applied Research Reports 5 No. 4 (EUR 8805 EN).

[9] E. J. Axton, (1985), Report IAEA Tecdoc-335, 214, IAEA, Vienna.

[10] E. G. Fuller and H. Gerstenberg, Photonuclear Data-Abstract Sheets, 1955-1982, NBSIR 83-2742 (1986).

8. Initial Spectra of Neutron-Induced Secondary Charged Particles (H. M. Gerstenberg, R. S. Caswell, and J. J. Coyne)

Initial spectra of secondary-charged particles (such as p, α, C, N, O) which result from neutron interactions with material such as tissue, will be tabulated in 200 keV neutron energy bin sizes from 0 to 20 MeV. Tabulations will also be made for 76 almost logarithmic bins extending from thermal energy for 2 MeV. These calculations use as input the neutron cross section data from the ENDF/B nuclear data file from the National Nuclear Data Center at Brookhaven. Supplementary information is also needed on the angular distribution of neutron reactions leading to charged particles and on the final excitation of residual nuclei. The calculations for these tables will be started when the final version of the total neutron cross section above 14 MeV is evaluated by Axton.[11]

9. Comparison of Measured and Calculated Microdosimetric Energy Spectra for a ^{252}Cf Source and a Reactor Spectrum* (H. M. Gerstenberg, J. J. Coyne, and R. B. Schwartz)

The microdosimetric energy spectra, or y spectra, have been measured for a ^{252}Cf source and a TRIGA reactor source shielded by six inches of lead to reduce the γ-ray contribution. Using calculated neutron fluence spectra for these sources, the y spectra were also calculated using the NBS analytical code[12,13]. Although both spectra are essentially due to fission neutrons, the calculations predicted a significant difference in the shape of the y-spectra; this difference was confirmed by the measurements.

10. Calculated Microdosimetric Energy Distribution Spectra and Their Use to Indicate Neutron Source Quality* (H. M. Gerstenberg and J. J. Coyne)

Microdosimetric energy distribution spectra, or y spectra, have been calculated for four different distributed neutron sources using the analytical computer code developed at the National Bureau of Standards[12,13]. The code is currently in use on the new NBS computer. The neutron spectra used as the input for the code were obtained from calculations of the neutron fluence expected from a ^{252}Cf source, a source with a large component of high-energy neutrons up to 16.9 MeV, and a source of neutrons from a pulsed thermal reactor with and without a lead shield. The resulting energy distribution spectra for each of the four input neutron spectra are compared and explained in terms of the proportion of low-energy neutrons to high-energy neutrons in the input neutron spectra. The variations, as well as the similarities, in the shape of the resulting energy distribution spectra show that the y spectra can be a useful tool in understanding the quality of different neutron spectra. A paper describing this work is being prepared for the Eighth International Congress of Radiation Research to be held in Edinburgh, Scotland.

---

* Supported in part by the Armed Forces Radiobiology Research Institute, Bethesda, MD, and the Defense Nuclear Agency, Washington, DC.

11 See Item C-3.

12 Randall S. Caswell, Radiation Research 27, 92-107 (1966).

13 Randall S. Caswell, J. Joseph Coyne, Radiation Research, 52, 448-470 (1972).

UNIVERSITY OF NEW MEXICO

THE $^{64}Zn(n,2n)$ ^{63}Zn AND $^{64}Zn(n,p)$ ^{64}Cu CROSS SECTION MEASUREMENTS AT 14.8 MeV

D. A. Rutherford

Cross section data is fundamental for many types of research, ranging from nuclear weapons testing to fusion research; consequently, in order to fulfill the needs for nuclear data, cross section analyses have been prioritized by the Nuclear Data Committee. In addition to this committee's work, in 1982 the Department of Energy initiated a program entitled, "Coordination of Magnetic Fusion Energy Nuclear Data Needs and Activities," which not only determined the nuclear data needs but also prioritized these needs for magnetic fusion. These measurements should be the most applicable to fusion blanket and the shield development research. One of these highly prioritized interactions is the $^{64}Zn(n,p)^{64}Cu$ cross section that provides data for the fission and fusion community. This cross section and the $^{64}Zn(n,2n)^{63}Zn$ cross section were measured for this work. The results which established an accurate measuring standard for these two cross sections are discussed in the contribution from LANL by Phil Young and Debra Rutherford.

OAK RIDGE NATIONAL LABORATORY

A. CROSS SECTION MEASUREMENTS

1. Capture, Total and Reactions

a. Modifications of the High-Energy Transport Code (HETC) and Comparisons with Experimental Results,[1] (R. G. Alsmiller, Jr., F. S. Alsmiller, T. A. Gabriel, and O. W. Hermann)

The High-Energy Transport Code HETC has been revised by incorporating the multi-chain fragmentation model of J. Ranft et al. to describe particle production from high-energy hadron-nucleus collisions. The revised code is briefly described and its validity is tested by comparing calculated results with experimental data from 29.4-GeV protons incident on an iron-air beam stop and with experimental data from 800-GeV protons incident on a large iron block. Some comparisons with calculated results obtained with other available transport codes, FLUKA82, CASIM, and MARS10 are also included.

b. Gamma-Ray Production Cross Sections for 0.9 to 20 MeV Neutron Interactions with 10-B,[2] (R. L. Bywater, Jr.[3])

Gamma-ray spectral data previously obtained at the 20-meter station of the Oak Ridge Electron Linear Accelerator flight-path 8 were studied to determine cross sections for 0.9- to 20-MeV neutron interactions with ^{10}B. Data reduction techniques, including those for determination of incident neutron fluences as well as those to compensate for Doppler-broadened gamma-ray-detection responses, are given in some detail in this report.

c. Nuclear Structure of Ca-49 Above 5 MeV Excitation from n + Ca-48 and Astrophysics for 30 keV Neutrons,[4] (R. F. Carlton,[5] J. A. Harvey, R. L. Macklin, C. H. Johnson, and Boris Castel[6])

The level structure of ^{49}Ca has been investigated above the neutron separation energy by measurements of the total and capture cross

---

[1]ANS Topical Conference on Theory and Practices in Radiation Protection and Shielding, Knoxville, Tenn., April 22-24, 1987. Proceedings will be published.

[2]ORNL/TM-10191 (October 1986).

[3]Student research participant from Nebraska Wesleyan College, Lincoln, Nebraska, under sponsorship of the Oak Ridge Associated University Summer Research Participation Program.

[4]Accepted by Nuclear Physics.

[5]Middle Tennessee State University, Murfreesboro, Tennessee 37132.

[6]Queen's University, Kingston, Ontario, Canada K71 3N6.

sections for neutron energies up to 10 MeV. Transmission data were obtained for two $^{48}CaCO_3$ samples enriched to 96% in ^{48}Ca and were analyzed in the R-matrix formalism up to 2 MeV. An upper limit of 0.07×10^{-4} was placed upon the s-wave strength function ($<\Gamma_n{}^{\circ}>/D$) and an optical model real potential was deduced from the low energy total cross section. Approximately 45% of the $2d_{5/2}$ single particle strength is observed in the region below 2 MeV neutron energy. Model configurations based on continuum shell model calculations which describe this strength and its distribution are presented. Combined low-energy results are used to obtain the Maxwellian-averaged capture cross section, and the result is discussed in relation to the nucleosynthesis of ^{49}Ca and the anomalous abundances observed in an inclusion of the Allende meteorite.

d. Resonance Structure of S-33 + n from Transmission Measurements,[1] (G. Coddens,[2] M. Salah,[3] J. A. Harvey, N. W. Hill, and N. M. Larson)

The total neutron cross section for ^{33}S has been determined for energies from 10 keV up to 2 MeV at the Oak Ridge Electron Linear Accelerator (ORELA) by a TOF transmission experiment. By combining these results with (n,α) data obtained at the Geel Electron Linear Accelerator (GELINA), resonance parameters (E_λ, J^π, and Γ_γ) have been determined up to 270 keV.

e. Half Life of 57-Ni,[4] (J. K. Dickens)

f. Neutron Capture Cross Sections of 151-Eu and 153-Eu from 3 to 2200 keV,[5] (R. L. Macklin and P. G. Young[6])

Neutron capture by enriched stable isotopes of europium was measured as a function of energy by time-of-flight at the Oak Ridge Electron Linear Accelerator. Deformed optical model and reaction theory calculations using the published total cross section for natural europium and low-energy resonance parameters were made to compare with the present data. Maxwellian-average capture at kT=30 keV was calculated as (3.40 ± 0.14) b for ^{151}Eu and (2.48 ± 0.10) b for ^{153}Eu.

g. A Self-Calibrated Neutron-Capture Measurement of the 1.15-keV Resonance of Iron[7] (R. L. Macklin)

---

[1]Accepted by Nuclear Physics.
[2]Commisariat a L'Energie Atomique, Laboratoire Leon Brillouin, France.
[3]Graduate student from Minia University, Egypt.
[4]Journal of Radioanalytical and Nuclear Chemistry Letters **103**, 273 (1986).
[5]Nucl. Sci. Eng. **95**, 189 (1987).
[6]Los Alamos National Laboratory, Los Alamos, New Mexico 87545.
[7]Nucl. Sci. Eng. **95**, 200 (1987).

h. Neutron Transmission Measurement and Resonance Analysis of 93-Zr from 60 to 6000 eV[1] (R. L. Macklin, J. A. Harvey, and N. W. Hill)

i. Neutron Capture Resonances of Gadolinium 152 and 154,[2] (R. L. Macklin)

Neutron resonance parameters were found for ^{152}Gd up to 2700 eV. An average s-wave spacing D_o = (17.4 ± 1.0) eV and radiation width (58.6 ± 3.0) eV were found. The resonance contribution to the capture integral was found as (397 ± 32) barns, exclusive of a 1/v term. Resonance parameters for ^{154}Gd were extended from 490 to 2760 eV.

j. Neutron Capture Cross Sections of Rhenium from 3 keV to 1900 keV,[3] (R. L. Macklin and P. G. Young[4])

The neutron capture cross section of elemental rhenium was measured to neutron energies between 3 and 1900 keV at the Oak Ridge Electron Linear Accelerator time-of-flight facility. A deformed optical model was used to analyze published neutron total cross sections for rhenium and low-energy average resonance parameters for ^{185}Re and ^{187}Re. The optical model results were used with reaction theory to calculate radiative capture cross sections for comparison with the present experimental data.

k. Maxwellian-Averaged Neutron Capture Cross Sections for 99-Tc and 96,98-Mo,[5] (R. R. Winters[6] and R. L. Macklin)

l. A Spherical Optical Model Potential for the Re/Os Stellar Nucleosynthesis Chronometer from s-Wave Neutrons on 186,187,188-Os,[7] (R. R. Winters,[6], R. F. Carlton,[8] J. A. Harvey, and N. W. Hill)

m. The 189-Os(n,γ) Cross Section and Implications for the Duration of Stellar Nucleosynthesis,[9] (R. R. Winters,[6] R. L. Macklin, and R. L. Hershberger[10])

This paper reports the results of a measurement of the ^{189}Os(n,γ) cross sections over the energy ranges 200 to 500 eV and 2.6 to 500

---

[1]Nucl. Sci. Eng. **92**, 525 (1986).
[2]Nucl. Sci. Eng. **95**, 189 (1987).
[3]Submitted to Nuclear Science and Engineering.
[4]Los Alamos National laboratory, Los Alamos, New Mexico 87545.
[5]Astrophysical Journal (in press).
[6]Department of Physics, Denison University, Granville, Ohio 43023.
[7]Phys. Rev. C34, 840 (1986).
[8]Middle Tennessee State University, Murfreesboro, Tennessee 37132.
[9]Astronomy and Astrophysics (in press).
[10]University of Kentucky, Lexington, Kentucky.

keV. We report resonance parameters for the lower energy region and these results yield an observed s-wave mean level spacing $D_0 = (3.4 \pm 0.2)$ eV, a neutron strength function $S_0 = (2.9 \pm 0.5) \times 10^{-4}$ and an average total radiation width $\langle\Gamma_\gamma\rangle = (83 \pm 5)$ meV. The averaged cross sections over the upper energy range provide constraints on the optical model potential and giant dipole resonance model used to represent the cross section. For astrophysical applications we report the 30-keV Maxwellian-averaged cross section $\langle\sigma_\gamma\rangle$ = 1168 ± 47) mb and use the ^{187}Re beta decay to estimate the duration of stellar nucleosynthesis as (11.0 ± 2.5) Gyr.

n. Maxwellian-Averaged Neutron-Capture Cross Sections for 99-Te and 96,98Mo,[1] (R. R. Winters[2] and R. L. Macklin)

This paper presents the the Maxwellian-averaged neutron capture cross sections for ^{99}Tc and ^{95,96,97,98}Mo. An extensive temperature range (5-100 keV) is included to encompass the model calculations for ongoing s-process nucleosynthesis in red giant stars where technetium has been observed. At T = 30 keV, the most often chosen temperature for the s-process, we find (782 ± 39) mb for ^{99}Tc, (292 ± 2) mb for ^{95}Mo, (112 ± 6) mb for ^{96}Mo, (339 ± 2) mb for ^{97}Mo, and (99 ± 5) mb for ^{98}Mo. These results are used to estimate the duration of the third dredge-up phase for two thermally pulsing asymptotic giant branch stars for which the technetium to molybdenum abundances have been measured.

2. Actinides

a. R-Matrix Analysis of the Pu-239 Cross Sections Up to 600 eV,[3] (H. Derrien,[4] G. de Saussure, R. B. Perez, N. M. Larson, and Roger L. Macklin)

b. R-Matrix Analysis of the 239-Pu Cross Sections up to 1 keV,[5] (H. Derrien,[4] G. de Saussure, R. B. Perez, N. M. Larson, and Roger Macklin)

We report here the results of an R-matrix resonance analysis of the ^{239}Pu neutron cross sections up to 1 keV. After a description of the method of analysis we list the nearly 1600 resonance parameters obtained and present extensive graphical and numerical comparisons between calculated and measured cross-section and transmission data.

---

[1]Astronomy and Astrophysics (in press).
[2]Department of Physics, Denison University, Granville, Ohio 43023.
[3]Trans. Am. Nucl. Soc. **52**, 635 (1986).
[4]Commissariat a l'Energie Atomique, Centre d'Etudes Nucleaires de Cadarache, Boite Postale No. 1, 13115, Saint-Paul-Lez-Durance, France.
[5]ORNL/TM-10098 (June 1986).

c. <u>R-Matrix Analysis of the 241-Pu Cross Sections Up to 100 eV,</u>[1] (H. Derrien,[2] N. M. Larson, G. de Saussure, and R. B. Perez)

The ^{241}Pu total cross-section measurement of Kolar and Carraro and the neutron fission cross-section measurements of Blons et al. and Weston and Todd were analyzed with the R-matrix resonance analysis program SAMMY which uses Bayes' equation to extract resonance parameters from the experimental data. A set of Reich-Moore-type resonance parameters was obtained which describes the cross sections up to 100 eV. It is shown that existing data are not adequate for a precise evaluation of the resonance cross sections and the need for additional work is discussed.

d. <u>Fission-Product Yield Data from the US/UK Joint Experiment in the Dounreay Prototype Fast Reactor,</u>[3] (J. K. Dickens and S. Raman)

The United States and the United Kingdom have been engaged in a joint research program in which samples of fissile and fertile actinides are irradiated in the Dounreay Prototype Fast Reactor in Scotland. The purposes of the program are to study the materials behavior and nuclear physics characteristics of selected actinide elements and/or isotopes. Samples of the actinides were incorporated in fuel pins inserted in the core. For the fission-yield measurements of this report, the samples were milligram quantities of actinide oxides of ^{248}Cm, ^{246}Cm, ^{244}Cm, ^{243}Cm, ^{243}Am, ^{241}Am, ^{244}Pu, ^{241}Pu, ^{240}Pu, ^{239}Pu, ^{238}Pu, ^{238}U, ^{236}U, ^{235}U, ^{234}U, ^{233}U, ^{231}Pa, ^{232}Th, and ^{230}Th encapsulated in vanadium holders. The samples were in core for about 14 months and were exposed to a total fluence of approximately 2.7 x 10^{22} fast neutrons.

Following irradiation the samples were prepared for further study using high-resolution gamma- and x-ray detectors. One series of measurements was made approximately nine months following the end of the irradiation, and a second series of measurements was made approximately six months later. Gamma rays and x-rays were observed (and quantitatively measured) corresponding to decay of several long-lived fission products, namely ^{91}Y, ^{95}Zr, ^{95}Nb, ^{103}Ru, ^{106}Rh (following decay of ^{106}Ru), ^{110m}Ag, ^{125}Sb, ^{134}Cs, ^{137}Cs, ^{141}Ce, ^{144}Ce, and ^{144}Pr, and ^{155}Eu. The gamma-ray yield data were analyzed to obtain fission-product yields. However, because of uncertainties associated with various parameters of the experiment (e.g., initial sample compositions, effective fission cross sections, etc.), it was found that all of the experimental data could not be reported on an absolute basis. Instead, the yield data for the fission product ^{137}Cs were designated as monitor data for the yield data of the other fission products.

---

[1]Accepted by Nuclear Science and Engineering.
[2]Commissariat a l'Energie Atomique, Centre d'Etudes Nucleaires de Cadarache, Boite Postale No. 1, 13115, Saint-Paul-Lez-Durance, France.
[3]ORNL-6266 (May 1986).

In addition to the fission-product yield data, the spectral measurements provided information on amounts of heavy elements in the samples. These results provided information on the initial sample composition as well as on actinides created during the irradiation.

The experimental relative-yield fission-product data were manipulated to provide data to compare with presently existing evaluated data. The comparisons are generally favorable and the exceptions are discussed.

e. Fission-Product Yields for Fast Neutron Fission of 243,244,246,248-Cm,[1] (J. K. Dickens)

Recent measurements of relative yields for ^{95}Zr, ^{125}Sb, ^{137}Cs, ^{141}Ce, ^{144}Ce, and ^{155}Eu for fast-neutron fission of samples enriched in the actinides $^{243,244,246,248}Cm$ have been combined with a simple mass-distribution model to predict complete mass distributions for fast-neutron fission of each of these four Cm actinides. Complete descriptions of the data analysis and of the model and its application and limitations are given.

f. Yields of Fission Products Produced by Thermal-Neutron Fission of 243-Cm,[2] (J. K. Dickens and J. W. McConnell)

On the basis of measured yields for 72 gamma rays and known nuclear data, cumulative fission-product yields were deduced for 69 fission products having half-lives between 36 seconds and 65 days representing 41 mass chains created during thermal-neutron fission of ^{243}Cm.

g. Measurements of the Energy Dependence of Prompt Neutron Emission from 233-U, 235-U, and 239-Pu for E_n = 0.0005 to 10 MeV Relative to Emission from Spontaneous Fission of 252-Cf,[3] (R. Gwin, R. R. Spencer, and R. W. Ingle)

h. High Resolution Measurement of the 238-U Neutron Capture Yield for Incident Neutron Energies Between 1 and 100 keV,[4] (Roger Macklin, R. B. Perez, G. de Saussure, R. W. Ingle)

The capture cross section of ^{238}U in the energy range up to 100 keV is one of the important nuclear parameters in reactor design. Nevertheless, the uncertainties in this parameter are still above reactor design requirements. These uncertainties, which were discussed at the Antwerp Conference on Nuclear Data (September 1982), led to the formation of the U-238 Task Force of the Nuclear Energy Agency Nuclear Data Committee

---

[1]Accepted for publication in Nuclear Science and Engineering.
[2]Phys. Rev. C 34(2), 722 (August 1986).
[3]Nucl. Sci. Eng. 94, 365 (1986).
[4]1987 ANS Summer Meeting, Dallas, Texas, June 7-11, 1987; Transactions of the American Nuclear Society.

(NEANDC). Among the most relevant conclusions arrived at by the NEANDC task force were that since most of the capture cross-section measurements were old and disagreed among themselves by more than expected from their respective error assignment, a new high resolution measurement was needed, and that the resolved resonance energy region should be extended above its present 4 keV limit.

In response to these requests a measurement of the ^{238}U capture yield was performed at the 150-meter flight-path section of the Oak Ridge Linear Electron Accelerator (ORELA) facility.

i. Resolved Resonance Parameters for 238-U from 1 to 10 keV,[1] (D. K. Olsen)

j. Parameters of the 1.056-eV Resonance in 240-Pu and the 2200-m/s Neutron Total Cross Sections of 235-U, 239-Pu, and 240-Pu,[2] (R. R. Spencer, J. A. Harvey, N. W. Hill, and L. W. Weston)

The Bayesian Method was applied to the simultaneous fitting of neutron transmission measurements on five thin and two thick samples of 240-Pu in order to obtain the parameters of the very large resonance near 1 eV. The results of the analysis are: $E_0 = 1.0564 \pm 0.0006$ eV, $\Gamma_\gamma = 30.3 \pm 0.3$ meV, and $\Gamma_n = 2.45 \pm 0.02$ meV. Some evidence in the data of a small deviation from the usual "weak binding" model for Doppler broadening of the theoretical resonance shape is presented. Transmission measurements on samples of 235-U, 239-Pu, and 240-Pu also were made over the thermal energy region and their neutron total cross sections were derived. Fits of the form $A/\sqrt{E} + B$ to the cross-section data in the interval 0.02 - 0.03 eV resulted in the values 690 ± 5, 1025 ± 6, and 284 ± 2 barns for the 2200 m/s total cross sections of 235-U, 239-Pu, and 240-Pu, respectively.

3. Experimental Techniques

a. Calculated Fraction of an Incident Current Pulse That Will be Accelerated by an Electron Linear Accelerator and Comparisons with Experimental Data,[3] (R. G. Alsmiller Jr., F. S. Alsmiller, and T. A. Lewis)

In a series of previous papers, calculated results obtained using a one-dimensional ballistic model were presented to aid in the design of a prebuncher for the Oak Ridge Electron Linear Accelerator. As part of this work, a model was developed to provide limits on the fraction of an incident current pulse that would be accelerated by the existing accelerator. In this paper experimental data on this fraction are presented and the

---

[1]Nucl. Sci. Eng. **94**, 102 (1986).
[2]Submitted to Nuclear Science and Engineering.
[3]ORNL/TM-10010 (May 1986). Also submitted to Nucl. Instrum. Meth.

validity of the model developed previously is tested by comparing calculated and experimental data. Part of the experimental data is used to fix the physical parameters in the model and then good agreement between the calculated results and the rest of the experimental data is obtained.

b. Scintillation Light Transport and Detection,[1] (T. A. Gabriel and R. A. Lillie)

The MORSE neutron gamma-ray transport code has been modified to allow for the transport of scintillation light. This modified code is used to analyze the light collection characteristics of a large liquid scintillator module (18 x 18 x 350 cm^3).

B. DATA ANALYSIS

1. Theoretical

a. Parameterization of High Intense Neutron Sources and the Design of the CNR Reactor,[2] (F. C. Difilippo)

The neutron source of a scattering facility for solid-state physics studies can be visualized as a two-region system. At the center there is a core where fast neutrons are produced via spallations or fission reactions, the core is surrounded by a moderator-reflector where extraction tubes are located. The requirement of unprecedented high-thermal neutron fluxes ($\approx 10^{16}/cm^2 sec$) makes necessary a careful analysis of the neutronic efficiency of the facility in order to minimize the power dissipated in the core. This paper presents a general theory that relates the efficiency to a few parameters which has direct application to the design of the neutron source for the Center for Neutron Research (CNR) a major facility proposed to be built at the Oak Ridge National Laboratory.

b. Validation of the TNG Code with Double Differential (n,xn) Data at 14 and 26 MeV,[3] (C. Y. Fu)

A simplified method for approximating precompound nuclear reaction effects in the TNG Hauser-Feshbach code for the calculation of double differential cross sections is validated. The method is developed from existing quantum-mechanical formulas of unified compound and precompound reaction theories. The compound part of the unified formulas is made

---

[1] ORNL/TM-10047 (August 1986). Also submitted to Nucl. Instrum. Methods.

[2] International Conference on Advances in Reactor Physics, Mathematics, and Computation, Paris, France, April 27-30, 1987.

[3] Proceedings of the Fifth Coordination Meeting of Participants in the Office of Basic Energy Sciences Program to Meet High Priority Nuclear Data Needs of the Office of Fusion Energy, Argonne, Illinois, September 17-19, 1986, Ohio Univ. Report DOE/ER/02490-4 (1986).

identical to the Hauser-Feshbach formula by applying the unified level density formulas derived previously for the two theories. The precompound part, much more complicated than the compound part, is simplified and globally parameterized for practical purposes. Double differential (n,xn) cross sections at 14 and 26 MeV for iron, niobium, and bismuth calculated with global parameters are shown to be in good agreement with the available experimental data. In use at ORNL and JAERI, the TNG code has been applied with ease and success to the evaluation of double differential (n,xn) cross sections from 1 to 20 MeV for the dominant isotopes of chromium, manganese, iron, and nickel.

c. <u>Calculations of Double Differential 184-W (n,xn) Cross Sections at 25.76 MeV by the TNG Code</u>,[1] (C. Y. Fu and D. M. Hetrick)

Neutron-induced cross sectrions of W-184 at 25.7 MeV were calculated using the TNG code for participation in an international intercomparison of precompound nuclear model codes organized by the NEA data bank. Cross sections reported here include the total, elastic, nonelastic, inelastic to the 2^+ and 4^+ states, first neutron emission spectrum, total neutron emission spectrum, and angular distributions for outgoing neutron energies of 13.5, 15.5, 18.5, and 21.5 MeV. Reactions contributing to the total neutron spectrum are (n,n'), (n,2n), (n,3n), and (n,4n). Direct inelastic cross sections for the 2^+ and 4^+ states were predicted using the DWUCK code.

d. <u>Evaluation and Testing of Double Differential Fe(n,n') Cross Sections</u>,[2] (C. Y. Fu and D. M. Hetrick)

Analyses of integral experiments that include thick (>15-cm) iron regions have shown a consistent underprediction of neutron transmission. One explanation that has been offered is that the angular distributions of the inelastically scattered neutrons in the continuum in the current ENDF/B-V iron evaluation were assumed to be isotropic. In reality, these distributions are forward peaked, especially if the incident neutron energies are a few MeV greater than the continuum Q-value. The forward peaking also increases with increasing outgoing neutron energies, giving rise to correlated energy-angle distributions. To understand their effects on neutron penetration through iron, we generated such correlated distributions in a special update of the ENDF/B-V Mod-3 iron evaluation and reanalyzed an iron sphere problem with a central DT source. It is shown that the predicted neutron leakage using the revised data set is increased, particularly near 10 MeV where the increase is 80%. A reduction of the total inelastic cross section above 3 MeV, a result of better nuclear model fit to the available data, also enhances neutron leakage, especially near 5 MeV where the reduction is the largest.

---

[1]Submitted to the NEA Data Bank Report "Blind Intercomparisons for n + ^{184}W at 25.7 MeV," P. Nagel, Ed., France.
[2]Trans. Am. Nucl. Soc. <u>53</u>, 409 (1986).

e. Simplified Spin Cutoff Factors for Particle-Hole Level Densities in Precompound Nuclear Reaction Theory,[1] (C. Y. Fu)

f. 208-Pb + n Reaction and the Mean Nuclear Field Near Threshold,[2] (D. J. Horen, C. H. Johnson, J. L. Fowler, A. D. MacKellar,[3] and B. Castel[4])

Measurement of the total and differential elastic cross sections for the ^{208}Pb + n reaction are reported for the neutron energy range E = 50 - 1005 keV. The data have been analyzed in terms of partial waves using the R-matrix formalism. The results were used to deduce optical model potentials near threshold. When the real part is expressed solely in terms of an "effective" volume and surface spin-orbit components, it is found that the depth of the "effective" volume potential exhibits an LJ dependence. It is noted that because of differences in the continuum wave functions in the surface region, such an effect could arise if the actual potential contained a real surface term. Relevance to the "Fermi surface anomaly" is mentioned. The observed reduced neutron strengths are compared with predictions from three microscopic models and good agreement is found.

g. Optical Models in the Resolved Resonance Region,[5] (C. H. Johnson)

Using modern time-of-flight facilities the resolved resonance region can be extended upward to about 1 MeV for nuclei with A < 60 and for heavier nuclei near closed shells. A careful measurement both on and off resonances followed by an R-matrix analysis yields partial wave scattering functions which are easily energy averaged for comparison to those from an optical model. A comparison of average scattering functions of opposite parities can provide information on surface effects because the wave functions for different parities are out of phase at the surface. Thus, a unique supplement is made to the information that can be obtained from other types of measurements for both the bound region and higher energies.

h. Dice, Entropy and Probabilities,[6] (F. G. Perey)

It has recently been suggested that the classical Bayesian solution to the die problem where we are only given the arithmetic mean of the numbers obtained in the N first rolls of the die does not correspond to

---

[1]Nucl. Sci. Eng. 92, 440 (1986).
[2]Physical Review C, 34(2) (August 1986).
[3]University of Kentucky, Lexington, Kentucky 40506.
[4]Queen's University, Kingston, Ontario, Canada K7L 3N6.
[5]Proceedings of Specialists Meeting on the Use of the Optical Model for the Calculation of Cross Sections Below 20 MeV, Paris, November 1985, NEANDC 222"U", Paris, 1986.
[6]Submitted to Foundations of Physics.

the Maximum Entropy solution. We show that the solution to this problem in Laplace's theory of probabilities does converge to the Maximum Entropy solution when N becomes large. This solution is based upon controversial Laws of the classical theory of probabilities. We show that every step in the derivation of this solution in the classical theory of probabilities admits a group-theoretical interpretation related to certain groups of transformations. These groups of transformations can be viewed as generating the various possibilities that arise due to the apparent symmetries in the problem. The probabilities assigned in the classical theory of probabilities are the invariant additive measures in the manifolds of these groups of transformations.

i. Recent Improvements of the TNG Statistical Model Code,[1] (K. Shibata and C. Y. Fu)

The applicability of the nuclear model code TNG to cross-section evaluations has been extended. The new TNG is capable of using variable bins for outgoing particle energies. Moreover, three additional quantities can now be calculated: capture gamma-ray spectrum, the precompound mode of the (n,γ) reaction, and fission cross section. In this report, the new features of the code are described together with some sample calculations and a brief explanation of the input data.

2. ENDF/B Related Work

a. Current Status of Decay Heat Measurements, Evaluations, and Needs,[2] (J. K. Dickens)

Over a decade ago serious concern over possible consequences of a loss-of-coolant accident in a commercial light-water reactor prompted support of several experiments designed specifically to measure the latent energy of beta-ray and gamma-ray emanations from fission products for thermal reactors. This latent energy was termed Decay Heat. At about the same time the American Nuclear Society convened a working group to develop a standard for use in computing decay heat in real reactor environs primarily for regulatory requirements. This working group combined the new experimental results and best evaluated data into a standard which was approved by the ANS and by the ANSI. The primary work since then has been (a) on improvements to computational efforts and (b) experimental measurements for fast reactors. In addition, the need for decay-heat data has been extended well beyond the time regime of a loss-of-coolant accident; new concerns involve, for example, away-from-reactor shipments and storage. The efficacy of the ANS standard

---

[1]ORNL/TM-10093 (August 1986).
[2]ORNL/TM-10094 (July 1986). Also will be published in the Proceedings of the National Topical Conference on Reactor Physics and Safety, Saratoga, New York, September 17-19, 1986.

for these longer time regimes has been a subject of study with generally positive results. However, a specific problem, namely, the consequences of fission-product neutron capture, remains contentious. Satisfactory resolution of this problem merits a high priority.

b. Update of ENDF/B-V MOD-3 Iron: Neutron-Producing Reaction Cross Sections and Energy-Angle Correlations,[1] (C. Y. Fu and D. M. Hetrick)

An update of the ENDF/B-V Mod-3 evaluation for natural iron is described. The cross sections of (n,n') and (n,2n) reactions are revised. Energy-angle correlations in the secondary (n,n') neutrons are introduced in the ENDF/B-V formats. Anisotropic angular distributions are provided for the secondary neutrons in (n,2n), (n,np) and (n,nα) reactions. Relevant integral results, microscopic data, and nuclear model calculations that influence the revised results are summarized.

c. Group Structure and Weighting Function Effects on Neutron Penetration Through Thick Sodium-Iron Shields,[2] (C. Y. Fu and D. T. Ingersoll)

The effects of group structures and weighting functions on neutron penetration through a thick Na-Fe geometry are studied. The recommended broad-group (61-neutron/23-gamma-ray) and few-group (22-neutron/10-gamma-ray) structures are tailored to the sodium and iron resonances, windows, and capture gamma-ray spectra. The best weighting functions are shown to be fine-group fluxes selected from a few key locations in the geometry. These group structures and weighting functions, relative to existing group structures and conventional weighting functions, improve the accuracy of the computed 61-neutron-group Bonner ball responses by up to 100% and of the computed 22-neutron-group results by up to 600%.

d. Calculation and Evaluation of 58,60-Ni for ENDF/B-VI,[3] (D. M. Hetrick)

It has been shown that deficiencies exist in the neutron emission spectra from contributing reactions for nickel in the present Evaluated Nuclear Data File (ENDF/B-V). Gamma rays produced in the (n,p) and (n,2n) reactions are significant for $E_\gamma < 0.5$ MeV, a gamma-ray energy region not represented in ENDF/B-V since measured data solely influenced the

---

[1] ORNL/TM-9964 (ENDF-341) (July 1986).

[2] To be published in Proceedings of ANS Topical Conference on Theory and Practices in Radiation Protection and Shielding, Knoxville, Tenn., April 22-24, 1987.

[3] Proceedings of Fifth Coordination Meeting of Participants in the Office of Basic Energy Sciences Program to Meet High-Priority Nuclear Data Needs of the Office of Fusion Energy, Argonne, Ill., September 17-19, 1986, Ohio University Report DOE/ER/02490-4 (1986).

evaluation. Also, an isotropic angular distribution is given for the continuum (MT=91) which is not adequate for the wide incident neutron energy range between the threshold of the highest-energy discrete level and 20 MeV. Calculations for neutron-induced cross sections of ^{58,60}Ni from the Hauser-Feshbach/precompound model code TNG are compared to both measured data and ENDF/B-V. An example of representing the energy-angle correlations of inelastically scattered neutrons in the new ENDF/B-VI format will be shown.

e. Report on Task Force A - Measurement Activities,[1] (D. C. Larson)

This report presents the activities and results of Task Force A from the Fifth Coordination Meeting. The task force reviewed the following six areas of data needs for fusion: (1) fuel cycle reactions, (2) neutron multiplying and tritium breeding data, (3) neutron and gamma-ray emission data, (4) dosimetry cross sections, (5) activation cross sections, and (6) radiation damage-charged particle production cross sections. Results of the reviews are presented in the report. Three task forces were set up to (1) study the available data base for the ^{7}Li(n,n't) reaction, (2) review the high priority activation cross-section list, and (3) provide a short subset of the activation cross-section list for inclusion in the present DOENDC Data Request List.

f. Evaluating Nuclear Data Uncertainty: Progress, Pitfalls, and Prospects,[2] (R. W. Peelle)

The reasons for including variance-covariance information in evaluated nuclear data files are reviewed. Accomplishments and obstacles in meeting these needs are identified. The capability to develop and utilize evaluated cross-section covariance files has been largely demonstrated, but comprehensive files of soundly based covariance data remain to be evaluated and not all types of cross-section data have yet been included. The status of the ENDF-VI covariance formats is discussed. Priorities are suggested for further development. Most effort should be concentrated to fully develop the capability to estimate the nuclear data uncertainties in quantities calculated for a broad energy spectrum.

---

[1] Office of Basic Energy Sciences Program to Meet High Priority Nuclear Data Needs of the Office of Fusion Energy 1986 Review, Ohio University Report No. DOE/ER/02490-4 (1986).

[2] To be published in Proceedings of the IAEA Specialists' Meeting on Covariance Methods and Practices in the Field of Nuclear Data, Rome, Italy, November 17-19, 1986.

OHIO UNIVERSITY

A. MEASUREMENTS

1. Neutron Scattering from ^{6,7}Li at 8.0 and 24.0 MeV.* (L.F. Hansen,** J. Rapaport, X. Wang,*** and F.A. Barrios)

Elastic and inelastic differential cross sections for 8.0 and 24.0 MeV neutrons scattered from ^{6}Li and ^{7}Li have been measured in the angular range from 15° to 150° using the Ohio University time-of-flight facility. The targets were cylinders 2.54 cm diameter by 2.54 cm height of separated lithium isotopes (^{6}Li 94.73% and ^{7}Li 99.94%). The neutron elastic and inelastic angular distributions for ^{6}Li (Q = -2.184 MeV) and those for ^{7}Li (Q = -4.63 MeV) at 24 MeV have been analyzed in conjunction with the respective elastic and inelastic proton data (1) at 24.4 MeV and (p,n) charge exchange data (2) at 24.0 MeV. Coupled-channel calculations using the Lane formalism have been carried out.

2. The ^{6}Li(n,p)^{6}He Reaction at 120 MeV from 0° to 12.5°.† (D. Pocanic,†† K. Wang,†† C.J. Martoff,†† S.S. Hanna,†† R.C. Byrd,††† C.C. Foster,††† D.L. Friesel,††† J. Rapaport and D. Wang)

Spectra from the neutron facility (3) at IUCF for the (n,p) reaction on ^{6}Li have been obtained at 120 MeV. Cross sections have been extracted from 0° to 12.5° for transitions to the ground state and the excitation energy range up to 35 MeV. The results are compared with ^{6}Li(π^-,γ)^{6}He, ^{6}Li(p,p')^{6}Li, ^{6}Li(γ,x), ^{6}Li(e,e')^{6}Li and ^{6}Li(p,n)^{6}Be data. From the 0° cross section the $v^c_{\sigma\tau}(0)$ (the isovector part of the effective spin-flip N-N interaction) is extracted and compared with theories.

---

* Work performed under the auspices of the U.S. Department of Energy and the National Science Foundation by Lawrence Livermore National Laboratory and Ohio University, respectively.

** Present Address: Lawrence Livermore National Laboratory, Livermore, CA 94550.

*** Present Address: Institute of Atomic Energy, Beijing, China.

† Work supported by a grant from the National Science Foundation.

†† Present Address: Stanford University, Stanford, CA 94305

††† Present Address: Indiana University Cyclotron Facility, Bloomington, IN 47405

(1) F. Petrovich et al., Nucl. Phys. A383, 355 (1982).

(2) C.H. Poppe et al., Phys. Rev. C14, 438 (1976).

(3) C.J. Martoff et al., to be published.

3. Elastic and Inelastic Scattering of Neutrons from ^{10}B.* (E.T. Sadowski, H.D. Knox, D.A. Resler and R.O. Lane)

As part of the study of the higher energy-level structure of ^{11}B, cross sections for elastic and inelastic scattering of neutrons from isotopically enriched ^{10}B samples have been measured for incident neutron energies from 3.02 MeV to 6.45 MeV in 250 keV increments and from 7.02 MeV to 12.01 MeV in 500 keV increments. Inelastic angular distributions for scattering to the states in ^{10}B in parentheses have been measured from the indicated energy up to 12.01 MeV: (0.718) from 3.02 MeV; (1.74) from 3.27 MeV; (2.15) from 3.77 MeV; (3.59) from 5.52 MeV; (4.77) from 7.02 MeV. The measurements at 3.02, 3.51, 4.02 and 4.51 MeV were done at nine laboratory angles from 20° to 158° in 17.5° increments with a sample that is isotopically 95.86% ^{10}B. All other distributions measured scattering at 11 lab angles from 18° to 158° in 15° increments from a sample that is isotopically 99.49% ^{10}B. The data are corrected for air scattering, sample attenuation, minor isotope impurity and multiple scattering effects.

4. Asymmetry Measurements in $(\vec{p},n)$ Reaction of $^{12,13,14}C$ at 160 MeV.** (J. Rapaport, D. Wang, J. Carr,*** F. Petrovich,***, C. Foster,† C. Goodman,† C. Gaarde,†† J. Larsen,†† D. Horen,††† C. Goulding,‡ T. Taddeucci,‡ and E. Sugarbaker‡‡)

Analyzing powers have been measured for the $(\vec{p},n)$ reaction on carbon isotopes using 160 MeV protons from the Indiana University Cyclotron Facility. The measured Ay values for the $^{12}C(p,n)^{12}N$ (g.s.) transition agree very well with similar values obtained in the analog transition $^{12}C(p,p')^{12}C$ (15.1 MeV). Data up to $\theta_L = 50°$ were obtained for the observed Gamow-Teller transitions. Comparisons with DWIA calculations were made for these GT transitions.

---

* Work supported by the U.S. Department of Energy.

** Work supported in part by the National Science Foundation, Department of Energy and the Danish National Science Council.

*** Present Address: Florida State University, Tallahassee, FL 32306.

† Present Address: Indiana University Cyclotron Facility, Bloomington, IN 47405.

†† Present Address: The Niels Bohr Institute, Copenhagen, DENMARK.

††† Present Address: Oak Ridge National Laboratory, Oak Ridge, TN 37830.

‡ Present Address: Los Alamos National Laboratory, Los Alamos, NM 87545.

‡‡ Present Address: Ohio State University, Columbus, OH 43212.

5. Selective Sequential 2n-Decay of $^{14}C^*$ States Populated by ^{13}C+n.* (D.A. Resler, R.O. Lane and H.D. Knox)

In the double-differential time-of-flight spectrum of emerging neutrons from neutrons incident on ^{13}C, a sharp substantial peak was observed whose energy remained constant as the incident neutron energy varied over at least 1.2 MeV. The results show that this peak is almost surely the secondary neutron group in the sequential 2n-decay of levels in $^{14}C^*$ where the primary neutron decay (inelastic scattering) is to the $5/2^-$ (7.547 MeV) level in $^{13}C^*$ which then decays via a 3-MeV secondary neutron to the ground state of ^{12}C. This reaction appears to be very selective in that from 15.8 MeV to 18.4 MeV the states of $^{13}C^*$ do have substantial overlap with $^{13}C^*$ ($5/2^-$, 7.547 MeV) coupled to a neutron, whereas from 8 MeV to 18.4 MeV they appear to have small or negligible overlap with the positive parity states of $^{13}C^*$ in this region.

6. Elastic and Inelastic Scattering of Nucleons from ^{16}O.** (M.S. Islam,*** R.W. Finlay and J.S. Petler†)

Measurements of differential elastic and inelastic cross sections for neutron scattering from ^{16}O at incident energies 18 to 26 MeV have been carried out. In addition to cross sections for neutron scattering, differential cross sections for proton scattering up to 66 MeV were described in terms of phenomenological optical model potentials. At 24.5 MeV incident energy inelastic scattering up to 11.5 MeV excitation were measured. The elastic and inelastic compound nucleus contributions were examined. Direct inelastic scattering from the normal parity states was calculated using the DWBA and coupled-channel formalisms. The inelastic scattering cross section from non-normal parity parity state 2^- was calculated using the coupled-channel formalism via multi-step processes. Cross sections due to inelastic scattering from some of the states, which are thought to be members of an excited state rotational band were calculated using both vibrational and rotational approaches and were compared.

---

* Work supported by the U.S. Department of Energy.

** This investigation was supported by PHS Grant Number CA-25193 awarded by the National Cancer Institute, DHHS.

*** Present Address: Physics Department, Ohio State University, Columbus, OH 43212.

† Present Address: British Petroleum Research Center, Sunbury-on-Thames, Middlesex, UK.

7. Proton Transfer to States in ^{24}Mg and ^{33}Cl via (d,n) Reaction.* (P.M. Egun, C.E. Brient, S.M. Grimes, J. Rapaport, S.K. Saraf and H. Satyanarayana**)

Angular distributions have been measured for neutron groups leading to states in ^{24}Mg up to an excitation energy of 9.0 MeV using ^{23}Na(d,n)^{24}Mg reaction at 8.0 MeV deuteron energy. The angular distributions for the ^{32}S(d,n)^{33}Cl reaction were measured at incident deuteron energies of 8.0, 8.3 and 8.6 MeV for states up to 4.0 MeV excitation energy in ^{33}Cl. The results of these measurements on both nuclei have been compared to DWBA and statistical model calculations. Analysis of stripping to unbound states in ^{33}Cl has also been studied.

8. The ^{26}Mg(p,n)^{26}Al and ^{23}Na(α,n)^{26}Al Reactions Near Threshold.*** (G. Doukellis† and J. Rapaport)

Cross sections and angular distributions for the ^{26}Mg(p,n)^{26}Al and ^{23}Na(α,n)^{26}Al reactions, populating the ground state and the first three excited states in ^{26}Al, have been measured between 5.3 and 7.0 MeV proton bombarding energy and between 3.9 and 5.9 MeV alpha bombarding energy, using the neutron time-of-flight technique. The measured total cross sections were used to derive the cross sections for the astrophysical interesting reactions ^{26}Al(n,p_0)^{26}Mg and ^{26}Al(n,α_0)^{23}Na. The ^{26}Mg(p,p')^{26}Mg and ^{26}Mg(p,α)^{23}Na cross sections were also measured at E_p = 5.3-6.1 MeV. A resonance analysis of the measured ^{26}Mg+p excitation functions was used to obtain information on cross sections for the ^{26}Al(n,p')^{26}Mg reaction.

9. Neutron Scattering and Neutron Emission Cross Sections on ^{27}Al, ^{93}Nb and ^{209}Bi at 7 MeV.*** (X. Wang,†† Y. Wang, D. Wang and J. Rapaport)

Elastic and inelastic neutron scattering and neutron emission at 7 MeV incident energy have been studied for monoisotopic samples of ^{27}Al, ^{93}Nb and ^{209}Bi. Time-of-flight spectra were taken at nine angles between 30 and 140 degrees using the beam-swinger spectrometer. The efficiency of the neutron detectors was maximized using a dynamic bias; low background was obtained throughout the neutron energy detected which correspond to about 6 MeV excitation energy. The data were converted to energy spectra

---

* Work supported by the U.S. Department of Energy.

** Present Address: School of Medicine, University of California, Irvine, CA 92717

*** Work supported in part by the National Science Foundation.

† Present Address: N.R.C. Democritos, Tandem Laboratory, Agia Paraskevi, Attikis, GREECE.

†† Present Address: Institute of Atomic Energy, Beijing, CHINA.

and corrected for sample attenuation, finite geometry and multiple scattering. For unresolved states the data were averaged over 0.5 MeV energy bins. Calculations for elastic and inelastic transitions and for compound and precompound processes have been carried out.

10. Neutron Elastic and Inelastic Scattering from ^{28}Si, ^{32}S and ^{34}S.* (R. Alarcon** and J. Rapaport)

Differential cross sections for the elastic and inelastic scattering of neutrons from the sd-shell nuclei ^{28}Si, ^{32}S and ^{34}S have been measured in the 20-26 MeV region. The data are analyzed in terms of the rotation-vibration (^{28}Si) and anharmonic vibration (^{32,34}S) collective models. Isoscalar E2, E3 and E4 transition matrix elements are obtained from the normalized multipole moments of the real potential and the results are compared with those obtained from electromagnetic probes and from nuclear structure theoretical calculations.

11. Measurement of B(GT/B(F) for the Anomalous ^{35}Ar β^+ Decay via the (p,n) Reaction.*** (A.J. Wagner,† E. Sugarbaker,† D. Krofcheck,† L.J. Rybarcyk,† C.D. Goodman,†† R. Byrd,†† W. Huang,†† T.N. Taddeucci,††† T. Carey,††† J. McClelland,††† J. Rapaport, D. Horen,‡ H. Sakai,‡‡ and D. Cisnowski‡‡‡)

Since the anomalously high vector coupling constant extracted from the mixed Fermi and Gamow-Teller β decay of the ground state of ^{35}Ar is consistent with a vanishing Cabibbo angle, there is considerable interest in resolving the source of the anomaly. The most suspect input to this result is thought to be the ratio of F to GT contributions, which has previously been extracted from β-decay asymmetry data on polarized ^{35}Ar nuclei. We have measured the transverse spin-flip probability S_{NN} in

---

* Work supported in part by a grant from the National Science Foundation.

** Present Address: University of Illinois at Champaign, Nuclear Physics Laboratory, Champaign, IL 61820.

*** Work supported in part by the National Science Foundation and the U.S. Department of Energy.

† Present Address: Ohio State University, Columbus, OH 43212.

†† Present Address: Indiana University Cyclotron Facility, Bloomington, IN 47405.

††† Present Address: Los Alamos National Laboratory, Los Alamos, NM 87545.

‡ Present Address: Oak Ridge National Laboratory, Oak Ridge, TN 37830.

‡‡ Present Address: Osaka University, Osaka, JAPAN.

‡‡‡ Present Address: University of Texas, Austin, TX 78712.

the $^{35}Cl(p,n)^{35}Ar$ (gs) reaction at 160 MeV, which can also be used to extract the F to GT ratio in such mixed transitions (1).

12. Neutron Inelastic Scattering from ^{40}Ca at 21.7 and 25.5 MeV.*
(R. Alarcon** and J. Rapaport)

Differential cross sections for the scattering of neutrons from ^{40}Ca for states up to 5 MeV excitation energy have been measured at 21.7 and 25.5 MeV. The analysis is done using a coupled channel formalism in terms of a vibration collective model. The results using a usual standard Woods-Saxon form factor for the transitions are compared with those obtained using form factors derived from a model independent analysis to the elastic cross sections.

13. Nucleon Elastic Scattering from ^{40}Ca Between 11 and 48 MeV.*
(R. Alarcon**, J. Rapaport and R.W. Finlay)

Differential cross sections for the elastic scattering of neutrons from ^{40}Ca have been measured in the 19-26 MeV region. The neutron elastic scattering data, previous neutron measurements and additional proton elastic scattering data are analyzed using three different approaches to the optical model potential: Woods-Saxon parameterization, model independent analysis and microscopic calculations. The difference between the phenomenological neutron and proton real potentials is studied in terms of Coulomb effects, nuclear polarization and charge symmetry breaking in the nuclear mean field.

14. Neutron Inelastic Scattering from $^{54,56}Fe$.*** (S. Mellema,† R.W. Finlay and F.S. Dietrich††)

Differential cross sections for inelastic scattering of neutrons to numerous levels in $^{54,56}Fe$ have been measured at incident neutron energies of 11 and 26 MeV. The data have been analyzed in terms of a collective model using a distorted-wave Born approximation as well as a full coupled-channels treatment. Analysis has also been performed with a microscopic folding model using an energy- and density-dependent effective interaction.

---

* Work supported by the National Science Foundation.

** Present Address: University of Illinois at Champaign, Nuclear Physics Laboratory, Champaign, IL 61820.

*** Work performed under the auspices of the National Science Foundation and the U.S. Department of Energy by Ohio University and Lawrence Livermore National Laboratory, respectively.

† Present Address: Gustavus-Adolphus College, St. Peter, MN 56082.

†† Present Address: Lawrence Livermore National Laboratory, Livermore, CA 94550.

(1) C.D. Goodman *et al.*, Phys. Rev. Lett. 54, 877 (1985).

Both collective and microscopic analyses have also been applied to inelastic proton scattering in the same energy region in order to extract information on the isospin nature of the measured excitations.

15. Charged-Particle Emission in Reactions of 9- and 11-MeV Neutrons with ^{63,65}Cu.* (Munir Ahmad,** C.E. Brient, P.M. Egun, S.M. Grimes, S. Saraf and H. Satyanarayana***)

Cross sections for the emission of protons, deuterons, and alpha particles from enriched targets of ^{63}Cu and ^{65}Cu bombarded with 9- and 11-MeV neutrons were measured. A charged-particle time-of-flight spectrometer capable of detecting particles with energies as low as 1 MeV was used to make these measurements. Cross sections and spectra are compared with statistical and pre-equilibrium model calculations. Level density parameters of various nuclei resulting from the best simultaneous fit to present and previous 15-MeV data are inferred.

16. Measurement of the Gamow-Teller Strength Distribution in ^{81}Kr.† (D. Krofcheck,†† E. Sugarbaker,†† A. Wagner,†† J. Rapaport, D. Wang, J.N. Bahcall,††† R.C. Byrd,‡ C.C. Foster,‡ C.D. Goodman,‡ I.J. Heerden,‡ W. Huang,‡ C. Gaarde,‡‡ J.S. Larsen,‡‡ D. Horen,‡‡‡ T. Carey,*† T.N. Taddeucci*†)

The predicted capture rate of a ^{81}Br solar neutrino detector requires knowledge of GT transition strengths to final states in ^{81}Kr. These strengths can be obtained from 0° (p,n) differential cross sections at intermediate energies (1). Neutron TOF measurements on the ^{81}Br(p,n)^{81}Kr reaction at E_p = 120 MeV and E_p = 200 MeV were performed at IUCF. $d\sigma/d\Omega$

---

* Work supported by the U.S. Department of Energy.

** Present Address: TRIUMF, Vancouver, British Columbia.

*** Present Address: School of Medicine, University of California, Irvine, CA 92717

† Work supported in part by the National Science Foundation, the U.S. Department of Energy and the Danish Natural Science Research Council.

†† Present Address: Ohio State University, Columbus, OH 43212.

††† Present Address: Institute for Advanced Studies, Princeton, NJ 08540.

‡ Present Address: Indiana University Cyclotron Facility, Bloomington, IN 47405.

‡‡ Present Address: The Niels Bohr Institute, Copenhagen, DENMARK.

‡‡‡ Present Address: Oak Ridge National Laboratory, Oak Ridge, TN 37830.

*† Present Address: Los Alamos National Laboratory, Los Alamos, NM 87545.

(1) C.D. Goodman et al., Phys. Rev. Lett. 44, 1755 (1980).

data at laboratory angles of 0.2°, 5.2° and 9.8° and implications for solar neutrino detection have been studied.

17. Hadronic Excitation of the Second 0^+ State in ^{90}Zr.* (J.P. Delaroche,** Y. Wang and J. Rapaport)

Coupled-channel analyses of new (n,n') and existing (p,p') as well as (α,α') scattering measurements for the second 0^+ state (1.761 MeV) in ^{90}Zr have been carried out. Macroscopic form factors are assumed for the E0 and E2 transitions. Multistep E2 transitions are found to dominate the direct inelastic excitations. Compound (n,n') and (p,p') scattering processes are also found to be important at incident energies up to 16 MeV. A rather good description of shapes and magnitudes of the differential cross sections is achieved.

B. MODEL CALCULATIONS AND ANALYSES

1. Cross Sections for Two-Body Sequential Decay Reactions.*** (M.D. Baker,† H.D. Knox and E. Breitenberger)

A general procedure has been developed for calculating the double differential cross section for a two-body sequential decay reaction, given the angular distributions for the initial and decay reactions. The kinematics, reference frame transformations and the Jacobians required for transforming the cross sections are developed for the general two-body sequential decay reaction.

2. The Optical Model Potential for Low-Energy Nucleons.†† (Y. Wang and J. Rapaport)

It is proposed that in the description of the empirical optical model potential to be used in global analysis a term equal to the empirical value of the average Fermi energy be included. This additional term explains the anomalous behavior of the real well depth when plotted as a function of (N-Z)/A reported by Perey in the analysis of 11 MeV proton scattering.

---

* Work supported in part by grants from the National Science Foundation and from the National Cancer Institute, Department of Health and Human Services.

** Permanent Address: Service de Physique et Techniques Nucleaires, Centre d'Etudes de Bruyères-le-Châtel, Bôite Postale No. 12, 91680 Bruyères-le-Châtel, FRANCE.

*** Work supported in part by the U.S. Department of Energy.

† Present Address: Massachusetts Institute of Technology, Cambridge, MA 02139.

†† Work supported in part by the National Science Foundation.

3. Reactions Leading to the ^{7}Li and ^{8}Li Systems: Shell Model and R-Matrix Calculations.* (H.D. Knox, D.A. Resler and R.O. Lane)

Level energies and reduced width amplitudes obtained from shell model calculations for ^{7}Li and ^{8}Li are incorporated into multilevel, multichannel R-matrix calculations of cross sections for reactions leading to these compound systems. With changes to a very few of the large number of parameters obtained from the model calculations, cross sections for eight reactions leading to the ^{7}Li system and for five reactions leading to the ^{8}Li system are calculated. For reactions where data are available, the calculated cross sections are in good agreement with experimental measurements. Comparisons of the present work to other structure studies have been carried out and possible improvements in the model calculations have been investigated.

4. Giant Resonance Coupling and ℓ-Dependent Potentials for ^{16}O.** (J.P. Delaroche,*** M.S. Islam† and R.W. Finlay)

The effects of giant resonance couplings on the elastic scattering of nucleons from light, spherical nuclei are examined over a wide range of incident energies (18-46 MeV). General trends in the large-angle elastic scattering data for ^{16}O that are poorly described with the conventional optical model are qualitatively reproduced with an uncomplicated picture for the giant states. Comparison is made between this approach and earlier calculations involving giant resonances and ℓ-dependent potentials.

5. Expansion Methods for Level Density Parameters.* (H. Satyanarayana,†† S.M. Grimes, D.A. Resler and B.A. Strohmaier†††)

Level density calculations using moment methods have usually been based on Hermite polynomial expansions. They have the significant drawback that they are not positive definite. We have obtained results for positive definite expansion utilizing moments up to the sixth and have made comparisons for ^{24}Mg. Calculations have been compared with data for isotopes of Mg, Al and Si.

---

* Work supported by the U.S. Department of Energy.

** Work supported by the National Cancer Institute, DHHS.

*** Permanent Address: Service de Physique et Techniques Nucleaires, Centre d'Etudes de Bruyères-le-Châtel, Bôite Postale No. 12, 91680 Bruyères-le-Châtel, FRANCE.

† Present Address: Ohio State University, Columbus, OH 43212.

†† Present Address: School of Medicine, University of California, Irvine, CA 92717.

††† Permanent Address: Institut für Radiumforschung und Kernphysik, Vienna, AUSTRIA.

C. INSTRUMENTS AND METHODS

1. Charged Particle Telescope System to Measure (n,z) Reactions with $7 < E_n < 30$ MeV.* (D. Wang and J. Rapaport)

A system consisting of four telescope detector array has been designed to measure neutron induced charged particle spectra. The detectors are mounted in a specially designed scattering chamber that may be rotated between $\theta_L = 0°$ and $90°$. The ΔE detectors are 0.015" thick plastic scintillators; the E detectors are ¼" thick NaI(Tl) scintillators with particle pulse shape discrimination properties. We have used this system to measure (n,p) and (n,d) cross sections on ^6Li and ^{54}Fe at $E_n = 26$ MeV.

2. Efficiency Calibration of Large Volume Liquid Scintillation Detectors.** (S. Mellema*** and J. Petler†)

An array of seven large (10 cm thick by 20 cm diameter) NE213 scintillation detectors for use in neutron time-of-flight experiments has been calibrated to determine a matrix of relative detection efficiency as a function of incident neutron energy and detector bias. This matrix is then used to determine the relative efficiency for neutron groups in time-of-flight spectra to which an efficiency-optimizing dynamic bias has been applied.

---

* Work supported in part by the National Science Foundation.

** Work supported by the National Science Foundation and the National Cancer Institute, DHHS.

*** Present Address: Gustavus-Adolphus College, St. Peter, MN 56082.

† Present Address: British Petroleum Research Centre, Sunbury-on-Thames, Middlesex, UK.

PACIFIC NORTHWEST LABORATORY

A. DELAYED NEUTRON HALF-LIVES AND EMISSION PROBABILITIES (P. L. Reeder, R. A. Warner, and R. L. Gill*)

The TRISTAN on-line mass separator facility at Brookhaven National Laboratory has been used to measure half-lives and delayed neutron emission probabilities (P_n) of fission-product delayed-neutron precursors. Because delayed neutron emission can be detected with high sensitivity in the presence of large intensities of beta and gamma radiations, we also used neutron counting to search for new isotopes among the very neutron-rich fission products.

Mass separated beams of fission products from TRISTAN were deposited on an aluminized Mylar tape in the center of a high efficiency neutron counter. Beta particles at the deposition point were counted with a totally depleted surface barrier Si detector. The experiments consisted of simultaneous multiscaler measurements of growth and decay curves for the beta counting rate, neutron counting rate, beta-neutron coincidence rate, and accidental coincidence rate.

With an improved High Temperature Plasma ion source, we have recently observed delayed neutron activity at mass 76 and have assigned it to a new precursor ^{76}Cu. From the neutron growth and decay curve, the half-life was determined to be 0.61 ± 0.10 s. The beta activity from longer lived ^{76}Zn and ^{76}Ga was too intense to allow determination of the half-life from the beta decay curve. By use of the half-life from the neutron decay, we obtained a rough estimate of the beta activity of the new activity and an approximate P_n of 3 ± 2%. The half-life is intermediate between two theoretical estimates[1,2] for ^{76}Cu as is the situation for other neutron-rich Cu isotopes.[3] The P_n is within a factor of two of the value we calculated using the Kratz-Herrmann formula.[4,5]

---

*Brookhaven National Laboratory, Upton NY 11973

1 Takahashi, Yamada, and Kondoh, At. Data Nucl. Data Tables 12, 101(1973).

2 Klapdor, Metzinger, and Oda, At. Data Nucl, Data Tables 31, 81(1984).

3 Reeder, Warner, Liebsch, Gill, and Pitrowski, Phys. Rev. C 31, 1029(1985).

4 P. L. Reeder and R. A. Warner, Nucl. Sci. Eng. 87, 181(1984).

5 K. L. Kratz and G. Herrmann, Z. Physik 263, 435(1973).

Both ^{98}Rb and ^{100}Rb are known to be beta-delayed two-neutron precursors. We have previously measured the P_{2n} for ^{98}Rb to be (0.060 ± 0.009%).[6] For ^{100}Rb, the ratio of P_{2n}/P_n was measured by a group working at ISOLDE[7] to be 0.027 ± 0.007, but because the P_n was not known, they could not report the value of P_{2n}. We have now measured the P_n of ^{100}Rb to be (5.0 ± 1.0%). Combining the ratio from ISOLDE with the P_n measured here gives the P_{2n} of (0.14 ± 0.04%) for ^{100}Rb. The experimental P_{2n} is almost a factor of 10 lower than a theoretical calculation.[8] Ground state deformation in the vicinity of mass 100 was ignored in the calculation which may account for the large discrepancy.

We have previously noted[9,10] that P_n values for deformed nuclides in the vicinity of mass 100 are unusually low compared to predictions of the Kratz-Herrmann formula.[5] Deformation parameters from the Moeller-Nix mass formula[11] are not sufficiently correlated with experimental deformations (as defined by the energy of the first excited 2^+ state in the daughter nuclide) to be useful in estimating unknown P_n values.[12] A plot of the ratio of the experimental to calculated P_n versus the excitation energy of the first excited 2^+ state in the daughter nuclide does show a significant correlation. The reduction in P_n values for deformed nuclides is probably due to increased level density below the neutron binding energy in the daughter nuclide thus resulting in a larger fraction of beta decay to non neutron-emitting levels.

---

6 Reeder, Warner, Yeh, Chrien, Gill, Shmid, Liou, and Stelts, Phys. Rev. Lett. 47, 483(1981).

7 Jonson, Gustafsson, Hansen, Hoff, Larsson, Mattsson, Nyman, Ravn, and Schardt, Proceedings of the IVth Int. Conf. Nuclei Far from Stability, Helsingor, June 7-13, 1981, CERN, Geneva, 1981. CERN 81-09.

8 Lyutostanskii, Panov, and Sirotkin, Sov. J. Nucl. Phys. 37, 163(1983).

9 R. A. Warner and P. L. Reeder, Int. Conf. Nuclear Data for Basic and Applied Science, Santa Fe, NM, May 13-17, 1985. PNL-SA-12858.

10 Reeder, Warner, Edmiston, Gill, and Piotrowski, Symposium on Recent Advances in the Study of Nuclei Off the Line of Stability, Am. Chem. Soc. National Meeting, Chicago, IL, September 8-13, 1985. PNL-SA-13117.

11 P. Moeller and J. R. Nix, At. Data Nucl. Data Tables, 26, 165(1981).

12 Reeder, Warner, Gill, and Piotrowski, Specialists Meeting on Delayed Neutrons, Birmingham, England, September 15-19, 1986. PNL-SA-14026.

B. DELAYED NEUTRON ENERGY SPECTRA (Atwater,** Goulding,** Moss,** Pederson,** Reeder, Robba,** Warner, and Wimett**)

Energy spectra of delayed neutrons from separated precursors are being measured at TRISTAN with a NE213 liquid scintillator spectrometer. The goal of these experiments is to obtain neutron spectra from 1 MeV up to the maximum energy allowed by the energy window. These data are being compared to predictions of nuclear model calculations performed at Los Alamos. Data up to 4 MeV have been obtained on $^{96,97,98}Rb$ although the energy windows are 5.9, 6.5, and 6.7 MeV, respectively. Our present data indicate that the nuclear model code BETA[13] overpredicts the number of high energy neutrons. Preliminary results of this work have been reported.[14,15]

C. INDEPENDENT ISOMER YIELD RATIO FOR ^{138}Cs (Ford,** Reeder, Warner, and Wilmes***)

We have measured the isomer yield ratio for ^{138}Cs from the thermal neutron fission of ^{235}U by use of the SOLAR on-line mass spectrometer facility at Washington State University. The data are currently being analyzed. A statistical model[16] has been used to provide a calibration curve for ^{138}Cs of isomer yield ratio versus average angular momentum J value.

Due to funding constraints, the SOLAR facility has been dismantled and no further experiments in this area are anticipated.

**Los Alamos National Laboratory, Los Alamos, NM 87545

***University of Idaho, Moscow, ID 83843

13 Mann, Dunn, and Schenter, Phys. Rev. C 25, 524(1982).

14 Atwater, Goulding, Moss, Pederson, Robba, Wimett, Reeder, and Warner, Specialists' Meeting on Delayed Neutrons, Birmingham, England, September 15-19, 1986. LA-UR-86-3114.

15 Goulding, Robba, Atwater, Moss, Pederson, Wimett, Reeder, Warner, Meeting of American Physical Society, Division of Nuclear Physics, Vancouver, B.C., October 9-11, 1986.

16 Ford, Wolfsberg, and Erdal, Phys. Rev. C 32, 1327(1984).

UNIVERSITY OF PENNSYLVANIA

A. NUCLEAR DATA COMPILATIONS (F. Ajzenberg-Selove, G. C. Marshall)

1. "Energy Levels of Light Nuclei - A = 13-15" by F. Ajzenberg-Selove has been published in Nuclear Physics A449 (1986) pp. 1-186.

2. "Energy Levels of Light Nuclei - A = 16-17" by F. Ajzenberg-Selove has been published in Nuclear Physics A460 (1986) pp. 1-148.

3. "Energy Levels of Light Nuclei - A = 18" was sent out as a preprint (PPP 3-86) in August 1986.

4. "Energy Levels of Light Nuclei - A = 19" was sent out as a preprint (PPP 5-86) in November 1986.

5. "Energy Levels of Light Nuclei - A = 20" was sent out as a preprint (PPP 1-87) in February 1987.

This work is proceeding on the exact schedule which we projected some years ago and which was approved by the Panel on Basic Nuclear Data Compilations, Numerical Data Advisory Board, National Research Council.

B. EXPERIMENTAL RESEARCH (F. Ajzenberg-Selove)

1. Indiana University Cyclotron Facility

We are planning to study T = 2 states in A = 16 nuclei using the $^{14}C(^{3}He, p)^{16}N$, $^{18}O(p, ^{3}He)^{16}N$ and $^{18}O(p, t)^{16}O$ reactions and the K-600 spectrometer, in collaboration with G. P. A. Berg, L. C. Bland, D. W. Miller and H. Nann of IUCF.

2. Daresbury Nuclear Structure Facility (England)

Daresbury is the only facility in the world at which intermediate energy tritons are available. Unfortunately there have been difficulties in obtaining an intense triton beam and in operating the QSD spectrometer. We have proposed to study a number of $(t, ^{3}He)$ reactions on light nuclei as well as on ^{56}Fe, ^{58}Ni, ^{124}Sn and a few selected heavy nuclides, in collaboration with J. S. Lilley of Daresbury and B. R. Fulton, O. Karban and G. C. Morrison of the University of Birmingham. We hope that this will prove to be possible during the coming year.

C. <u>TALKS</u> (F. Ajzenberg-Selove)

1. "(t, ^{3}He) Reactions and Astrophysics", February 21 (1986), Lawrence Berkeley Laboratory; April 3 (1986), Indiana University Cyclotron Facility.

2. "The Structure of the Light Nuclei", September 26, 1986, International School-Seminar on Heavy Ion Physics, Dubna, U.S.S.R. [to be published in the Proceedings]. [Sent out as preprint PPP 4-86 in September 1986.]

RENSSELAER POLYTECHNIC INSTITUTE

A. NUCLEAR DATA

1. "Measurement of the Fission Cross Section of ^{242}Cm" (B. Alam, R.C. Block, R.E. Slovacek (KAPL), R.W. Hoff (LLL)

The neutron-induced fission cross section of ^{242}Cm is of interest in understanding its nuclear properties as related to structure and fission systematics. In addition, the fission cross section of this isotope is useful in the prediction of accumulation of heavy actinides in spent fuel pins and in the optimization of the production chain of actinides, particularly ^{252}Cf. There are no resonance energy data available for ^{242}Cm except one transmission measurement.[1] The measurement of ^{242}Cm is extremely difficult because of its very high alpha decay rate and intense spontaneous fission background. The technique employed for the present measurement was to use the large neutron flux from the Rensselaer Intense Neutron Spectrometer (RINS) to obtain an adequate ratio of the neutron-induced fission signal to that due to spontaneous fission background. A special fission chamber design employing up to six pairs of hemispherical electrodes coupled with nanosec rise time electronics combine to suppress the alpha pile-up effects. The electrodes inside the chamber were coated with 1.15 μg of ^{242}Cm, 12.5 μg of 99.995 a/o ^{238}Pu, a mixture of 6.4 μg of highly enriched ^{235}U and 2.86 pg of ^{252}Cf, and 960 pg of ^{252}Cf.

The fission chamber was filled with 2 atm (absolute) of research grade methane. All four pairs of electrodes were operated at a 500-V bias. The LINAC was run for 25.8 h at a repetetive rate of 140 pps with 725 W of power on the photoneutron target to record fission data. A 19.8-h run of background data was recorded when the machine was off.

The counting data were corrected for dead time losses, spontaneous fission background and flux shape variations. The flux normalization factor was determined from the present experimentally measured ^{235}U fission data and the resolution-broadened ^{235}U ENDF/B-V data. The ^{242}Cm data so obtained are presented in Fig. A. It is observed that the 13.6 and 60.1 eV resonances are clearly resolved. The broad resolution of RINS could not individually resolve the 30.3 and 37.5 eV resonances. However, a combined peak appears around 31 eV, while the clusters of resonances can be seen near 130, 220 and 620 eV. A broad peak appears around 3000 eV which suggests intermediate structure.

The resonance parameters of low energy resonances below 100 eV have been determined and presented in Table I. The fission width Γ_f for the 30.3 and 37.5 eV resonances was assumed to be the same and this was determined from the relationship

$$A_f = \frac{\pi}{2} (\sigma_0^{30.3} + \sigma_0^{37.5}) \Gamma_f$$

where A_f is the measured area and σ_0 is the total cross section at resonance.

In summary, the RINS method once again demonstrated its capability to measure microgram quantities of highly active actinides. This is the first reported fission data for ^{242}Cm over the resonance energy range of practical interest to thermal and fast reactors.

[1] V.S. Artamonov et al., Conf. Proc. 4th All Union Conf. Neutron Physics, Kiev, 2, 257 (1977).

TABLE I: ^{242}Cm RESONANCE PARAMETERS

E_0 (eV) From Ref.(1)	Measured A_f (b-eV)	g	Γ_n (meV) From Ref.(1)	Γ_γ (meV)	Γ_f (meV)
13.62	20.8 ± 1.9	1	1.82 ± 0.05	34 ± 6 From Ref.(5)	1.42 ± 0.27
30.33 37.49	130 ± 8 (Area under ~31 eV peak)	1	3.1 ± 0.3 4.4 ± 0.3	34 34 (Assumed)	6.41 ± 1.53
60.1	52.8 ± 5.5	1	23.6 ± 4.0	34 (Assumed)	1.96 ± 0.46

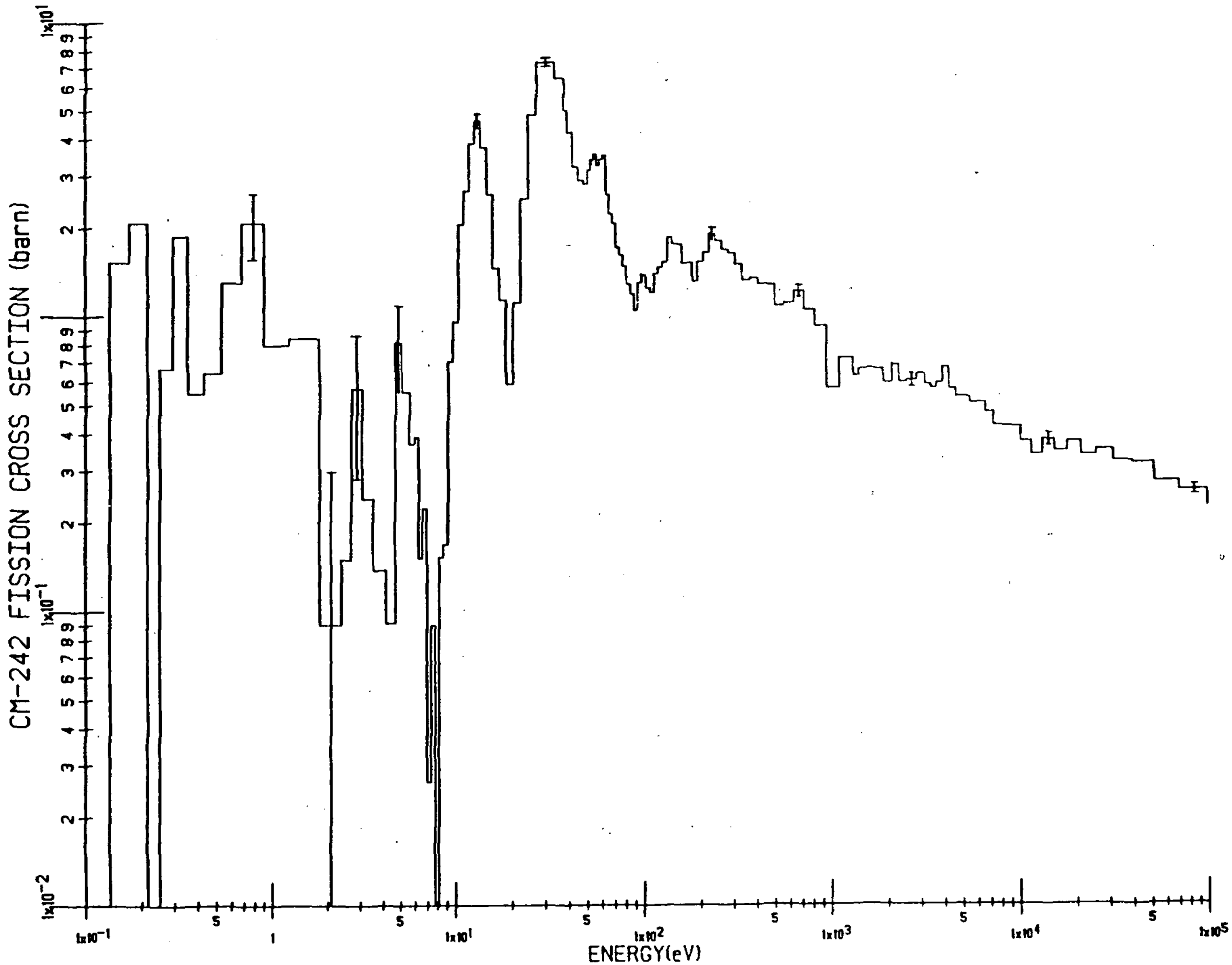

FIGURE 1. Fission cross section versus neutron energy for the ^{242}Cm isotope.

A. NEUTRON PHYSICS

1. Helium Generation Cross Sections for Fusion Applications (D. W. Kneff, B. M. Oliver, and R. P. Skowronski)

Neutron-induced helium generation is a major consideration in the development of materials for fusion reactor environments. Rockwell International is engaged in the measurement of helium production in fusion-energy neutron environments and in other neutron environments used for fusion reactor materials testing. Current emphasis is on the measurement of the cross sections of pure elements and separated isotopes for fast (~8-15 MeV) monoenergetic neutrons, and of helium production rates of pure elements irradiated in mixed-spectrum (comparable fast and thermal neutron flux) fission reactors. Most of this work is performed as a collaborative effort with L. R. Greenwood of Argonne National Laboratory (ANL), and has been sponsored by the Department of Energy's Office of Basic Energy Sciences and Office of Fusion Energy.

The helium measurement technique is based on the passive irradiation of an array of materials in the neutron spectrum of interest. The amount of helium generated in each sample is subsequently measured by isotope-dilution gas mass spectrometry, with typical measurement uncertainties of ~1-3%. The neutron fluence and spectral information are derived from a comprehensive set of ANL radiometric dosimeters, augmented by helium accumulation neutron dosimetry. For experiments using monoenergetic neutron sources, the helium measurements are combined with the neutron fluence data to derive cross sections. For broad neutron energy spectrum distributions, the spectrum-integrated helium measurements are compared directly with helium predictions made at ANL using energy spectrum unfolding techniques and ENDF/B-V cross sections. The comparisons provide an integral test of the ENDF cross sections and the helium plus radiometric measurements provide information on the contributing reaction processes.

Four new monoenergetic-neutron irradiation experiments were initiated during the present reporting period. They include one primary-volume 14.8-MeV neutron irradiation at the Rotating Target Neutron Source-II (RTNS-II) at the Lawrence Livermore National Laboratory, two add-on irradiations at RTNS-II, and a 10-MeV neutron irradiation at the Los Alamos National Laboratory (LANL). The primary-volume RTNS-II irradiation included a number of new materials (N, Mg, S, Ge, W, and W isotopes) to extend our helium production cross section data base.[1,2] It also included several other materials to

[1] Kneff, Oliver, Farrar, and Greenwood, "Helium Production in Pure Elements, Isotopes, and Alloy Steels by 14.8-MeV Neutrons," Nucl. Sci. Eng. 92, 491 (1986).

[2] Kneff, Oliver, Goldberg, and Haight, "Helium Production Cross Sections for 15-MeV Neutrons on ^{6}Li and ^{7}Li," Nucl. Sci. Eng. 94, 136 (1986).

improve previous measurement uncertainties (e.g., O, F, Ta), and to provide cross section information for a range of neutron energies in the 14-MeV neutron energy region (e.g., Be, C, N, O). The RTNS-II add-on experiments will provide additional energy-dependent cross section information.

The 10-MeV neutron irradiation is a joint experiment with R. C. Haight of LANL. The neutrons were generated by the $^{1}H(t,n)$ reaction, using 16.2-MeV tritons incident upon a rotating hydrogen gas target developed by Haight. Irradiated materials included 11 pure elements and the 9 separated isotopes of Fe and Ni. Neutron dosimetry is based on an array of radiometric foils counted at ANL.

Joint Rockwell-ANL work on mixed-spectrum reactor-irradiated materials is continuing with the further analysis of reactions producing enhanced helium production at high thermal neutron fluences. The ^{58}Ni two-step reaction[3] is well-known and has become an important tool for simulating fusion-neutron helium production in fission reactor environments. We recently reported on a ^{63}Cu three-step reaction process that has potential application to radiation effects simulations in copper alloys.[4] Our recent measurements for iron demonstrate a small helium enhancement with increasing thermal neutron fluence, indicating an ^{54}Fe two-step process. We are now using a combination of radiometric and helium production measurements to determine the contributing and competing reaction cross sections for iron. The goal is to provide a technique for simulating fusion-neutron helium production in ferritic alloys in mixed-spectrum fission reactors.

Future work will include analysis of the RTNS-II and $^{1}H(t,n)$ experiments to derive total helium production cross sections, and continued irradiation and analysis of materials in mixed-spectrum fission reactors. The latter will be used for cross section measurements and their application to fusion neutron radiation effects simulation in mixed-spectrum reactors.

[3] Greenwood, Kneff, Skowronski, and Mann, "A Comparison of Measured and Calculated Helium Production in Nickel Using Newly Evaluated Neutron Cross Sections for ^{59}Ni," J. Nucl. Mater. 122 & 123, 1002 (1984).

[4] Kneff, Greenwood, Oliver, and Skowronski, "Helium Production in Copper by a Thermal Three-Stage Reaction," Radiat. Eff. 93, 217 (1986).

TRIANGLE UNIVERSITIES NUCLEAR LABORATORY

A. NEUTRON CROSS SECTIONS

1. Overview (R. L. Walter, C. R. Howell, W. Tornow, C. R. Gould, P. O. Felsher, G. M. Honoré*, K. Murphy**, R. S. Pedroni+, H. P. Pfützner, M. L. Roberts, J. P. Delaroche++)

The FN tandem facility at TUNL and the neutron time-of-flight system is well-suited to providing neutron scattering cross-section information in the 8 to 17 MeV region. For these measurements the high flux at 0° from the $^{2}H(d,n)^{3}He$ reaction is used for a source of mono-energetic neutrons. The technique provides valuable information, particularly between 12 to 17 MeV - a region in which it has been difficult to make systematic energy-dependent measurements at other laboratories. The interpretation of the data is enhanced by using differential cross sections $\sigma(\theta)$ obtained at other labs in the 20 to 40 MeV range, total cross sections from about 1 to 80 MeV, s- and p-wave strength functions at 10 to 200 keV, and analyzing power $A_y(\theta)$ data obtained at TUNL, usually in the 10 to 17 MeV range. These sizeable neutron data bases for individual nuclei, combined in some cases with complementary (p,p) scattering data and (p,n) cross section data, permit some well-constrained analysis, both in TUNL projects as well as analyses at other labs.

A variety of neutron polarization experiments have also been conducted at TUNL. Much relates to the nucleon-nucleus interaction, and such data are incorporated into the nuclear model studies which attempt to explain the above cross-section data. Other TUNL polarization data, such as for the fundamental scattering processes $^{1}H(n,n)^{1}H$ and $^{2}H(n,n)^{2}H$ are important for providing a more accurate understanding of the basic nuclear interactions. This knowledge is important for obtaining accurate predictions of the cross sections for n+p and n+d reactions, as well as permitting improved calculations for neutron scattering from heavier nuclei when the appropriate model is based on an accurate knowledge of the nucleon-nucleon potential.

Analyses have been underway for many nuclei ranging from ^{1}H to ^{208}Pb. Some of these are presented in this section and the remaining in the neutron polarization section (Section B) of TUNL XXIV (Annual Report 1986). The division is somewhat arbitrary. Because of the demands on the personnel, a few of the analyses have had little progress during the past 12 months; the main emphasis has been on completing the projects for ^{10}B, ^{11}B, $^{54,56}Fe$, $^{58,60}Ni$, ^{89}Y and ^{93}Nb. The ^{10}B and ^{11}B reactions were viewed from a Lane model picture where all the available information of (N,N) channels was utilized. The analyses for Fe and Ni have been conducted in the framework of the conventional coupled channel (CC) analysis, but using the Fermi-energy anomoly feature to parametrize the energy dependence of the imaginary potential. The work on ^{89}Y and ^{93}Nb used a simple form of the spherical optical model (SOM), since no data on inelastic scattering were obtained.

Additional work has been done in the $^{12}C(n,n)$ study at energies above 11 MeV.

---

* Present address: Division of Radiology, Duke Medical Center, Durham, NC
** Present address: Indiana University Cyclotron Facility, Bloomington, IN
\+ Present address: Department of Physics, Ohio University, Athens, OH
\++ Permanent address: Centre d'Études de Bruyères-le-Châtel, France

New $\sigma(\theta)$ data was obtained at 8 MeV for ^{208}Pb, and a new approach to understanding the ^{208}Pb(n,n) process below 10 MeV is being developed in cooperation with ORNL scientists.

Considerable progress was made in determining and parametrizing the detection efficiency of the two main neutron time-of-flight detectors; a new code was designed, and the Monte Carlo code from the PTB lab was installed on the TUNL VAX computer. Several changes in the equipment were made, the foremost being the modifications at the injection end of the tandem in preparation for the insertion of a new buncher in a few months. This new system eventually will permit us to improve the width of the deuteron beam burst to about 0.8 ns from the present 1.8 ns routinely obtained at present. Additional tests for installing a detector array at 7 to 10 m flight path for the backward scattering hemisphere were performed; some $A_y(\theta)$ data were obtained with a total of 8 detectors, 2 forward and 6 backward.

2. Studies of $\sigma(\theta)$ in the 1p Shell

a. ^{9}Be (N,N) Reactions

The Lane model analysis of ^{9}Be(n,n), ^{9}Be(p,n) and ^{9}Be(p,p) has been published in Nucl. Phys. A455 (1986) 525.

b. ^{6}Li(n,n) Scattering

To complement $\sigma(\theta)$ data obtained previously at TUNL for energies below 15 MeV and to supplement our $A_y(\theta)$ data, a measurement was made at 17 MeV. A self-consistent analysis in the SOM framework is intended for the ^{6}Li(n,n) and ^{6}Li(p,p) data. Since N=Z for ^{6}Li, no symmetry term is needed in the potential, which greatly simplifies the analysis.

c. ^{10}B and ^{11}B(N,N) Scattering

A spherical optical model in the Lane formulation that was developed at TUNL has given a fairly respectable description of the (n,n) and (p,n) cross section and analyzing power for ^{11}B. The same approach worked quite well for representing the (n,n) and (p,p) cross section and analyzing power for ^{10}B. The analyses led to a determination of the nature of the terms for both the real and imaginary parts of the central, spin-orbit and isospin potentials. (See TUNL XXIV.) As no useable data for $\sigma(\theta)$ or $A_y(\theta)$ for ^{11}B(p,p) was available, and only a single $A_y(\theta)$ distribution for ^{10}B(p,p) has been reported, some of the conclusions were left somewhat ambiguous, however. In order to obtain a larger body of (p,p) data with the goal of obtaining a complete (N,N) data set in the region from 10 to 17 MeV, the $\sigma(\theta)$ and $A_y(\theta)$ distributions were measured in this energy range in about 1 MeV steps for ^{10}B and ^{11}B. The measurements were analyzed and the data was put into "final" form. The Lane model calculations were retuned with the new results incorporated, and reasonable agreement was achieved everywhere, except that the magnitude of the back angle (p,p) $A_y(\theta)$ data is overpredicted. The real and imaginary Coulomb correction terms were obtained; the real part is similar to that found in Lane-type analyses for heavier nuclei.

d. Neutron Scattering from ^{12}C

The cross section for $^{12}C(n,n_0)$ and $^{12}C(n,n_1)$ have been determined at 11 and 14 MeV in a careful measurement to provide an accurate confirmation of the calibration data[1] obtained at the PTB (Braunschweig, FRG). These PTB results are in serious disagreement with the ENDF/B-V evaluation. The discrepancy calls into question earlier data obtained at TUNL and also at Bruyères-le-Châtel about 10 years ago. Since the n+^{12}C interaction is particularly important for applied purposes, it is important to resolve this question. The uncertainties on the new data are about ±3% for both the the (n,n_0) and (n,n_1) data. The reduced coefficients derived from the polynomial expansions which fit the (n,n_0) data are in excellent agreement with those derived by PTB from their data. This verification of the PTB findings points out the need for revising the ENDF/B-V evaluation before accurate use can be made of the evaluation files for applied purposes. The results for $^{12}C(n,n_1)$ seem to disagree with PTB's results and comparison of the actual $\sigma(\theta)$ data will be done when the PTB results are released.

In a second project we have completed a paper on the extension of our previous phase shift analysis upward into the 12 to 17 MeV region. The paper has been accepted for publication in Journal Phys. G: Nucl. Phys. The abstract follows:

"Analyzing power data for elastic scattering of neutrons from ^{12}C have been obtained at selected angles in small energy steps between incident energies of 15.55 and 17.35 MeV. The excitation energy, spin and parity of levels in ^{13}C have been determined for excitation energies around 20 MeV via a phase-shift analysis of these data and of previously measured n-^{12}C total cross section data. In addition, an auxilary phase-shift analysis has been performed in the neutron energy range from 12 to 15 MeV. All experimental data are well reproduced by the phase shifts obtained. The need for further experimental data is pointed out."

An extension of this work is underway: first, $\sigma(\theta)$ for scattering to the ground and first 2^+ excited states have been measured at 16.75 and 17.27 MeV. The 17.27 MeV elastic scattering data are shown in Fig. A2-1 in comparison to the 15 year old data of Deconninck and Meulders.[2] Second, analyzing power data, as discussed in Sec. B, have been measured at selected energies and angles between 15.5 MeV and 16.5 MeV.

In order to extend our present phase-shift analysis to even higher energies, in a first step, analyzing power data $A_y(\theta)$, as described in Sec. B, have been measured at 18.25 MeV to complement the existing $\sigma(\theta)$ data at this energy.

e. $^{14}N(n,n)$ Cross Sections

A paper titled "Neutron Scattering from ^{14}N and ^9B at 11, 14 and 17 MeV" has been published in Nuclear Science and Engineering 91 (1985) 451.

---

1. R. Bottger et al. in Nuclear Data for Basic and Applied Science, ed. P. G. Young et al. (Gordon and Breach Science Publ., 1986) p. 1455.
2. G. Deconninck and J.-P. Meulders, Phys. Rev. C 1 (1970) 1326

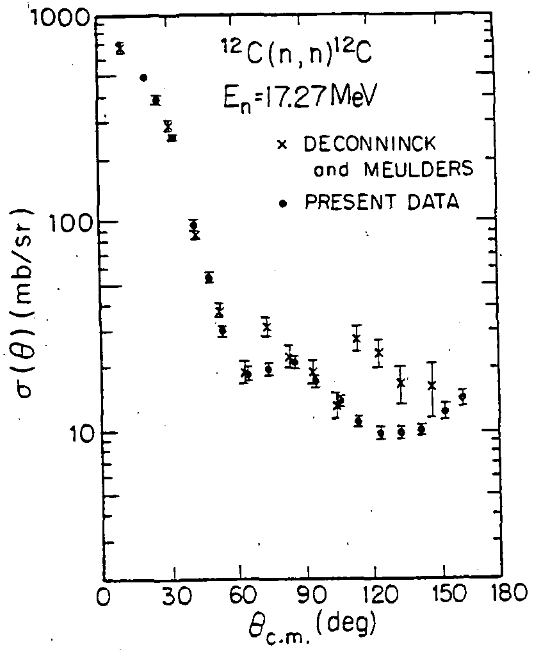

Fig. A2-1 Comparison of new σ(θ) data at 17.27 MeV to the apparently errant data from Ref. 2.

3. Elastic Neutron Scattering from ^{27}Al

The TUNL σ(θ) data reported in Phys. Rev. C 30 (1984) 1435 was combined with our newly measured $A_y(\theta)$ data at 14 and 17 MeV to form another unique data set. The data were analyzed using a conventional spherical optical model with Woods-Saxon form factors. Good agreement was obtained between the data and the calculations. The results have been published in Phys. Rev. C 34 (1986) 384.

4. ^{28}Si and ^{32}S Cross Sections

The σ(θ) for (n,n_0) and (n,n_1) for E_n=8, 10, 12, 14 and 17 MeV have been shown in previous TUNL reports. A coupled-channel analysis of these data and complementary $A_y(\theta)$ data has been completed. The final publication of this study will include an analysis of the complimentary data for (p,p_0) and (p,p_1).

5. ^{40}Ca Cross Sections and Analyzing Powers

The analysis of ^{40}Ca(n,n) up to 80 MeV has been published in Phys. Rev. C 33 (1986) 1129. The abstract follows:

"Differential cross sections σ(θ) and analyzing powers $A_y(\theta)$ for neutron scattering to the ground and first 3^- excited state of ^{40}Ca have been measured in the energy range from 11 to 17 MeV. Elastic and inelastic scattering measurements have been obtained for $A_y(\theta)$ at energies of 11.0, 13.9, and 16.9 MeV, the inelastic scattering data representing the first (n,n') measurements of $A_y(\theta)$ for this nucleus. Differential cross section for (n,n) and (n,n') have been obtained at 13.9 and 16.9 MeV. Both the σ(θ) and $A_y(\theta)$ data at 13.9 MeV have been compared with previous measurements at this energy and the agreement is good, typically within less than 3%. These results have been combined with other $\sigma(\theta)$ and $A_y(\theta)$ data and total cross section σ_T measurements to form a large set of neutron scattering and reaction data for incident energies up to 80 MeV. This data set, along with $\sigma(\theta)$ and $A_y(\theta)$ measurements available for proton scattering in this energy range, has been described in the framework of the coupled-channel formalism. This highly constrained analysis has led to a precise determination of geometries, energy dependencies, and deformation parameters. Further analyses, which dealt with simultaneous couplings to low- and high-energy excited states, have led to improved descriptions of the elastic scattering measurements for $\sigma(\theta)$ and $A_y(\theta)$ at backward angles. These results confirm that real and virtual excitations of giant resonances cannot be ignored in the description of the reaction mechanism. In this context, it has also been found that corrections to the real central potentials, as estimated by Mahaux and Ngô from dispersion relations, help to further improve the fits to elastic scattering observables."

6. Elastic and Inelastic Scattering from ^{54}Fe and ^{58}Ni

The CC analyses of neutron scattering from ^{54}Fe and ^{58}Ni have been completed and a paper is being prepared. The new data, both $\sigma(\theta)$ and $A_y(\theta)$, at 17 MeV and new total cross section σ_T of D. Larson et al. from ORNL for energies up to 80 MeV were used to specify the energy dependence of the real and imaginary potential more accurately than in our previous publications on these nuclei. The form employed here incorporates the Fermi-surface anomaly in the imaginary surface potential. Fig. A6-1 for ^{58}Ni shows the energy dependence of the strength of the real potential V and the surface and volume imaginary potentials, W_D and W_V, respectively. The potentials have Woods-Saxon form factors. The $\sigma(\theta)$ and $A_y(\theta)$ data from 10 to 26 MeV and σ_T are quite well described with these energy dependences. The total cross section calculation is compared in Fig. A6-2 to the unpublished ORELA data of Larson et al. There is some difficulty representing σ_T in the energy range below 4 MeV; solution of this problem might require an energy dependent potential radius and non-linear energy dependence of the central potential, as was

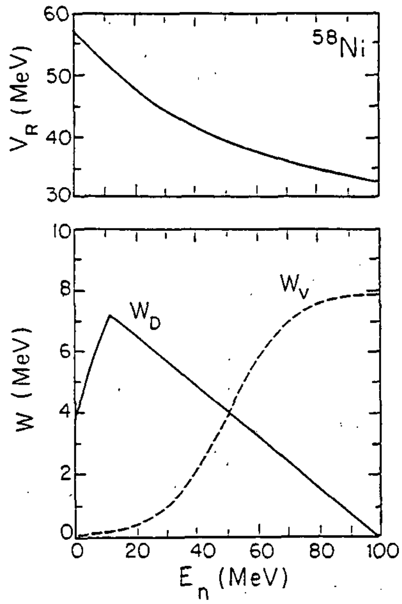

Fig. A6-1 Energy dependence of the real and imaginary potential for ^{58}Ni(n,n).

reported by the Ohio University group for ^{208}Pb in Nuclear Physics A443 (1985) 249. Unfortunately, one of the limitations in such analyses is the relatively large uncertainties in the σ_T data due to the inability to measure self-shielding corrections for isotopically enriched samples of Fe and Ni.

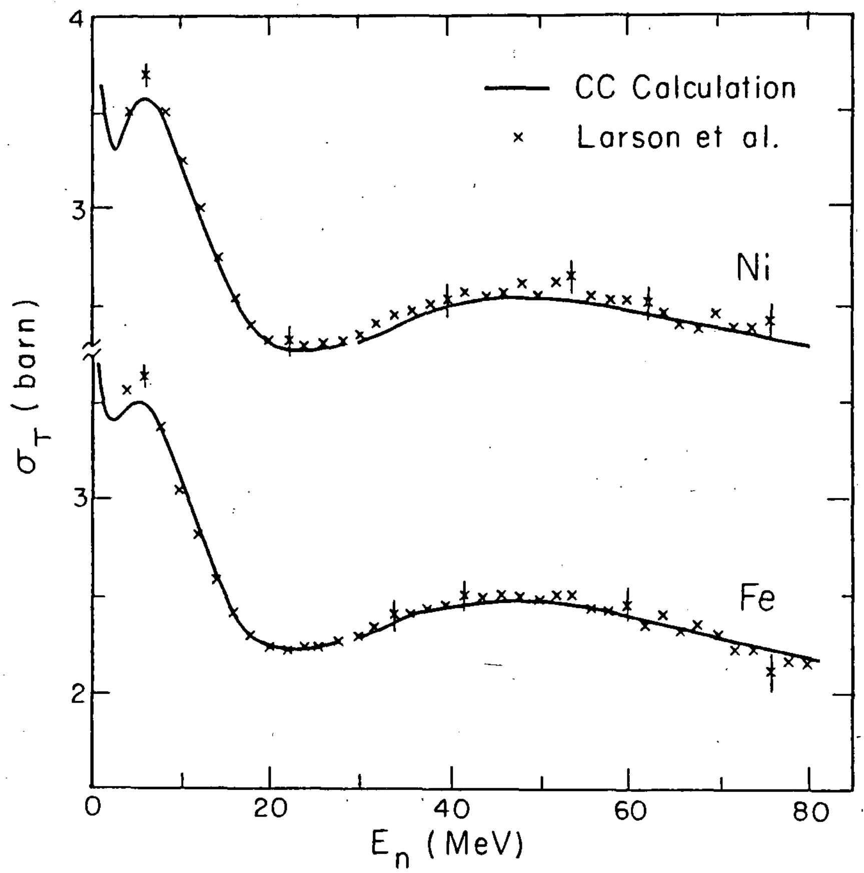

Fig. A6-2 Comparison of σ_T data to the CC calculations for n + ^{58}Ni and n + ^{54}Fe.

7. Elastic Scattering from ^{89}Y and ^{93}Nb

A phenomenological SOM description for ^{89}Y(n,n) was performed and has been accepted for publication in Phys. Rev. C. The abstract follows:

"Differential cross sections and analyzing powers for neutron elastic scattering from ^{89}Y have been measured at energies from 8 to 17 MeV using the neutron time-of-flight facility at TUNL. The data have been analyzed with the spherical optical model and excellent representations are achieved at all energies with the derived optical potential parameters, which were constrained to vary linearly with energy. Comparisons have been made to two previously reported global spherical optical models as well."

A similar set of data for ^{93}Nb has been included in the Ph.D. thesis of R. Pedroni (1986). A report of this measurement and the SOM analysis is being prepared for publication.

8. Elastic and Inelastic Scattering from $^{116,120}Sn$

A paper on the $\sigma(\theta)$ and $A_y(\theta)$ analysis for the 8 to 14 MeV $^{116,120}Sn$ data has been submitted for publication. The analysis, which gives quite good agreement with the data, used a straightforward CC framework with simple energy dependencies of the potential strengths. A comparison of the deformation lengths for the (n,n) and (p,p) central potentials was made through a consistent analysis of some of the available (p,p) scattering data. The deformation length of the spin-orbit potential was observed to be the same as that for the central potential.

9. Scattering from ^{208}Pb

The $\sigma(\theta)$ for ^{208}Pb has been measured previously at TUNL at 10, 14 and 17 MeV. High accuracy $\sigma(\theta)$ data are available from Ohio University from 4 to 7 MeV and above 20 MeV. In order to understand detailed features in the n+^{208}Pb interaction, TUNL had also previously obtained $A_y(\theta)$ data at 10 and 14 MeV. We are now obtaining $A_y(\theta)$ data with high accuracy at 6, 7, 8 and 9 MeV. In order to correct the 8-Mev $A_y(\theta)$ measurement for multiple scattering in the sample, it is necessary to have an accurate determination of $\sigma(\theta)$ at this energy. Also, since this energy appears to be a transition region below which energy dependences apparently must be introduced into the geometry parameters of the potential wells, it is important to have a good determination of $\sigma(\theta)$ at this energy. Such an experiment was performed using optimum resolution of our neutron TOF spectrometers so that backgrounds were low and could be well determined, and so that inelastic scattering to the 3^- state could be well resolved.

B. NEUTRON POLARIZATION STUDIES

1. Overview (C. R. Howell, W. Tornow, R. L. Walter, P. D. Felsher, G.Honoré*, K. Murphy**, R. Pedroni***, H. Pfützner, M. Roberts, M. Al Ohali, G. Weisel, Z. Chen+, A. A. Naqvi++, I. Slaus+++, J. P. Delaroche#)

During the past year the experiments were concentrated in three major areas: n-p scattering, n+d interactions and neutron scattering from ^{12}C, ^{28}Si and ^{208}Pb. In all these cases the source of polarized neutrons is the $^2H(\vec{d},\vec{n})^3He$ reaction at 0°.

---

* Present address: Division of Radiology, Duke University Medical Center
** Present address: Indiana University Cyclotron Facility
*** Present address: Dept. of Physics, Ohio University
\+ Permanent address: Dept. of Physics, Tsinghua Univ., Beijing
\++ Permanent address: Dept. of Physics, Univ. of Petroleum and Minerals, Dhahran
\+++ Permanent address: Ruder Boskovic Institute, Zagreb
\# Permanent address: Service de Physique et Techniques Nucléaires, Bruyères-le-Châtel

In the n-p study, new data were needed to permit verification of an earlier TUNL measurement of Tornow et al. at 16.9 MeV where discrepancies were found to exist between the nucleon-nucleon model predictions of the Paris potential and the data at backward angles. Two new measurements were made in collaboration with G. Mertens of Tübingen. In the first case the $A_y(\theta)$ for the recoil protons in the $^1H(n,n)^1H$ reaction was observed at 2 angles corresponding to backward angle neutron scattering. The measurements were made to a statistical accuracy of ±0.003, which was sufficient to make an initial test of the previous data. The second was to measure the $A_y(\theta)$ for $0°<\theta<16°$ in about 2° steps to an accuracy of ±0.002 for the $^2H(\vec{d},\vec{n})^3He$ reaction, the neutron source reaction in the previous n-p experiment of Tornow et al. The measurement was made at the deuteron energy of 14.1 MeV, the energy which provides the 16.9 MeV polarized neutron beam for the n-p study. Having this detailed information about the source reaction, it is now possible to apply corrections in the original n-p measurement for effects previously believed to be negligible.

The interaction of 12 MeV polarized neutrons with ^2H has been further investigated during the past year. The $A_y(\theta)$ data for $^2H(n,n)^2H$ scattering have been corrected for multiple-scattering and finite geometry effects. In collaboration with Y. Koike of Osaka, few-nucleon predictions using meson-theory based nucleon-nucleon potentials as input have been compared to our elastic data. The accuracy of the data is sufficient for testing various nucleon-nucleon interactions. Progress has been made on the interpretation of the two-dimensional spectra obtained in the experiment to measure $A_y(\theta)$ in the breakup reaction $^2H(n,n)np$.

The neutron scattering group devoted considerable accelerator time to measure $A_y(\theta)$ for $^{208}Pb(n,n)$ from E_n = 8 MeV down to our lowest practical energy 6 MeV. These data have been obtained to a relatively high accuracy of about ±0.03 in order to provide a critical test of several nuclear models for $n+^{208}Pb$. In order to obtain such data, the tandem Van de Graaff must be run at a low terminal voltage, i.e., down to 1.5 MV, a value at which the polarized deuteron beam is transmitted poorly through the accelerator. Such experiments of this accuracy are therefore quite time consuming. These data are also being used to investigate the need for a parity-dependent potential which has been proposed by our collaborator, D. Horen of ORNL.

Another breakthrough was the successful test of the $^2H(\vec{d},\vec{n})^3He$ reaction as a monoenergetic source of 19 MeV polarized neutrons. (Our previous measurements had always been conducted below 17 MeV.) For this work the tandem must run reliably near its maximum voltage of 8.1 MV. We chose the nucleus ^{28}Si as a target for this test, since several interesting features in $A_y(\theta)$ for $n+^{28}Si$ were anticipated above 17 MeV. Later we will return to measure $\sigma(\theta)$ for $n+^{28}Si$ at this energy using the unpolarized deuteron beam. A wide range of experiments will be feasible at this energy, especially since the time resolution of the TOF system is to be improved during the next year.

Several measurements for $n+^{12}C$ were also conducted around 16 MeV. We see no sign of the resonance at an excitation energy of about 20 MeV reported by Benetskii et al. last year; their $A_y(\theta)$ results could not be duplicated in our measurement. These new data also will be valuable for the phase shift analysis currently underway at TUNL for $15<E_n<17$ MeV.

The multi-detector arrays mentioned in Sec. A1 actually have already been employed to obtain $A_y(\theta)$ data in the ^{208}Pb experiment. A permanent installation of such a system would greatly expedite the accumulation of $A_y(\theta)$ data for neutron scattering, since it can take 8-12 hours to accumulate high-accuracy $A_y(\theta)$ data at backward angles with the standard 2-detector system at TUNL.